Mechanisms of Arsenic Toxicity in Humans: Interplay of Arsenic, Glutathione, and DNA Methylation in Bangladeshi Adults

Megan Marie Niedzwiecki

Submitted in partial fulfillment of the
requirements for the degree of
Doctor of Philosophy
under the Executive Committee
of the Graduate School of Arts and Sciences

COLUMBIA UNIVERSITY

2014

Abstract

Mechanisms of Arsenic Toxicity in Humans: Interplay of Arsenic, Glutathione, and DNA Methylation in Bangladeshi Adults

Megan Marie Niedzwiecki

Background: Over 200 million individuals worldwide are chronically exposed to arsenic (As) in drinking water at concentrations above the World Health Organization (WHO) guideline of 10 µg/L. Arsenic exposure is of particular concern in Bangladesh, where it is estimated that 35-77 million people are exposed to As in well water at concentrations above the WHO guideline. Chronic As exposure is associated with neurological impairments, respiratory disease, cardiovascular disease, skin lesions, and cancers of the skin, liver, lung and bladder. The mechanisms of As toxicity in humans are not well-characterized: there are considerable interspecies differences in As toxicokinetics, and until recently, there were no animal models to study As carcinogenesis. However, two of several proposed pathways of As toxicity in humans involve DNA methylation and oxidative stress. Arsenic metabolism, DNA methylation, and glutathione (GSH) are metabolically connected through the one-carbon metabolism and transsulfuration pathways, and their interactions are remarkably complex. The epidemiologic studies in this dissertation are designed to address the overarching hypothesis that one-carbon metabolism and the transsulfuration pathway interact to influence susceptibility to As toxicity.

Introduction: Arsenic is methylated in the liver to monomethyl (MMA) and dimethyl (DMA) arsenical species by arsenic(III)-methyltransferase (AS3MT), which requires a methyl group from *S*-adenosylmethionine (SAM) and the presence of a reductant, such as glutathione (GSH). SAM is the universal methyl donor for transmethylation reactions, including DNA methylation,

and is a product of folate-dependent one-carbon metabolism. GSH is the primary endogenous antioxidant and determinant of the intracellular redox state, and the rate-limiting precursor for GSH synthesis, cysteine (Cys), is a product of the transsulfuration pathway. One-carbon metabolism and the transsulfuration pathway are connected through homocysteine (Hcys). In humans, aberrant DNA methylation, oxidative stress, hyperhomocysteinemia (HHcys), and impaired As methylation capacity have been identified as risk factors for As-related conditions, including As-induced skin lesions. However, there are knowledge gaps regarding the relationships among these risk factors in humans, namely (1) the dose-response relationship between chronic As exposure and global DNA methylation over a wide range of As concentrations, as well as the influence of As exposure on the newly-discovered epigenetic modification, 5-hydroxymethylcytosine (5hmC); (2) whether an oxidized GSH redox state impairs the capacity to methylate As and DNA; and (3) whether variants in one-carbon metabolism genes are associated with HHcys and susceptibility to As-induced skin lesions.

Methods: We addressed these questions in five self-contained epidemiological studies of As-exposed Bangladeshi adults, which employed cross-sectional (Chapters 3-6) and nested case-control (Chapter 7) designs. First, we examined the dose-response relationship between As exposure and global methylation of peripheral blood mononuclear cell (PBMC) DNA (Chapter 3). Second, we optimized a high-throughput liquid chromatography-tandem mass spectrometry (LC-MS/MS) assay to measure global 5-methylcytosine (5mC) and 5hmC content in human DNA samples, and we examined the associations of As exposure with global %mC and %hmC in two independent samples of As-exposed adults (Chapter 4). Third, we measured GSH and its "oxidized" form, glutathione disulfide (GSSG) in plasma, and we examined the interaction of plasma GSH redox state and folate nutritional status on As methylation capacity (Chapter 5).

Fourth, we examined the relationships between blood GSH redox, blood SAM, and global methylation of PBMC DNA (Chapter 6). Fifth, we conducted a nested case-control study (Chapter 7) to determine whether nonsynonymous single nucleotide polymorphisms (SNPs) in methylene-tetrahydrofolate reductase (*MTHFR*) and other one-carbon metabolism genes were associated with HHcys and risk for As-induced precancerous skin lesions, and we conducted an exploratory genome-wide association study (GWAS) of Hcys in a subset of participants.

Results: Chronic As exposure was associated with increased global DNA methylation over a wide range of well water As concentrations (Chapter 3), but the relationship between As exposure and global %hmC was gender-specific, with a positive association in males and negative association in females (Chapter 4). We found that an oxidized GSH redox state was associated with both decreased As methylation capacity (Chapter 5) and global DNA hypomethylation (Chapter 6). Finally, in the nested-case control study, we confirmed previous findings that serum HHcys was a risk factor for As-induced skin lesions, and gene variants in *MTHFR* were found to explain a substantial proportion of the variance in serum Hcys concentrations (Chapter 7). However, we did not find that one-carbon metabolism gene variants were risk factors for As-induced skin lesions. The GWAS of serum Hcys identified one genome-wide significant SNP in the pregnane X receptor (PXR) gene, along with other SNPs in genes involved in cell signaling and the establishment of epithelial cell polarity.

Taken together, our findings suggest that indices of one-carbon metabolism and the transsulfuration pathway—DNA methylation, GSH redox, and As methylation—interact with one another to influence susceptibility to As toxicity in humans. In addition, to our knowledge, this is the first report of an association between As exposure and global 5hmC.

Table of Contents

Chapter 4: Arsenic exposure and age are associated with global hydroxymethylcytosine content in two subpopulations of human peripheral blood cell DNA

Chapter 5: Interactions of plasma glutathione redox and folate deficiency on arsenic methylation capacity

List of Tables and Figures

Chapter 1

Figures

Chapter 2

Figures

Tables

Chapter 3

Figures

Tables

Chapter 4

Figures

Tables

Chapter 5

Figures

Tables

Chapter 6

Tables

Chapter 7

Figures

Tables

List of Abbreviations

5mTHF	5-methyltetrahydrofolate
5,10 methylene-THF	5,10-methylenetetrahydrofolate
5hmC	5-hydroxymethylcytosine
5mC	5-methylcytosine
AAS	age-associated skewing
AML	acute myeloid leukemia
AP-1	activator protein-1
AQP	aquaporin
APL	acute promyelocytic leukemia
ARE	antioxidant response element
As	arsenic
As^{III}	arsenite
As^{V}	arsenate
AS3MT	arsenic(III)-methyltransferase
ASTDR	Agency for Toxic Substances and Disease Registry
ATC^{III}	arsenic tricysteine
ATG	arsenic triglutathione
ATRA	all-trans retinoic acid
bAs	blood arsenic
BER	base excision repair
BH_4	tetrahydrobiopterin
BMI	body mass index
CAT	catalase
CBS	cystathionine-beta-synthase
CI	confidence interval
CSE	cystathionine gamma-lyase
CV	coefficient of variation
CVD	cardiovascular disease
CYP	cytochrome
Cys	cysteine
CySS	cystine
DHF	dihydrofolate
DHFR	dihydrofolate reductase
DMA^{III}	dimethylarsinous acid
DMA^{V}	dimethylarsinic acid
$DAMC^{III}$	dimethylarsinic cysteine
DMAG	dimethylarsinic glutathione
$DMDTA^{V}$	dimethyldithioarsinic acid

$DMMTA^V$	dimethylmonothioarsinic acid
DNMT	DNA methyltransferase
DP	dipeptidase
DPM	disintegrations per minute
DRC	dynamic reaction cell
dUMP	deoxyuridine monophosphate
dTMP	deoxythymidine monophosphate
ER	endoplasmic reticulum
ERK	extracellular signal-regulated protein kinase
ES	embryonic stem
FA	folic acid
FAD	flavin adenine dinucleotide
FMN	flavin mononucleotide
FOX	Folate and Oxidative Stress study
FPGS	folylpolyglutamate synthase
FR	folate receptor
GAMT	guanidinoacetate methyltransferase
GCL	glutamate cysteine ligase
GCLC	glutamate cysteine ligase catalytic subunit
GCLM	glutamate cysteine ligase modifier subunit
GEMMA	Genome-wide Efficient Mixed Model Association
GENI	Gene-Environment-Nutrition Interactions study
GFAA	graphite furnace atomic absorption spectrometry
GGH	gamma-glutamyl hydrolase
GGT	gamma-glutamyltransferase
Glu	glutamate
GLUT	glucose transporter
Gly	glycine
GPx	glutathione peroxidase
GR	glutathione reductase
GS	glutathione synthase
GS^*	glutathione thiyl radical
GSH	glutathione
GSSG	glutathione disulfide
GST	glutathione-*S*-transferase
GWAS	genome-wide association study
H_2O_2	hydrogen peroxide
HC	haptocorrin
Hcys	homocysteine
HDAC	histone deacetylase

HEALS	Health Effects of Arsenic Longitudinal Cohort
HHcys	hyperhomocysteinemia
holoTC	holotranscobalamin
HPLC	high performance liquid chromatography
ICP-MS	inductively coupled mass spectrometry
IDH	isocitrate dehydrogenase
IκB	inhibitor of κB
IKK	IκB kinase
JNK	c-Jun N-terminal kinase/stress-activated protein kinase
Keap1	kelch like-ECH-associated protein 1
LC-MS/MS	liquid chromatography-tandem mass spectrometry
LD	linkage disequilibrium
LINE-1	long interspersed element-1
LOESS	locally estimated scatterplot smoothing
LSD1	lysine-specific demethylase 1
$MADC^{III}$	monomethylarsonic dicysteine
MADG	monomethylarsonic diglutathione
MAF	minor allele frequency
MAPK	mitogen-activated protein kinase
MAT	methionine adenosyltransferase
MBP	methyl binding protein
Met	methionine
MKK	mitogen-activated protein kinase kinase
MKP	mitogen-activated protein kinase phosphatase
MLL	mixed lineage leukemia
MMA^{III}	methylarsonous acid
MMA^{V}	methylarsonic acid
$MMMTA^{V}$	monomethylmonothioarsonic acid
MRP	multidrug resistance protein
MTHFD1	methylenetetrahydrofolate dehydrogenase 1
MTHFR	methylenetetrahydrofolate reductase
MTR	methionine synthetase
MTRR	methionine synthase reductase
$NaAsO_2$	sodium arsenite
NAC	*N*-acetyl-*L*-cysteine
NADH	nicotinamide adenine dinucleotide
$NADP^{+}$	nicotinamide adenine dinucleotide phosphate
NADPH	nicotinamide adenine dinucleotide phosphate (reduced)
NER	nucleotide excision repair
NF-κB	nuclear factor-kappaB

NIAT	Nutritional Influences of Arsenic Toxicity study
NIK	NF-κB inducing kinase
NOS	nitric oxide synthase
NOX	NADPH oxidase
Nrf2	nuclear factor (erythroid-derived 2)-like 2
$O_2^{-\bullet}$	superoxide anion
OATPB	organic anion transporting polypeptide
•OH	hydroxyl radical
$ONOO^-$	peroxynitrite
OR	odds ratio
PBL	peripheral blood leukocytes
PBMC	peripheral blood mononuclear cells
PBS	phosphate buffered saline
PC	phosphatidylcholine
PCA	perchloric acid
PCFT	protein-coupled folate transport
PDH	pyruvate dehydrogenase
PEMT	phosphatidylethanolamine N-methyltransferase
PML	promyelocytic leukaemia
PRC	polycomb repressive complex
PTK	protein tyrosine kinase
PTP	protein tyrosine phosphatase
PXR	pregnane X receptor
Q	ubiquinone
QH_2	ubiquinol
Q-Q	quantile-quantile
RARα	retinoic acid receptor alpha
RCS	restricted cubic spline
RFC1	reduced folate carrier 1
RHD	rel-homology domain
ROS	reactive oxygen species
RXR	retinoid X receptor
SAH	*S*-adenosylhomocysteine
SAHH	*S*-adenosylhomocysteine hydrolase
SAM	*S*-adenosylmethionine
SD	standard deviation
SE	standard error
SDH	succinate dehydrogenase
SLC19A1	solute carrier family 19, member 1
SLC46A1	solute carrier family 46, member 1

SMI	secondary methylation index
SNP	single nucleotide polymorphism
SOD	superoxide dismutase
TC	transcobalamin
TCblR	transcobalamin receptor
TDG	thymine DNA glycosylase
TET1	ten-eleven translocation-1
THF	tetrahydrofolate
Trx	thioredoxin
TSS	transcription start site
TYMS	thymidylate synthase
uAs	urinary arsenic
uCr	urinary creatinine
UHRF1	ubiquitin-like, containing PHD and RING finger domains, 1
WBC	white blood cell
WHO	World Health Organization
wAs	water arsenic

Acknowledgements

This dissertation could not have been completed without extensive support from my colleagues, friends, and family. First and foremost, I would like to thank my mentor, Dr. Mary Gamble, for shaping my graduate school career, and for being the model of the public health scientist who I can only hope to become. I cannot thank her enough for her mentorship, and for providing me the intellectual freedom to explore my research questions. I would also like to thank my dissertation committee members, Drs. Joseph Graziano, Regina Santella, Robert Wright, and William Blaner, for their guidance over the past three years.

I want to specifically thank Dr. Megan Hall for her mentorship and emotional support. I would not have made it through without her.

To the Gamble lab, past and present—Vesna Iliveski, Shelley Qu, Dr. Kristin Harper, Julie Oka, Larissa Calancie, Tyler McClintock, and my fellow doctoral students Brandilyn Peters and Caitlin Howe—I could not have asked for better labmates. I would also like to thank the members of the Graziano lab for their technical support, including Vesna Slavkovich, Olga Balac, David Santiago, Angela Lomax, and Tiffany Sanchez, and the members of the Freyer, Santella, Tang, Perzanowski, and Guilarte labs, specifically J.D. Knotts, Adnan Divjan, and Drs. Maya Kappil and Maria Jose Rosa.

I am grateful to all of the members of the Columbia SRP for their guidance, including Nancy Lolacono and Drs. Pam Factor-Litvak, Jennie Kline, Gail Wasserman, Yu Chen, Faruque Parvez, Khalid Khan, Alexander van Geen, and Jacob Mey. Having to present at the Tuesday morning lab meetings was one of the most fear-inducing—but intensely valuable—experiences during graduate school, and I truly appreciated the constructive feedback. Special thanks to Dr. Xinhua Liu for her biostatistics expertise and Diane Levy for her database management expertise, and to everyone at the Columbia University Arsenic & Health Research office in Bangladesh.

This work would not have been possible without our collaborators at other institutions. I would like to thank Drs. Habibul Ahsan, Maria Argos, Muhammad Kibriya, and Lin Tong at University of Chicago for their help with the GENI study. I am grateful to Drs. Richard Finnell and Huiping Zhu at University of Texas at Austin, along with the members of the Finnell Lab, for their extensive help with the OpenArray genotyping platform and for their hospitality during my trip to Austin, and to Drs. William Stewart and David Greenberg at The Ohio State University for their expertise in statistical genetics.

My graduate school experience would not have been the same without my fellow doctoral students, specifically Drs. Maria Jose Rosa, Maya Kappil, Allan Just, Robert Prins, Christine George, and Ann Marie Reardon, and current students Caitlin Howe, Brandilyn Peters, Tiffany Sanchez, Ashlinn Quinn, Medina Jackson-Browne, and Richard Gill.

I am also grateful to the EHS department, specificially Nina Kulacki and Drs. Tom Guilarte, Greg Freyer, and Alysa Turkowitz, for their academic and administrative support. In addition, I want to thank Drs. Greg Freyer and Matt Perzanowski for supervising my research

laboratory rotations during my first year in the program, and Dr. Rachel Miller for serving as my TRANSFORM mentor and helping me write my first journal article.

I would like to acknowledge the funding sources that have supported my studies, including the EHS departmental NIH T32 training fellowship, the NIH T32 translational science award through the Irving Institute, the Columbia University NIEHS Center for Environmental Health, and the Columbia University Cancer Epidemiology Training Program T32 award—with a special thanks to the Cancer Training Program Director, Dr. Al Neugut, and the Training Program faculty for their support, both financial and academic.

I am forever indebted to the HEALS and FOX study participants for agreeing to donate their time—and urine—in support of our research. In return for their generosity, I hope that my research will lead to a better understanding of how to combat the health effects of As toxicity, even in a small way.

Finally, I want my family to know that their love and emotional support was integral to my success. Specifically, I want my husband Robert to know how much I appreciate everything that he does for our family; without him, none of this would have been possible.

Dedication

For Robert and Cora

Chapter 1: Statement of hypotheses

In Bangladesh, over 35 million people are chronically exposed to As in drinking water above the World Health Organization (WHO) guideline of 10 µg/L, which has been described as "the largest mass poisoning of a population in history." Chronic As exposure is associated with respiratory and cardiovascular diseases, neurological impairments, and cancers of the skin, liver, lung and bladder. Although the mechanisms of As toxicity in humans are not well-characterized, two proposed pathways involve DNA methylation and oxidative stress. Arsenic metabolism, DNA methylation, and glutathione (GSH) are metabolically connected through one-carbon metabolism and the transsulfuration pathway (Figure 1). This dissertation is an epidemiologic investigation of the metabolic interplay between As metabolism, GSH, and DNA methylation to address the overarching hypothesis that one-carbon metabolism and the transsulfuration pathway interact to influence susceptibility to As toxicity in humans.

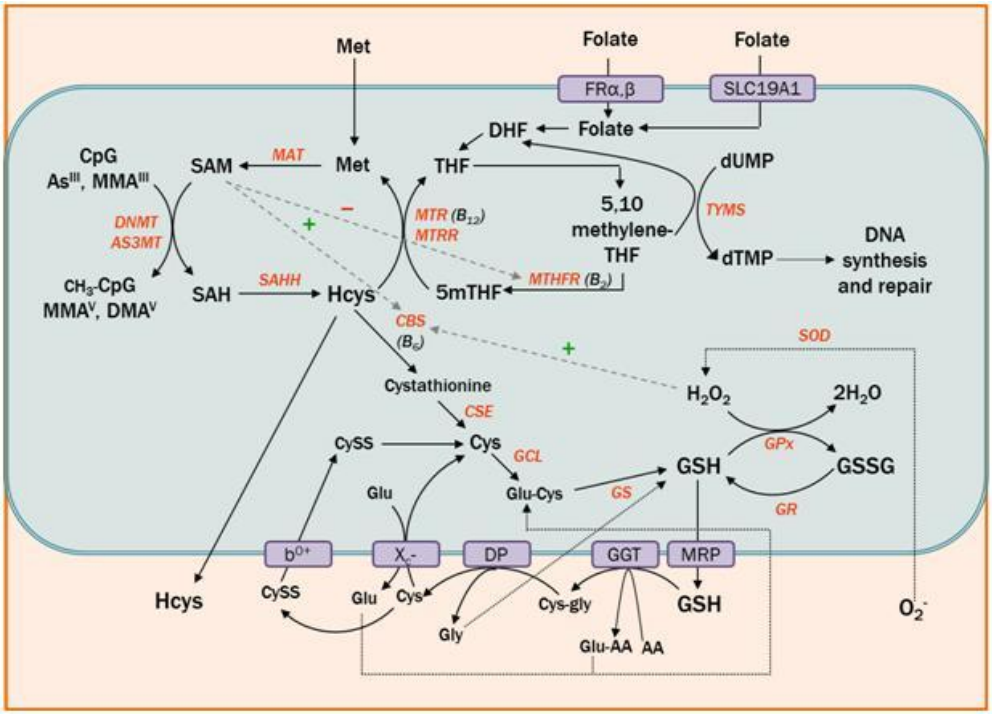

Figure 1. One-carbon metabolism and the transsulfuration pathway: metabolic interactions of arsenic metabolism, DNA methylation, and glutathione.

Hypothesis 1.

We hypothesize that chronic As exposure is associated with alterations of global DNA methylation and hydroxymethylation.

Specific Aim 1A: Arsenic exposure and global DNA methylation

We will explore the dose-response relationship between As exposure and global methylation of peripheral blood mononuclear cell (PBMC) DNA, measured using the [^{3}H]-methyl incorporation assay, in the Folate and Oxidative Stress (FOX) study, a cross-sectional study of 378 Bangladeshi adults who were exposed to a wide range of As in well water. Additionally, we will examine whether there is evidence of a non-linear relationship.

Specific Aim 1B: Arsenic exposure and global 5-hydroxymethylcytosine

We will optimize a high-throughput liquid chromatography-tandem mass spectrometry (LC-MS/MS) assay to measure global percent 5-methylcytosine (%5mC) and 5-hydroxymethylcytosine (%5hmC) in human DNA samples. We will then examine the cross-sectional associations between As exposure and global %mC and %hmC in peripheral blood cell DNA in two independent samples of As-exposed Bangladeshi adults.

Hypothesis 2.

We hypothesize that an oxidized intracellular GSH redox state is associated with a reduced capacity to methylate DNA and As.

Specific Aim 2A: Plasma GSH redox status, As methylation capacity, and folate

We will examine the associations between plasma GSH redox status and urinary As metabolites (urinary %MMA and %DMA) in the FOX study, and test whether these associations are modified by plasma folate nutritional status.

Specific Aim 2B: Blood GSH redox status and global DNA methylation

We will examine the association between whole blood glutathione (GSH) redox status and [^{3}H]-methyl incorporation of PBMC DNA in the FOX study, and additionally, we will assess whether blood *S*-adenosylmethionine (SAM) is a mediator of this association.

Hypothesis 3.

We predict that aberrant regulation of one-carbon metabolism contributes to increased susceptibility to As-induced skin lesions. Specifically, we predict that nonsynonymous variants in one-carbon metabolism genes, specifically variants that are known to influence enzymatic activities, and elevated serum homocysteine (Hcys) are risk factors for As-induced skin lesion incidence.

Specific Aim 3: One-carbon metabolism genes, serum Hcys, and As-induced skin lesions

We will conduct a nested case-control study within the Health Effects of Arsenic Longitudinal Study (HEALS) cohort of 876 incident skin lesions and matched controls, and we will measure single nucleotide polymorphisms (SNPs) in genes involved in one-carbon metabolism—with a focus on nonsynonymous SNPs in methylenetetrahydrofolate reductase (MTHFR)—and homocysteine (Hcys) concentrations in serum samples. We will examine whether SNP genotypes are associated with serum Hcys concentrations separately in the case and control groups, and we will use conditional logistic regression to examine the associations between SNPs and risk of As-induced skin lesions. In an exploratory analysis, we will conduct a genome-wide association study (GWAS) of serum Hcys in a subset of participants.

Chapter 2: Background

A. One-carbon metabolism and the transsulfuration pathway.

1. One-carbon metabolism.

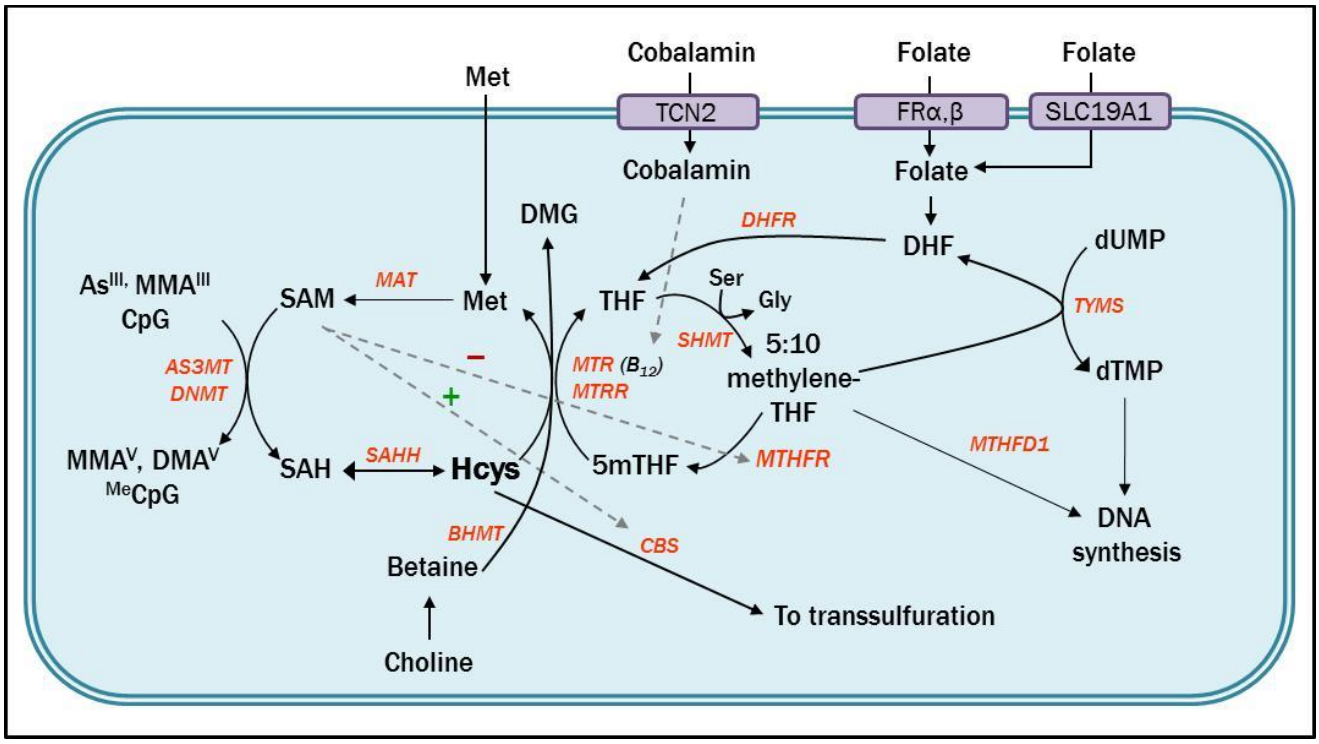

Figure 1. Mammalian one-carbon metabolism.

a. Overview of biochemistry.

One-carbon metabolism is a folate- and cobalamin-dependent pathway involved in two major biologic processes: (1) the synthesis of thymidines and purine bases for DNA replication, synthesis, and repair; and (2) the generation of methyl groups for transmethylation reactions. The functions and biochemistry of mammalian one-carbon metabolism are outlined in several excellent review articles (Fox and Stover 2008; Tibbetts and Appling 2010). The major

components of the pathway are shown in Figure 1. Briefly, folate, in the forms of naturally-occurring 5-methyltetrahydrofolate (5mTHF) and as folic acid (FA), is transported into the cell via a receptor-mediated (folate receptor alpha [FRα], beta [FRβ], or gamma [FRγ]) or carrier-mediated (solute carrier family 19, member 1 [SLC19A1], also known as RFC1) transport mechanisms; FA is subsequently reduced to dihydrofolate (DHF) and tetrahydrofolate (THF). THF enters the one-carbon metabolic pathway and picks up a methyl group from serine, forming 5,10-methylenetetrahydrofolate (5,10 methylene-THF). 5,10 methylene-THF can be used for synthesis of nucleotide bases (*de novo* thymidine synthesis) or reduced to 5mTHF via the enzyme methylenetetrahydrofolate reductase (MTHFR). 5mTHF derived from the metabolism of FA and that originating from naturally-occurring food folates are chemically indistinguishable. The methyl group of 5mTHF is transferred to homocysteine (Hcys) via methionine synthetase (MTR), generating methionine (Met) and THF. Met is activated by ATP to form *S*-adenosylmethionine (SAM), the universal methyl donor for transmethylation reactions. The donation of the methyl group yields the methylated product and *S*-adenosylhomocysteine (SAH), which is hydrolyzed by *S*-adenosylhomocysteine hydrolase (SAHH) to generate Hcys.

b. Folate and cobalamin.

Folates. Folates (Vitamin B_9, pteroyl-L-glutamates) comprise a family of cofactors required for the transfer of methyl groups in one-carbon metabolism. Naturally-occuring folates (generally the polyglutamated forms of 5mTHF and 5-formylTHF) are found in a variety of food sources, with high amounts found in beef liver, spinach, and green vegetables (USDA 2012). Folic acid (pteroylmonoglutamic acid), a synthetic form of folate, does not occur in nature but is used for supplementation and food fortification (Wright et al. 2007). Based on World Health

Organization (WHO) guidelines, the normal range of serum folate concentrations in humans is between 13.5 and 45.3 nmol/L, with marginal folate deficiency classified as concentrations between 6.8 to 13.4 nmol/L, and severe deficiency at concentrations <6.8 nmol/L (WHO 2012).

Folate absorption and transport. In the intestinal wall, dietary polyglutamates are deconjugated to their monoglutamate forms through the cleavage of their polyglutamate tails by folylpolyglutamate carboxypeptidase (Chandler et al. 1986). Folic acid and reduced monoglutamyl folates are transported into enterocytes through a proton-coupled folate transport mechanism (SLC46A1, also known as PCFT), which has equal binding affinity for folic acid and reduced folates (Qiu et al. 2006). Folate enters the hepatic portal vein and is transported to the liver, the primary site of one-carbon metabolism activity, folate storage (Rogers et al. 1997), and conversion of folic acid to reduced folates by dihydrofolate reductase (DHFR) (Wright et al. 2007). A portion of the folate pool is excreted in "first pass" hepatic metabolism, where folic acid is removed at a higher rate than other folates (Steinberg et al. 1979).

Folate, predominately in the form of 5mTHF, can proceed into systemic circulation and taken into tissues through two mechanisms: (1) a bidirectional carrier-mediated system (RFC1), which has higher binding affinity for reduced folates compared to folic acid and is ubiquitously expressed in normal human tissues (Whetstine et al. 2002), or (2) a unidirectional receptor-mediated system (FR), which has similar binding affinity for folic acid and reduced folates (Antony 1996). The major FR isoforms in adult humans are FRα and FRβ: FRα is expressed on the apical surface of polarized epithelial cells (Basal et al. 2009), whereas FRβ is primarily found on myeloid hematopoietic cells (Reddy et al. 1999). Once folate enters the cell, folylpolyglutamate synthase (FPGS) converts monoglutamyl folates to polyglutamates forms,

which have longer intracellular retention than monoglutamates (McGuire et al. 1980). The glutamate moiety can be removed by gamma-glutamyl hydrolase (GGH) to regulate the intracellular folate pool (Rhee et al. 1998). Folate is exported from cells via ATP-dependent efflux transporters called multidrug resistance proteins (MRP1-5) (Ifergan and Assaraf 2008).

Cobalamin. Cobalamin (Vitamin B_{12}) is the cofactor for MTR, which catalyzes the regeneration of Met from Hcys (Banerjee and Matthews 1990). The only naturally-occurring sources of Vitamin B_{12} (primarily in the forms of methylcobalamin, deoxyadenosylcobalamin and hydroxycobalamin) are in animal products, including clams, liver, various types of fish, beef, and dairy products; vegetarians and vegans must rely on supplementation or fortified foods, such as breakfast cereals, to meet their required intakes (USDA 2012). In the circulation, cobalamin is bound to one of two carrier proteins, transcobalamin (TC) or haptocorrin (HC). Approximately 20% of total plasma cobalamin is bound to TC, which is normally 10% saturated with cobalamin (Obeid et al. 2006), while the majority of plasma cobalamin is bound to HC, a glycoprotein which is nearly 100% saturated with cobalamin, and whose biologic function is unclear (Seetharam and Li 2000). Only cobalamin complexed to TC, known as holotranscobalamin (holoTC), can be transported into cells through a receptor-mediated endocytosis process mediated by the transcobalamin receptor (TCblR) (Quadros and Sequeira 2013).

c. Key functions of one-carbon metabolism.

Synthesis of nucleotides. Folate is involved in the *de novo* synthesis of purine and pyrimidine bases for DNA synthesis and repair. Thymidine is synthesized through the methylation of deoxyuridine monophosphate (dUMP) by thymidylate synthase (TYMS), using 5,10 methylene-THF as the methyl donor, yielding deoxythymidine monophosphate (dTMP) and DHF (Longley

et al. 2003). The synthesis of purine bases requires 10-formylTHF, which is produced from 5,10 methylene-THF by methylenetetrahydrofolate dehydrogenase 1 (MTHFD1) (Christensen et al. 2013). Due to the essential role of folate in DNA synthesis, folate deficiency impairs cell cycle progression (James et al. 1993) and increases uracil misincorporation (Blount et al. 1997; Duthie et al. 2000), leading to DNA strand breaks (Reidy 1988) and genomic instability (Melnyk et al. 1999). Folate for DNA synthesis is especially important during periods of rapid growth and development, such as the prenatal period (Antony 2007).

Remethylation of Hcys. The methylation of Hcys to Met can occur through the enzymatic transfer of a methyl group from one of two methyl donors: (1) 5mTHF via MTR, the primary route or (2) betaine via betaine-homocysteine *S*-methyltransferase (BHMT), an alternative route active during folate-deficient conditions (Reed et al. 2006). MTHFR catalyzes the rate-limiting step in the synthesis of 5mTHF (irreversible reduction of 5,10 methylene-THF to 5mTHF), and its enzymatic activity is thus a major determinant of Hcys concentrations in humans (Ueland et al. 2001). MTHFR activity is dependent upon riboflavin (vitamin B_2), the precursor to the MTHFR cofactor flavin adenine dinucleotide (FAD) (Bates and Fuller 1986; Hustad et al. 2000; McNulty et al. 2002).

The MTR-catalyzed methylation of Hcys to Met involves a two-step reaction, with cobalamin bound to MTR. First, a methyl group is transferred from 5mTHF to cob(I)alamin, yielding methyl(III)cobalamin and THF; then, the methyl group from methyl(III)cobalamin is transferred to Hcys, yielding cob(I)alamin and Met (Matthews et al. 1998). Occasionally, cob(I)alamin is oxidized to cob(II)alamin, rendering MTR inactive (Drummond et al. 1993). MTR activity can be restored through the regeneration of methyl(III)cobalamin, which occurs

via the reductive methylation of cob(II)alamin by the enzyme methionine synthase reductase (MTRR) and SAM (Wolthers and Scrutton 2007).

Deficiencies in folate and cobalamin result in elevated concentrations of Hcys, a condition known as hyperhomocysteinemia (HHcys) (Klee 2000). Moderate HHcys is a well-established risk factor for cardiovascular disease (Wald et al. 2002), cancer (Wu and Wu 2002), and neurodegeneration (Herrmann and Obeid 2011). Hcys concentrations are sensitive to folate status and can be reduced with folic acid supplementation (Vermeulen et al. 2000). However, under conditions of severe cobalamin deficiency, MTR cannot metabolize 5mTHF for Hcys methylation, resulting in a buildup of 5mTHF in a "methyl trap" (Scott and Weir 1981).

Synthesis of S-adenosylmethionine. SAM, the universal methyl donor for transmethylation reactions, is formed from the ATP-dependent activation of Met by a family of methionine adenosyltransferases (MATs); MAT1 is expressed in liver, while MAT2 is expressed in extrahepatic tissues (Roje 2006). Although numerous enzymes use SAM, including DNA methyltransferases (DNMTs) and arsenic(III)-methyltransferase (AS3MT), two enzymes—guanidinoacetate methyltransferase (GAMT) and phosphatidylethanolamine N-methyltransferase (PEMT)—consume over 70% of SAM-derived methyl groups (Williams and Schalinske 2007). GAMT regulates creatine synthesis from guanidinoacetate, and PEMT catalyzes the transfer of three SAM-derived methyl groups to phosphatidylethanolamine for the synthesis of the phospholipid phosphatidylcholine (PC), an important component of cell membranes (Williams and Schalinske 2007). Upon donation of its methyl group, SAM is converted to SAH, a potent inhibitor of most methylation reactions (Chen et al. 2010). SAH can be reversibly hydrolyzed to Hcys by SAH hydrolase (SAHH) in a reaction that favors SAH synthesis over Hcys synthesis (James et al. 2002). Two long-range interactions—feedback inhibition of MTHFR by SAM and

GNMT by 5mTHF—ensure that intracellular SAM concentrations remain within a tight range (Reed et al. 2006). SAM is also an allosteric activator of cystathionine-β-synthase (CBS), an enzyme catalyzing the conversion of Hcys to Cys in the first step of the transsulfuration pathway (Prudova et al. 2006).

2. The transsulfuration pathway.

a. Overview of biochemistry.

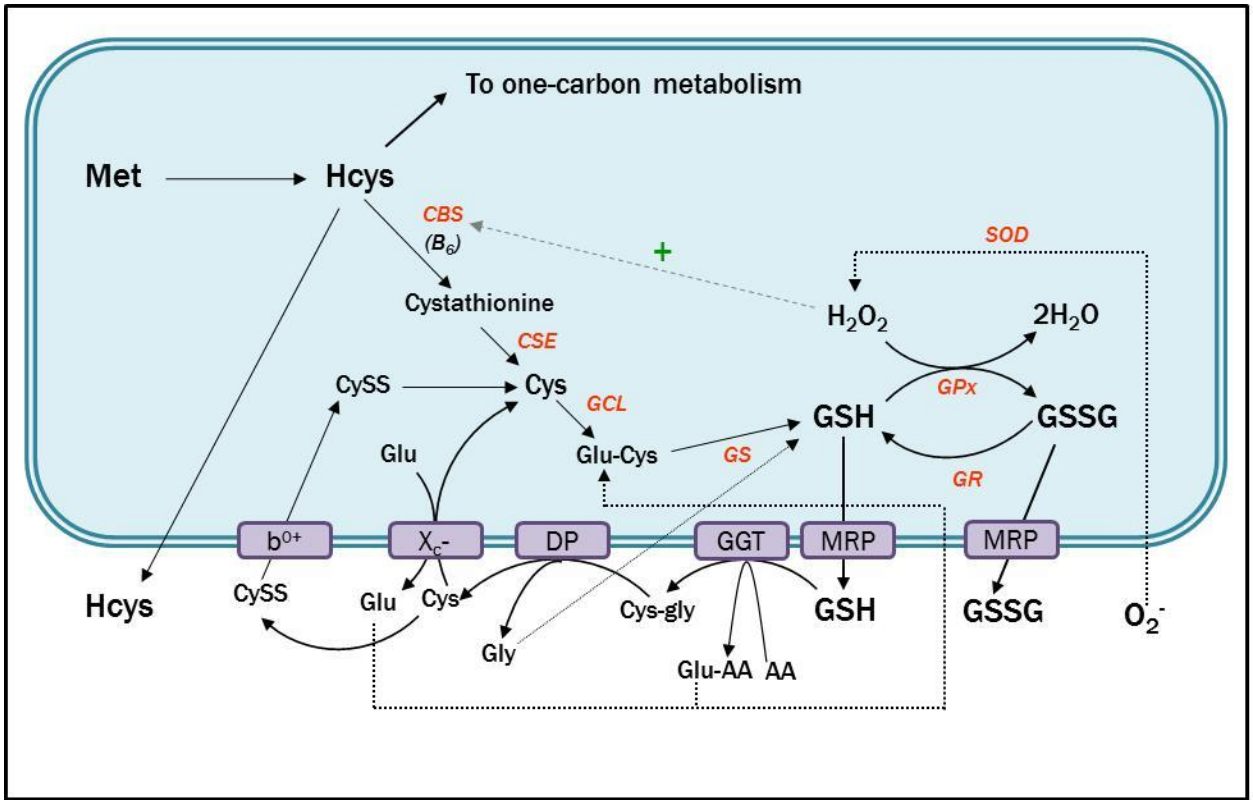

Figure 2. The transsulfuration pathway and glutathione synthesis in mammalian cells.

The transsulfuration pathway involves the conversion of homocysteine (Hcys) to cysteine (Cys), the rate-limiting precursor for the synthesis of the primary endogenous antioxidant

glutathione (GSH) (reviewed in McBean 2012; Wu et al. 2004). As shown in Figure 2, Hcys can be directed through the transsulfuration pathway via the vitamin B_6-dependent enzyme CBS to form cystathionine, which is cleaved to Cys and α-ketobutyrate by cystathionine gamma-lyase (CSE). Glutamate cysteine ligase (GCL) catalyzes the ATP-dependent condensation of Cys and glutamate (Glu) to form γ-glutamylcysteine (Glu-Cys). Glycine (Gly) is then added to Glu-Cys by a condensation reaction catalyzed by glutathione synthase (GS), resulting in the formation of GSH. Intracellular GSH can be used in antioxidant conjugation reactions, or can be exported out of the cell and catabolized via the cell membrane enzyme γ-glutamyltransferase (GGT). GGT transfers the γ-glutamyl group to an amino acid, producing cysteinylglycine (Cys-Gly), which can be broken down to Cys and Gly via dipeptidase. Cys is unstable extracellularly and rapidly oxidizes to cystine (CySS). The xC^- antiporter can import CySS using a transmembrane Glu gradient, and the b^{0+} system can directly import CySS, which can be converted back to Cys to maintain the intracellular Cys pool.

b. Glutathione.

Glutathione synthesis. GSH, a low-molecular weight tripeptide thiol comprised of the amino acids Cys, Glu, and Gly, is the primary mammalian intracellular antioxidant, with concentrations between 0.5–10 mmol/L in cells (Dringen 2000; Wu et al. 2004). Plasma GSH concentrations are markedly lower, with estimated concentrations between 2–20 μmol/L (Wu et al. 2004), and is believed to originate mainly from hepatic GSH synthesis (Griffith 1999). The antioxidant activity of GSH results from the reducing activity of the thiol group of its Cys moiety (Dringen 2000), and GSH depletion is a primary indicator of oxidative stress (Mytilineou et al. 2002).

Although the rate-limiting precursor in GSH synthesis—the semi-essential amino acid Cys—can be obtained from dietary sources, most of the Cys used for GSH production is derived from endogenous synthesis from Met via the transsulfuration pathway (Wu et al. 2004). However, a functional transsulfuration pathway is not found in all tissues: intact pathways are found in liver, kidney, small intestine and pancreas tissues (Finkelstein 1990) and were recently identified in brain (Vitvitsky et al. 2006) and T cells (Garg et al. 2011). Under conditions of oxidative stress, Hcys flux through the transsulfuration pathway is enhanced 2-3 fold times its normal rate to increase Cys availability for GSH synthesis (Mosharov et al. 2000); this occurs through the upregulation of CBS, which contains a redox-sensitive heme domain (Taoka et al. 1998; Taoka et al. 2002). In tissues lacking active transsulfuration pathways, CySS is imported into cells through membrane transport mechanisms and converted to Cys, as described in (a). In addition to its role as an antioxidant, GSH also serves as a reservoir and transport mechanism for Cys (Meister et al. 1986), which can be cytotoxic at high concentrations (Stipanuk et al. 2006).

B. Biologic processes associated with one-carbon metabolism and transsulfuration.

1. DNA methylation.

The term "epigenetics" refers to the study of modifications that influence gene expression without altering the underlying DNA sequence. The most widely studied epigenetic modification is DNA methylation, a process involving the covalent addition of a methyl group to the 5'-position of cytosines to form 5-methylcytosine (5mC) (Smith and Meissner 2013). 5mC is generally found in the context of CpG dinucleotides, but non-CpG 5mC has been detected in low quantities in mammalian genomes (Ramsahoye et al. 2000; Ziller et al. 2011). In mammals, methylation reactions are catalyzed by three conserved enzymes known as DNA methyltransferases (DNMT1, DNMT3A, and DNMT3B), and the methyl groups are donated from SAM, a product of one-carbon metabolism (Figure 3) (Smith and Meissner 2013). Proper maintenance of genomic 5mC distribution is essential for normal mammalian development (Razin and Shemer 1995).

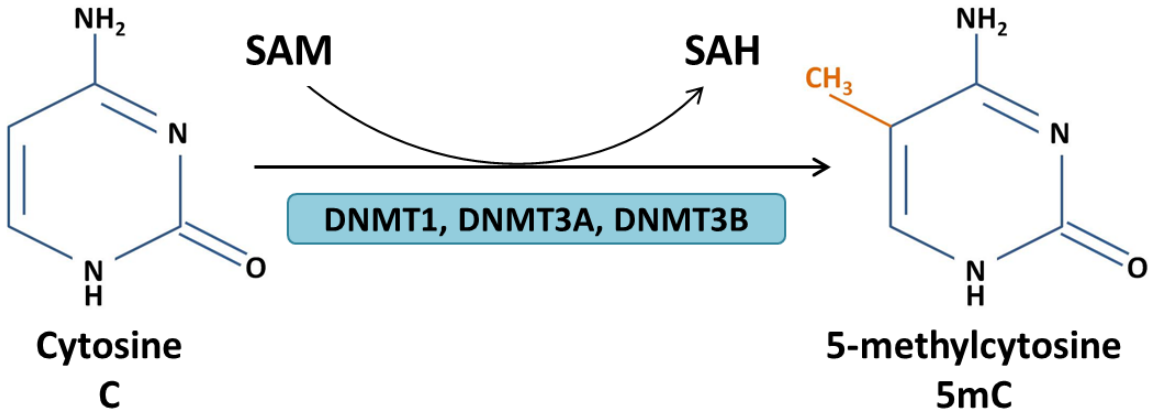

Figure 3. Methylation of cytosines by DNMTs and SAM.

a. CpG methyltransferases.

Dnmt1. Riggs (1975) and Holliday and Pugh (1975) first proposed that DNA methylation is a heritable mechanism of gene regulation, but it was not until 1988 that Bestor and colleagues (Bestor 1988) cloned the first mammalian DNA methyltransferase enzyme, Dnmt1. The Dnmt1 enzyme preferentially methylates hemimethylated CpGs and is essential for the maintenance of DNA methylation patterns during DNA replication throughout S-phase (Leonhardt et al. 1992). The Dnmt1 protein is composed of two domains, the N-terminal regulatory domain and the C-terminal catalytic domain, which are connected through a glycine-lysine $(GlyLys)_6$ repeat (Margot et al. 2003) (Figure 4). The N-terminus contains sequences that regulate interactions of DNMT1 with other proteins, including a zinc finger Cys-X-X-Cys (CXXC) domain that recognizes unmethylated CpG sites (Lee et al. 2001), while the C-terminus contains conserved amino acid methyltransferases motifs (e.g., I, IV and X), the catalytic center, and coenzyme binding site (Margot et al. 2003). Dnmt1 is recruited by ubiquitin-like, containing PHD and RING finger domains, 1 (UHRF1), a protein that specifically binds hemimethylated CpGs (Arita et al. 2008).

Dnmt3s. In 1996, Lei et al. (1996) discovered that *de novo* CpG methylation occurred in *Dnmt1*-null mouse embryonic stem (ES) cells, suggesting the presence of other independently-encoded Dnmt enzymes. Two years later, colleagues from the same group cloned the *de novo* methyltransferases Dnmt3a and Dnmt3b and found that these enzymes catalyzed the methylation of unmethylated- and hemimethylated-CpG sites at equal rates (Okano et al. 1998). The Dnmt3 family contains the same conserved amino acid motifs at their C-termini as in Dnmt1, but the N-termini of Dnmt1 and Dnmt3s do not share sequence similarity (Chen and Li 2004; Okano et al. 1998) (Figure 4). Their N-termini contain a Cys-rich domain and a PWWP domain; the latter

binds DNA in Dnmt3b (Qiu et al. 2002), but not in Dmnt3a (Chen et al. 2004), and is involved in directing the Dnmt3s to pericentric heterochromatin (Chen et al. 2004).

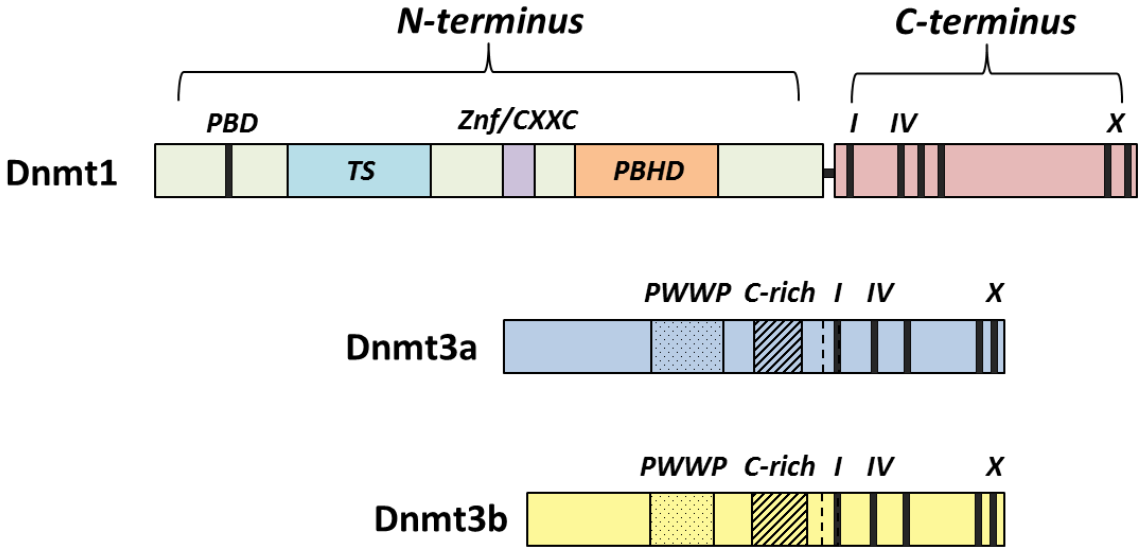

Figure 4. Organization of Dnmt1 and Dnmt3 family. (adapted from Margot et al. 2003)

b. Chromatin structure and gene expression.

*Histones and the nucleosome***.** In eukaryotes, DNA is packed around eight histone core proteins (H2A, H2B, H3 and H4; two H2A-H2B dimers and one H3-H4 tetramer) in structural units called nucleosomes (Bartova et al. 2008). DNA segments of 20-60 base pairs, known as "linker DNA," connect the nucleosomes, and histone H1 "sits" on top of the DNA-core histone complex to stabilize the nucleosome and bind the linker DNA (Bartova et al. 2008) (Figure 5). The core histones contain amino acid "tails" at their N-terminal domains that are subject to post-translational epigenetic modifications such as acetylation (Ac), methylation (Me), and phosphorylation (Bannister and Kouzarides 2011).

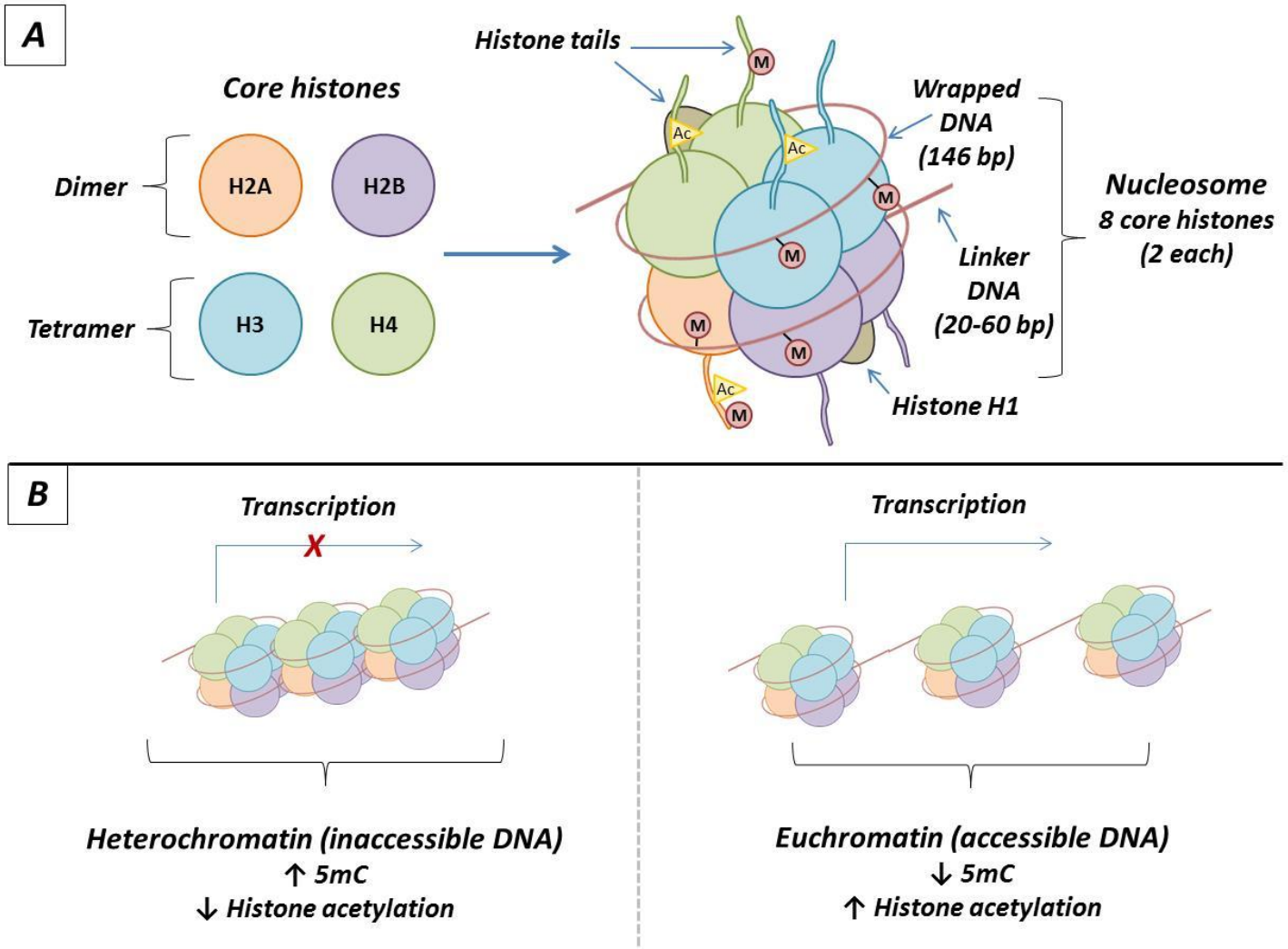

Figure 5. Chromatin structure, DNA methylation, and histone tail modifications. (A) Nucleosome structure. (B) Chromatin structure. Heterochromatin is associated with transcriptional silencing and is characterized by increased 5mC and decreased histone acetylation, while euchromatin is associated with transcriptional activation and is characterized by decreased 5mC and increased histone acetylation.

*DNA methylation, chromatin structure, and gene expression***.** Chromatin exists in two broad structural states that are associated with gene transcription: "euchromatin" refers to a relaxed, open structure that is associated with gene expression, while "heterochromatin" refers to a densely-packed structure linked to gene repression (Dillon 2004). Heterochromatin can further be classified into *constitutive* and *facultative* heterochromatin, depending upon the reversibility of the state (Dillon 2004). Constitutive heterochromatin is stable and associated with repetitive sequences, including telomeres and the transposable element sequences long interspersed element-1 (LINE-1) and Alu. Conversely, facultative heterochromatin is reversible and generally localized to gene promoter regions, and the heterochromatic state is maintained by transcriptional repressors and epigenetic modifications associated with repression.

DNA methylation is associated with gene repression through complex interactions with repressive proteins and histone modifications (Cedar and Bergman 2009). CpG methylation is believed to block transcriptional machinery from accessing DNA (Curradi et al. 2002) and/or recruit methyl binding proteins (MBPs) that initiate chromatin remodeling (Klose and Bird 2006). Across the human genome, approximately 70% of all CpGs are methylated (Bird 1986), and the frequency of CpG dinucleotides is 25% lower than the expected frequency based upon GC content (Bird 1980). CpG sites are more frequently found in exons, intronic regions, and gene promoters, with a particularly high enrichment of CpG sites around transcription start sites (TSS) (Saxonov et al. 2006). These CpGs clusters, known as "CpG islands," are around 1,000 bp long and are less methylated than CpG sites in other regions (~3% in gene promoters) (Deaton and Bird 2011). Although increased promoter CpG methylation is associated with gene repression, several *in vitro* studies have found that CpG methylation increases only after the initiation of gene silencing and the recruitment of other epigenetic silencing marks (including

H3K27me3), suggesting that enhanced CpG methylation may be a consequence, and not an initiator, of gene silencing (Deaton and Bird 2011). CpGs outside of CpG islands tend to have high levels of methylation, which is associated with the silencing of constitutive heterochromatin and genome stabilization (Ma et al. 2005).

c. The "sixth base," 5-hydroxymethylcytosine.

A new level of epigenetic complexity was unveiled by the recent discovery of 5-hydroxymethylcytosine (5hmC), dubbed the "sixth base" in the genome (Rusk 2012). Tahiliani et al. (2009) first discovered that the ten-eleven translocation-1 (TET1) protein catalyzes the conversion of 5mC to 5-hydroxymethylcytosine (5hmC). Follow-up studies by Ito et al. (2010) in mouse ES cells established that all three Tet family proteins (Tet1, Tet2 and Tet3) catalyze the same reaction. TET enzymes depend upon the presence of iron (Fe^{2+}) and alpha-ketoglutarate (α-ketoglutarate) as cofactors (Tahiliani et al. 2009); α-ketoglutarate is a product of the oxidative decarboxylation of isocitrate by isocitrate dehydrogenase (IDH) enzymes (Reitman and Yan 2010) (Figure 6) and is an intermediate in the Krebs cycle (Tretter and Adam-Vizi 2005).

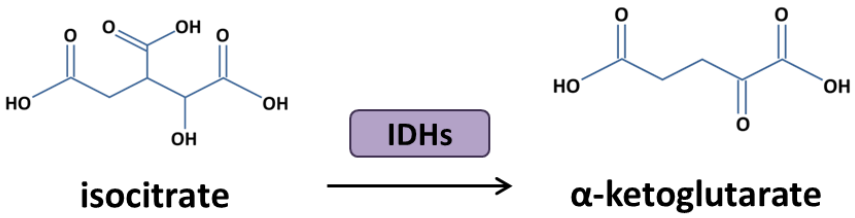

Figure 6. Oxidative decarboxylation of isocitrate to alpha-ketoglutarate by isocitrate dehydrogenases.

Initial speculation following the discovery by Tahiliani et al. (2009) was that 5hmC is an intermediate in a DNA demethylation pathway (Ito et al. 2010). The proposed mechanisms involve active and passive processes (Figure 7). Since DMNT1 poorly recognizes 5hmC (Valinluck and Sowers 2007), the accumulation of 5hmC results in passive loss of 5mC through successive rounds of DNA replication. Additionally, DNA repair pathways involving thymine DNA glycosylase (TDG) and base excision repair (BER) have been shown to actively remove 5hmC (Guo et al. 2011) (Figure 7). 5hmC might also have independent regulatory roles in gene expression (C-X Song et al. 2011), embryogenesis (Wossidlo et al. 2011), and neurodevelopment (Kriaucionis and Heintz 2009; Szulwach et al. 2011).

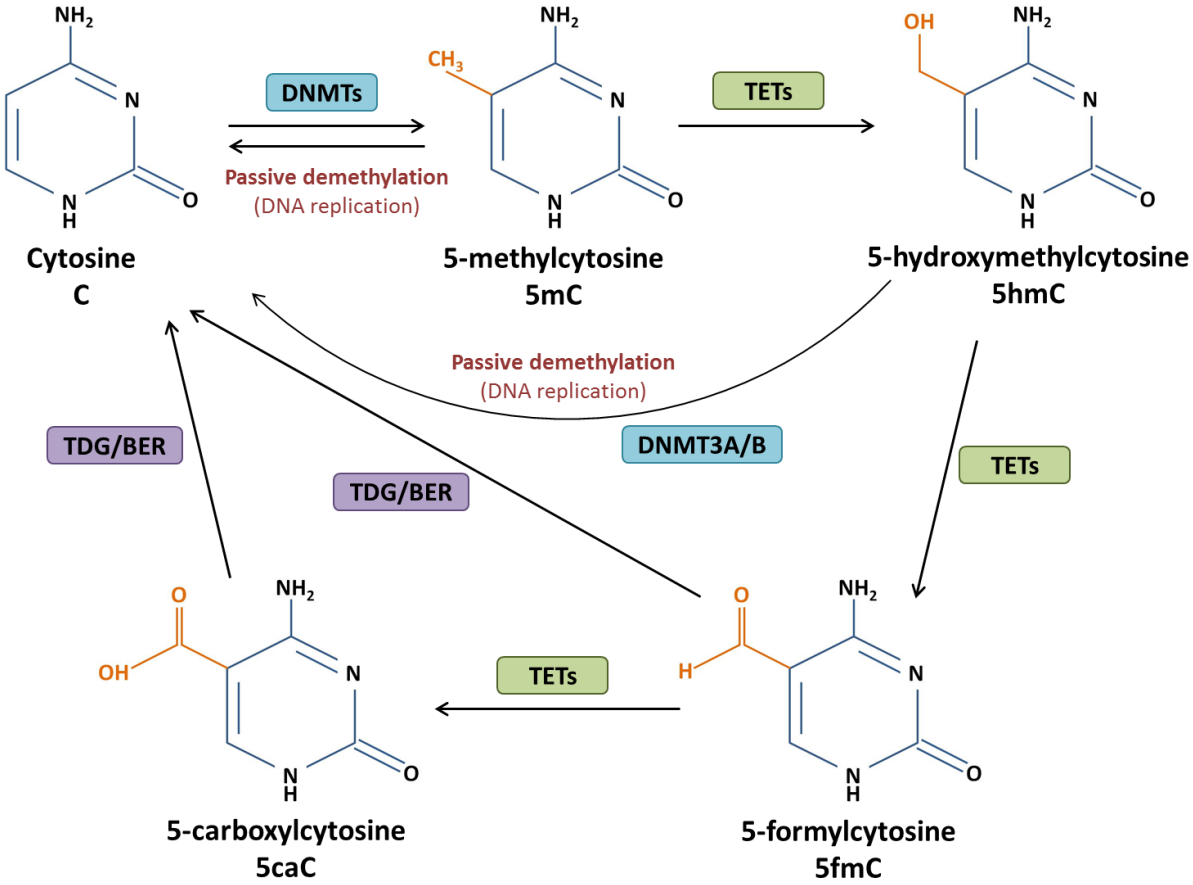

Figure 7. Mechanisms of DNA demethylation through 5-hydroxymethylcytosine. DNMTs catalyze the conversion of cytosine (C) to 5-methylcytosine (5mC) and are responsible for the establishment and maintenance of genomic 5mC patterns. TETs catalyze the stepwise oxidation of 5mC to 5-hydroxymethylcytosine (5hmC), 5-formylcytosine (5fC), and 5-carboxylcytosine (5caC), which results in DNA demethylation through active and passive mechanisms. Through active pathways, the oxidation products 5fC and 5caC are removed by thymine DNA glycosylases (TDGs), generating abasic sites that are converted back to C through base excision repair (BER). 5hmC can also be actively converted to C by DNMT3s, which exhibit dehydroxymethylase activities in oxidized environments. Additionally, since the maintenance DNA methyltransferase DNMT1 does not readily recognize 5hmC, passive conversion of 5hmC to C occurs over successive rounds of DNA replication.

2. Oxidative stress, redox regulation, and glutathione.

a. Oxidative stress and redox environment.

Oxidative stress and ROS. "Oxidative stress" refers to an imbalance in the production of reactive oxygen species (ROS) and a biological system's ability to detoxify the reactive intermediates (Jones 2008). Aptly-named, ROS are oxygen-containing molecules that are highly damaging to sensitive targets. Certain types of ROS, known as "free radicals," contain unpaired electrons in their chemical structures and are thus extremely reactive; examples include superoxide anion ($O_2^{-\cdot}$), peroxide ($O_2^{-2\cdot}$), and hydroxyl radical (•OH) (Halliwell 1989). Free radicals can induce macromolecular oxidative damage, such as protein oxidation (e.g., carbonyls), lipid peroxidation (e.g., malondealdyhyde), and oxidative DNA damage (e.g., 8-oxo-2'-deoxyguanosine) (Parman et al. 1999). Nonradical oxidants (e.g., hydrogen peroxide, or H_2O_2) are less reactive than free radicals, but they have strong oxidizing capabilities and are prone to decomposing to free radical species (Campos-Martin et al. 2006).

Redox couples and redox state. Antioxidants are compounds that inhibit or remove ROS (Jones 2008). Many antioxidants are *reducing agents*, which are compounds that donate electrons to ROS and as a result, become oxidized themselves. A pair of reduced and oxidized species is known as a *redox couple* (Schafer and Buettner 2001). The term *redox state* refers to the ratio of reduced and oxidized species, as well as the concentrations of the reduced and oxidized species, within a particular redox couple; thus, the redox state reflects a redox couple's reducing capacity (Schafer and Buettner 2001). The reduction potential of a redox couple can be calculated using the Nernst equation, $E_h(mV) = E_0(-RT/nF) * \ln([\text{reductant}]/[\text{oxidant}])$, where E_0 = standard reduction state at pH 7.0, R = gas constant, T = temperature in Kelvin, n = number of transferred

electrons, and F = Faraday's constant. There are several interconnected redox systems of biological importance:

(1) *Glutathione system (GSSG/2GSH).* The predominant redox couple within cells is GSH and glutathione disulfide (GSSG), with estimated cytosolic GSH concentrations between 1–11 mM (Lu 2009). Cellular GSH and GSSG concentrations can be used in the Nernst equation as an indicator of the intracellular redox environment: for the GSH/GSSG redox couple, the equation simplifies to $E_h(mV) = -264 - 30 \log([GSH]^2/[GSSG])$ (Jones et al. 2000). Since two free radical GSH molecules react to form GSSG, the redox state is dependent both on the concentrations and ratio of the GSH/GSSG couple, reflected in the Nernst equation by the squared GSH term.

(2) *Thioredoxin system ($TrxSS/Trx(SH)_2$).* Thioredoxins (Trx) are small redox proteins that are found at intracellular concentrations 100- to 1000-fold lower than GSH, with estimated concentrations between 1 to 10 μM (Mari et al. 2009). The $TrxSS/Trx(SH)_2$ system is important for the reduction of CySS in intramolecular disulfide bonds and regulates transcription factor binding (e.g., NF-kappaB [NF-kB]) and cellular signaling (Schenk et al. 1994)

(3) *Nicotinamide adenine dinucleotide phosphate system ($NADP^+/NADPH$).* The cofactor nicotinamide adenine dinucleotide phosphate (NADPH) provides a pool of reducing equivalents for reduction reactions, notably for the regeneration of reducing agents in the GSH and Trx redox systems (Watson et al. 2003). Each molecule of NADPH donates two electrons upon its conversion to its oxidized form, $NADP^+$. NADPH is primarily synthesized in the liver via the pentose phosphate pathway, but it can also be generated in mitochondria by isocitrate dehydrogenase (IDH) and NADH kinase (Dang 2012).

Redox disruption vs. oxidative damage. The *redox environment* of a cell or tissue refers to the reducing capacity of the systems of redox couples within the specified milieu (Schafer and Buettner 2001). Although macromolecular damage caused by oxidative stress has long been implicated as the causative factor in aging and disease, Dean Jones proposed that the pathological impact of oxidative stress might instead result from disruption of the redox environment (Jones 2008). Based upon antioxidant enzyme kinetics, he proposed a scenario of "oxidative stress" (Figure 8) where the initial rates of free radicals versus nonradical oxidant generation is 10% and 90%, respectively, with a rate of radical scavenging of >99%, resulting in a total rate of production of nonradical oxidants of > 99.9% and macromolecular oxidative damage of < 0.1% (Jones 2008). Thus, the greater impact of oxidative stress would be seen through the disruption of redox control, and macromolecular damage would correlate with redox disruption but would not likely be the causative factor in oxidative stress-related pathology.

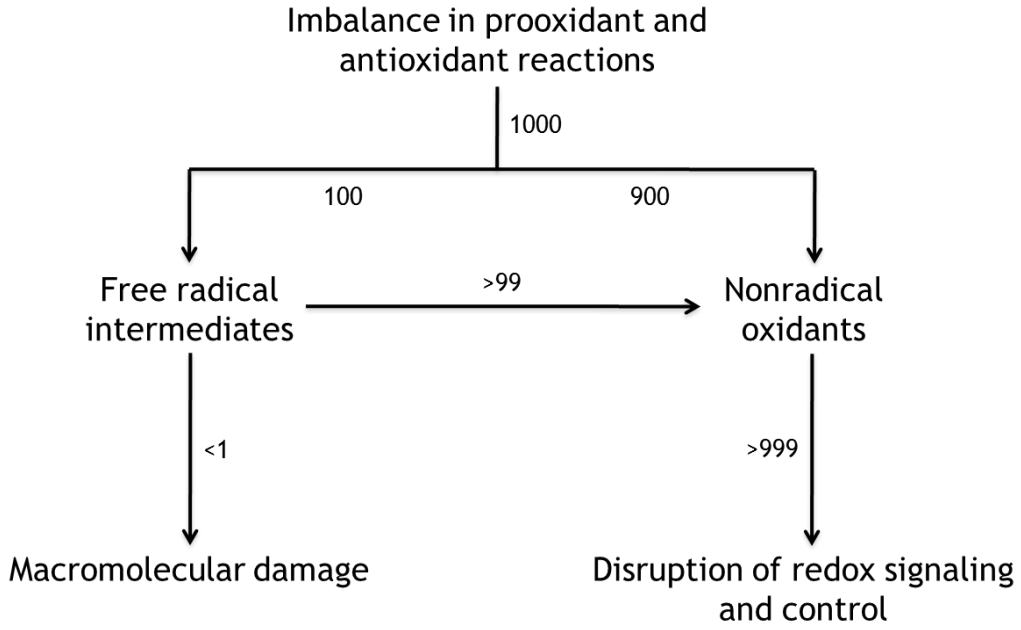

Figure 8. Relative impacts of macromolecular damage versus redox disruption during conditions of oxidative stress. (adapted from Jones et al. 2008)

b. Antioxidant enzymes and systems.

Glutathione enzymes. GSH readily donates a reducing equivalent from the thiol group of its Cys moiety via the glutathione peroxidase (GPx) enzyme family, and the free radical GSH molecule quickly reacts with another free radical GSH to form GSSG; e.g., the conversion of H_2O_2 to two molecules of H_2O is characterized by the reaction $2GSH + H_2O_2 \rightarrow GSSG + 2H_2O$ (Figure 9). There are eight isoforms of GPx in humans (GPx1 through 8). Five of the eight GPx isforms (Gpx1-4, Gpx6) are selenoproteins and are dependent upon selenium (Se) for their enzymatic activities (Moghadaszadeh and Beggs 2006). GSH can be regenerated from GSSG via glutathione reductase (GR), which requires NADPH and FAD as cofactors (Berkholz et al. 2008).

Superoxide dismutases. Superoxide dismutases (SODs) are metalloprotein enzymes that catalyze the dismutation of $O_2^{-\cdot}$ to H_2O_2 and O_2 ($2\ O_2^{-\cdot} + 2\ H^+ \rightarrow O_2 + H_2O_2$) (Figure 9). There are three types of human SODs: SOD1 and SOD3 bind copper (Cu) and zinc (Zn) ions (Cu/Zn) and are found in the cytoplasm and extracellular space, respectively, while SOD2 binds manganese (Mn) ions and is found in mitochondria (Noor et al. 2002).

Catalases. Catalase (CAT) is a heme-containing enzyme that converts two molecules of H_2O_2 into O_2 and two molecules of H_2O ($2\ H_2O_2 \rightarrow 2\ H_2O + O_2$) (Figure 9). Catalases are contained within peroxisomes (Sies 1974) and are expressed in every organ, with the highest expression in liver (Schisler and Singh 1987; Tiedge et al. 1997).

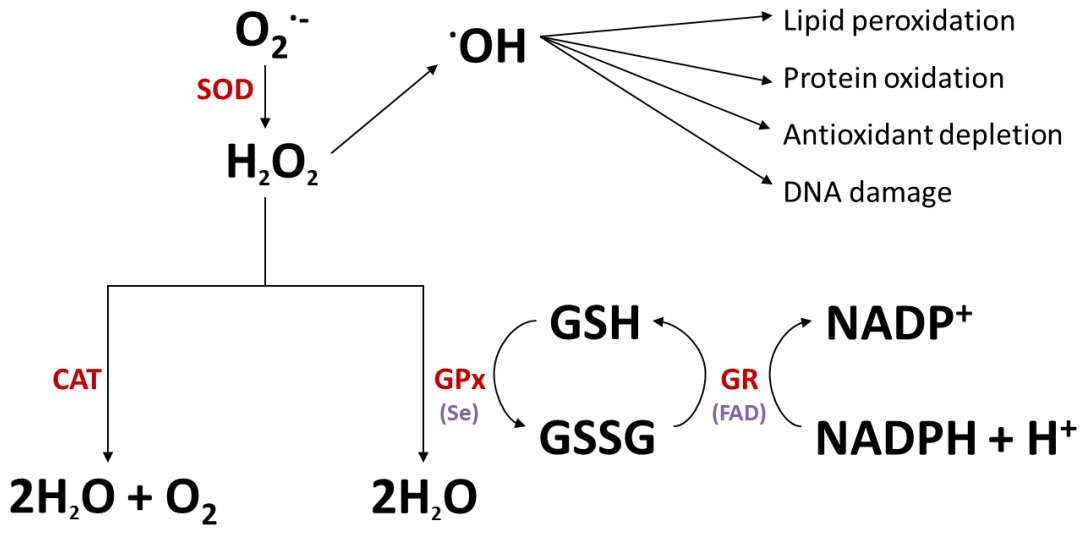

Figure 9. Detoxification of superoxide by antioxidant enzymes.

Nrf2-mediated defense system. Oxidative stress stimulates the nuclear factor (erythroid-derived 2)-like 2 (Nrf2) antioxidant response pathway, the primary cellular defense against ROS (Nguyen et al. 2009). Nrf2 is a leucine zipper transcription factor that is normally kept in the cytoplasm by a protein complex of Kelch like-ECH-associated protein 1 (Keap1) and Cullin-3, which quickly degrades Nrf2 by ubiquitination (Zhang et al. 2004). Under conditions of oxidative stress, the formation of Keap1 intermolecular disulfide bonds (via Cys^{151}) prevents the Keap1/Cullin-3 complex from degrading Nrf2, which allows Nrf2 to accumulate and enter the nucleus (Fourquet et al. 2010; Zhang and Hannink 2003). Nrf2 heterodimerizes with small Maf proteins and binds antioxidant response elements (AREs), *cis*-acting enhancer sequences in promoter regions that regulate gene transcription (Itoh et al. 1997). AREs are located in promoters of numerous antioxidant and Phase II detoxification genes, including CAT and SOD1 (Itoh et al. 1997).

Nrf2 and GSH. Nrf2 regulates the transcription of several GSH-associated genes (Chan and Kwong 2000). The rate-limiting step in GSH production is the conjugation of Glu and Cys by GCL, a heterodimeric enzyme composed of a catalytic subunit (glutamate cysteine ligase catalytic subunit, or GCLC) and a modifier subunit that improves catalytic efficiency by lowering the K_m for Glu (glutamate cysteine ligase modifier subunit, or GCLM); both subunits contain AREs in their promoter regions (Erickson et al. 2002), and the Nrf2 pathway upregulates GSH biosynthesis by inducing GCL expression (Wild et al. 1999). Nrf2 also increases GR expression for the reduction of GSSG back to GSH (Harvey et al. 2009).

c. Sources of reactive oxygen species.

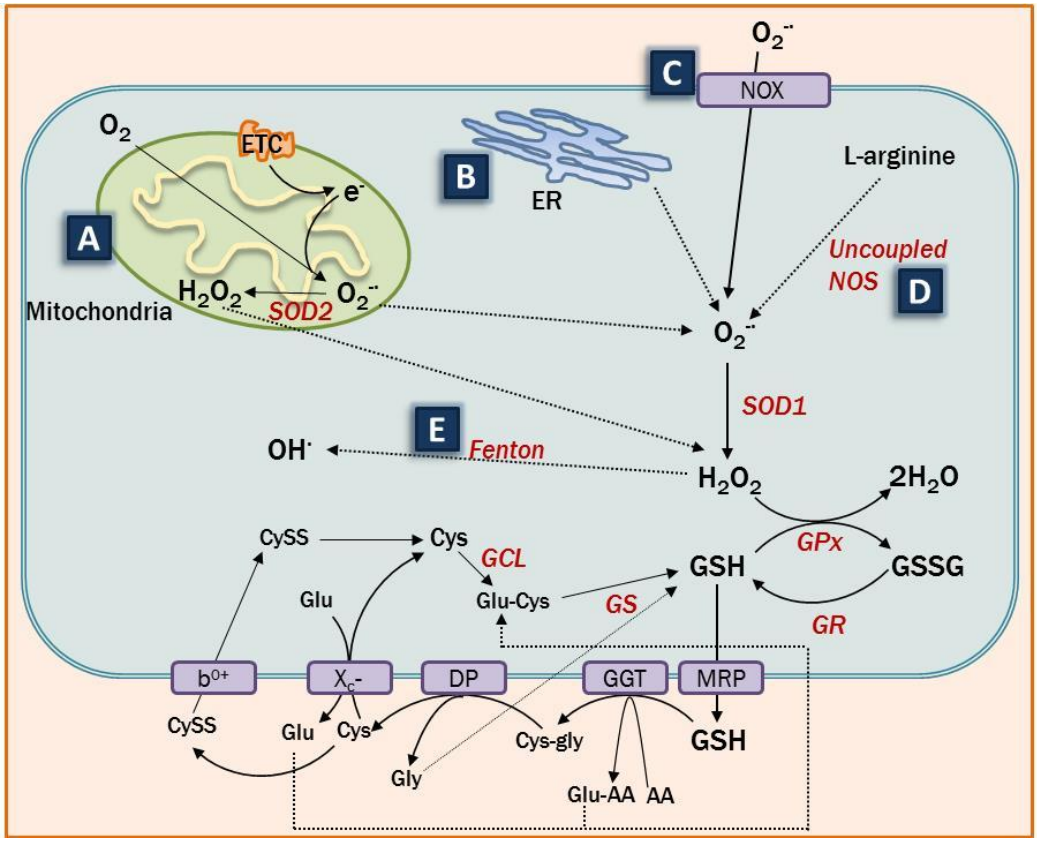

Figure 10. Sources of endogenous ROS. Major sources of ROS include (A) mitochondrial oxidative phosphorylation, (B) endoplasmic reticulum stress, (C) NADPH oxidase enzyme activity, (D) nitric oxide synthase uncoupling, and (E) the Fenton reaction.

Endogenous ROS are normal byproducts of various cellular processes, illustrated in Figure 10. *A. Oxidative phosphorylation in mitochondria.* Mitochondrial ATP production (oxidative phosphorylation) involves a series of redox reactions at the mitochondrial inner membrane that release free energy for the pumping of protons (H+) into the intermembrane space, creating an electrochemical gradient for the synthesis of ATP (Brookes et al. 2004). Electrons are donated from reduced nicotinamide adenine dinucleotide (NADH) and succinate, products of the Krebs cycle, and electron transport occurs at four protein membrane complexes, Complexes I through IV. Occasionally, electrons leak from the chain and react with O_2, resulting in the formation of $O_2^{-\cdot}$ (Murphy 2009). The "vicious cycle" theory of aging postulates that the accumulation of ROS-induced mutations in mitochondrial DNA (mtDNA) leads to increased leakage of electrons from the transport chain, thereby increasing ROS production and additional mtDNA mutations in a "vicious cycle" of ever-increasing oxidative stress (Cui et al. 2012).

Complex I (NADH dehydrogenase). NADH is oxidized to NAD+ through the reduction of riboflavin-5′-phosphate (FMN) to $FMNH_2$. Two electrons are transferred from $FMNH_2$ to ubiquinone (Q) in a two-step process involving the formation of two semiquinone (free radical) intermediates. Complex I is the primary source of mitochondrial $O_2^{-\cdot}$ production in aging and neurological conditions.

Complex II (succinate dehydrogenase). Succinate is oxidized to fumarate through the reduction of Q to ubiquinol (QH_2).

Complex III (Cytochrome bc1 complex). Two electrons are transferred from QH_2 to two molecules of cytochrome c. Complex III is the primary source of $O_2^{-\cdot}$ production in heart and lung mitochondria.

Complex IV (Cytochrome c Oxidase). Four electrons are transferred from cytochrome c to molecular oxygen (O_2) to produce two molecules of H_2O.

B. Endoplasmic reticulum stress. The redox environment within the endoplasmic reticulum (ER) is oxidized relative to other cellular compartments due to its involvement in protein folding, which requires an oxidized environment for disulfide bond formation (Csala et al. 2010). ROS can be produced as a byproduct of protein oxidation and folding (Malhotra and Kaufman 2007) and through alterations of intra-ER Ca^{2+} homeostasis (Bhandary et al. 2012).

C. NOX enzymes. The NADPH oxidase (NOX) family is comprised of seven membrane-bound enzymes (NOX1-5, DUOX1, and DUOX2) (Ajayi et al. 2013) that produce $O_2^{-\cdot}$ from O_2 and NADPH in the reaction NADPH + 2 O_2 → $NADP^+$ + 2 H^+ + 2 $O_2^{-\cdot}$ (Ago et al. 1999). NOX enzymes catalyze the transfer of electrons across membranes for multiple functions, including first-line host defense against microbes in phagocytes and cell signaling regulation in various tissues (Suh et al. 1999). The NOX–mediated generation of ROS is vital for redox signaling pathway regulation under normal conditions and during the cellular response to oxidants and exogenous stressors (Jiang et al. 2011). For example, NOX-mediated ROS production plays an important role in the inhibition of enzymes in the protein tyrosine phosphatase (PTP) superfamily, which contain a conserved redox-sensitive Cys residue in their catalytic domains (Jiang et al. 2011). PTPs, along with protein tyrosine kinases (PTKs), are essential for the regulation of tyrosine phosphorylation, a mechanism of signal transduction pathway activation (Alho et al. 2013; Alonso et al. 2004). However, the overexpression of NOX leads to excessive generation of $O_2^{-\cdot}$ (Hamilton et al. 2001), and NOX dysregulation is implicated in carcinogenesis, aging, and neurodegeneration (Nauseef 2008).

D. Nitric oxide synthase uncoupling. Nitric oxide synthase (NOS) enzymes catalyze the five-electron oxidation of L-arginine to nitric oxide (NO), a free radical signaling molecule that is a potent vasodilator and is involved in the cardiovascular system, immunity, and neurologic function (Jiang et al. 2013). NOS enzymes require five cofactors—FAD, FMN, heme, tetrahydrobiopterin (BH_4), and Ca^{2+}/calmodulin-—and the electron flow occurs as follows: NADPH → FAD → FMN → heme → O_2, characterized by the reaction L-arginine + 3/2 NADPH + H^+ + 2 O_2 → citrulline + nitric oxide + 3/2 $NADP^+$. There are three human isoforms of NOS (Forstermann and Kleinert 1995):

(1) Neuronal NOS (nNOS), encoded by NOS, constitutively expressed in brain;

(2) Inducible NOS (iNOS) is encoded by NOS2, expressed in liver, induced by lipopolysaccharides and cytokines, and involved in immunity; and

(3) Endothelial NOS (eNOS) is encoded by NOS3, constitutively expressed in the endothelium, and involved in vasodilation and maintaining vascular tone.

If BH_4 is depleted, the NOS enzyme becomes "uncoupled," and electron flow is diverted away from NO production and toward $O_2^{-\bullet}$ generation (Verhaar et al. 2004). $O_2^{-\bullet}$ can react with NO to form peroxynitrite ($ONOO^-$), a powerful oxidant that can oxidize BH_4 to 7,8-dihydro-biopterin (BH_2), leading to further BH_4 depletion and NOS uncoupling (Kuzkaya et al. 2003).

E. Fenton reaction. Iron (Fe) and other transition metals react with H_2O_2 to produce •OH in a reaction known as the Fenton reaction, Fe^{2+} + H_2O_2 → Fe^{3+} + •OH + $^-$OH (Jozefczak et al. 2012). The production of •OH through the Fenton reaction is a key mechanism in the toxicity of transition metals (Stohs and Bagchi 1995).

Exogenous ROS are derived from many types of environmental exposures, including xenobiotics, pollution, and radiation (Waris and Ahsan 2006). This section will briefly discuss the roles of GSH and ROS in xenobiotic metabolism, a hepatic detoxification pathway with three phases, (A) Phase I oxidation, (B) Phase II conjugation, and (C) Phase III transport (reviewed in Omiecinski et al. 2011; Xu et al. 2005).

A. Phase I oxidation. Phase I metabolism is catalyzed primarily by the cytochrome (CYP) P450 superfamily of heme enzymes, which involves xenobiotic monooxidation in a reaction requiring two electrons from NADPH: $S + O_2 + 2e^- + 2H^+ \rightarrow SO + H_2O$ (Meunier et al. 2004). Certain P450 families (2, 4, 7, 11, 17, 19, 21, 24, 27, 46, and 51) are involved in metabolism of endogenous steroid hormones, cholesterol, vitamin D, and eicosanoids, in addition to the metabolism of exogenous compounds (Pikuleva and Waterman 2013). Although there are 57 total human P450 enzymes, over 95% of all drug metabolism reactions involve only five P450s enzymes, CYP3A4, 2C9, 2C19, 2D6, and 1A2 (Guengerich 2008). The production of O_2^{-*} and H_2O_2 can occur through the uncoupling of NADPH oxidation with substrate oxygenation (Cederbaum et al. 2001; Gillette et al. 1957; Imaoka et al. 2004; Nordblom and Coon 1977).

B. Phase II conjugation. Phase II metabolism involves the conjugation of activated xenobiotics to increase their solubility and reduce their reactivity (unlike Phase I metabolism, which often involves bioactivation) (Omiecinski et al. 2011). One of the major Phase II enzyme families is the glutathione *S*-transferase (GST) superfamily, which is comprised of eight cytosolic families (alpha, mu, pi, sigma, theta, tau, omicron, and kappa GSTs) that catalyze the conjugation of GSH to xenobiotic substrates (Katoh et al. 2008). Phase II xenobiotic detoxification can result in depletion of the hepatic GSH pool (Hayes and Pulford 1995). GSTs are also involved in the detoxification of ROS (Hayes and Pulford 1995) and are important components of the cellular

oxidative stress defense system (Board and Menon 2013). Activities of GSTs, like most Phase II enzymes, are upregulated by the Nrf2 pathway during oxidative stress (Xu et al. 2005).

C. Phase III transport. In Phase III transport, GSH-xenobiotic conjugates are excreted through MRP-mediated cellular efflux (Zaman et al. 1995). ATP-dependent MRPs mediate biliary excretion of most Phase II conjugates (Kullak-Ublick et al. 2002) and are also involved in cellular efflux of GSSG (Mueller et al. 2005) and folates (Ifergan and Assaraf 2008).

d. Redox signaling.

In addition to GSH's roles in ROS scavenging and xenobiotic detoxification, the intracellular GSH/GSSG redox state influences redox signaling pathways involved in various physiologic processes, including gene expression and cell cycle progression (Zhang and Forman 2012). The subcellular compartmentalization of redox states, which do not exist in equilibrium with one another, allows for organelle-specific control of redox signaling (Jones and Go 2010).

Redox-sensitive enzymes. Redox-sensitive enzymes contain Cys residues that are susceptible to oxidative post-translational modifications, which influence their catalytic activities in response to changes in the redox environment (Klomsiri et al. 2011). The redox reactivity of a Cys residue is largely dependent upon its susceptibility to deprotonation at a physiologic pH (pH 7.0-7.4); thus, low pKa thiols are generally considered to be "redox-sensitive" Cys residues (Paulsen and Carroll 2013). The sulfhydryl group (-SH) group of redox-sensitive Cys residues can undergo a number of reversible oxidative modifications, including disulfide bond formation and *S*-glutathionylation (Guttmann and Powell 2012).

Disulfide bonds. Under conditions of oxidative stress, the reversible formation of intramolecular disulfide bonds between redox-sensitive Cys residues (Figure 11) induces

structural changes that act as "switches" to activate or inhibit the enzyme in response to the redox environment (Cumming et al. 2004). The functions of the disulfide bridges are directly related to the distance between the Cys residues and their placement within the protein (Wu et al. 2012). GSH can serve as a reducing agent for disulfide bond cleavage (Chakravarthi and Bulleid 2004), and intracellular GSH/GSSG status is an indicator of the frequency of disulfide bond formation (Hansen et al. 2009).

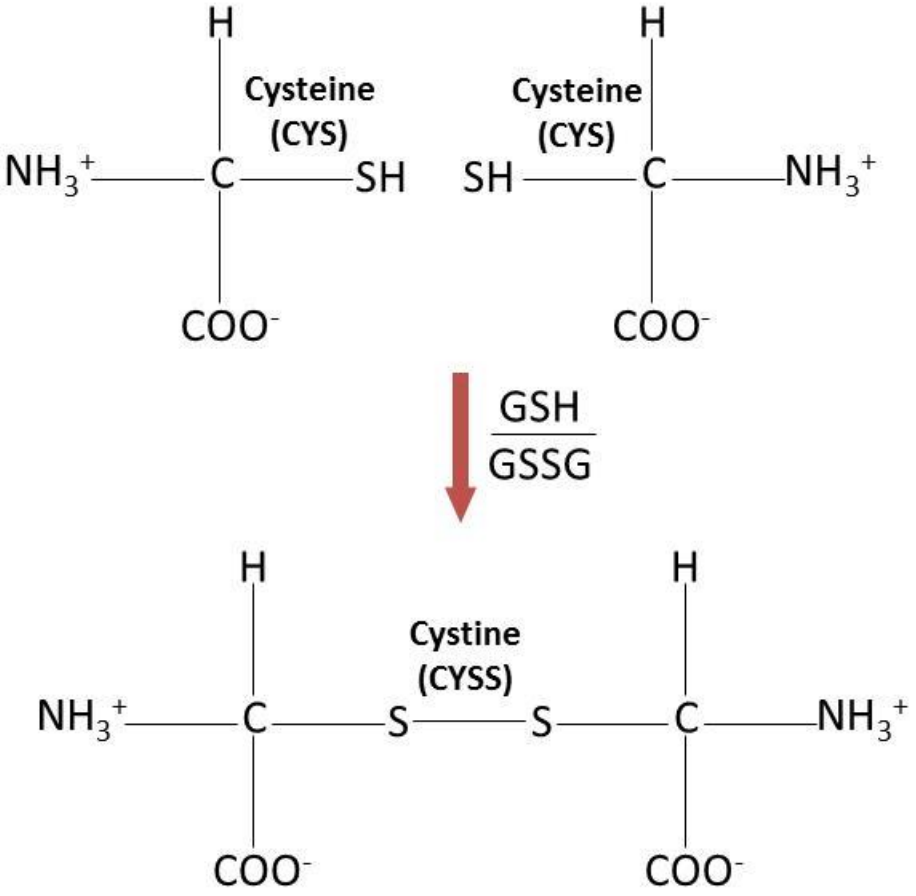

Figure 11. Disulfide bond formation under oxidized conditions.

S-glutathionylation. Protein *S*-glutathionylation involves the formation of a mixed disulfide between GSH and redox-sensitive Cys residues (Dalle-Donne et al. 2007), which can occur spontaneously or through a reaction catalyzed by glutathione *S*-transferase pi (GSTP) (Grek et al. 2013). The forward and reverse *S*-glutathionylation reactions can also be catalyzed by glutaredoxin (Grx) and Trx proteins (Beer et al. 2004; Kalinina et al. 2008; Starke et al. 2003). *S*-glutathionylation occurs through the attack of the sulfhydryl group of GSSG by a deprotonated Cys thiol, or under conditions of oxidative or nitrosative stress, *S*-glutathionylation can occur through the interaction of the Cys thiol with the GSH-thiyl radical (GS^{*}) and/or the interaction of a modified Cys thiol with GSH (Grek et al. 2013). *S*-glutathionylation also occurs via a disulfide/thiol exchange reaction between GSSG and the Cys thiol (Grek et al. 2013). However, for the majority of redox-sensitive Cys residues, the intracellular GSH/GSSG ratio would need to change 100-fold to induce *S*-glutathionylation through disulfide/thiol exchange, indicating that this mechanism is only applicable to a small group of Cys residues with very low pKa values (Dalle-Donne et al. 2007; Shelton et al. 2005).

NF-κB signaling. The nuclear factor-kappaB (NF-κB)-dependent signaling pathway is involved in the upregulation of target genes in response to cellular stressors (Li and Stark 2002) and is important for cytokine transcription in inflammation and immunity (Vallabhapurapu and Karin 2009) and gene expression in cell cycle regulation and apoptosis (Morgan and Liu 2011). The NF-κB pathway also upregulates the expression of many antioxidant enzymes, including CAT, SOD2, Trx1, Trx2, GSTP, and GPX (Morgan and Liu 2011). The mammalian NF-κB family of transcription factors is comprised of five proteins (RelA [also known as p65], RelB, c-Rel, NF-κB1 [p50], and NF-κB2 [p52], which contain a conserved Rel-homology domain (RHD) for

dimerization and DNA binding (Basak and Hoffmann 2008). In the cytosol, the NF-κB protein is complexed with inhibitor of κB (IκB) protein, which keeps NF-κB inactivated (Sun and Andersson 2002). In the canonical activation pathway, IκB kinase (IKK) phosphorylates two serine residues within IκB, which leads to lysine ubiquitination and proteasomal degradation of IκB; active NF-κB can then dimerize and translocate to the nucleus to bind κB enhancers in target genes (Gilmore 2006). Certain stimuli activate NF-κB through a non-canonical pathway involving NF-κB inducing kinase (NIK), which triggers the processing of the NF-κB2 precursor protein into its mature p52 subunit through phosphorylation and degredation of p100, a subunit complexed with p52 in the NF-κB2 precursor (Sun 2011).

The first study examining ROS and NF-κB by Schreck and colleagues (1991) found that H_2O_2 was a potent activator of NF-κB in human T cells, and pretreatment with *N*-acetyl-*L*-cysteine (NAC) and GSH blocked H_2O_2-mediated NF-κB activation (Flohe et al. 1997; Li and Karin 1999). However, subsequent studies of NF-κB redox regulation have produced mixed findings, which is explained by the fact that redox influences NF-κB through multiple, cell type-specific mechanisms (Morgan and Liu 2011).

First, oxidative stress influences IKK activity in a context-dependent manner. For example, H_2O_2 can irreversibly inhibit IKK through the direct oxidation of Cys^{179} of its β-subunit (IKK-β) (Korn et al. 2001). This oxidative inhibition of IKK was later found to correspond with *S*-glutathionylation of the same Cys residue, which could be reversed by GRX1; the authors postulated that redox-mediated *S*-glutathionylation might be a mechanism to protect IKK-β from irreversible oxidation by H_2O_2 and allow the rapid regulation of enzymatic activity (Reynaert et al. 2006). Alternatively, H_2O_2 can *increase* IKK activity by inducing dimerization of its IKK-γ regulatory subunit, which requires intermolecular disulfide bond formation involving Cys^{54} and

Cys^{347} (Herscovitch et al. 2008), and can also increase IKK activity by inducing phosphorylation of serines in the IKK activation loop (Kamata et al. 2002).

Oxidative stress also regulates NF-κB through IKK-independent mechanisms. During IL-1β induction of NFκB, H_2O_2 upregulates NIK activity at low concentrations (1–10 μM) but inhibits NIK at higher concentrations (Li and Engelhardt 2006). Under hypoxic conditions, NF-κB activation can occur through an atypical pathway in which IκB degradation is trigged by phosphorylation of Tyr^{42} in the IκBα subunit (Imbert et al. 1996; Koong et al. 1994; Siomek 2012), which is dependent upon the H_2O_2-mediated activation of c-Src kinases (Fan et al. 2003). The IκBα subunit also contains a Cys residue (Cys^{189}) that is a target for *S*-glutathionylation under oxidized conditions, which *prevents* IκBα degredation (Kil et al. 2008). In addition, the redox state in the nucleus influences the ability of the NF-κB complex to bind DNA (Toledano and Leonard 1991). This inhibition can occur through direct oxidation of a Cys residue (Cys^{62}) in the RHD of NF-κB (Matthews et al. 1993). When nuclear GSH/GSSG ratios are low, DNA binding inhibition occurs through *S*-glutathionylation of Cys^{62} (Pineda-Molina et al. 2001).

Due to the intricate crosstalk between oxidative stress and NF-κB signaling, it is impossible to summarize the "general" influence of oxidative stress on NF-κB activation. However, the complex interplay among ROS, GSH, and NF-κB allows the cell to initiate finely-tuned redox signaling cascades in response to a variety of stimuli, in a manner that is dependent upon the physiologic state of the cell (Flohe et al. 1997). Given the key role of NF-κB in the regulation of cell cycle progression, aberrant regulation of NF-κB signaling and ROS crosstalk is believed to play a role in carcinogenesis (Ben-Neriah and Karin 2011).

AP-1 signaling. The activator protein 1 (AP-1) family of leucine zipper transcription factors (comprised of Jun, Fos, Fra, and ATF subfamilies) regulates the expression of genes involved in

cell cycle control, DNA repair, and oncogenesis (Karin and Shaulian 2001). AP-1 activity can be induced by numerous stimuli, including growth factors, stress signals, bacterial and viral infections, and UV radiation (Angel and Karin 1991; Hess et al. 2004). The AP-1 complex is formed by the dimerization of different AP-1 proteins (usually a c-Jun/c-Fos heterodimer), which have different DNA binding affinities based upon the components of the dimer (Halazonetis et al. 1988), and the dimer binds to TPA response elements in promoter regions to enhance gene expression (Zhou et al. 2005).

One of the most widely-studied mechanisms of redox-associated AP-1 upregulation is via the mitogen-activated protein kinase (MAPK) family, which is comprised of three subfamilies of serine/threonine protein kinases (extracellular signal-regulated protein kinase [ERK], c-Jun N-terminal kinase/stress-activated protein kinase [JNK/SAPK], and p38) that phosphorylate c-Jun and c-Fos (Torres and Forman 2003; Wang et al. 1998). Activation of MAPKs requires phosphorylation by mitogen-activated protein kinase kinases (MKKs), which can be reversed by MAPK phosphatases (MKPs) (Boutros et al. 2008). The dual-specificity MKPs are PTPs and thus, contain a conserved redox-sensitive Cys residue; H_2O_2 oxidizes this Cys residue in JNK phosphatases, resulting in sustained JNK activation (Kamata et al. 2005). ROS have also been shown to downregulate ERK phosphatases, which can be reversed by pretreatment with NAC (Traore et al. 2008). In addition, ROS activates JNK via the inactivation of GSTP, which normally binds the c-terminal of JNK to suppress its activity (Shen and Liu 2006). MAPK activation is postulated to be a primary mechanism of ROS-induced apoptotic initiation (Circu and Aw 2010).

C. Inorganic arsenic.

1. Background.

Arsenic (As), a naturally-occurring metalloid, is a ubiquitous environmental contaminant in food, water, soil, and air (Mandal and Suzuki 2002). Over 200 million people worldwide are chronically exposed to As in drinking water, predominately in the form of arsenate (As^{V}) or arsenite (As^{III}), at concentrations greater than the WHO guideline of 10 µg/L (2008). Countries with As-exposed populations include, but are not limited to, Argentina, Bangladesh, Chile, China, Ghana, India, Mexico, Taiwan, the United States, and Vietnam (Naujokas et al. 2013). Arsenic exposure is of particular concern in Bangladesh: in a well-intentioned effort to prevent waterborne diseases from the consumption of pathogen-contamined surface water, humanitarian organizations installed tube wells throughout the country during the 1960s and 1970s (Flanagan et al. 2012). Unfortunately, it was not until the early 1990s that As was first detected in these wells (Flanagan et al. 2012). It is estimated that 35 to 77 million people in Bangladesh are chronically-exposed to As through drinking water (Kinniburgh and Smedley 2001).

The Agency for Toxic Substances and Disease Registry (ASTDR) calculates a ranking of toxic chemicals that pose the greatest hazards to public health; in 2011, arsenic had the highest ranking on the priority list (Naujokas et al. 2013). The relative toxicities of As compounds are strongly tied to their valence states. In general, trivalent arsenicals are more reactive than pentavalent arsenicals (Styblo et al. 2000), which can be attributed primarily to the binding affinity of trivalent arsenicals to sulhydryl groups in proteins and enzymes (Hughes et al. 2011). The toxicity of As^{V} stems from its structural similarity to phosphate and its ability to replace phosphate in chemical reactions (ter Welle and Slater 1967).

2. Metabolism of ingested arsenic.

a. Absorption and tissue uptake.

Following ingestion, inorganic arsenic (InAs) is readily absorbed (>90%) by the gastrointestinal tract: As^{V} is transported into enterocytes by the high-affinity phosphate transporter NaPiIIb (Villa-Bellosta and Sorribas 2008), while As^{III} uptake is mediated through a variety of transport mechanisms, including glucose transporters (GLUT2, GLUT5), organic anion transporting polypeptides (OATPB) and aquaporins (AQP3 and AQP10) (Calatayud et al. 2012). Arsenic exits the enterocyte via basolateral transporters (GLUT2, AQP3, AQP4, and MRPs, likely MRP3) and enters the circulation (Calatayud et al. 2012), where As^{III} can be transported into tissues via AQPs (Maciaszczyk-Dziubinska et al. 2012).

b. Methylation.

Within cells, As^{III} is metabolized through a series of methylation reactions, resulting in the formation of monomethyl (MMAs) and dimethyl arsenicals (DMAs) (Lin et al. 2002). The reaction is catalyzed by the enzyme arsenic(III)-methyltransferase (AS3MT), which is absolutely dependent upon a methyl group from SAM and the presence of a reductant (Lin et al. 2002), such as GSH (Thomas 2009; Waters et al. 2004b) or the TR/Trx/NADPH system (Waters et al. 2004a; Waters et al. 2004b). Although the primary site of As methylation is the liver, AS3MT is also expressed in kidney, lung, heart, and bladder tissues (Lin et al. 2002). Three distinct AS3MT-catalyzed methylation pathways have been proposed in the literature (Figure 10 A-C):
A. Oxidative methylation. In this pathway first proposed by Challenger (1945, 1951), AS3MT catalyzes the oxidative methylation of As^{III} and methylarsonous acid (MMA^{III}) to methylarsonic

acid (MMA^V) and dimethylarsinic acid (DMA^V), respectively. A reductant (such as GSH) is required for the reduction of the pentavalent arsenicals (As^V and MMA^V) to their trivalent counterparts (As^{III} and MMA^{III}).

B. Successive methylation via As-GSH complexes. Hayakawa et al. (2005) proposed a pathway in which As-GSH complexes are substrates for AS3MT. Here, As^{III} nonenzymatically complexes with GSH to generate arsenic triglutathione (ATG), which is methylated by AS3MT to form monomethylarsonic diglutathione (MADG). MADG can be further methylated to dimethylarsinic glutathione (DMAG). As-GSH complexes (ATG, MADG, and DMAG) are in equilibrium with trivalent arsenicals (As^{III}, MMA^{III}, and DMA^{III}) based on the concentration of GSH. The trivalent methylated arsenicals (MMA^{III} and DMA^{III}) can be oxidized to pentavalent arsenicals (MMA^V and DMA^V) by environmental oxygen.

C. Ordered methylation mechanism. Wang et al. (2012) proposed a model in which a reductant (thiol or nonthiol) changes the conformation of AS3MT to influence enzyme activity. In this scheme, SAM binds to AS3MT; then, a reductant (such as GSH) cleaves a disulfide bond in the enzyme, which exposes active-site cysteine (Cys) residues for As^{III} binding. As^{III} binds the Cys residues, forming arsenic tricysteine (ATC^{III}), and the methyl group from SAM is transferred to ATC^{III} on the AS3MT enzyme, resulting in monomethylarsonic dicysteine ($MADC^{III}$). $MADC^{III}$ can remain bound to AS3MT and be further methylated to dimethylarsinic cysteine ($DMAC^{III}$). $MADC^{III}$ and $DMAC^{III}$ can dissociate from AS3MT, forming MMA^{III} and DMA^{III}, respectively. Trivalent species are then oxidized to pentavalent arsenicals by environmental oxygen.

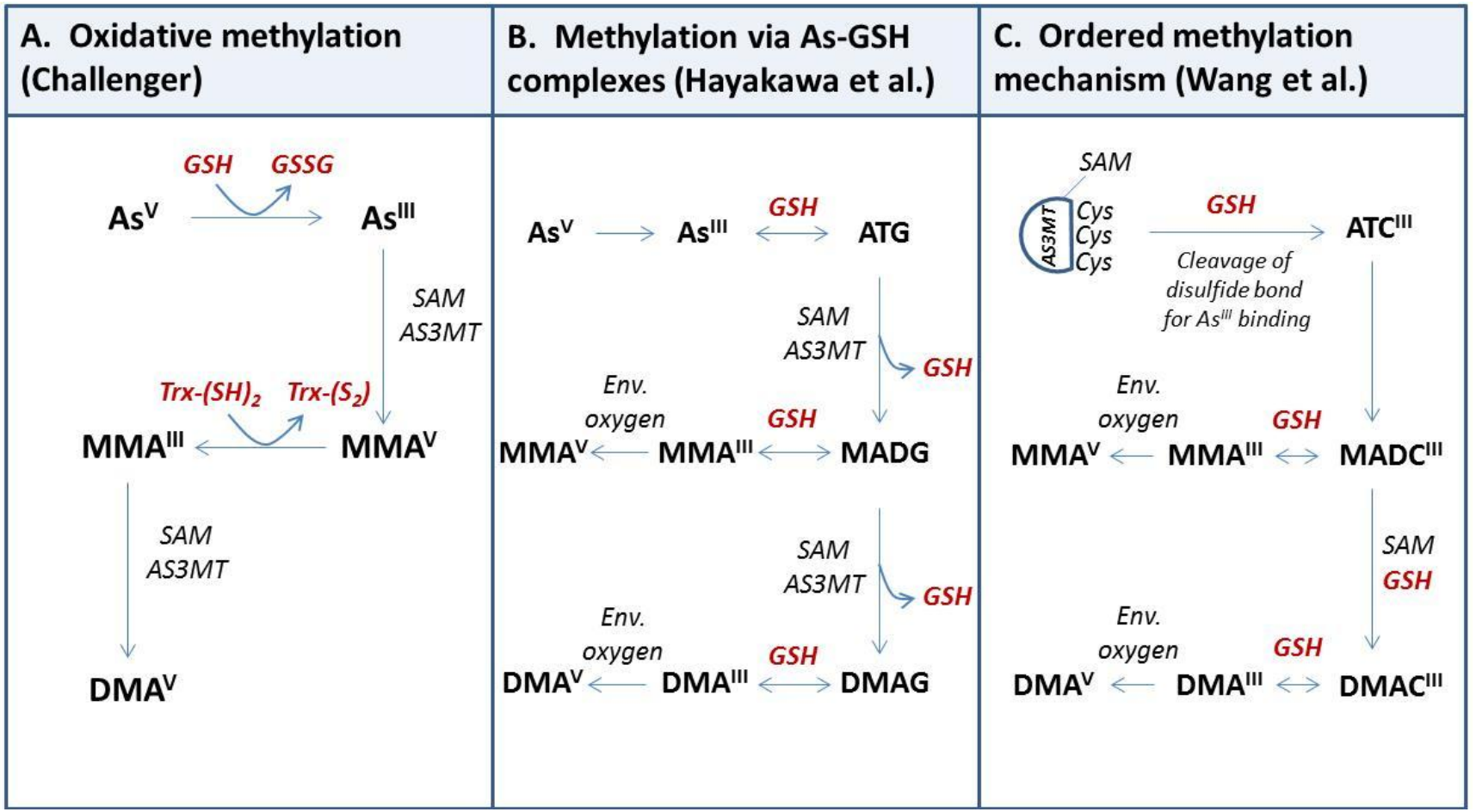

Figure 12. Proposed mechanisms of arsenic methylation. (A) Oxidative methylation pathway, first proposed by Challenger in 1945; (B) Methylation via As-GSH complexes, first proposed by Hayakawa et al. 2005; (C) Ordered methylation mechanism, first proposed by Wang et al. 2012. Pathways are described in detail on pages 38-39.

There are twelve conserved Cys residues in the human AS3MT (hAS3MT) structure (X Song et al. 2011). The hAS3MT binding site for As^{III} contains two Cys residues (Cys^{156} and Cys^{206}) that serve as the catalytic binding sites, and another Cys residue (Cys^{250}) in this site is involved in an intramolecular disulfide bond to maintain structural stability (Song et al. 2009), possibly with Cys^{72} (X Song et al. 2011). The structure of the hAS3MT binding site for SAM is less defined, but models indicate that Asp^{102} forms hydrogen bonds with ribose hydroxyl groups of SAM (Li et al. 2013b) and Tyr^{59} forms a hydrogen bond with the carboxyl group (Li et al. 2013a). Additionally, Cys^{156} and Cys^{206} within the As^{III} binding site are also found in the SAM binding pocket, with Cys^{156} predicted to interact with the S^{+}-CH_3 of SAM to orient the methyl group for As^{III} binding (Li et al. 2013a).

Arsenic methylation: detoxification.or bioactivation?

Studies of As3mt-knockout mice suggest that As methylation plays a key role in As excretion and detoxification (Drobna et al. 2009; Hughes et al. 2010). Following an acute As exposure of 0.5 mg As^{V}/kg, compared to wildtype mice at 24 h, As3mt knockouts had markedly higher proportions of MMA in liver and higher As retention in liver, kidneys, bladder, lungs, and heart; whole-body retention of the As dose at 24 h was 6% in wildtype mice and 50% in As3mt-knockout mice (Drobna et al. 2009). Further examination of this same As^{V} dose over 10 daily doses (to achieve steady-state exposures) found that the whole body burden of As was 16 to 20 times greater in As3mt-knockout mice compared to wildtype (Hughes et al. 2010).

The methyl donor for As methylation is SAM, a product of folate-dependent one-carbon metabolism. Early animal studies found that folate deficiency increased As retention and decreased urinary As excretion (Spiegelstein et al. 2005; Tice et al. 1997; Vahter and Marafante 1987), and recent studies using Mthfr-knockout mice found impaired urinary As excretion in

Mthfr knockouts compared to wildtype (Wlodarczyk et al. 2012). In humans, folate deficiency has been associated with impaired As methylation capacity in numerous cross-sectional studies (Basu et al. 2011; Gamble et al. 2005; Heck et al. 2007). A randomized controlled trial (RCT) in a folate-deficient, As-exposed Bangaldeshi population examining the influence of folic acid supplementation on As methylation capacity found that compared to placebo, daily supplementation with 400 µg folic acid for 12 weeks decreased urinary %MMA, increased urinary %DMA, and decreased total blood As (Gamble et al. 2006; Gamble et al. 2007).

Despite the experimental evidence linking As methylation capacity with whole-body As excretion, it has been argued that As methylation involves bioactivation rather than detoxification (Thomas et al. 2001; Vahter and Concha 2001). The first examination of the *in vitro* toxicities of the methylated arsenicals found that MMA^{III} was the most cytotoxic, with an LC_{50} of 6.3 µM, and was considerably more toxic than the second-most toxic species, As^{III}, with an LC_{50} of 19.8 µM (Petrick et al. 2000). Based on these findings and results from other *in vitro* and *in vivo* cytotoxicity studies (Petrick et al. 2001; Styblo et al. 2000), the relative toxicities of the As metabolites are estimated to be $MMA^{III} > DMA^{III} > As^{III} > As^{V} > MMA^{V} > DMA^{V}$ (reviewed in Hall and Gamble 2012). Recent studies have also examined the toxicities of the minor thiolated As metabolites, dimethylmonothioarsinic acid ($DMMTA^{V}$), dimethyldithioarsinic acid ($DMDTA^{V}$), and monomethylmonothioarsonic acid ($MMMTA^{V}$), and found that $DMMTA^{V}$ was extremely cytotoxic in human bladder cells, second only to DMA^{III} (Naranmandura et al. 2011). In sum, evidence suggests that As methylation increases As excretion; however, incomplete As methylation resulting in increased MMA production, and endogenous environments supporting the formation of trivalent and thiol methylated metabolites, might enhance toxicity.

c. Excretion.

The primary route of As elimination in humans is through urinary excretion. Two toxicokinetic studies in healthy human adults found that, in conditions of chronic exposure to varying oral doses of sodium arsenite ($NaAsO_2$) with steady-state excretion, approximately 60% of the $NaAsO_2$ dose is excreted in urine within 24 h (Buchet et al. 1981b), while another experiment from the same group found that a single oral dose of 500 µg As^{III} is excreted in urine within 4 days (Buchet et al. 1981a). Among individuals who are chronically-exposed to As in well water, the predominant urinary As metabolite is DMA (typically ranging from 45-85%), followed by InAs (10-30%) and MMA (5-25%) (Gamble et al. 2005; Meza et al. 2004; Vahter and Concha 2001). Arsenic (as As-GSH and As-GSH-Se complexes) can also be excreted in bile via MRP-mediated transport mechanisms (Figure 13) (Carew and Leslie 2010; Kala et al. 2000).

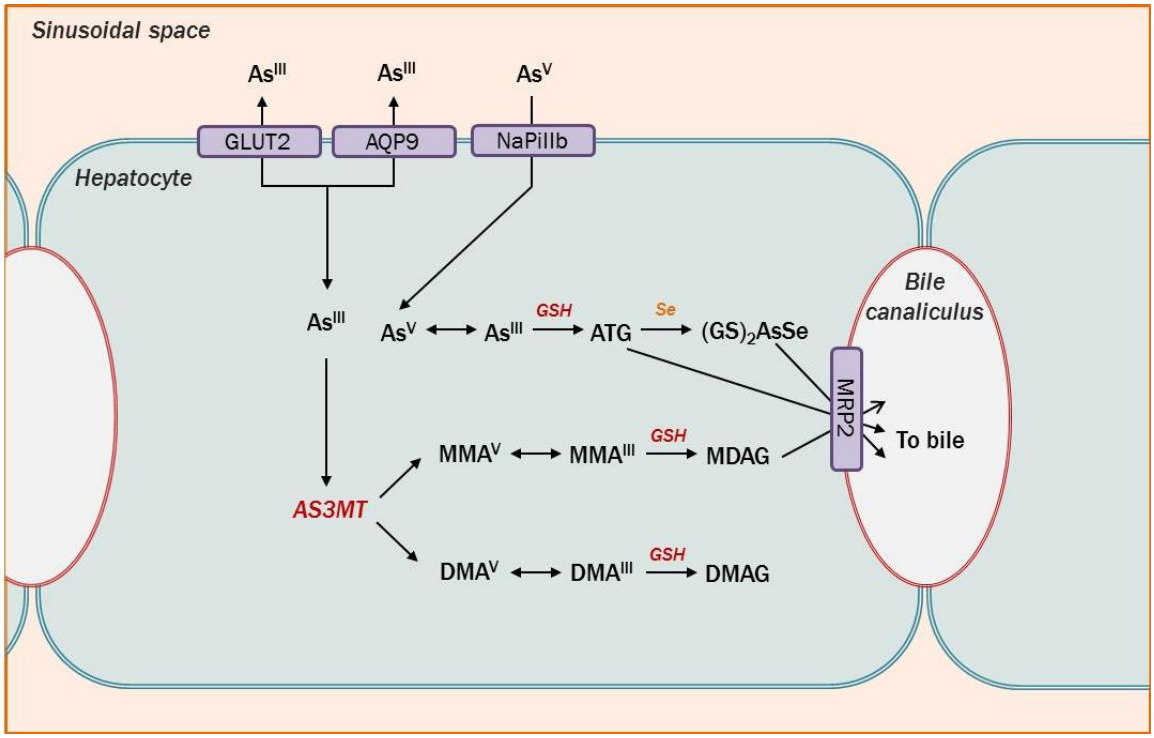

Figure 13. Biliary excretion of conjugated arsenicals. Arsenical species (As^{III} and MMA^{III}) can form As-GSH complexes, which are transported to the bile canaliculus via MRP2.

3. Health effects of chronic arsenic exposure in adults.

a. Arsenic-induced skin lesions.

Arsenic tends to accumulate in keratin-rich peripheral tissues, such as the skin, nails, and hair (Yu et al. 2006). As such, one of the most common As-associated health outcomes is the appearance of skin lesions (melanosis, keratosis, and/or leukomelanosis), which are often the first visible sign of arsenicosis (Chakraborty and Saha 1987; Tseng et al. 1968). Melanosis, the most common and early-presenting manifestation, is characterized by hyperpigmentation of the chest, back, and limbs; keratosis is a sign of moderate-to-severe As toxicity and is characterized by rough, dark nodules on the palms and soles of the feet; and leukomelanosis, an uncommon manifestation, is characterized by hypopigmentation and is associated with advanced-stage toxicity (Saha et al. 1999).

Multiple studies have confirmed that As exposure is associated with a dose-dependent increase in risk for skin lesions (Argos et al. 2011; Guo et al. 2001; Haque et al. 2003; Tondel et al. 1999), and skin lesions are considered to be a specific biomarker of long-term As exposure (Chen et al. 2005), as well as a biomarker of increased susceptibility to As toxicity (Hsu et al. 2013). A recent study in Taiwan found that the presence of skin lesions was associated with increased risk of lung and endothelial cancer, even years after the cessation of As exposure (Hsu et al. 2013). In addition, the prevalence of skin lesions in As-exposed populations is fairly high compared to other health outcomes, allowing for large sample sizes in epidemiologic studies: For example, in 1968, a large study of an As-exposed population in Taiwan found that the prevalence (per 1,000 individuals) of melanosis was 183.5 and keratosis was 71.0, while the prevalence of skin cancer was only 10.6 (Tseng et al. 1968). Although skin lesions do not

progress to skin cancer at a high rate, examining the risk factors that increase the risk of As-induced skin lesions might provide insight into mechanisms of As toxicity and factors that influence susceptibility.

b. Health outcomes.

Chronic As exposure is associated with increased all-cause and chronic-disease mortality rates (Argos et al. 2010) and increased risks for numerous health outcomes (Table 1).

Table 1. Examples of health outcomes associated with chronic As exposure in adult humans. (adapted from Hughes 2002; Naujokas et al. 2013, Yoshida et al. 2004)

System	**Disease/condition**
Skin	Skin lesions, squamous cell carcinoma
Respiratory	Asthma, chronic obstructive pulmonary disorder
Cardiovascular	Ischemic heart disease, hypertension
Nervous	Peripheral neuropathy, impaired motor function
Hepatic	Liver cancer
Hematological	Bone marrow depression
Endocrine	Diabetes, thyroid disruption, glucose tolerance
Renal	Proximal tubule degeneration, kidney cancer, bladder cancer

c. As methylation and disease risk.

In human studies, impaired As methylation capacity (as indicated by increased %MMA and/or decreased %DMA in urine) has been associated with increased susceptibility to a variety of As-related diseases, including skin lesions, atherosclerosis, cardiovascular disease (CVD), and cancers of the lung, bladder, and skin (reviewed in Steinmaus et al. 2010). Although the studies included in Steinmaus et al. examined prevalent cases, raising the possibility that the relationship between As methylation capacity and disease might not be temporal, a recent prospective study in Bangladesh observed a significant association between increased %MMA and risk for CVD (Chen et al. 2013).

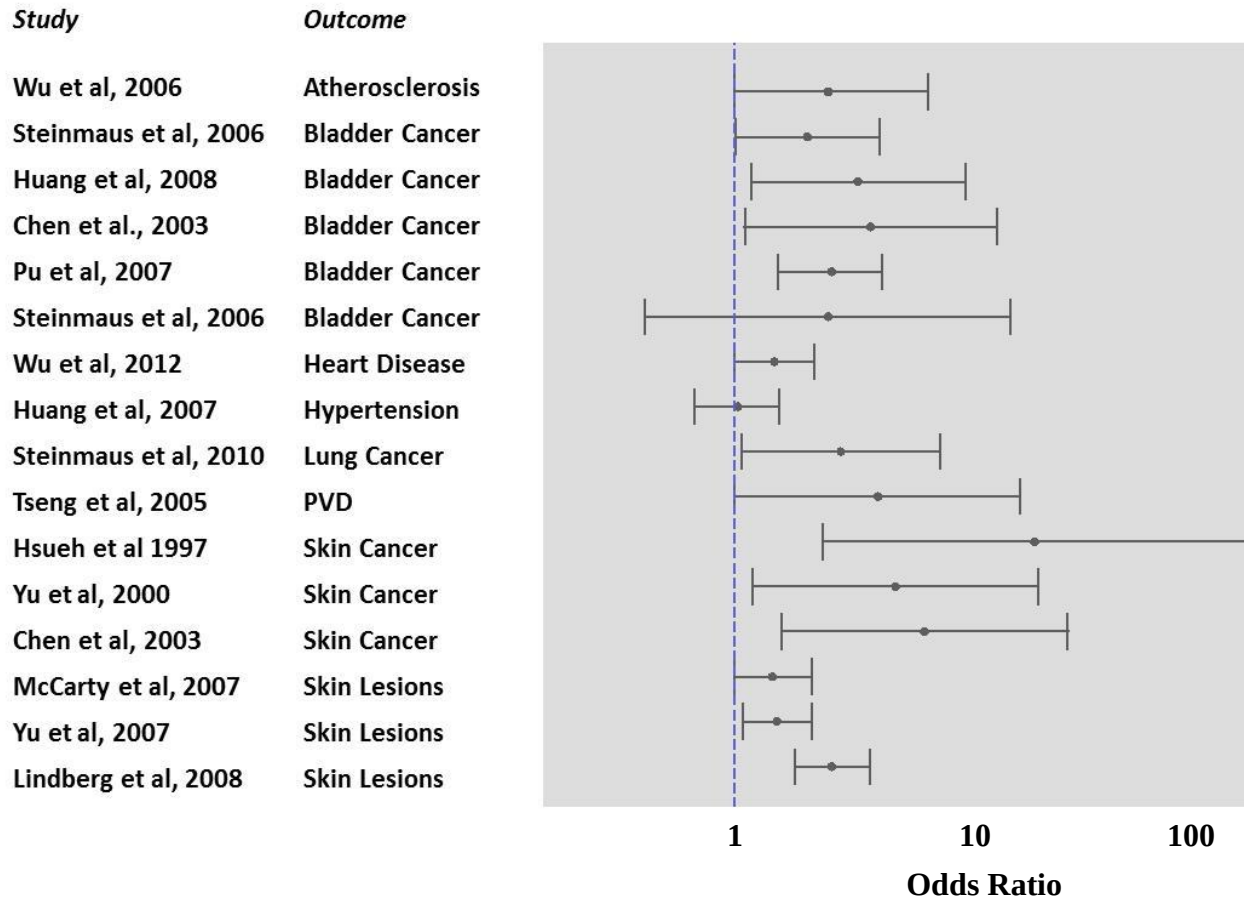

Figure 14. Forest plot displaying odds ratios (95% CIs) of As-related disease by high vs. low urinary %MMA(^{III}+^{V}). Elevated urinary %MMA is associated with increased disease risks across 16 independent studies. Courtesy of Dr. Megan Hall, adapted from Steinmaus et al. 2010.

4. Mechanisms of arsenic toxicity and carcinogenesis in humans.

The exact mechanism(s) of action of As toxicity are unknown, but several pathways have been proposed (Figure 15) (Hughes 2002). Unlike the majority of known chemical carcinogens, As is a weak point mutagen (Kligerman et al. 2003; Rossman et al. 1980). Despite its inability to induce DNA mutations, in a study published in *Science* in 1988, $NaAsO_2$ was shown to be a strong inducer of gene amplification *in vitro* (Lee et al. 1988), and subsequent *in vitro* studies have confirmed that As exposure induces genomic instability (reviewed in Bhattacharjee et al. 2013). In humans, As exposure in drinking water has been significantly associated with chromosomal aberrations and micronuclei formation in numerous studies (Ghosh et al. 2006; Gonsebatt et al. 1997; Lerda 1994; Mahata et al. 2003), which are hypothesized to occur through the pathways presented in Figure 15.

Elucidating mechanisms of As toxicity in humans has proven difficult due to substantial interspecies differences in AS3MT expression and As toxicokinetics (Drobna et al. 2010). This is a particular concern in the study of As carcinogenesis. Although As is a known human carcinogen, there is a lack of evidence for As carcinogenicity from *in vivo* experimental models, and until recently, there were no animal models of As carcinogenesis (Huff et al. 2000; Tokar et al. 2010). Additionally, recently-developed rodent models generally administer As at doses (drinking water As in the ppm range) that are orders of magnitude higher than environmentally-relevant exposures (drinking water As in the ppb range) (Tokar et al. 2010). Since As exposure is likely to exert its toxic effects through multiple, dose-dependent mechanisms (Singh et al. 2011), it is uncertain whether findings from animal models can be directly translated to humans. It is thus essential to complement experimental studies of As toxicity with mechanistic studies in human populations.

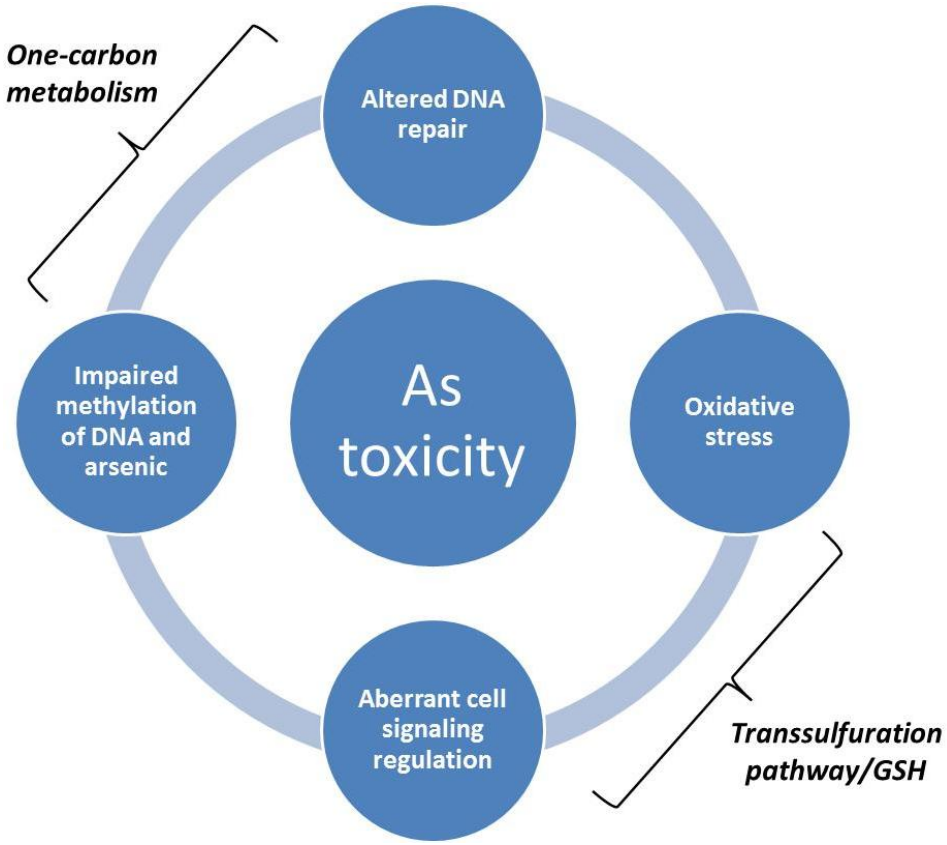

Figure 15. Proposed mechanisms of arsenic toxicity. Four of several proposed mechanisms of As toxicity include (A) decreased capacity to methylate DNA and/or arsenic; (B) impaired DNA repair capacity; (C) oxidative stress; and (D) aberrant cell signaling. As outlined in sections A and B of the introduction, transmethylation reactions and DNA repair capacity are regulated, in part, by folate and one-carbon metabolism, and oxidative stress and cell signaling cascades are regulated, in part, by GSH and the transsulfuration pathway.

5. Metabolic interactions and unanswered questions.

As outlined in Sections A and B of the introduction, these proposed mechanisms of As toxicity are not metabolically independent, and they are all influenced, in part, by one-carbon metabolism and the transsulfuration pathway (Figure 16). Given the complex metabolic interactions between As metabolism, GSH redox regulation, and DNA methylation, it is important to understand how these factors might interact with one another to influence As toxicity. In this dissertation, we examined the relationships and metabolic interactions among these factors in a human population that is chronically-exposed to As in drinking water.

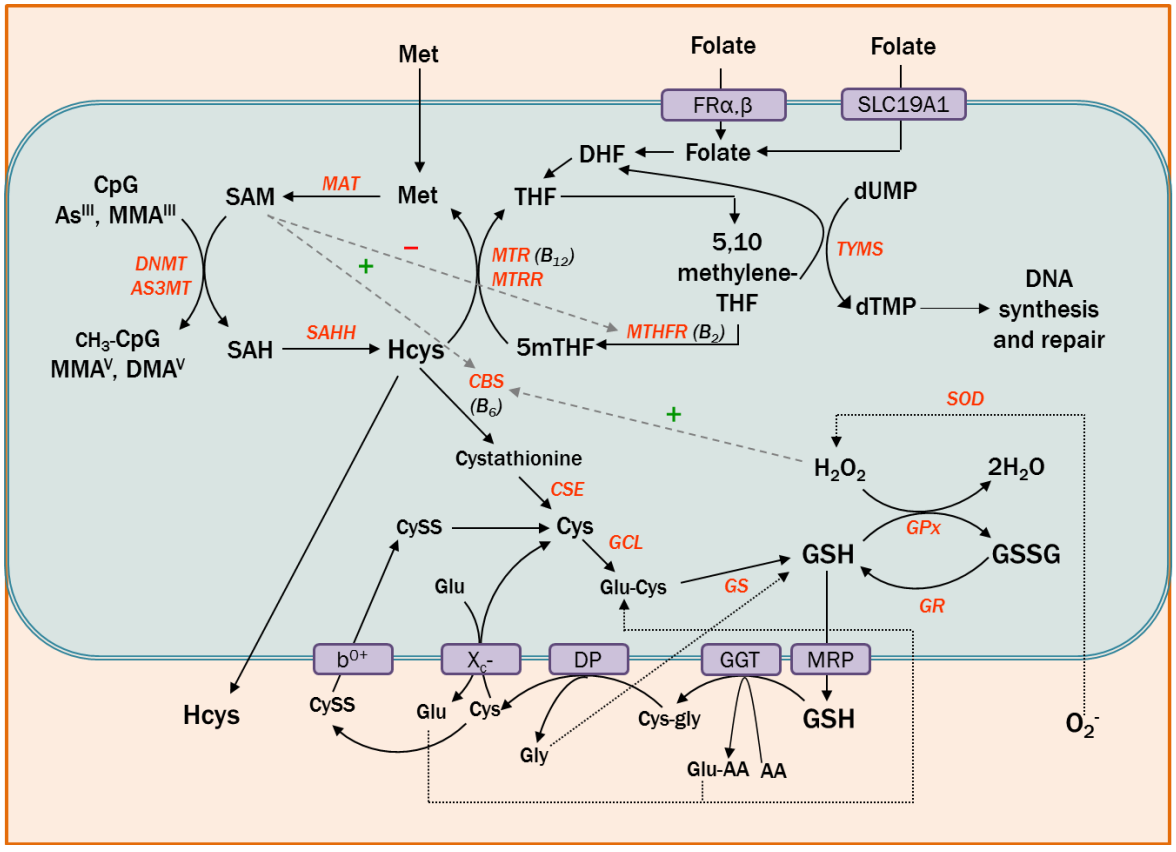

Figure 16. Metabolic interactions between DNA methylation, glutathione redox regulation, and arsenic metabolism: a simplified diagram.

REFERENCES

Ago T, Nunoi H, Ito T, Sumimoto H. 1999. Mechanism for phosphorylation-induced activation of the phagocyte nadph oxidase protein p47(phox). Triple replacement of serines 303, 304, and 328 with aspartates disrupts the sh3 domain-mediated intramolecular interaction in p47(phox), thereby activating the oxidase. J Biol Chem 274:33644-33653.

Ajayi A, Yu X, Ström A-L. 2013. The role of nadph oxidase (nox) enzymes in neurodegenerative disease. Front Biol 8:175-188.

Alho I, Costa L, Bicho M, Coelho C. 2013. The role of low-molecular-weight protein tyrosine phosphatase (lmw-ptp acp1) in oncogenesis. Tumour biology : the journal of the International Society for Oncodevelopmental Biology and Medicine 34:1979-1989.

Alonso A, Sasin J, Bottini N, Friedberg I, Friedberg I, Osterman A, et al. 2004. Protein tyrosine phosphatases in the human genome. Cell 117:699-711.

Angel P, Karin M. 1991. The role of jun, fos and the ap-1 complex in cell-proliferation and transformation. Biochim Biophys Acta 1072:129-157.

Antony AC. 1996. Folate receptors. Annual review of nutrition 16:501-521.

Antony AC. 2007. In utero physiology: Role of folic acid in nutrient delivery and fetal development. The American Journal of Clinical Nutrition 85:598S-603S.

Argos M, Kalra T, Rathouz PJ, Chen Y, Pierce B, Parvez F, et al. 2010. Arsenic exposure from drinking water, and all-cause and chronic-disease mortalities in bangladesh (heals): A prospective cohort study. The Lancet 376:252-258.

Argos M, Kalra T, Pierce BL, Chen Y, Parvez F, Islam T, et al. 2011. A prospective study of arsenic exposure from drinking water and incidence of skin lesions in bangladesh. American journal of epidemiology 174:185-194.

Arita K, Ariyoshi M, Tochio H, Nakamura Y, Shirakawa M. 2008. Recognition of hemi-methylated DNA by the sra protein uhrf1 by a base-flipping mechanism. Nature 455:818-821.

Banerjee RV, Matthews RG. 1990. Cobalamin-dependent methionine synthase. The FASEB Journal 4:1450-1459.

Bannister AJ, Kouzarides T. 2011. Regulation of chromatin by histone modifications. Cell research 21:381-395.

Bartova E, Krejci J, Harnicarova A, Galiova G, Kozubek S. 2008. Histone modifications and nuclear architecture: A review. The journal of histochemistry and cytochemistry : official journal of the Histochemistry Society 56:711-721.

Basak S, Hoffmann A. 2008. Crosstalk via the nf-kappab signaling system. Cytokine Growth Factor Rev 19:187-197.

Basal E, Eghbali-Fatourechi GZ, Kalli KR, Hartmann LC, Goodman KM, Goode EL, et al. 2009. Functional folate receptor alpha is elevated in the blood of ovarian cancer patients. PLoS One 4:e6292.

Basu A, Mitra S, Chung J, Guha Mazumder DN, Ghosh N, Kalman D, et al. 2011. Creatinine, diet, micronutrients, and arsenic methylation in west bengal, india. Environ Health Perspect 119:1308-1313.

Bates CJ, Fuller NJ. 1986. The effect of riboflavin deficiency on methylenetetrahydrofolate reductase (nadph) (ec 1.5.1.20) and folate metabolism in the rat. The British journal of nutrition 55:455-464.

Beer SM, Taylor ER, Brown SE, Dahm CC, Costa NJ, Runswick MJ, et al. 2004. Glutaredoxin 2 catalyzes the reversible oxidation and glutathionylation of mitochondrial membrane thiol proteins: Implications for mitochondrial redox regulation and antioxidant defense. J Biol Chem 279:47939-47951.

Ben-Neriah Y, Karin M. 2011. Inflammation meets cancer, with nf-[kappa]b as the matchmaker. Nat Immunol 12:715-723.

Berkholz DS, Faber HR, Savvides SN, Karplus PA. 2008. Catalytic cycle of human glutathione reductase near 1 a resolution. Journal of molecular biology 382:371-384.

Bestor TH. 1988. Cloning of a mammalian DNA methyltransferase. Gene 74:9-12.

Bhandary B, Marahatta A, Kim HR, Chae HJ. 2012. An involvement of oxidative stress in endoplasmic reticulum stress and its associated diseases. International journal of molecular sciences 14:434-456.

Bhattacharjee P, Banerjee M, Giri AK. 2013. Role of genomic instability in arsenic-induced carcinogenicity. A review. Environment International 53:29-40.

Bird AP. 1980. DNA methylation and the frequency of cpg in animal DNA. Nucleic Acids Research 8:1499-1504.

Bird AP. 1986. Cpg-rich islands and the function of DNA methylation. Nature 321:209-213.

Blount BC, Mack MM, Wehr CM, MacGregor JT, Hiatt RA, Wang G, et al. 1997. Folate deficiency causes uracil misincorporation into human DNA and chromosome breakage: Implications for cancer and neuronal damage. Proc Natl Acad Sci U S A 94:3290-3295.

Board PG, Menon D. 2013. Glutathione transferases, regulators of cellular metabolism and physiology. Biochim Biophys Acta 1830:3267-3288.

Boutros T, Chevet E, Metrakos P. 2008. Mitogen-activated protein (map) kinase/map kinase phosphatase regulation: Roles in cell growth, death, and cancer. Pharmacol Rev 60:261-310.

Brookes PS, Yoon Y, Robotham JL, Anders MW, Sheu SS. 2004. Calcium, atp, and ros: A mitochondrial love-hate triangle. American journal of physiology Cell physiology 287:C817-833.

Buchet JP, Lauwerys R, Roels H. 1981a. Comparison of the urinary excretion of arsenic metabolites after a single oral dose of sodium arsenite, monomethylarsonate, or dimethylarsinate in man. Int Arch Occup Environ Health 48:71-79.

Buchet JP, Lauwerys R, Roels H. 1981b. Urinary excretion of inorganic arsenic and its metabolites after repeated ingestion of sodium metaarsenite by volunteers. Int Arch Occup Environ Health 48:111-118.

Calatayud M, Barrios JA, Vélez D, Devesa V. 2012. In vitro study of transporters involved in intestinal absorption of inorganic arsenic. Chemical Research in Toxicology 25:446-453.

Campos-Martin JM, Blanco-Brieva G, Fierro JL. 2006. Hydrogen peroxide synthesis: An outlook beyond the anthraquinone process. Angewandte Chemie (International ed in English) 45:6962-6984.

Carew MW, Leslie EM. 2010. Selenium-dependent and -independent transport of arsenic by the human multidrug resistance protein 2 (mrp2/abcc2): Implications for the mutual detoxification of arsenic and selenium. Carcinogenesis 31:1450-1455.

Cedar H, Bergman Y. 2009. Linking DNA methylation and histone modification: Patterns and paradigms. Nat Rev Genet 10:295-304.

Cederbaum AI, Wu D, Mari M, Bai J. 2001. Cyp2e1-dependent toxicity and oxidative stress in hepg2 cells. Free Radic Biol Med 31:1539-1543.

Chakraborty AK, Saha KC. 1987. Arsenical dermatosis from tubewell water in west bengal. The Indian journal of medical research 85:326-334.

Chakravarthi S, Bulleid NJ. 2004. Glutathione is required to regulate the formation of native disulfide bonds within proteins entering the secretory pathway. Journal of Biological Chemistry 279:39872-39879.

Challenger F. 1945. Biological methylation. Chemical Reviews 36:315–361.

Challenger F. 1951. Biological methylation. Advances in enzymology and related subjects of biochemistry 12:429-491.

Chan JY, Kwong M. 2000. Impaired expression of glutathione synthetic enzyme genes in mice with targeted deletion of the nrf2 basic-leucine zipper protein. Biochim Biophys Acta 1517:19-26.

Chandler CJ, Wang TT, Halsted CH. 1986. Pteroylpolyglutamate hydrolase from human jejunal brush borders. Purification and characterization. J Biol Chem 261:928-933.

Chen CJ, Hsu LI, Wang CH, Shih WL, Hsu YH, Tseng MP, et al. 2005. Biomarkers of exposure, effect, and susceptibility of arsenic-induced health hazards in taiwan. Toxicol Appl Pharmacol 206:198-206.

Chen NC, Yang F, Capecci LM, Gu Z, Schafer AI, Durante W, et al. 2010. Regulation of homocysteine metabolism and methylation in human and mouse tissues. FASEB J 24:2804-2817.

Chen T, Li E. 2004. Structure and function of eukaryotic DNA methyltransferases. Current topics in developmental biology 60:55-89.

Chen T, Tsujimoto N, Li E. 2004. The pwwp domain of dnmt3a and dnmt3b is required for directing DNA methylation to the major satellite repeats at pericentric heterochromatin. Mol Cell Biol 24:9048-9058.

Chen Y, Wu F, Liu M, Parvez F, Slavkovich V, Eunus M, et al. 2013. A prospective study of arsenic exposure, arsenic methylation capacity, and risk of cardiovascular disease in bangladesh. Environ Health Perspect 121:832-838.

Christensen KE, Deng L, Leung KY, Arning E, Bottiglieri T, Malysheva OV, et al. 2013. A novel mouse model for genetic variation in 10-formyltetrahydrofolate synthetase exhibits disturbed purine synthesis with impacts on pregnancy and embryonic development. Hum Mol Genet 22:3705-19.

Circu ML, Aw TY. 2010. Reactive oxygen species, cellular redox systems, and apoptosis. Free Radic Biol Med 48:749-762.

Csala M, Margittai E, Banhegyi G. 2010. Redox control of endoplasmic reticulum function. Antioxid Redox Signal 13:77-108.

Cui H, Kong Y, Zhang H. 2012. Oxidative stress, mitochondrial dysfunction, and aging. Journal of Signal Transduction 2012:13.

Cumming RC, Andon NL, Haynes PA, Park M, Fischer WH, Schubert D. 2004. Protein disulfide bond formation in the cytoplasm during oxidative stress. Journal of Biological Chemistry 279:21749-21758.

Curradi M, Izzo A, Badaracco G, Landsberger N. 2002. Molecular mechanisms of gene silencing mediated by DNA methylation. Molecular and Cellular Biology 22:3157-3173.

Dalle-Donne I, Rossi R, Giustarini D, Colombo R, Milzani A. 2007. S-glutathionylation in protein redox regulation. Free Radic Biol Med 43:883-898.

Dang CV. 2012. Links between metabolism and cancer. Genes & Development 26:877-890.

Deaton AM, Bird A. 2011. Cpg islands and the regulation of transcription. Genes & Development 25:1010-1022.

Dillon N. 2004. Heterochromatin structure and function. Biology of the cell / under the auspices of the European Cell Biology Organization 96:631-637.

Dringen R. 2000. Metabolism and functions of glutathione in brain. Progress in neurobiology 62:649-671.

Drobna Z, Naranmandura H, Kubachka KM, Edwards BC, Herbin-Davis K, Styblo M, et al. 2009. Disruption of the arsenic (+3 oxidation state) methyltransferase gene in the mouse alters the phenotype for methylation of arsenic and affects distribution and retention of orally administered arsenate. Chem Res Toxicol 22:1713-1720.

Drobna Z, Walton FS, Harmon AW, Thomas DJ, Styblo M. 2010. Interspecies differences in metabolism of arsenic by cultured primary hepatocytes. Toxicol Appl Pharmacol 245:47-56.

Drummond JT, Huang S, Blumenthal RM, Matthews RG. 1993. Assignment of enzymatic function to specific protein regions of cobalamin-dependent methionine synthase from escherichia coli. Biochemistry 32:9290-9295.

Duthie SJ, Narayanan S, Blum S, Pirie L, Brand GM. 2000. Folate deficiency in vitro induces uracil misincorporation and DNA hypomethylation and inhibits DNA excision repair in immortalized normal human colon epithelial cells. Nutrition and cancer 37:245-251.

Erickson AM, Nevarea Z, Gipp JJ, Mulcahy RT. 2002. Identification of a variant antioxidant response element in the promoter of the human glutamate-cysteine ligase modifier subunit gene: Revision of the are consensus sequence. Journal of Biological Chemistry 277:30730-30737.

Fan C, Li Q, Ross D, Engelhardt JF. 2003. Tyrosine phosphorylation of i kappa b alpha activates nf kappa b through a redox-regulated and c-src-dependent mechanism following hypoxia/reoxygenation. J Biol Chem 278:2072-2080.

Finkelstein JD. 1990. Methionine metabolism in mammals. The Journal of nutritional biochemistry 1:228-237.

Flanagan SV, Johnston RB, Zheng Y. 2012. Arsenic in tube well water in bangladesh: Health and economic impacts and implications for arsenic mitigation. Bulletin of the World Health Organization 90:839-846.

Flohe L, Brigelius-Flohe R, Saliou C, Traber MG, Packer L. 1997. Redox regulation of nf-kappa b activation. Free Radic Biol Med 22:1115-1126.

Forstermann U, Kleinert H. 1995. Nitric oxide synthase: Expression and expressional control of the three isoforms. Naunyn-Schmiedeberg's archives of pharmacology 352:351-364.

Fourquet S, Guerois R, Biard D, Toledano MB. 2010. Activation of nrf2 by nitrosative agents and h2o2 involves keap1 disulfide formation. Journal of Biological Chemistry 285:8463-8471.

Fox JT, Stover PJ. 2008. Folate-mediated one-carbon metabolism. Vitamins and hormones 79:1-44.

Gamble MV, Liu X, Ahsan H, Pilsner R, Ilievski V, Slavkovich V, et al. 2005. Folate, homocysteine, and arsenic metabolism in arsenic-exposed individuals in bangladesh. Environ Health Perspect 113:1683-1688.

Gamble MV, Liu X, Ahsan H, Pilsner JR, Ilievski V, Slavkovich V, et al. 2006. Folate and arsenic metabolism: A double-blind, placebo-controlled folic acid-supplementation trial in bangladesh. Am J Clin Nutr 84:1093-1101.

Gamble MV, Liu X, Slavkovich V, Pilsner JR, Ilievski V, Factor-Litvak P, et al. 2007. Folic acid supplementation lowers blood arsenic. Am J Clin Nutr 86:1202-1209.

Garg SK, Yan Z, Vitvitsky V, Banerjee R. 2011. Differential dependence on cysteine from transsulfuration versus transport during t cell activation. Antioxid Redox Signal 15:39-47.

Ghosh P, Basu A, Mahata J, Basu S, Sengupta M, Das JK, et al. 2006. Cytogenetic damage and genetic variants in the individuals susceptible to arsenic-induced cancer through drinking water. International journal of cancer Journal international du cancer 118:2470-2478.

Gillette JR, Brodie BB, La Du BN. 1957. The oxidation of drugs by liver microsomes: On the role of tpnh and oxygen. J Pharmacol Exp Ther 119:532-540.

Gilmore TD. 2006. Introduction to nf-[kappa]b: Players, pathways, perspectives. Oncogene 25:6680-6684.

Gonsebatt ME, Vega L, Salazar AM, Montero R, Guzman P, Blas J, et al. 1997. Cytogenetic effects in human exposure to arsenic. Mutat Res 386:219-228.

Grek CL, Zhang J, Manevich Y, Townsend DM, Tew KD. 2013. Causes and consequences of cysteine s-glutathionylation. Journal of Biological Chemistry 288:26497-26504.

Griffith OW. 1999. Biologic and pharmacologic regulation of mammalian glutathione synthesis. Free Radic Biol Med 27:922-935.

Guengerich FP. 2008. Cytochrome p450 and chemical toxicology. Chem Res Toxicol 21:70-83.

Guo Junjie U, Su Y, Zhong C, Ming G-l, Song H. 2011. Hydroxylation of 5-methylcytosine by tet1 promotes active DNA demethylation in the adult brain. Cell 145:423-434.

Guo X, Fujino Y, Kaneko S, Wu K, Xia Y, Yoshimura T. 2001. Arsenic contamination of groundwater and prevalence of arsenical dermatosis in the hetao plain area, inner mongolia, china. Molecular and cellular biochemistry 222:137-140.

Guttmann RP, Powell TJ. 2012. Redox regulation of cysteine-dependent enzymes in neurodegeneration. International Journal of Cell Biology 2012:8.

Halazonetis TD, Georgopoulos K, Greenberg ME, Leder P. 1988. C-jun dimerizes with itself and with c-fos, forming complexes of different DNA binding affinities. Cell 55:917-924.

Hall MN, Gamble MV. 2012. Nutritional manipulation of one-carbon metabolism: Effects on arsenic methylation and toxicity. Journal of toxicology 2012:595307.

Halliwell B. 1989. Free radicals, reactive oxygen species and human disease: A critical evaluation with special reference to atherosclerosis. British journal of experimental pathology 70:737-757.

Hamilton CA, Brosnan MJ, McIntyre M, Graham D, Dominiczak AF. 2001. Superoxide excess in hypertension and aging: A common cause of endothelial dysfunction. Hypertension 37:529-534.

Hansen RE, Roth D, Winther JR. 2009. Quantifying the global cellular thiol–disulfide status. Proceedings of the National Academy of Sciences 106:422-427.

Haque R, Mazumder DN, Samanta S, Ghosh N, Kalman D, Smith MM, et al. 2003. Arsenic in drinking water and skin lesions: Dose-response data from west bengal, india. Epidemiology 14:174-182.

Harvey CJ, Thimmulappa RK, Singh A, Blake DJ, Ling G, Wakabayashi N, et al. 2009. Nrf2-regulated glutathione recycling independent of biosynthesis is critical for cell survival during oxidative stress. Free Radic Biol Med 46:443-453.

Hayakawa T, Kobayashi Y, Cui X, Hirano S. 2005. A new metabolic pathway of arsenite: Arsenic-glutathione complexes are substrates for human arsenic methyltransferase cyt19. Arch Toxicol 79:183-191.

Hayes JD, Pulford DJ. 1995. The glutathione s-transferase supergene family: Regulation of gst and the contribution of the isoenzymes to cancer chemoprotection and drug resistance. Critical reviews in biochemistry and molecular biology 30:445-600.

Heck JE, Gamble MV, Chen Y, Graziano JH, Slavkovich V, Parvez F, et al. 2007. Consumption of folate-related nutrients and metabolism of arsenic in bangladesh. Am J Clin Nutr 85:1367-1374.

Herrmann W, Obeid R. 2011. Homocysteine: A biomarker in neurodegenerative diseases. Clinical chemistry and laboratory medicine : CCLM / FESCC 49:435-441.

Herscovitch M, Comb W, Ennis T, Coleman K, Yong S, Armstead B, et al. 2008. Intermolecular disulfide bond formation in the nemo dimer requires cys54 and cys347. Biochem Biophys Res Commun 367:103-108.

Hess J, Angel P, Schorpp-Kistner M. 2004. Ap-1 subunits: Quarrel and harmony among siblings. J Cell Sci 117:5965-5973.

Holliday R, Pugh JE. 1975. DNA modification mechanisms and gene activity during development. Science 187:226-232.

Hsu L-I, Chen G-S, Lee C-H, Yang T-Y, Chen Y-H, Wang Y-H, et al. 2013. Use of arsenic-induced palmoplantar hyperkeratosis and skin cancers to predict risk of subsequent internal malignancy. American journal of epidemiology 177:202-212.

Huff J, Chan P, Nyska A. 2000. Is the human carcinogen arsenic carcinogenic to laboratory animals? Toxicological Sciences 55:17-23.

Hughes MF. 2002. Arsenic toxicity and potential mechanisms of action. Toxicology Letters 133:1-16.

Hughes MF, Edwards BC, Herbin-Davis KM, Saunders J, Styblo M, Thomas DJ. 2010. Arsenic (+3 oxidation state) methyltransferase genotype affects steady-state distribution and clearance of arsenic in arsenate-treated mice. Toxicol Appl Pharmacol 249:217-223.

Hughes MF, Beck BD, Chen Y, Lewis AS, Thomas DJ. 2011. Arsenic exposure and toxicology: A historical perspective. Toxicological Sciences 123:305-332.

Hustad S, Ueland PM, Vollset SE, Zhang Y, Bjørke-Monsen AL, Schneede J. 2000. Riboflavin as a determinant of plasma total homocysteine: Effect modification by the methylenetetrahydrofolate reductase c677t polymorphism. Clinical Chemistry 46:1065-1071.

Ifergan I, Assaraf YG. 2008. Chapter 4 molecular mechanisms of adaptation to folate deficiency. In: Vitamins & hormones, Vol. Volume 79, (Gerald L, ed):Academic Press, 99-143.

Imaoka S, Osada M, Minamiyama Y, Yukimura T, Toyokuni S, Takemura S, et al. 2004. Role of phenobarbital-inducible cytochrome p450s as a source of active oxygen species in DNA-oxidation. Cancer Lett 203:117-125.

Imbert V, Rupec RA, Livolsi A, Pahl HL, Traenckner EB, Mueller-Dieckmann C, et al. 1996. Tyrosine phosphorylation of i kappa b-alpha activates nf-kappa b without proteolytic degradation of i kappa b-alpha. Cell 86:787-798.

Ito S, Dalessio AC, Taranova OV, Hong K, Sowers LC, Zhang Y. 2010. Role of tet proteins in 5mc to 5hmc conversion, es-cell self-renewal and inner cell mass specification. Nature 466:1129-1133.

Itoh K, Chiba T, Takahashi S, Ishii T, Igarashi K, Katoh Y, et al. 1997. An nrf2/small maf heterodimer mediates the induction of phase ii detoxifying enzyme genes through antioxidant response elements. Biochem Biophys Res Commun 236:313-322.

James SJ, Miller BJ, Cross DR, McGarrity LJ, Morris SM. 1993. The essentiality of folate for the maintenance of deoxynucleotide precursor pools, DNA synthesis, and cell cycle progression in pha-stimulated lymphocytes. Environ Health Perspect 101 Suppl 5:173-178.

James SJ, Melnyk S, Pogribna M, Pogribny IP, Caudill MA. 2002. Elevation in s-adenosylhomocysteine and DNA hypomethylation: Potential epigenetic mechanism for homocysteine-related pathology. The Journal of Nutrition 132:2361S-2366S.

Jencks DA, Mathews RG. 1987. Allosteric inhibition of methylenetetrahydrofolate reductase by adenosylmethionine. Effects of adenosylmethionine and nadph on the equilibrium between active and inactive forms of the enzyme and on the kinetics of approach to equilibrium. J Biol Chem 262:2485-2493.

Jiang F, Zhang Y, Dusting GJ. 2011. Nadph oxidase-mediated redox signaling: Roles in cellular stress response, stress tolerance, and tissue repair. Pharmacological Reviews 63:218-242.

Jiang S, Cheng R, Wang X, Xue T, Liu Y, Nel A, et al. 2013. Real-time electrical detection of nitric oxide in biological systems with sub-nanomolar sensitivity. Nat Commun 4.

Jones DP, Carlson JL, Mody VC, Cai J, Lynn MJ, Sternberg P. 2000. Redox state of glutathione in human plasma. Free Radic Biol Med 28:625-635.

Jones DP. 2008. Radical-free biology of oxidative stress. American Journal of Physiology - Cell Physiology 295:C849-C868.

Jones DP, Go YM. 2010. Redox compartmentalization and cellular stress. Diabetes, obesity & metabolism 12 Suppl 2:116-125.

Jozefczak M, Remans T, Vangronsveld J, Cuypers A. 2012. Glutathione is a key player in metal-induced oxidative stress defenses. International journal of molecular sciences 13:3145-3175.

Kala SV, Neely MW, Kala G, Prater CI, Atwood DW, Rice JS, et al. 2000. The mrp2/cmoat transporter and arsenic-glutathione complex formation are required for biliary excretion of arsenic. Journal of Biological Chemistry 275:33404-33408.

Kalinina EV, Chernov NN, Saprin AN. 2008. Involvement of thio-, peroxi-, and glutaredoxins in cellular redox-dependent processes. Biochemistry Biokhimiia 73:1493-1510.

Kamata H, Manabe T, Oka S, Kamata K, Hirata H. 2002. Hydrogen peroxide activates ikappab kinases through phosphorylation of serine residues in the activation loops. FEBS Lett 519:231-237.

Kamata H, Honda S, Maeda S, Chang L, Hirata H, Karin M. 2005. Reactive oxygen species promote tnfalpha-induced death and sustained jnk activation by inhibiting map kinase phosphatases. Cell 120:649-661.

Karin M, Shaulian E. 2001. Ap-1: Linking hydrogen peroxide and oxidative stress to the control of cell proliferation and death. IUBMB Life 52:17-24.

Katoh T, Yamano Y, Tsuji M, Watanabe M. 2008. Genetic polymorphisms of human cytosol glutathione s-transferases and prostate cancer. Pharmacogenomics 9:93-104.

Kil IS, Kim SY, Park JW. 2008. Glutathionylation regulates ikappab. Biochem Biophys Res Commun 373:169-173.

Kinniburgh D, Smedley P. 2001. Arsenic contamination of groundwater in bangladesh. Vol. 2: Final report. [accessed October 10 2013].

Klee GG. 2000. Cobalamin and folate evaluation: Measurement of methylmalonic acid and homocysteine vs vitamin b12 and folate. Clinical Chemistry 46:1277-1283.

Kligerman AD, Doerr CL, Tennant AH, Harrington-Brock K, Allen JW, Winkfield E, et al. 2003. Methylated trivalent arsenicals as candidate ultimate genotoxic forms of arsenic: Induction of chromosomal mutations but not gene mutations. Environmental and molecular mutagenesis 42:192-205.

Klomsiri C, Karplus PA, Poole LB. 2011. Cysteine-based redox switches in enzymes. Antioxid Redox Signal 14:1065-1077.

Klose RJ, Bird AP. 2006. Genomic DNA methylation: The mark and its mediators. Trends in biochemical sciences 31:89-97.

Koong AC, Chen EY, Giaccia AJ. 1994. Hypoxia causes the activation of nuclear factor kappa b through the phosphorylation of i kappa b alpha on tyrosine residues. Cancer Res 54:1425-1430.

Korn SH, Wouters EF, Vos N, Janssen-Heininger YM. 2001. Cytokine-induced activation of nuclear factor-kappa b is inhibited by hydrogen peroxide through oxidative inactivation of ikappab kinase. J Biol Chem 276:35693-35700.

Kriaucionis S, Heintz N. 2009. The nuclear DNA base 5-hydroxymethylcytosine is present in purkinje neurons and the brain. Science 324:929-930.

Kullak-Ublick GA, Baretton GB, Oswald M, Renner EL, Paumgartner G, Beuers U. 2002. Expression of the hepatocyte canalicular multidrug resistance protein (mrp2) in primary biliary cirrhosis. Hepatology research : the official journal of the Japan Society of Hepatology 23:78-82.

Kuzkaya N, Weissmann N, Harrison DG, Dikalov S. 2003. Interactions of peroxynitrite, tetrahydrobiopterin, ascorbic acid, and thiols: Implications for uncoupling endothelial nitric-oxide synthase. J Biol Chem 278:22546-22554.

Lee J-H, Voo KS, Skalnik DG. 2001. Identification and characterization of the DNA binding domain of cpg-binding protein. Journal of Biological Chemistry 276:44669-44676.

Lee TC, Tanaka N, Lamb PW, Gilmer TM, Barrett JC. 1988. Induction of gene amplification by arsenic. Science 241:79-81.

Lei H, Oh SP, Okano M, Juttermann R, Goss KA, Jaenisch R, et al. 1996. De novo DNA cytosine methyltransferase activities in mouse embryonic stem cells. Development (Cambridge, England) 122:3195-3205.

Leonhardt H, Page AW, Weier HU, Bestor TH. 1992. A targeting sequence directs DNA methyltransferase to sites of DNA replication in mammalian nuclei. Cell 71:865-873.

Lerda D. 1994. Sister-chromatid exchange (sce) among individuals chronically exposed to arsenic in drinking water. Mutat Res 312:111-120.

Li N, Karin M. 1999. Is nf-kappab the sensor of oxidative stress? FASEB J 13:1137-1143.

Li Q, Engelhardt JF. 2006. Interleukin-1beta induction of nfkappab is partially regulated by h2o2-mediated activation of nfkappab-inducing kinase. J Biol Chem 281:1495-1505.

Li X, Stark GR. 2002. Nfkappab-dependent signaling pathways. Experimental hematology 30:285-296.

Li X, Cao J, Wang S, Geng Z, Song X, Hu X, et al. 2013a. Residues in human arsenic (+3 oxidation state) methyltransferase forming potential hydrogen bond network around s-adenosylmethionine. PLoS ONE 8:e76709.

Li X, Geng Z, Wang S, Song X, Hu X, Wang Z. 2013b. Functional evaluation of asp76, 84, 102 and 150 in human arsenic(iii) methyltransferase (has3mt) interacting with s-adenosylmethionine. FEBS Letters 587:2232-2240.

Lin S, Shi Q, Nix FB, Styblo M, Beck MA, Herbin-Davis KM, et al. 2002. A novel s-adenosyl-l-methionine:Arsenic(iii) methyltransferase from rat liver cytosol. J Biol Chem 277:10795-10803.

Longley DB, Harkin DP, Johnston PG. 2003. 5-fluorouracil: Mechanisms of action and clinical strategies. Nat Rev Cancer 3:330-338.

Lu SC. 2009. Regulation of glutathione synthesis. Mol Aspects Med 30:42-59.

Ma Y, Jacobs SB, Jackson-Grusby L, Mastrangelo M-A, Torres-Betancourt JA, Jaenisch R, et al. 2005. DNA cpg hypomethylation induces heterochromatin reorganization involving the histone variant macroh2a. Journal of Cell Science 118:1607-1616.

Maciaszczyk-Dziubinska E, Wawrzycka D, Wysocki R. 2012. Arsenic and antimony transporters in eukaryotes. International journal of molecular sciences 13:3527-3548.

Mahata J, Basu A, Ghoshal S, Sarkar JN, Roy AK, Poddar G, et al. 2003. Chromosomal aberrations and sister chromatid exchanges in individuals exposed to arsenic through drinking water in west bengal, india. Mutat Res 534:133-143.

Malhotra JD, Kaufman RJ. 2007. Endoplasmic reticulum stress and oxidative stress: A vicious cycle or a double-edged sword? Antioxid Redox Signal 9:2277-2293.

Mandal BK, Suzuki KT. 2002. Arsenic round the world: A review. Talanta 58:201-235.

Margot J, Ehrenhofer-Murray A, Leonhardt H. 2003. Interactions within the mammalian DNA methyltransferase family. BMC Molecular Biology 4:7.

Mari M, Morales A, Colell A, Garcia-Ruiz C, Fernandez-Checa JC. 2009. Mitochondrial glutathione, a key survival antioxidant. Antioxid Redox Signal 11:2685-2700.

Matthews JR, Kaszubska W, Turcatti G, Wells TN, Hay RT. 1993. Role of cysteine62 in DNA recognition by the p50 subunit of nf-kappa b. Nucleic Acids Res 21:1727-1734.

Matthews RG, Sheppard C, Goulding C. 1998. Methylenetetrahydrofolate reductase and methionine synthase: Biochemistry and molecular biology. European journal of pediatrics 157 Suppl 2:S54-59.

McBean GJ. 2012. The transsulfuration pathway: A source of cysteine for glutathione in astrocytes. Amino acids 42:199-205.

McGuire JJ, Hsieh P, Coward JK, Bertino JR. 1980. Enzymatic synthesis of folylpolyglutamates. Characterization of the reaction and its products. Journal of Biological Chemistry 255:5776-5788.

McNulty H, McKinley MC, Wilson B, McPartlin J, Strain J, Weir DG, et al. 2002. Impaired functioning of thermolabile methylenetetrahydrofolate reductase is dependent on riboflavin status: Implications for riboflavin requirements. The American Journal of Clinical Nutrition 76:436-441.

Meister A, Anderson ME, Hwang O. 1986. Intracellular cysteine and glutathione delivery systems. Journal of the American College of Nutrition 5:137-151.

Melnyk S, Pogribna M, Miller BJ, Basnakian AG, Pogribny IP, James SJ. 1999. Uracil misincorporation, DNA strand breaks, and gene amplification are associated with tumorigenic

cell transformation in folate deficient/repleted chinese hamster ovary cells. Cancer Lett 146:35-44.

Meunier B, de Visser SP, Shaik S. 2004. Mechanism of oxidation reactions catalyzed by cytochrome p450 enzymes. Chem Rev 104:3947-3980.

Meza MM, Kopplin MJ, Burgess JL, Gandolfi AJ. 2004. Arsenic drinking water exposure and urinary excretion among adults in the yaqui valley, sonora, mexico. Environ Res 96:119-126.

Moghadaszadeh B, Beggs AH. 2006. Selenoproteins and their impact on human health through diverse physiological pathways. Physiology (Bethesda, Md) 21:307-315.

Morgan MJ, Liu Z-g. 2011. Crosstalk of reactive oxygen species and nf-[kappa]b signaling. Cell research 21:103-115.

Mosharov E, Cranford MR, Banerjee R. 2000. The quantitatively important relationship between homocysteine metabolism and glutathione synthesis by the transsulfuration pathway and its regulation by redox changes. Biochemistry 39:13005-13011.

Mueller CFH, Widder JD, McNally JS, McCann L, Jones DP, Harrison DG. 2005. The role of the multidrug resistance protein-1 in modulation of endothelial cell oxidative stress. Circulation Research 97:637-644.

Murphy MP. 2009. How mitochondria produce reactive oxygen species. Biochem J 417:1-13.

Mytilineou C, Kramer BC, Yabut JA. 2002. Glutathione depletion and oxidative stress. Parkinsonism & related disorders 8:385-387.

Naranmandura H, Carew MW, Xu S, Lee J, Leslie EM, Weinfeld M, et al. 2011. Comparative toxicity of arsenic metabolites in human bladder cancer ej-1 cells. Chem Res Toxicol 24:1586-1596.

Naujokas MF, Anderson B, Ahsan H, Aposhian HV, Graziano JH, Thompson C, et al. 2013. The broad scope of health effects from chronic arsenic exposure: Update on a worldwide public health problem. Environ Health Perspect 121:295-302.

Nauseef WM. 2008. Biological roles for the nox family nadph oxidases. Journal of Biological Chemistry 283:16961-16965.

Nguyen T, Nioi P, Pickett CB. 2009. The nrf2-antioxidant response element signaling pathway and its activation by oxidative stress. J Biol Chem 284:13291-13295.

Noor R, Mittal S, Iqbal J. 2002. Superoxide dismutase--applications and relevance to human diseases. Medical science monitor : international medical journal of experimental and clinical research 8:RA210-215.

Nordblom GD, Coon MJ. 1977. Hydrogen peroxide formation and stoichiometry of hydroxylation reactions catalyzed by highly purified liver microsomal cytochrome p-450. Arch Biochem Biophys 180:343-347.

Obeid R, Morkbak AL, Munz W, Nexo E, Herrmann W. 2006. The cobalamin-binding proteins transcobalamin and haptocorrin in maternal and cord blood sera at birth. Clin Chem 52:263-269.

Okano M, Xie S, Li E. 1998. Cloning and characterization of a family of novel mammalian DNA (cytosine-5) methyltransferases. Nat Genet 19:219-220.

Omiecinski CJ, Vanden Heuvel JP, Perdew GH, Peters JM. 2011. Xenobiotic metabolism, disposition, and regulation by receptors: From biochemical phenomenon to predictors of major toxicities. Toxicological Sciences 120:S49-S75.

Parman T, Wiley MJ, Wells PG. 1999. Free radical-mediated oxidative DNA damage in the mechanism of thalidomide teratogenicity. Nature medicine 5:582-585.

Paulsen CE, Carroll KS. 2013. Cysteine-mediated redox signaling: Chemistry, biology, and tools for discovery. Chem Rev 113:4633-4679.

Petrick JS, Ayala-Fierro F, Cullen WR, Carter DE, Vasken Aposhian H. 2000. Monomethylarsonous acid (mma(iii)) is more toxic than arsenite in chang human hepatocytes. Toxicol Appl Pharmacol 163:203-207.

Petrick JS, Jagadish B, Mash EA, Aposhian HV. 2001. Monomethylarsonous acid (mma(iii)) and arsenite: Ld(50) in hamsters and in vitro inhibition of pyruvate dehydrogenase. Chem Res Toxicol 14:651-656.

Pikuleva IA, Waterman MR. 2013. Cytochromes p450: Roles in diseases. J Biol Chem 288:17091-17098.

Pineda-Molina E, Klatt P, Vazquez J, Marina A, Garcia de Lacoba M, Perez-Sala D, et al. 2001. Glutathionylation of the p50 subunit of nf-kappab: A mechanism for redox-induced inhibition of DNA binding. Biochemistry 40:14134-14142.

Prudova A, Bauman Z, Braun A, Vitvitsky V, Lu SC, Banerjee R. 2006. S-adenosylmethionine stabilizes cystathionine beta-synthase and modulates redox capacity. Proc Natl Acad Sci U S A 103:6489-6494.

Qiu A, Jansen M, Sakaris A, Min SH, Chattopadhyay S, Tsai E, et al. 2006. Identification of an intestinal folate transporter and the molecular basis for hereditary folate malabsorption. Cell 127:917-928.

Qiu C, Sawada K, Zhang X, Cheng X. 2002. The pwwp domain of mammalian DNA methyltransferase dnmt3b defines a new family of DNA-binding folds. Nature structural biology 9:217-224.

Quadros EV, Sequeira JM. 2013. Cellular uptake of cobalamin: Transcobalamin and the tcblr/cd320 receptor. Biochimie 95:1008-1018.

Ramsahoye BH, Biniszkiewicz D, Lyko F, Clark V, Bird AP, Jaenisch R. 2000. Non-cpg methylation is prevalent in embryonic stem cells and may be mediated by DNA methyltransferase 3a. Proceedings of the National Academy of Sciences 97:5237-5242.

Razin A, Shemer R. 1995. DNA methylation in early development. Human molecular genetics 4 Spec No:1751-1755.

Reddy JA, Haneline LS, Srour EF, Antony AC, Clapp DW, Low PS. 1999. Expression and functional characterization of the beta-isoform of the folate receptor on cd34(+) cells. Blood 93:3940-3948.

Reed MC, Nijhout HF, Neuhouser ML, Gregory JF, 3rd, Shane B, James SJ, et al. 2006. A mathematical model gives insights into nutritional and genetic aspects of folate-mediated one-carbon metabolism. J Nutr 136:2653-2661.

Reidy JA. 1988. Role of deoxyuridine incorporation and DNA repair in the expression of human chromosomal fragile sites. Mutat Res 200:215-220.

Reitman ZJ, Yan H. 2010. Isocitrate dehydrogenase 1 and 2 mutations in cancer: Alterations at a crossroads of cellular metabolism. Journal of the National Cancer Institute 102:932-941.

Reynaert NL, van der Vliet A, Guala AS, McGovern T, Hristova M, Pantano C, et al. 2006. Dynamic redox control of nf-κb through glutaredoxin-regulated s-glutathionylation of inhibitory κb kinase β. Proceedings of the National Academy of Sciences 103:13086-13091.

Rhee MS, Lindau-Shepard B, Chave KJ, Galivan J, Ryan TJ. 1998. Characterization of human cellular γ-glutamyl hydrolase. Molecular pharmacology 53:1040-1046.

Riggs AD. 1975. X inactivation, differentiation, and DNA methylation. Cytogenetics and cell genetics 14:9-25.

Rogers LM, Pfeiffer CM, Bailey LB, Gregory JF. 1997. A dual-label stable-isotopic protocol is suitable for determination of folate bioavailability in humans: Evaluation of urinary excretion and plasma folate kinetics of intravenous and oral doses of [13c5] and [2h2]folic acid. J Nutr 127:2321-2327.

Roje S. 2006. S-adenosyl-l-methionine: Beyond the universal methyl group donor. Phytochemistry 67:1686-1698.

Rossman TG, Stone D, Molina M, Troll W. 1980. Absence of arsenite mutagenicity in e coli and chinese hamster cells. Environmental mutagenesis 2:371-379.

Rusk N. 2012. Epigenetics: The sixth base and counting. Nat Meth 9:646-646.

Saha JC, Dikshit AK, Bandyopadhyay M, Saha KC. 1999. A review of arsenic poisoning and its effects on human health. Critical Reviews in Environmental Science and Technology 29:281-313.

Saxonov S, Berg P, Brutlag DL. 2006. A genome-wide analysis of cpg dinucleotides in the human genome distinguishes two distinct classes of promoters. Proceedings of the National Academy of Sciences of the United States of America 103:1412-1417.

Schafer FQ, Buettner GR. 2001. Redox environment of the cell as viewed through the redox state of the glutathione disulfide/glutathione couple. Free Radic Biol Med 30:1191-1212.

Schenk H, Klein M, Erdbrugger W, Droge W, Schulze-Osthoff K. 1994. Distinct effects of thioredoxin and antioxidants on the activation of transcription factors nf-kappa b and ap-1. Proc Natl Acad Sci U S A 91:1672-1676.

Schisler NJ, Singh SM. 1987. Inheritance and expression of tissue-specific catalase activity during development and aging in mice. Genome / National Research Council Canada = Genome / Conseil national de recherches Canada 29:748-760.

Schreck R, Rieber P, Baeuerle PA. 1991. Reactive oxygen intermediates as apparently widely used messengers in the activation of the nf-kappa b transcription factor and hiv-1. EMBO J 10:2247-2258.

Scott JM, Weir DG. 1981. The methyl folate trap. A physiological response in man to prevent methyl group deficiency in kwashiorkor (methionine deficiency) and an explanation for folic-acid induced exacerbation of subacute combined degeneration in pernicious anaemia. Lancet 2:337-340.

Seetharam B, Li N. 2000. Transcobalamin ii and its cell surface receptor. Vitamins and hormones 59:337-366.

Shelton MD, Chock PB, Mieyal JJ. 2005. Glutaredoxin: Role in reversible protein s-glutathionylation and regulation of redox signal transduction and protein translocation. Antioxid Redox Signal 7:348-366.

Shen HM, Liu ZG. 2006. Jnk signaling pathway is a key modulator in cell death mediated by reactive oxygen and nitrogen species. Free Radic Biol Med 40:928-939.

Sies H. 1974. Biochemistry of the peroxisome in the liver cell. Angewandte Chemie (International ed in English) 13:706-718.

Singh AP, Goel RK, Kaur T. 2011. Mechanisms pertaining to arsenic toxicity. Toxicology international 18:87-93.

Siomek A. 2012. Nf-kappab signaling pathway and free radical impact. Acta biochimica Polonica 59:323-331.

Smith ZD, Meissner A. 2013. DNA methylation: Roles in mammalian development. Nat Rev Genet 14:204-220.

Song C-X, Szulwach KE, Fu Y, Dai Q, Yi C, Li X, et al. 2011. Selective chemical labeling reveals the genome-wide distribution of 5-hydroxymethylcytosine. Nat Biotech 29:68-72.

Song X, Geng Z, Zhu J, Li C, Hu X, Bian N, et al. 2009. Structure–function roles of four cysteine residues in the human arsenic (+3 oxidation state) methyltransferase (has3mt) by site-directed mutagenesis. Chemico-Biological Interactions 179:321-328.

Song X, Geng Z, Li X, Zhao Q, Hu X, Zhang X, et al. 2011. Functional and structural evaluation of cysteine residues in the human arsenic (+3 oxidation state) methyltransferase (has3mt). Biochimie 93:369-375.

Spiegelstein O, Lu X, Le XC, Troen A, Selhub J, Melnyk S, et al. 2005. Effects of dietary folate intake and folate binding protein-2 (folbp2) on urinary speciation of sodium arsenate in mice. Environmental toxicology and pharmacology 19:1-7.

Starke DW, Chock PB, Mieyal JJ. 2003. Glutathione-thiyl radical scavenging and transferase properties of human glutaredoxin (thioltransferase). Potential role in redox signal transduction. J Biol Chem 278:14607-14613.

Steinberg SE, Campbell CL, Hillman RS. 1979. Kinetics of the normal folate enterohepatic cycle. J Clin Invest 64:83-88.

Steinmaus C, Yuan Y, Kalman D, Rey OA, Skibola CF, Dauphine D, et al. 2010. Individual differences in arsenic metabolism and lung cancer in a case-control study in cordoba, argentina. Toxicol Appl Pharmacol 247:138-145.

Stipanuk MH, Dominy JE, Jr., Lee JI, Coloso RM. 2006. Mammalian cysteine metabolism: New insights into regulation of cysteine metabolism. J Nutr 136:1652S-1659S.

Stohs SJ, Bagchi D. 1995. Oxidative mechanisms in the toxicity of metal ions. Free Radic Biol Med 18:321-336.

Styblo M, Del Razo LM, Vega L, Germolec DR, LeCluyse EL, Hamilton GA, et al. 2000. Comparative toxicity of trivalent and pentavalent inorganic and methylated arsenicals in rat and human cells. Arch Toxicol 74:289-299.

Suh YA, Arnold RS, Lassegue B, Shi J, Xu X, Sorescu D, et al. 1999. Cell transformation by the superoxide-generating oxidase mox1. Nature 401:79-82.

Sun SC. 2011. Non-canonical nf-kappab signaling pathway. Cell research 21:71-85.

Sun Z, Andersson R. 2002. Nf-kappab activation and inhibition: A review. Shock (Augusta, Ga) 18:99-106.

Szulwach KE, Li X, Li Y, Song CX, Wu H, Dai Q, et al. 2011. 5-hmc-mediated epigenetic dynamics during postnatal neurodevelopment and aging. Nat Neurosci 14:1607-1616.

Tahiliani M, Koh KP, Shen Y, Pastor WA, Bandukwala H, Brudno Y, et al. 2009. Conversion of 5-methylcytosine to 5-hydroxymethylcytosine in mammalian DNA by mll partner tet1. Science 324:930-935.

Taoka S, Ohja S, Shan X, Kruger WD, Banerjee R. 1998. Evidence for heme-mediated redox regulation of human cystathionine beta-synthase activity. J Biol Chem 273:25179-25184.

Taoka S, Lepore BW, Kabil O, Ojha S, Ringe D, Banerjee R. 2002. Human cystathionine beta-synthase is a heme sensor protein. Evidence that the redox sensor is heme and not the vicinal cysteines in the cxxc motif seen in the crystal structure of the truncated enzyme. Biochemistry 41:10454-10461.

ter Welle HF, Slater EC. 1967. Uncoupling of respiratory-chain phosphorylation by arsenate. Biochim Biophys Acta 143:1-17.

Thomas DJ, Styblo M, Lin S. 2001. The cellular metabolism and systemic toxicity of arsenic. Toxicol Appl Pharmacol 176:127-144.

Thomas DJ. 2009. Unraveling arsenic--glutathione connections. Toxicol Sci 107:309-311.

Tibbetts AS, Appling DR. 2010. Compartmentalization of mammalian folate-mediated one-carbon metabolism. Annual review of nutrition 30:57-81.

Tice RR, Yager JW, Andrews P, Crecelius E. 1997. Effect of hepatic methyl donor status on urinary excretion and DNA damage in b6c3f1 mice treated with sodium arsenite. Mutat Res 386:315-334.

Tiedge M, Lortz S, Drinkgern J, Lenzen S. 1997. Relation between antioxidant enzyme gene expression and antioxidative defense status of insulin-producing cells. Diabetes 46:1733-1742.

Tokar EJ, Benbrahim-Tallaa L, Ward JM, Lunn R, Sams RL, 2nd, Waalkes MP. 2010. Cancer in experimental animals exposed to arsenic and arsenic compounds. Critical reviews in toxicology 40:912-927.

Toledano MB, Leonard WJ. 1991. Modulation of transcription factor nf-kappa b binding activity by oxidation-reduction in vitro. Proc Natl Acad Sci U S A 88:4328-4332.

Tondel M, Rahman M, Magnuson A, Chowdhury IA, Faruquee MH, Ahmad SA. 1999. The relationship of arsenic levels in drinking water and the prevalence rate of skin lesions in bangladesh. Environ Health Perspect 107:727-729.

Torres M, Forman HJ. 2003. Redox signaling and the map kinase pathways. BioFactors (Oxford, England) 17:287-296.

Traore K, Sharma R, Thimmulappa RK, Watson WH, Biswal S, Trush MA. 2008. Redox-regulation of erk1/2-directed phosphatase by reactive oxygen species: Role in signaling tpa-induced growth arrest in ml-1 cells. Journal of cellular physiology 216:276-285.

Tretter L, Adam-Vizi V. 2005. Alpha-ketoglutarate dehydrogenase: A target and generator of oxidative stress. Philosophical transactions of the Royal Society of London Series B, Biological sciences 360:2335-2345.

Tseng WP, Chu HM, How SW, Fong JM, Lin CS, Yeh S. 1968. Prevalence of skin cancer in an endemic area of chronic arsenicism in taiwan. Journal of the National Cancer Institute 40:453-463.

Ueland PM, Hustad S, Schneede J, Refsum H, Vollset SE. 2001. Biological and clinical implications of the mthfr c677t polymorphism. Trends in pharmacological sciences 22:195-201.

U.S. Department of Agriculture, Agricultural Research Service. 2013. USDA National Nutrient Database for Standard Reference, Release 26. Available: http://www.ars.usda.gov/ba/bhnrc/ndl [accessed October 15 2013].

Vahter M, Marafante E. 1987. Effects of low dietary intake of methionine, choline or proteins on the biotransformation of arsenite in the rabbit. Toxicol Lett 37:41-46.

Vahter M, Concha G. 2001. Role of metabolism in arsenic toxicity. Pharmacol Toxicol 89:1-5.

Valinluck V, Sowers LC. 2007. Endogenous cytosine damage products alter the site selectivity of human DNA maintenance methyltransferase dnmt1. Cancer Res 67:946-950.

Vallabhapurapu S, Karin M. 2009. Regulation and function of nf-kappab transcription factors in the immune system. Annual review of immunology 27:693-733.

Verhaar MC, Westerweel PE, van Zonneveld AJ, Rabelink TJ. 2004. Free radical production by dysfunctional enos. Heart (British Cardiac Society) 90:494-495.

Vermeulen EG, Stehouwer CD, Twisk JW, van den Berg M, de Jong SC, Mackaay AJ, et al. 2000. Effect of homocysteine-lowering treatment with folic acid plus vitamin b6 on progression of subclinical atherosclerosis: A randomised, placebo-controlled trial. Lancet 355:517-522.

Villa-Bellosta R, Sorribas V. 2008. Role of rat sodium/phosphate cotransporters in the cell membrane transport of arsenate. Toxicol Appl Pharmacol 232:125-134.

Vitvitsky V, Thomas M, Ghorpade A, Gendelman HE, Banerjee R. 2006. A functional transsulfuration pathway in the brain links to glutathione homeostasis. J Biol Chem 281:35785-35793.

Wald DS, Law M, Morris JK. 2002. Homocysteine and cardiovascular disease: Evidence on causality from a meta-analysis. BMJ 325:1202.

Wang S, Li X, Song X, Geng Z, Hu X, Wang Z. 2012. Rapid equilibrium kinetic analysis of arsenite methylation catalyzed by recombinant human arsenic (+3 oxidation state) methyltransferase (has3mt). J Biol Chem 287:38790-38799.

Wang X, Martindale JL, Liu Y, Holbrook NJ. 1998. The cellular response to oxidative stress: Influences of mitogen-activated protein kinase signalling pathways on cell survival. Biochem J 333 (Pt 2):291-300.

Waris G, Ahsan H. 2006. Reactive oxygen species: Role in the development of cancer and various chronic conditions. Journal of Carcinogenesis 5:14.

Waters SB, Devesa V, Del Razo LM, Styblo M, Thomas DJ. 2004a. Endogenous reductants support the catalytic function of recombinant rat cyt19, an arsenic methyltransferase. Chem Res Toxicol 17:404-409.

Waters SB, Devesa V, Fricke MW, Creed JT, Styblo M, Thomas DJ. 2004b. Glutathione modulates recombinant rat arsenic (+3 oxidation state) methyltransferase-catalyzed formation of trimethylarsine oxide and trimethylarsine. Chem Res Toxicol 17:1621-1629.

Watson WH, Chen Y, Jones DP. 2003. Redox state of glutathione and thioredoxin in differentiation and apoptosis. BioFactors (Oxford, England) 17:307-314.

Whetstine JR, Flatley RM, Matherly LH. 2002. The human reduced folate carrier gene is ubiquitously and differentially expressed in normal human tissues: Identification of seven non-coding exons and characterization of a novel promoter. Biochem J 367:629-640.

World Health Organization. 2008. Guidelines for drinking-water quality: Incorporating first and second addenda to third edition. Vol. 1—recommendations. Available: http://www.who.int/water_sanitation_health/dwq/gdwq3/en/index.html [accessed October 15 2013].

World Health Organization. 2012. Serum and red blood cell folate concentrations for assessing folate status in populations. Vitamin and Mineral Nutrition Information System. Geneva:World Health Organization.

Wild AC, Moinova HR, Mulcahy RT. 1999. Regulation of gamma-glutamylcysteine synthetase subunit gene expression by the transcription factor nrf2. J Biol Chem 274:33627-33636.

Williams KT, Schalinske KL. 2007. New insights into the regulation of methyl group and homocysteine metabolism. The Journal of Nutrition 137:311-314.

Wlodarczyk B, Spiegelstein O, Hill D, Le XC, Finnell RH. 2012. Arsenic urinary speciation in mthfr deficient mice injected with sodium arsenate. Toxicol Lett 215:214-218.

Wolthers KR, Scrutton NS. 2007. Protein interactions in the human methionine synthase-methionine synthase reductase complex and implications for the mechanism of enzyme reactivation. Biochemistry 46:6696-6709.

Wossidlo M, Nakamura T, Lepikhov K, Marques CJ, Zakhartchenko V, Boiani M, et al. 2011. 5-hydroxymethylcytosine in the mammalian zygote is linked with epigenetic reprogramming. Nat Commun 2:241.

Wright AJ, Dainty JR, Finglas PM. 2007. Folic acid metabolism in human subjects revisited: Potential implications for proposed mandatory folic acid fortification in the uk. The British journal of nutrition 98:667-675.

Wu C, Leroux J-C, Gauthier MA. 2012. Twin disulfides for orthogonal disulfide pairing and the directed folding of multicyclic peptides. Nat Chem 4:1044-1049.

Wu G, Fang YZ, Yang S, Lupton JR, Turner ND. 2004. Glutathione metabolism and its implications for health. J Nutr 134:489-492.

Wu LL, Wu JT. 2002. Hyperhomocysteinemia is a risk factor for cancer and a new potential tumor marker. Clin Chim Acta 322:21-28.

Xu C, Li CY, Kong AN. 2005. Induction of phase i, ii and iii drug metabolism/transport by xenobiotics. Archives of pharmacal research 28:249-268.

Yoshida T, Yamauchi H, Fan Sun G. 2004. Chronic health effects in people exposed to arsenic via the drinking water: Dose-response relationships in review. Toxicol Appl Pharmacol 198:243-252.

Yu HS, Liao WT, Chai CY. 2006. Arsenic carcinogenesis in the skin. Journal of biomedical science 13:657-666.

Zaman GJ, Lankelma J, van Tellingen O, Beijnen J, Dekker H, Paulusma C, et al. 1995. Role of glutathione in the export of compounds from cells by the multidrug-resistance-associated protein. Proc Natl Acad Sci U S A 92:7690-7694.

Zhang DD, Hannink M. 2003. Distinct cysteine residues in keap1 are required for keap1-dependent ubiquitination of nrf2 and for stabilization of nrf2 by chemopreventive agents and oxidative stress. Mol Cell Biol 23:8137-8151.

Zhang DD, Lo SC, Cross JV, Templeton DJ, Hannink M. 2004. Keap1 is a redox-regulated substrate adaptor protein for a cul3-dependent ubiquitin ligase complex. Mol Cell Biol 24:10941-10953.

Zhang H, Forman HJ. 2012. Glutathione synthesis and its role in redox signaling. Seminars in cell & developmental biology 23:722-728.

Zhou H, Zarubin T, Ji Z, Min Z, Zhu W, Downey JS, et al. 2005. Frequency and distribution of ap-1 sites in the human genome. DNA Res 12:139-150.

Ziller MJ, Müller F, Liao J, Zhang Y, Gu H, Bock C, et al. 2011. Genomic distribution and inter-sample variation of non-cpg methylation across human cell types. PLoS Genet 7:e1002389.

Chapter 3: A dose–response study of arsenic exposure and global methylation of peripheral blood mononuclear cell DNA

Megan M. Niedzwiecki[1], Megan N. Hall[2], Xinhua Liu[3], Julie Oka[1], Kristin N. Harper[1], Vesna Slavkovich[1], Vesna Ilievski[1], Diane Levy[3], Alexander van Geen[4], Jacob L. Mey[4], Shafiul Alam[5], Abu B. Siddique[5], Faruque Parvez[1], Joseph H. Graziano[1], and Mary V. Gamble[1]

Affiliations: [1]Department of Environmental Health Sciences, [2]Department of Epidemiology, [3]Department of Biostatistics, [1-3]Mailman School of Public Health, Columbia University, New York NY,10032, USA; [4]Lamont-Doherty Earth Observatory of Columbia University, Palisades, NY, USA; [5]Columbia University Arsenic Project in Bangladesh, Dhaka, Bangladesh

Published: http://ehp.niehs.nih.gov/1206421

Niedzwiecki MM, Hall MN, Liu X, Oka J, Harper KN, Slavkovich V, Ilievski V, Levy D, van Geen A, Mey JL, Alam S, Siddique AB, Parvez F, Graziano JH, Gamble MV. **A Dose-Response Study of Arsenic Exposure and Global Methylation of Peripheral Blood Mononuclear Cell DNA in Bangladeshi Adults.** Environ Health Perspect. 2013 Nov-Dec;121(11-12):1306-12. doi: 10.1289/ehp.1206421.

ABSTRACT

BACKGROUND: Several studies employing cell culture and animal models suggest that arsenic (As) exposure induces global DNA hypomethylation. However, As has been associated with global DNA hypermethylation in human study populations. It has been hypothesized that this discrepancy may reflect a non-linear relationship between As dose and DNA methylation.

OBJECTIVE: The objective of this study was to examine the dose-response relationship between As and global methylation of peripheral blood mononuclear cell (PBMC) DNA in apparently healthy Bangladeshi adults chronically exposed to a wide range of As concentrations in drinking water.

METHODS: Global PBMC DNA methylation, plasma folate, blood *S*-adenosylmethionine (SAM), and concentrations of As in drinking water, blood, and urine were measured in 320 adults. DNA methylation was measured using the [^{3}H]-methyl incorporation assay, which provides disintegration per minute (DPM) values that are negatively associated with global DNA methylation.

RESULTS: Water, blood, and urinary As were positively correlated with global PBMC DNA methylation ($P < 0.05$). In multivariable adjusted models, 1-μg/L increases in water and urinary As were associated with 27.6 unit (95% CI, 6.3 to 49.0) and 22.1 unit (95% CI, 0.5 to 43.8) decreases in DPM per μg DNA, respectively. Categorical models indicated that estimated mean levels of PBMC DNA methylation were highest in participants with the highest As exposures.

CONCLUSIONS: These results suggest that As is positively associated with global methylation of PBMC DNA over a wide range of drinking water As concentrations. Further research is necessary to elucidate underlying mechanisms and physiologic implications.

INTRODUCTION

An estimated 70 million people in Bangladesh are chronically exposed to arsenic (As)-contaminated drinking water at levels over the World Health Organization (WHO) limit of 10 µg/L (Loewenberg 2007). Exposure to As has been associated with cancers of the skin, lung, bladder, liver, and kidney (Navarro Silvera and Rohan 2007), hypertension and cardiovascular disease (Chen et al. 1995; Chen et al. 2011; Tseng et al. 2003), respiratory outcomes (Chattopadhyay et al. 2010; Dauphine et al. 2011; Parvez et al. 2010), and reduced cognitive function in children (Hamadani et al. 2011; Wasserman et al. 2004). The mechanism(s) responsible for the pleiotropic health effects of As are not completely understood.

DNA methylation involves the covalent addition of a methyl group from *S*-adenosylmethionine (SAM) to the 5' position of cytosine bases in CpG dinucleotides (Zhao et al. 1997). SAM biosynthesis is regulated by one-carbon metabolism, a biochemical pathway for the methylation of numerous substrates that is dependent on folate for the recruitment of methyl groups from serine (Chiang et al. 1996). Methylation of CpG dinucleotides is associated with gene silencing: CpGs in intergenic regions and repetitive elements are usually methylated (Robertson 2001), while CpGs in gene promoter regions of transcriptionally active genes are generally less methylated than in other regions (Razin and Kantor 2005). Global DNA hypomethylation is associated with genomic instability, including loss of heterozygosity (Matsuzaki et al. 2005), aneuploidy (Dodge et al. 2005), and chromosomal alterations (Schulz et al. 2002), and is commonly observed in tumors and transformed cells (Gaudet et al. 2003). In addition, recent work by the ENCODE project (Consortium 2004) has highlighted important regulatory roles of methylation of transposable elements and other non-coding regions of the

genome (previously coined “junk DNA”) in cell-type dependent transcriptional regulation (Bernstein et al. 2012; Thurman et al. 2012).

Evidence based on *in vitro* and *in vivo* models suggests that chronic As exposure induces global DNA hypomethylation, in conjunction with hypermethylation of promoter regions of tumor suppressor genes (Benbrahim-Tallaa et al. 2005; Chen et al. 2004; Reichard et al. 2007; Ren et al. 2011). Based on this literature, we initially hypothesized that As exposure would be associated with a reduction in global methylation of DNA in a population chronically exposed to As-contaminated drinking water, providing a mechanistic link between As exposure and increased cancer risk. We further hypothesized that this would be exacerbated by folate deficiency. However, in our first population-based study on this subject, contrary to our *a priori* hypotheses, chronic As exposure was positively associated with global methylation of peripheral blood leukocyte (PBL) DNA among subjects with sufficient folate levels (Pilsner et al. 2007). While these findings were unanticipated, the positive association between As exposure and global DNA methylation in humans has been replicated by our group (Pilsner et al. 2012; Pilsner et al. 2009) and by others (Kile et al. 2012; Lambrou et al. 2012; Majumdar et al. 2010). We hypothesized that the discrepancy between the experimental and human studies is related to the dose and duration of As exposure: High acute As exposures might result in DNA hypomethylation, whereas a non-linear pattern of association might be observed within the range of As exposures in human populations, many of whom have been exposed to As for decades.

The primary objective of this analysis was to evaluate the relationship between As exposure and global methylation of peripheral blood mononuclear cell (PBMC) DNA. We used data from the Folate and Oxidative Stress (FOX) study (Hall et al. 2013), which selected study participants having a wide range of As exposure with the primary objective to assess the

relationship between As exposure and oxidative stress. This study provided a unique opportunity to examine the dose-response relationship between As exposure and global DNA methylation in a population with higher levels of As exposure than previous study populations.

SUBJECTS AND METHODS

Eligibility criteria and study design

For the FOX study, we recruited 379 men and women between the ages of 30 and 65 y between April 2007 and April 2008 in Araihazar, Bangladesh. Participants were selected based on well water As (wAs) exposure such that the final study sample represented the full range of wAs concentrations in the region. We aimed to recruit 75 participants from each of 5 exposure categories (Group A, 0-10 μg/L; Group B, 10-100 μg/L; Group C, 100-200 μg/L; Group D, 200-300 μg/L; and Group E, >300 μg/L) but had difficulty recruiting participants in the highest exposure categories because households using wells that tested positive for As (i.e., > 50 μg/L, the Bangladesh standard) were encouraged to switch to lower-As wells (Chen et al. 2007). Thus, the final participant numbers for the 5 categories were Group A, N=76; Group B, N=104; Group C, N=86; Group D, N=67, and Group E, N=45. Note that a random sample in this region would have likely yielded 40-50% of participants consuming wAs ≤ 50 μg/L. Participants must have been drinking from the same well for a minimum of 3 months prior to recruitment. Participants were excluded if they were pregnant; were currently taking nutritional supplements (or had done so within the past 3 months); or had known diabetes, cardiovascular, or renal disease.

Oral informed consent was obtained by our Bangladeshi field staff physicians, who read an approved consent form to the study participants. This study was approved by the institutional review boards of the Bangladesh Medical Research Council and of Columbia University Medical Center.

Analytic techniques

Sample collection and handling

Blood samples were drawn and processed immediately at our field clinic laboratory in Araihazar. Blood samples were centrifuged at 3,000 × g for 10 min at 4°C, and buffy coat and plasma were separated from red cells. Aliquots of blood and plasma were stored at –80°C. Urine samples were collected in 50 mL acid-washed polypropylene tubes and frozen at –20°C. Blood, plasma, and urine samples were transported to Dhaka on dry ice and stored at -80°C. Samples were then shipped, frozen on dry ice, to Columbia University for analysis.

Water As

Field sample collection and laboratory procedures have been described in detail (Cheng et al. 2004; Van Geen et al. 2005). Briefly, at the recruitment visit of the FOX study, new water samples were collected in 20 mL polyethylene scintillation vials and acidified to 1% with high-purity Optima HCl (Fisher Scientific, Pittsburg, PA, USA) at least 48 hr before analysis (van Geen et al. 2007). Water samples were analyzed by high-resolution inductively coupled plasma mass spectrometry (ICP-MS) after 1:10 dilution and addition of a Ge spike to correct fluctuations in instrument sensitivity. A standard with an As concentration of 51 µg/L was run multiple times in each batch; the intra- and inter-assay coefficients of variation (CVs) for this standard were 6.0% and 3.8%, respectively.

Total urinary As and urinary creatinine

Urinary As (uAs) metabolites were speciated using high performance liquid chromatography (HPLC) separation of arsenobetaine (AsB), arsenocholine (AsC), As^{V}, A^{sIII}, MMA (MMA^{III} + MMA^{V}), and DMA (DMA^{V}), followed by detection using ICP-MS (Vela et al. 2001). Total uAs was calculated by summing the concentrations of As^{V}, As^{III}, MMA, and DMA; AsC and AsB were not included in the sum. The limit of detection for each uAs metabolite was 0.1 µg/L. Arsenic levels in urine were determined with and without adjustment for urinary

creatinine (uCr), which was analyzed by a colorimetric assay based on the Jaffe reaction (Slot 1965). The intra-assay CVs were 4.5% for As^{V}, 3.8% for As^{III}, 1.5% for MMA, and 0.6% for DMA; inter-assay CVs were 10.6% for As^{V}, 9.6% for As^{III}, 3.5% for MMA, and 2.8% for DMA.

Total blood As

Total blood As (bAs) was analyzed using Perkin-Elmer Elan DRC II ICP-MS equipped with an AS 93+ autosampler, with a limit of detection of 0.1 μg/L, as previously described (Hall et al. 2006). The intra- and inter-assay CVs were 3.2% and 5.7%, respectively.

PBMC DNA isolation

PBMCs were isolated from fresh blood samples in the field clinic laboratory in Araihazar. To isolate PBMCs, 4 mL Ficoll solution was added to a tube containing 4 mL blood (with serum removed) and 11 mL PBS. Tubes were centrifuged at 400 x g for 30 min, and the mononuclear cell layer was extracted and washed with PBS. Cells were sedimented by centrifuging at 200 x g for 10 min. The cell pellet was resuspended with 4 mL lysis solution and 50 μl Proteinase K solution. PBMC lysates were stored at 4°C until shipment to Columbia University. PBMC DNA was isolated from 4 mL PBMC lysate using 1 mL Protein Precipitation Solution (5-Prime, New York, NY) and standard isopropanol extraction following the manufacturer's protocol. DNA was stored at -20°C until further analysis.

Global DNA methylation

Global DNA methylation was measured using the [^{3}H]-methyl incorporation assay developed by Balaghi and Wagner (Balaghi and Wagner 1993), as previously described (Pilsner et al. 2007). The assay employs ^{3}H-labeled SAM and SssI methylase to add ^{3}H-labeled methyl groups to unmethylated CpG sequences. Thus, disintegration per minute (DPM) values are negatively associated with global DNA methylation. Samples were run in duplicate, and each

run included a blank (mixture including all reaction components except SssI enzyme), hypomethylated control (HeLa cell DNA), and positive control (DNA extracted from whole blood sample). PicoGreen dsDNA Quantitation Reagent (Molecular Probes, Eugene, OR) was used to quantify the exact amount of double-stranded DNA (dsDNA) used in each reaction. The mean DPM values from the duplicate samples were expressed per µg DNA, as determined by PicoGreen. The intra- and inter-assay CVs were 3.4% and 10.4%, respectively.

Plasma folate

Plasma folate was analyzed by radioproteinbinding assay (SimulTRAC-S, MP Biomedicals, Orangeburg, NY). This method requires heating plasma to 100°C to denature endogenous binding substances. For folate concentration determination, folic acid as pteroylglutamic acid was used for calibration, and its ^{125}I-labeled analog was used as the tracer. The intra- and inter-assay CVs were 6% and 14%, respectively.

Blood *S*-adenosylmethionine

SAM was measured in whole blood as described previously (Poirier et al. 2001). SAM was detected at 254 nm using a 996 Photodiode Array ultraviolet absorbance detector (Waters Inc, Milford MA) and quantified relative to standard curves (Sigma, St. Louis, MO). The inter-assay CV was 9.6%.

Statistical methods

Descriptive statistics (means and standard deviations) were calculated for the overall sample. Spearman correlations (for continuous variables) and the Wilcoxon rank-sum test (for dichotomous variables) were used to examine bivariate associations between As variables and other covariates with [^{3}H]-methyl incorporation. Certain confounders (sex, age, and ever versus never cigarette smoking) were selected based on biologic plausibility and our previous studies

(Pilsner et al. 2007). Other potential confounders (BMI, years of education, plasma folate, plasma vitamin B_{12}, ever betelnut use, and television ownership) were selected based on bivariate associations with markers of As exposure and [^{3}H]-methyl incorporation in this dataset, but none met our criteria for inclusion in the final models ($P > 0.20$ for associations of the potential confounder with both the exposure and the outcome).

Urinary As was adjusted for urinary Cr using the residual method. To estimate these adjusted values, linear regression models were constructed with log-transformed uCr as the predictor of log-transformed uAs. The residuals from this model were added back to the mean log-transformed uAs and exponentiated to get the final uCr-adjusted urinary As values. The uCr-adjusted urinary As variable was used for all analyses involving urinary As.

We used locally estimated scatterplot smoothing (LOESS) curves of unadjusted associations between As exposure variables and [^{3}H]-methyl incorporation to visually identify potential nonlinear or nonmonotonic relationships. A SAS macro for restricted cubic splines (RCS) was used to estimate associations between markers of As exposure and [^{3}H]-methyl incorporation adjusted for sex, age, and smoking (Desquilbet and Mariotti 2010). An RCS function represents the sum of piecewise cubic polynomial splines with continuity and constraints at 3 to 5 specified knots on the continuous exposure variables (Desquilbet and Mariotti 2010). A Wald chi-square test with K-2 degrees of freedom, where K = number of knots and K-2 = number of spline variables, was used to test the null hypothesis of linear relationship between the exposure and outcome variables. Failure to reject the null hypothesis of linearity would support the use of linear regression to estimate associations between markers of As exposure (modeled as untransformed continuous variables) and [^{3}H]-methyl incorporation.

Associations were also estimated by modeling As exposure using categorical variables. Water As categories were created with the reference category reflecting the Bangladeshi drinking water standard for As of 50 µg/L: 0-50 µg/L, 50-100 µg/L, 100-200 µg/L, 200-300 µg/L, and 300-700 µg/L. Urinary As was first adjusted for urinary Cr using the residual method; quintiles of uAs exposures were then constructed based on these adjusted values. Blood As was categorized based on quintiles. General linear models with categorized exposure variables were used to estimate covariate-adjusted least squares means for [^{3}H]-methyl incorporation by As category.

[^{3}H]-methyl incorporation values were excluded from the analysis if duplicate assays had coefficients of variation > 15% (N=48), if less than 10 µg/mL of DNA was used in the assay (N=8), or if DPM values were extreme outliers, defined as values that exceeded the boxplot of the DPM values by more than three interquartile ranges (N=2). Additionally, we were unable to extract DNA from 1 lysate, leaving a final dataset of N=320 for the analyses. All statistical analyses were conducted using SAS (version 9.2; SAS Institute Inc., Cary, NC); statistical tests were two sided with a significance level of 0.05.

RESULTS

The characteristics of the study population are shown in Table 1. The mean age was 43.2 years, and there were roughly equal numbers of males and females. Water As concentrations ranged from 0.4 to 700 µg/L, with a mean of 145 µg/L. By design, wells that exceeded the Bangladeshi standard of 50 µg/L were the primary drinking water source for 70.9% of participants.

Table 1. Demographic and clinical data for current study (N=320).

Baseline variables	Mean ± SD (range) or N(%)
Age (yrs)	43.2 ± 8.3 (30 - 63)
Male	159 (49.7)
BMI (kg/m^2)	20.3 ± 3.5 (13.8 - 35.3)
Underweight ($BMI < 18.5\ kg/m^2$)	112 (35.1)
Ever cigarette smoking	123 (38.4)
Ever betel nut use	142 (44.4)
Television ownership	185 (57.8)
Water As (µg/L)[a]	145 ± 123 (0.4 - 700)
Water As > 50 µg/L[a]	226 (70.9)
Urinary As (µg/L)	213 ± 242 (2 - 1800)
Urinary creatinine (mg/dL)	54.5 ± 43.7 (4.3 - 223.5)
Urinary As adj. for urinary creatinine (µg/L)	167 ± 122 (10 - 548)
Blood As (µg/L)	13.9 ± 9.8 (1.2 - 57.0)
Plasma folate (nmol/L)[a]	12.6 ± 7.0 (2.4 - 60.6)
Folate deficient[a] (<9 nmol/L)	100 (31.3)
Blood SAM (µM)[b]	1.29 ± 0.50 (0.44 - 3.38)
DPM per µg DNA	149,123 ± 23,932 (61,398 - 215,666)

[a.] N=319; [b.] N=312

All As variables (wAs, bAs, and uAs adjusted for uCr) were negatively correlated with [^{3}H]-methyl incorporation (Table 2), indicating that As exposure was positively correlated with PBMC DNA methylation. Spearman correlation coefficients were similar between groups when stratified by folate deficiency (plasma folate < 9.0 nmol/L) (data not shown), suggesting that folate status did not modify associations between As exposure markers and [^{3}H]-methyl incorporation in this sample. Correlations also were similar between groups defined using more stringent definitions of folate deficiency (plasma levels < 8.0 nmol/L, N=69; or < 7.0 nmol/L, N=38) (data not shown). We also examined correlations of As and [^{3}H]-methyl incorporation with blood SAM, which has been hypothesized to mediate the relationship between As exposure and DNA methylation (Mass and Wang 1997). While blood SAM was negatively correlated with [^{3}H]-methyl incorporation, As was not correlated with blood SAM (Table 2). In addition, methylated metabolites of As were not correlated with [^{3}H]-methyl incorporation (data not shown). We did not observe significant correlations between plasma folate and [^{3}H]-methyl incorporation or blood SAM, or between age and [^{3}H]-methyl incorporation (Table 2).

The shapes of the LOESS curves suggested that [^{3}H]-methyl incorporation decreased linearly with increasing levels of wAs, bAs, and uAs (data not shown). Using RCS functions with 5 knots, we similarly observed a decrease in [^{3}H]-methyl incorporation as As levels increased (data not shown). Tests of departures from the null hypothesis of linear dose-response relations were not statistically significant for any of the As predictors (all $P > 0.30$).

Table 2. Spearman correlation coefficients for arsenic variables, blood *S*-adenosylmethionine, plasma folate, and [^{3}H]-methyl incorporation in PBMC DNA (N=320).

	Blood As	Urinary As	Urinary As, adj. for urinary Cr	DPM per µg DNA	Blood SAM[b]	Plasma folate[a]	Age
Water As[a]	0.75***	0.63***	0.75***	-0.14*	-0.03	-0.04	-0.01
Blood As	-	0.67***	0.93***	-0.13*	-0.03	-0.06	0.00
Urinary As	-	-	0.71***	-0.08	0.00	0.03	-0.02
Urinary As, adj. for urinary Cr	-		-	-0.12*	-0.04	0.00	0.01
DPM per µg DNA	-		-	-	-0.12*	0.03	0.07
Blood SAM[b]	-		-	-	-	-0.07	0.13*
Plasma folate[a]	-		-	-	-	-	-0.12*

*P<0.05; **P<0.01; ***P<0.0001; [a.] N=319; [b.] N=312

Unadjusted linear regression models of wAs, uAs, or bAs as predictors of [^{3}H]-methyl incorporation indicated negative associations between As exposure and [^{3}H]-methyl incorporation that were statistically significant for wAs (B = -28.2; 95% CI: -49.5, -6.8, *P* = 0.01) and borderline significant for uAs (B = -20.2; 95% CI: -41.9, 1.4, *P* = 0.07) and bAs (B = -254.5; 95% CI: -523.5, 14.6, *P* = 0.06) (Table 3). Estimates for the difference in mean DPM estimates associated with a 1-unit increase in As exposure adjusted for sex, age, ever smoking, and uCr (for uAs), were similar to unadjusted estimates for wAs (B = -27.6; 95% CI: -49.0, -6.3, *P* = 0.01) and uAs (B = -22.1; 95% CI: -43.8, -0.5, *P* = 0.045), but the association for bAs was attenuated (B = -211.7; 95% CI: -483.9, 60.5, *P* = 0.13 compared with B =-254.5; 95% CI: -523.5, 14.6 before adjustment).

Table 3. Estimated regression coefficients from linear regression models of associations between arsenic variables and [^{3}H]-methyl incorporation in PBMC DNA (N=320).

Predictor	Model	B (95% CI)	*P*
Water As[a]	Unadjusted	-28.2 (-49.5, -6.8)	0.01
	Adjusted[b]	-27.6 (-49.0, -6.3)	0.01
Urinary As, adjusted for urinary Cr	Unadjusted	-20.2 (-41.9, 1.4)	0.07
	Adjusted[b]	-22.1 (-43.8, -0.5)	0.045
Blood As	Unadjusted	-254.5 (-523.5, 14.6)	0.06
	Adjusted[b]	-211.7 (-483.9, 60.5)	0.13

[a.] N=319; [b.] Adjusted for sex, age, and ever cigarette smoking

Linear models were constructed to estimate covariate-adjusted mean [^{3}H]-methyl incorporation levels by As category (Figure 1). Adjusted mean [^{3}H]-methyl incorporation levels were similar between the lowest two wAs categories (Figure 1A) and among the lowest three uAs quintiles (Figure 1B). Higher wAs and uAs exposure categories were associated with lower estimated mean values for [^{3}H]-methyl incorporation: adjusted mean [^{3}H]-methyl incorporation was 7.0% lower (95% CI: 2.2, 11.8%) among participants in the highest wAs category (300-700 µg/L) compared with the 0-50 µg/L wAs referent group (P = 0.02, Figure 1A) and was 6.4% lower (95% CI: 2.5, 10.3%) among those in the highest uAs quintile compared with the lowest uAs quintile (P = 0.02, Figure 1B). While the pattern of association for [^{3}H]-methyl incorporation by quintile of bAs was similar to the pattern for wAs and uAs (Figure 1C), the adjusted means were not significantly different from one another.

Figure 1. Adjusted mean values of [^{3}H]-methyl incorporation by category means of water (A), urinary (B), and blood (C) arsenic. Data points represent estimated mean DPM values (with 95% CI) according to the mean As value for each As exposure category, adjusted for gender, age, and ever cigarette smoking. Categories for blood and urinary As are quintiles, while categories for water As reflect study sampling categories and the Bangladeshi As standard of 50 µg/L.

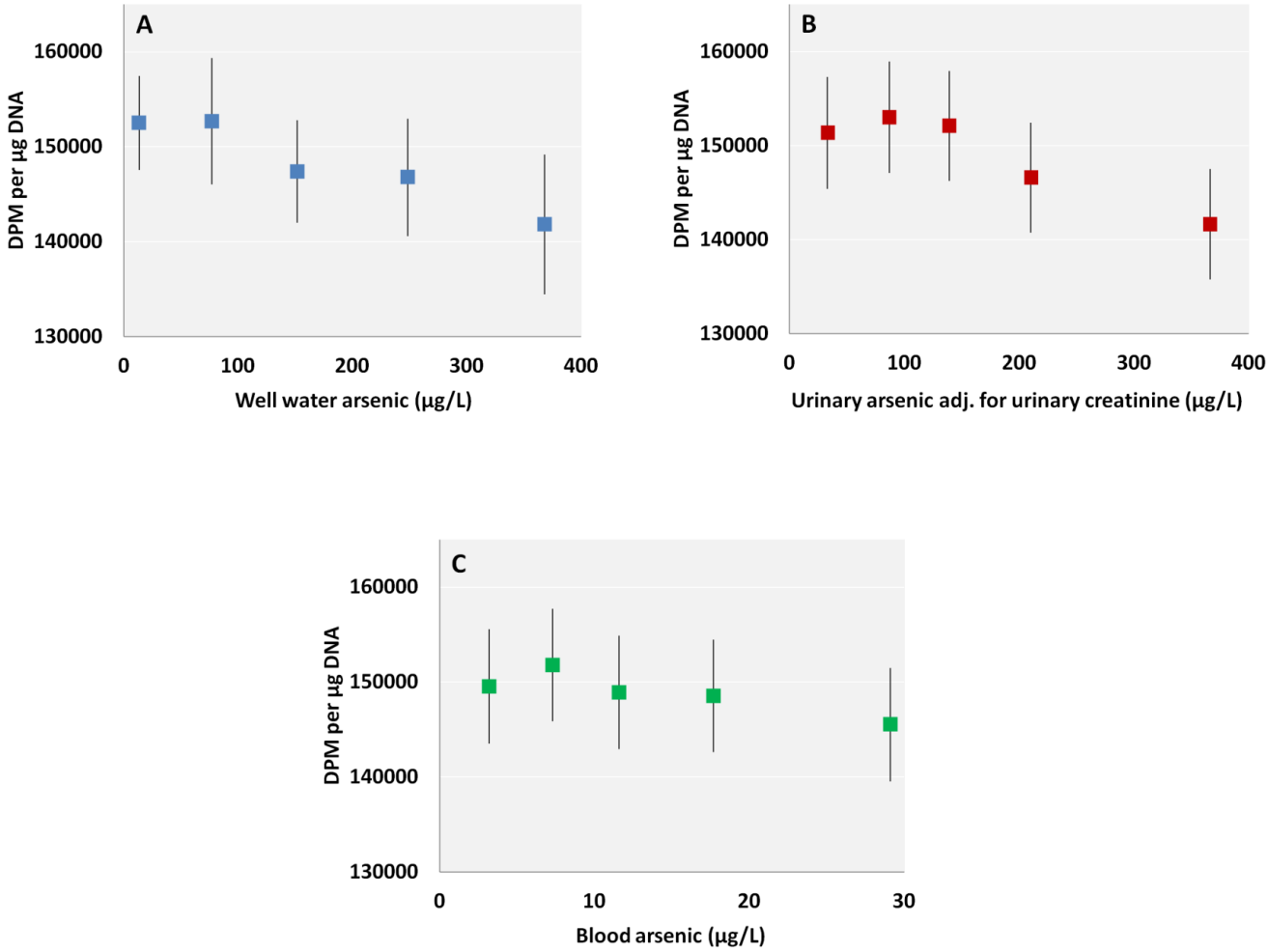

DISCUSSION

The primary objective of this study was to assess the dose-response relationship between As exposure and global methylation of PBMC DNA in adults chronically exposed to a wide range of As in drinking water in Bangladesh. In agreement with previous findings (Pilsner et al. 2007, 2009), As exposure was positively associated with global DNA methylation of PBMC DNA. Furthermore, within the range of As exposures in our study, we did not detect a statistically significant departure from linearity in the association between As and DNA methylation. Adjusted mean DNA methylation levels were similar among the lower As exposure categories but increased in the higher As exposure categories, with the highest estimated mean DNA methylation levels in the highest As exposure categories (water As > 300 µg/L). However, we cannot rule out the possibility of non-linearity at extremely high doses often used in animal studies, e.g., As exposures ranging from 1 to 85 ppm (1,000 to 85,000 µg/L) (Reichard and Puga 2010).

In the present study, we did not find a significant correlation between age and [^{3}H]-methyl incorporation. It is possible that this is attributable to the demographics of the study population. In our first study of As exposure and global DNA methylation (Pilsner et al. 2007), global DNA methylation decreased with age across the 18-29, 30-36, and 37-45 year age categories. However, global DNA methylation levels did not differ significantly between the 37-45 and 46-66 year age groups (Pilsner et al. 2007). The narrower age range of the FOX study (30-65 years) may therefore have contributed to the lack of a significant association between global DNA methylation and age in our study population.

We also did not find a correlation between plasma folate and [^{3}H]-methyl incorporation. The mean plasma folate level was higher in the FOX study population than in our first study of

As exposure and global DNA methylation (12.6 vs. 8.6 nmol/L, respectively), and a smaller proportion was folate deficient (31.3 vs. 64.6%). Folate might only influence DNA methylation under conditions in which folate is limiting. In support of this hypothesis, folic acid supplementation was not associated with higher global DNA methylation in study populations whose participants were folate sufficient at baseline (Basten et al. 2006; Jung et al. 2011). In the present study population, associations between As and DNA methylation were similar between those with and without folate deficiency, even when more stringent definitions of folate deficiency were used. However, our ability to evaluate an interaction may have been limited by the small numbers of participants with severe folate deficiency.

Other epidemiologic studies in adults have reported that associations between As exposure and global DNA methylation were modified by folate status. In a study of elderly men in Massachusetts, toenail As concentrations were positively associated with Alu methylation only among men with plasma folate levels below the study median (Lambrou et al. 2012). Although this seemingly contradicts our previous finding of an association between As exposure and DNA methylation that was limited to participants with sufficient plasma folate levels (Pilsner et al. 2007), as noted by Lambrou et al. (2012), plasma folate levels in our folate-sufficient group (> 9.0 nmol/L) overlapped with levels in their low folate group (< 32 nmol/L). In the present study, all but 6 participants had plasma folate levels < 32 nmol/L.

Two studies of prenatal As exposure have reported positive associations between As exposure and global DNA methylation. A study of 113 mother/newborn pairs in Bangladesh reported that As exposure was associated with higher methylation of LINE-1 in both umbilical cord blood and maternal leukocytes (Kile et al. 2012). In a similar study of 101 mother/newborn pairs in Bangladesh, maternal As exposure also was associated with increased global DNA

methylation based on [^{3}H]-methyl-incorporation in DNA extracted from umbilical cord blood leukocytes (Pilsner et al. 2012). However, the direction of the associations between maternal As exposure and other markers of global DNA methylation (Alu, LINE-1, and LUMA) differed by sex: associations were positive in male newborns, but negative in female newborns (Pilsner et al. 2012).

Several mechanisms of As-induced epigenetic dysregulation have been proposed. For example, because SAM is required for As metabolism, it has been hypothesized that As methylation may influence DNA methylation through competition for methyl groups (Mass and Wang 1997). In an *in vitro* model, low-dose As exposure decreased SAM concentrations in keratinocytes cultured in folic acid-deficient medium (Reichard et al. 2007). While blood SAM was positively correlated with DNA methylation in our study population, it was not correlated with markers of As exposure. In addition, in contrast with what one might expect if there were competition between DNA methyltransferases and arsenic methyltransferase for SAM, As metabolites also were not correlated with DNA methylation in our study population Quantitatively, methylation of As and DNA consumes only a very small proportion of total SAM (Gamble and Hall 2012).

There is growing evidence that As exposure may alter post-translational modifications of lysine residues in histone tails. For example, exposure to $NaAsO_2$ led to increased global histone acetylation and more open chromatin formation in human HepG2 hepatocarcinoma cells (Ramirez et al. 2008), and exposure to $InAs^{III}$ led to increased H3K9 dimethylation (H3K9me2) and decreased H3K27 trimethylation (H3K27me3) in human lung carcinoma A549 cells (Zhou et al. 2008). Occupational exposure to inhalable As was significantly associated with H3K4me2 and H3K9 acetylation (H3K9ac) in histones purified from WBCs in a study of steel workers in

Italy (Cantone et al. 2011). In ongoing studies, we are evaluating associations of As exposure on global histone modifications in As-exposed Bangladeshis (Chervona et al. 2012) and whether these histone marks are additionally associated with global DNA methylation.

The physiologic implications of increased global DNA methylation in apparently healthy adults are unclear, given that global DNA *hypo*methylation has been associated with multiple diseases, including As-induced skin lesions. An increase in global DNA methylation might be associated with an increased spontaneous mutation rate: methylated cytosines are more prone to deamination than unmethylated cytosines, which increases the likelihood of C→T transitions (Ehrlich et al. 1986). Additionally, DNA methylation is associated with heterochromatic regions (Beisel and Paro 2011), and somatic mutation density in human cancer genomes were found to be highest in heterochromatin-like domains (Schuster-Bockler and Lehner 2012).

Additionally, previous findings suggest that As-induced global DNA hypermethylation might be associated with concomitant increases in As-induced gene-specific promoter methylation of tumor suppressors or other disease-related genes. Kile et al. reported that urinary As was associated with both increased LINE-1 methylation and increased *P16* promoter methylation of leukocyte DNA from umbilical cord blood and maternal blood (Kile et al. 2012). Promoter methylation of *P16* and *P53* tumor suppressors was elevated in both As-exposed individuals and As-associated skin cancer cases in West Bengal, India (Chanda et al. 2006), and methylation of the tumor suppressors *RASSF1A* and *PRSS3* was associated with toenail As concentrations and invasive tumor stage in bladder cancer cases in New Hampshire (Marsit et al. 2006). In women from the Argentinean Andes, urinary As concentrations were positively associated with promoter methylation of *P16* and the DNA repair gene *MLH1* (Hossain et al. 2012).

We cannot dismiss the possibility that our findings may be explained by As-induced shifts in blood cell type distributions. In our previous studies (Pilsner et al. 2007, 2009), DNA was isolated from PBLs, while our current study used PBMCs. Because PBMCs are a subset of the cells present in PBLs, this would reduce cell type variability to some extent. Arsenic exposure was not significantly associated with proportions of total T, Tc, B, or NK cells in PBMCs isolated from As-exposed children in Mexico (Soto-Pena et al. 2006). Furthermore, average [^{3}H]-methyl incorporation levels were not significantly different among DNA samples isolated from granulocytes, mononuclear cells, and white blood cells (Wu et al. 2011).

In the present study population, the association of [^{3}H]-methyl-incorporation with blood As was less statistically significant than associations with water or urine As. Blood As is the most proximal marker of PBMC exposure, so one might expect that blood As would have the strongest and/or most significant association with PBMC DNA methylation. While blood As was strongly correlated with water As (Spearman $r = 0.75$) and urinary As adjusted for urinary Cr (Spearman $r = 0.93$), the range of concentrations of As in blood (1.2 – 57.0 ug/L) was much smaller than in urine (10 – 548 ug/L) or water (0.4 – 700 ug/L), resulting in reduced statistical power to predict [^{3}H]-methyl incorporation.

This study has several limitations. First, PBMCs are not known to be direct targets of As-induced carcinogenesis. However, As trioxide is a highly effective therapeutic drug for the treatment of acute promyelocytic leukemia (Powell et al. 2010), demonstrating that As distributes to bone marrow progenitor cells and influences their cellular function (Petrie et al. 2009; Soignet et al. 1998). We do not know the extent to which methylation of PBMC DNA reflects the methylation of other target tissues. Finally, it is possible that our results are explained by unmeasured confounding. Notably, we do not have measures of all possible

contaminants in well water that may co-occur with As and potentially confound our observed associations. However, mass spectrometry data for a panel of 33 elements from well water samples from our study area indicated that only As and Mn were elevated (Cheng et al. 2004), and Mn was not associated with DNA methylation (data not shown).

In conclusion, As exposure was positively associated with global methylation of PBMC DNA in Bangladeshi adults with a wide range of As exposures, consistent with previous studies. Furthermore, we did not observe statistical evidence of non-linear relationships between As and global DNA methylation within the range of As exposures in our population. Future studies, in addition to investigating the influence of As on histone modifications, should evaluate the potential physiological implications of increased global DNA methylation.

ACKNOWLEDGEMENTS

This work was supported by grants RO1 CA133595, RO1ES017875, P42 ES10349, P30 ES09089, and T32 CA009529-24 from the National Institutes of Health. The content is solely the responsibility of the authors and does not necessarily represent the official views of the National Institute of Environmental Health Sciences, the National Cancer Institute, or the National Institutes of Health.

REFERENCES

Balaghi M, Wagner C. 1993. DNA methylation in folate deficiency: use of CpG methylase. Biochem Biophys Res Commun 193(3): 1184-1190.

Basten GP, Duthie SJ, Pirie L, Vaughan N, Hill MH, Powers HJ. 2006. Sensitivity of markers of DNA stability and DNA repair activity to folate supplementation in healthy volunteers. Br J Cancer 94(12): 1942-1947.

Beisel C, Paro R. 2011. Silencing chromatin: comparing modes and mechanisms. Nat Rev Genet 12(2): 123-135.

Benbrahim-Tallaa L, Waterland RA, Styblo M, Achanzar WE, Webber MM, Waalkes MP. 2005. Molecular events associated with arsenic-induced malignant transformation of human prostatic epithelial cells: aberrant genomic DNA methylation and K-ras oncogene activation. Toxicol Appl Pharmacol 206(3): 288-298.

Bernstein BE, Birney E, Dunham I, Green ED, Gunter C, Snyder M. 2012. An integrated encyclopedia of DNA elements in the human genome. Nature 489(7414): 57-74.

Cantone L, Nordio F, Hou L, Apostoli P, Bonzini M, Tarantini L, et al. 2011. Inhalable Metal-Rich Air Particles and Histone H3K4 Dimethylation and H3K9 Acetylation in a Cross-sectional Study of Steel Workers. Environ Health Perspect 119(7): 964-969.

Chanda S, Dasgupta UB, GuhaMazumder D, Gupta M, Chaudhuri U, Lahiri S, et al. 2006. DNA Hypermethylation of Promoter of Gene p53 and p16 in Arsenic-Exposed People with and without Malignancy. Toxicological Sciences 89(2): 431-437.

Chattopadhyay BP, Mukherjee AK, Gangopadhyay PK, Alam J, Roychowdhury A. 2010. Respiratory effect related to exposure of different concentrations of arsenic in drinking water in West Bengal, India. J Environ Sci Eng 52(2): 147-154.

Chen CJ, Hsueh YM, Lai MS, Shyu MP, Chen SY, Wu MM, et al. 1995. Increased prevalence of hypertension and long-term arsenic exposure. Hypertension 25(1): 53-60.

Chen H, Li S, Liu J, Diwan BA, Barrett JC, Waalkes MP. 2004. Chronic inorganic arsenic exposure induces hepatic global and individual gene hypomethylation: implications for arsenic hepatocarcinogenesis. Carcinogenesis 25(9): 1779-1786.

Chen Y, Graziano JH, Parvez F, Liu M, Slavkovich V, Kalra T, et al. 2011. Arsenic exposure from drinking water and mortality from cardiovascular disease in Bangladesh: prospective cohort study. BMJ 342: d2431.

Chen Y, van Geen A, Graziano JH, Pfaff A, Madajewicz M, Parvez F, et al. 2007. Reduction in urinary arsenic levels in response to arsenic mitigation efforts in Araihazar, Bangladesh. Environ Health Perspect 115(6): 917-923.

Cheng Z, Zheng Y, Mortlock R, Van Geen A. 2004. Rapid multi-element analysis of groundwater by high-resolution inductively coupled plasma mass spectrometry. Anal Bioanal Chem 379(3): 512-518.

Chervona Y, Hall MN, Arita A, Wu F, Sun H, Tseng HC, et al. 2012. Associations between Arsenic Exposure and Global Posttranslational Histone Modifications among Adults in Bangladesh. Cancer Epidemiol Biomarkers Prev 21(12): 2252-2260.

Chiang PK, Gordon RK, Tal J, Zeng GC, Doctor BP, Pardhasaradhi K, et al. 1996. S-Adenosylmethionine and methylation. FASEB J 10(4): 471-480.

Consortium TEP. 2004. The ENCODE (ENCyclopedia Of DNA Elements) Project. Science 306(5696): 636-640.

Dauphine DC, Ferreccio C, Guntur S, Yuan Y, Hammond SK, Balmes J, et al. 2011. Lung function in adults following in utero and childhood exposure to arsenic in drinking water: preliminary findings. Int Arch Occup Environ Health 84(6): 591-600.

Desquilbet L, Mariotti F. 2010. Dose-response analyses using restricted cubic spline functions in public health research. Stat Med 29(9): 1037-1057.

Dodge JE, Okano M, Dick F, Tsujimoto N, Chen T, Wang S, et al. 2005. Inactivation of Dnmt3b in mouse embryonic fibroblasts results in DNA hypomethylation, chromosomal instability, and spontaneous immortalization. J Biol Chem 280(18): 17986-17991.

Ehrlich M, Norris KF, Wang RY, Kuo KC, Gehrke CW. 1986. DNA cytosine methylation and heat-induced deamination. Biosci Rep 6(4): 387-393.

Gamble MV, Hall MN. 2012. Relationship of creatinine and nutrition with arsenic metabolism. Environ Health Perspect 120(4): A145-146.

Gaudet F, Hodgson JG, Eden A, Jackson-Grusby L, Dausman J, Gray JW, et al. 2003. Induction of tumors in mice by genomic hypomethylation. Science 300(5618): 489-492.

Hall M, Chen Y, Ahsan H, Slavkovich V, van Geen A, Parvez F, et al. 2006. Blood arsenic as a biomarker of arsenic exposure: results from a prospective study. Toxicology 225(2-3): 225-233.

Hall MN, Niedzwiecki M, Liu X, Harper KN, Alam S, Slavkovich V, et al. 2013. Chronic arsenic exposure and blood glutathione and glutathione disulfide concentrations in bangladeshi adults. Environ Health Perspect 121:1068-74.

Hamadani JD, Tofail F, Nermell B, Gardner R, Shiraji S, Bottai M, et al. 2011. Critical windows of exposure for arsenic-associated impairment of cognitive function in pre-school girls and boys: a population-based cohort study. Int J Epidemiol 40(6): 1593-1604.

Hossain MB, Vahter M, Concha G, Broberg K. 2012. Environmental arsenic exposure and DNA methylation of the tumor suppressor gene p16 and the DNA repair gene MLH1: effect of arsenic metabolism and genotype. Metallomics 4(11): 1167-1175.

Jung AY, Smulders Y, Verhoef P, Kok FJ, Blom H, Kok RM, et al. 2011. No effect of folic acid supplementation on global DNA methylation in men and women with moderately elevated homocysteine. PLoS One 6(9): e24976.

Kile ML, Baccarelli A, Hoffman E, Tarantini L, Quamruzzaman Q, Rahman M, et al. 2012. Prenatal arsenic exposure and DNA methylation in maternal and umbilical cord blood leukocytes. Environ Health Perspect 120(7): 1061-1066.

Lambrou A, Baccarelli A, Wright RO, Weisskopf M, Bollati V, Amarasiriwardena C, et al. 2012. Arsenic exposure and DNA methylation among elderly men. Epidemiology 23(5): 668-676.

Loewenberg S. 2007. Scientists tackle water contamination in Bangladesh. The Lancet 370(9586): 471-472.

Majumdar S, Chanda S, Ganguli B, Mazumder DN, Lahiri S, Dasgupta UB. 2010. Arsenic exposure induces genomic hypermethylation. Environ Toxicol 25(3): 315-318.

Marsit CJ, Karagas MR, Danaee H, Liu M, Andrew A, Schned A, et al. 2006. Carcinogen exposure and gene promoter hypermethylation in bladder cancer. Carcinogenesis 27(1): 112-116.

Mass MJ, Wang L. 1997. Arsenic alters cytosine methylation patterns of the promoter of the tumor suppressor gene p53 in human lung cells: a model for a mechanism of carcinogenesis. Mutat Res 386(3): 263-277.

Matsuzaki K, Deng G, Tanaka H, Kakar S, Miura S, Kim YS. 2005. The relationship between global methylation level, loss of heterozygosity, and microsatellite instability in sporadic colorectal cancer. Clin Cancer Res 11(24 Pt 1): 8564-8569.

Navarro Silvera SA, Rohan TE. 2007. Trace elements and cancer risk: a review of the epidemiologic evidence. Cancer Causes Control 18(1): 7-27.

Parvez F, Chen Y, Brandt-Rauf PW, Slavkovich V, Islam T, Ahmed A, et al. 2010. A prospective study of respiratory symptoms associated with chronic arsenic exposure in Bangladesh: findings from the Health Effects of Arsenic Longitudinal Study (HEALS). Thorax 65(6): 528-533.

Petrie K, Zelent A, Waxman S. 2009. Differentiation therapy of acute myeloid leukemia: past, present and future. Curr Opin Hematol 16(2): 84-91.

Pilsner JR, Hall MN, Liu X, Ilievski V, Slavkovich V, Levy D, et al. 2012. Influence of prenatal arsenic exposure and newborn sex on global methylation of cord blood DNA. PLoS One 7(5): e37147.

Pilsner JR, Liu X, Ahsan H, Ilievski V, Slavkovich V, Levy D, et al. 2007. Genomic methylation of peripheral blood leukocyte DNA: influences of arsenic and folate in Bangladeshi adults. Am J Clin Nutr 86(4): 1179-1186.

Pilsner JR, Liu X, Ahsan H, Ilievski V, Slavkovich V, Levy D, et al. 2009. Folate deficiency, hyperhomocysteinemia, low urinary creatinine, and hypomethylation of leukocyte DNA are risk factors for arsenic-induced skin lesions. Environ Health Perspect 117(2): 254-260.

Poirier LA, Wise CK, Delongchamp RR, Sinha R. 2001. Blood determinations of S-adenosylmethionine, S-adenosylhomocysteine, and homocysteine: correlations with diet. Cancer Epidemiol Biomarkers Prev 10(6): 649-655.

Powell BL, Moser B, Stock W, Gallagher RE, Willman CL, Stone RM, et al. 2010. Arsenic trioxide improves event-free and overall survival for adults with acute promyelocytic leukemia: North American Leukemia Intergroup Study C9710. Blood 116(19): 3751-3757.

Ramirez T, Brocher J, Stopper H, Hock R. 2008. Sodium arsenite modulates histone acetylation, histone deacetylase activity and HMGN protein dynamics in human cells. Chromosoma 117(2): 147-157.

Razin A, Kantor B. 2005. DNA methylation in epigenetic control of gene expression. Prog Mol Subcell Biol 38: 151-167.

Reichard JF, Puga A. 2010. Effects of arsenic exposure on DNA methylation and epigenetic gene regulation. Epigenomics 2(1): 87-104.

Reichard JF, Schnekenburger M, Puga A. 2007. Long term low-dose arsenic exposure induces loss of DNA methylation. Biochem Biophys Res Commun 352(1): 188-192.

Ren X, McHale CM, Skibola CF, Smith AH, Smith MT, Zhang L. 2011. An emerging role for epigenetic dysregulation in arsenic toxicity and carcinogenesis. Environ Health Perspect 119(1): 11-19.

Robertson KD. 2001. DNA methylation, methyltransferases, and cancer. Oncogene 20(24): 3139-3155.

Schulz WA, Elo JP, Florl AR, Pennanen S, Santourlidis S, Engers R, et al. 2002. Genomewide DNA hypomethylation is associated with alterations on chromosome 8 in prostate carcinoma. Genes Chromosomes Cancer 35(1): 58-65.

Schuster-Bockler B, Lehner B. 2012. Chromatin organization is a major influence on regional mutation rates in human cancer cells. Nature 488(7412): 504-507.

Slot C. 1965. Plasma creatinine determination. A new and specific Jaffe reaction method. Scand J Clin Lab Invest 17(4): 381-387.

Soignet SL, Maslak P, Wang ZG, Jhanwar S, Calleja E, Dardashti LJ, et al. 1998. Complete remission after treatment of acute promyelocytic leukemia with arsenic trioxide. N Engl J Med 339(19): 1341-1348.

Soto-Pena GA, Luna AL, Acosta-Saavedra L, Conde P, Lopez-Carrillo L, Cebrian ME, et al. 2006. Assessment of lymphocyte subpopulations and cytokine secretion in children exposed to arsenic. FASEB J 20(6): 779-781.

Thurman RE, Rynes E, Humbert R, Vierstra J, Maurano MT, Haugen E, et al. 2012. The accessible chromatin landscape of the human genome. Nature 489(7414): 75-82.

Tseng CH, Chong CK, Tseng CP, Hsueh YM, Chiou HY, Tseng CC, et al. 2003. Long-term arsenic exposure and ischemic heart disease in arseniasis-hyperendemic villages in Taiwan. Toxicol Lett 137(1-2): 15-21.

van Geen A, Cheng Z, Jia Q, Seddique AA, Rahman MW, Rahman MM, et al. 2007. Monitoring 51 community wells in Araihazar, Bangladesh, for up to 5 years: implications for arsenic mitigation. J Environ Sci Health A Tox Hazard Subst Environ Eng 42(12): 1729-1740.

Van Geen A, Cheng Z, Seddique AA, Hoque MA, Gelman A, Graziano JH, et al. 2005. Reliability of a commercial kit to test groundwater for arsenic in Bangladesh. Environ Sci Technol 39(1): 299-303.

Vela NP, Heitkemper DT, Stewart KR. 2001. Arsenic extraction and speciation in carrots using accelerated solvent extraction, liquid chromatography and plasma mass spectrometry. The Analyst 126(7): 1011-1017.

Wasserman GA, Liu X, Parvez F, Ahsan H, Factor-Litvak P, van Geen A, et al. 2004. Water arsenic exposure and children's intellectual function in Araihazar, Bangladesh. Environ Health Perspect 112(13): 1329-1333.

Wu HC, Delgado-Cruzata L, Flom JD, Kappil M, Ferris JS, Liao Y, et al. 2011. Global methylation profiles in DNA from different blood cell types. Epigenetics 6(1): 76-85.

Zhao CQ, Young MR, Diwan BA, Coogan TP, Waalkes MP. 1997. Association of arsenic-induced malignant transformation with DNA hypomethylation and aberrant gene expression. Proc Natl Acad Sci U S A 94(20): 10907-10912.

Zhou X, Sun H, Ellen TP, Chen H, Costa M. 2008. Arsenite alters global histone H3 methylation. Carcinogenesis 29(9): 1831-1836.

Chapter 4: Arsenic exposure and age are associated with global hydroxymethylcytosine content in two subpopulations of human peripheral blood cell DNA

Megan M. Niedzwiecki[1], Megan N. Hall[2], Xinhua Liu[3], Vesna Slavkovich[1], Vesna Ilievski[1], Diane Levy[3], Shafiul Alam[4], Abu B. Siddique[4], Faruque Parvez[1], Joseph H. Graziano[1], and Mary V. Gamble[1]

Affiliations: [1]Department of Environmental Health Sciences, [2]Department of Epidemiology, [3]Department of Biostatistics, [1-3]Mailman School of Public Health, Columbia University, New York NY,10032, USA; [4]Columbia University Arsenic Project in Bangladesh, Dhaka, Bangladesh

ABSTRACT

BACKGROUND: The ten-eleven translocation (TET) family of proteins catalyze the conversion of 5-methylcytosine (5mC) to 5-hydroxymethylcytosine (5hmC). 5hmC is believed to be an intermediate in DNA demethylation pathways, and changes in global 5hmC levels are independently associated with disease. Arsenic (As) exposure is known to induce changes in global DNA methylation, but common methodologies used to assess global DNA methylation do not distinguish between 5mC and 5hmC.

OBJECTIVE: To assess the association between As exposure and global %hmC in blood cell DNA among As-exposed Bangaldeshi adults.

METHODS: We examined peripheral blood leukocyte (PBL) DNA from baseline in 200 folate-deficient adults who were enrolled in a folic acid supplementation trial in Araihazar, Bangladesh and peripheral blood mononuclear cell (PBMC) DNA in 378 As-exposed adults in the Folate and Oxidative Stress (FOX) cross-sectional study. Global %5mC and %5hmC of blood cell DNA was measured using LC-MS/MS. Total As in plasma, urine, blood, and well water were measured by GFAA spectrometry and/or ICP-MS.

RESULTS: In adjusted models, water, blood, urinary, and plasma As were positively associated with global %hmC in males and negatively associated with global %hmC in females, and the magnitudes of association were consistent between the two study samples. In addition, age was associated with a dose-dependent decrease in global %hmC in both study samples.

CONCLUSIONS: Arsenic exposure was positively associated with global %hmC of blood cell DNA in males and negatively associated with global %hmC in females. Further research should examine the relevance of As-induced changes in global %hmC in As-related carcinogenesis and examine mechanism(s) underlying a potential gender-specific effect.

INTRODUCTION

The most widely studied epigenetic process, DNA methylation, regulates gene expression through the covalent addition of a methyl group on cytosines, primarily in CpG dinucleotides, to form 5-methylcytosine (5mC) (Bird 1992). Increased abundance of genomic 5mC is negatively associated with chromatin accessibility (Thurman et al. 2012) and gene activation (Siegfried et al. 1999), presumably through the recruitment of methyl-CpG-binding proteins (MBPs) and disruption of transcriptional machinery (Kass et al. 1997). DNA methylation has important roles in cellular differentiation and mammalian development (Smith and Meissner 2013), and abnormal DNA methylation patterns are observed in human cancers (Bergman and Cedar 2013; Robertson 2005).

Although DNA methylation is known to be a dynamic process, the mechanisms of DNA demethylation are not well-characterized. Recently, the ten-eleven translocation (TET) enzymes (TET1, TET2, TET3) have been shown to catalyze the oxidation of 5mC to 5-hydroxymethylcytosine (5hmC) (Tahiliani et al. 2009), which is believed to be an intermediate in cytosine demethylation (Ito et al. 2010). The TET enzymes are dependent upon Fe^{2+} and alpha-ketoglutarate (α-ketoglutarate) as cofactors (Tahiliani et al. 2009); the latter is generated from the oxidative decarboxylation of isocitrate by the isocitrate dehydrogenase (IDH) enzyme family (Reitman and Yan 2010). The maintenance DNA methyltransferase DMNT1 poorly recognizes 5hmC (Valinluck and Sowers 2007), which results in passive loss of DNA methylation through DNA replication. 5hmC is also actively removed through pathways involving thymine DNA glycosylase (TDG) and base excision repair (BER) (Guo et al. 2011).

In addition, 5hmC might have independent regulatory roles in gene expression (Song et al. 2011), embryogenesis (Wossidlo et al. 2011), and neurodevelopment (Kriaucionis and Heintz

2009; K. E. Szulwach et al. 2011). In general, enrichment of 5hmC is positively correlated with gene expression and is associated with enhancer regions and exon bodies (Stroud et al. 2011; Keith E. Szulwach et al. 2011). *TET1* was originally identified as a partner gene to the *mixed lineage leukemia* (*MLL*) gene translocation that is commonly found in acute myeloid leukemia (AML) cases (Lorsbach et al. 2003; Ono et al. 2002). Mutations in *TET*s and *IDH*s have since been identified in myeloid malignant diseases, suggesting that 5hmC plays a role in hematopoietic differentiation and regulation (Murati et al. 2012).

Arsenic (As), a Class I human carcinogen, is a ubiquitous environmental contaminant worldwide (Hughes et al. 2011). Exposure to As is particularly high in Bangladesh, where over 70 million people are chronically exposed to As in well water at concentrations above the World Health Organization standard of 10 µg/L (Loewenberg 2007). While the mechanisms of As toxicity in humans are not fully understood, one proposed pathway is through epigenetic dysregulation (Ren et al. 2011). Chronic As exposure has been associated with changes in global and gene-specific methylation of human peripheral blood cell DNA in numerous population-based studies (Kile et al. 2012; Lambrou et al. 2012; Majumdar et al. 2010; Pilsner et al. 2009; Pilsner et al. 2012). Paradoxically, arsenic trioxide (As_2O_3), in combination with all-trans retinoic acid (ATRA), is a highly effective treatment for acute promyelocytic leukemia (APL) (Lo-Coco et al. 2013), a subtype of AML that is believed to occur, in part, through epigenetic dysregulation of myeloid cell differentiation (Uribesalgo and Di Croce 2011). However, the relationship between As exposure and 5hmC in human blood cell DNA is unknown.

To our knowledge, global %hmC has not been measured in white blood cell DNA in a population-based human study. In this study, we used liquid chromatography-tandem mass spectrometry (LC-MS/MS) to measure global %mC and %hmC in white blood cell DNA in two

independent samples of Bangladeshi adults, and we examined the associations of gender, age, and As exposure with global %mC and %hmC. The first sample examined peripheral blood leukocyte (PBL) DNA from baseline samples from the Nutritional Influences of Arsenic Toxicity (NIAT) randomized controlled trial (Gamble et al. 2006), which examined the influence of folic acid supplementation on As metabolism. Our second sample examined peripheral blood mononuclear cell (PBMC) DNA from subjects in the Folate and Oxidative Stress (FOX) study (Hall et al. 2013), a cross-sectional study designed to assess the relationship between chronic As exposure and oxidative stress.

SUBJECTS AND METHODS

Eligibility criteria and study design

The NIAT folic acid intervention study design has described previously (Gamble et al. 2006). Briefly, NIAT participants were selected from the Health Effects of Arsenic Longitudinal Study (HEALS) cohort, which at the time of NIAT recruitment, included 11,746 men and women between the ages of 18 and 65 years in Araihazar, Bangladesh (Ahsan et al. 2006). NIAT participants were drawn from a cross-sectional study of 1,650 HEALS participants designed to assess the prevalence of folate and cobalamin deficiencies in Bangladesh; we randomly selected 200 NIAT participants from the 550 subjects in the lowest tertile of plasma folate (Gamble et al. 2005). Participants were excluded if they were pregnant or cobalamin deficient (plasma cobalamin $\leq$ 185 pmol/L) or were taking nutritional supplements. As described elsewhere (Pilsner et al. 2007), high-quality DNA samples were obtained from 195 whole blood samples drawn from participants at baseline. For the purposes of the current study, only baseline samples were included in the analysis.

The details of the FOX study design are described in Chapter 3. Unlike in the NIAT study, participants in FOX were not selected based on folate or cobalamin nutritional status.

Oral informed consent was obtained by our Bangladeshi field staff physicians, who read an approved consent form to the FOX and NIAT study participants. The FOX and NIAT studies were approved by the institutional review boards of the Bangladesh Medical Research Council and of Columbia University Medical Center.

Analytic techniques

Methods for water As, urinary As, urinary Cr, blood As, PBMC DNA isolation, plasma folate and cobalamin, and plasma homocysteine for the FOX study are described in detail in

Chapter 3. Analytic methods for the NIAT study, brief descriptions of any discrepancies in methodology between the NIAT and FOX studies, and methods for global %mC and %hmC in NIAT and FOX are outlined in this chapter.

Sample collection and handling

For the NIAT study, blood samples were drawn in the field, as described previously (Pilsner et al. 2007). Blood was collected in heparin-containing evaporated tubes, placed in IsoRack cool packs (Brinkmann Instruments, Westbury, NY) in hand-carried coolers, and transported to the field clinic in Araihazar within 4 h of collection. For the FOX study, blood samples were drawn at the field clinic laboratory in Araihazar and immediately processed. All blood samples were centrifuged at 3,000 × g for 10 min at 4°C, and buffy coat and plasma were separated from red cells. Aliquots of blood and plasma were stored at –80°C, and urine samples were stored at –20°C in acid-washed polypropylene tubes. Blood, plasma, and urine samples were then shipped on dry ice to Columbia University.

Water As

In NIAT, well water As concentrations were measured in a survey of all tube wells in the NIAT study region from January to May 2000. Water samples were analyzed using graphite furnace atomic absorption (GFAA) spectrometry, with a detection limit of 5 µg/L; water samples with non-detectable As using GFAA were analyzed with inductively coupled mass spectrometry (ICP-MS), with a detection limit of 0.1 µg/L.

In FOX, well water samples were collected at the time of the FOX recruitment visit, and all water samples were analyzed using ICP-MS. The intra- and inter-assay coefficients of variation (CVs) were 6.0% and 3.8%, respectively.

Total urinary As and urinary creatinine

In NIAT and FOX, urinary As (uAs) metabolites—arsenobetaine (AsB), arsenocholine (AsC), As^{V}, A^{sIII}, MMA (MMA^{III} + MMA^{V}), and DMA (DMA^{V})—were separated using HPLC, and metabolite concentrations were measured using ICP-MS, with a limit of detection of 0.1 μg/L (Vela et al. 2001). To calculate total uAs, we summed the concentrations of As^{V}, As^{III}, MMA, and DMA, excluding the concentrations of AsC and AsB. Urinary creatinine (uCr) was analyzed by a colorimetric assay based on the Jaffe reaction (Slot 1965) and used to adjust for urine concentration. For FOX, the intra-assay CVs were 4.5% for As^{V}, 3.8% for As^{III}, 1.5% for MMA, and 0.6% for DMA, and the inter-assay CVs were 10.6% for As^{V}, 9.6% for As^{III}, 3.5% for MMA, and 2.8% for DMA.

Total blood As

Total blood As (bAs) was analyzed using Perkin-Elmer Elan DRC II ICP-MS equipped with an AS 93+ autosampler, with a limit of detection of 0.1 μg/L, as previously described (Hall et al. 2006). The intra- and inter-assay CVs were 3.2% and 5.7%, respectively.

Total plasma As

In NIAT, total plasma As was analyzed using dynamic reaction cell (DRC) technology (Elan DRC II ICP-MS; Perkin- Elmer) equipped with an AS 93+ autosampler, as previously described (Pilsner et al. 2007). The intra-assay CV was 10.4%. Plasma As was not measured in the FOX study.

PBL DNA isolation

In NIAT, to isolate DNA from PBLs, 1 mL red blood cell solution (GenomicPrep Blood DNA Isolation Kit; Amersham Biosciences, Piscataway, NJ) was added to the buffy coat, and tubes were centrifuged at 16,000 x g for 5 min. PBLs were stored in lysis solution at 4 °C until

shipment to Columbia University. DNA was isolated from PBL lysates using silica membrane spin columns according to the manufacturer's protocol.

PBMC DNA isolation

In FOX, the protocol for DNA isolation from PBMCs was outlined in Chapter 2. Briefly, PBMCs were isolated from whole blood using Ficoll solution, and DNA was isolated from PBMC lysates with Protein Precipitation Solution (5-Prime, New York, NY) and isopropanol extraction according to the manufacturer's protocol.

Global %mC and %hmC

Global %mC and %hmC was analyzed using liquid chromatography-tandem mass spectrometry (LC-MS/MS) with biosynthetic [U-^{15}N]deoxycytidine and [U-^{15}N]methyldeoxycytidine internal standards, with methods adapted from the protocols of Quinlivan and Gregory (Quinlivan and Gregory 2008). The LC-MS/MS method allows for the sensitive quantitation of mC and hmC concentrations in digested genomic DNA.

DNA samples were hydrolyzed into nucleosides according to the protocol of Quinlivan and Gregory (Quinlivan and Gregory 2008). A Digest Mix (per 100 samples) was prepared containing 250 U Benzonase (Sigma-Aldrich, St. Louis, MO), 300 mU phosphdiesterase (Sigma-Aldrich), and 200 U alkaline phosphatase (Sigma-Aldrich), made up to 5 mL with buffer [10 mM Tris–HCl, 50 mM NaCl, 10 mM $MgCl_2$ (pH 7.9)]. DNA samples were hydrolyzed by adding 50 μL Digest Mix to 50 μL DNA sample (1 μg DNA in 50 μL water) and incubating at 37°C for 6 h. All samples within each study were digested in one day, using one batch of Digest Mix.

An internal standard containing [U-$^{15}N_3$]-labeled deoxynucleosides ([$^{15}N_3$]-dC and [$^{15}N_3$]-mdC) was synthesized based on the protocol of Quinlivan and Gregory (Quinlivan and

Gregory 2008). Cryopreserved *Escherichia coli* K12 grown in minimal medium (New England Biolabs, Ipswich, MA) was inoculated into 10 ml [^{15}N]-labeled growth medium containing 50 mM NaCl, 25 mM KH_2PO_5, 70 μM CaCl, 2.1 mM $MgSO_4$, 10 mM glucose, and 50 mM [^{15}N]NH_4Cl (Cambridge Isotopes, Andover, MA), pH 7.2, and incubated while shaking at 37°C. After log-phase growth was reached, 10 μL of culture was transferred to 50 mL of fresh [^{15}N]-labeled growth medium and grown to lag-phase. [U-^{15}N]DNA was isolated using the ArchivePure DNA Extraction Kit (5-Prime) according to the manufacturer's protocol for gram-negative bacterial culture and reconstituted in buffer containing 10 mM Tris–HCl, 50 mM NaCl, 1 mM dithiothreitol, and 10 mM $MgCl_2$ (pH 7.9). [U-^{15}N]DNA concentrations were measured using NanoDrop and adjusted to ~50 μg/mL. To increase the abundance of [$^{15}N_3$]-mdC, 100 U SssI (CpG) methyltransferase (New England Biolabs) and 20 μl SAM (32 mM) were added to [U-^{15}N]DNA (per 100 ug DNA) and incubated at 37°C for 4 h. Hypermethylated [U-^{15}N]DNA samples were digested by adding 250 U Benzonase (Sigma), 300 mU phosphdiesterase (Sigma) and 200 U alkaline phosphatase (Sigma) (per 100 μg DNA), and incubating at 37°C for 12 h. Two separate batches of [U-^{15}N]DNA internal standard were synthesized (one batch for FOX, one batch for NIAT), but all experimental samples within the same study received [U-^{15}N]DNA internal standard from the same batch.

Hydrolyzed DNA samples (100 μL) were transferred to vials (Agilent Technologies, Santa Clara, CA) with 4 μL [U-^{15}N]DNA internal standard and analyzed in the Biomarkers Core Lab at Columbia University with the Agilent 6430 Triple Quadrupole LC-MS (Agilent Technologies, Santa Clara, CA). 10 μL of sample was injected onto a reverse phase UPLC column (Eclipse C18 2.1 × 50 mm, 1.8 μ particle size, Agilent) equilibrated and eluted (100 μL/min) with water/methanol/formic acid (95/5/0.1, all by volume). Isotopic nucleosides

enrichment scanning was performed in positive ionization mode using selected reaction monitoring (SRM) mode, monitoring the mass to charge (m/z) transitions of dC: 228.1→112.0; [$^{15}N_3$]dC: 231.1→115.0; mdC: 242.1→126.0; [$^{15}N_3$]mdC 245.1→129.0; and hmdC: 258.1→142.1.

A standard curve was run with each batch of experimental samples. Stock mixtures of dC, mC, and hmC were created with known concentrations and proportions of mC and hmC to dC, and a standard curve was prepared using serial dilutions. To correct for recovery, 4 ul of [U-^{15}N]DNA internal standard was added to 50 ul of each dilution. Standard curves were constructed by plotting the analyte/internal standard ratio (M+0/M+3) against the known concentrations of dC, mC, and hmC for each dilution. The concentrations of dC, mC, and hmC in each experimental sample were calculated from the standard curves using the analyte/internal standard ratio (M+0/M+3) by reverse prediction, and %mC and %hmC were calculated by dividing the concentrations of mC and hmC, respectively, by the total dC sum (dC + mC + hmC).

In the FOX study, one large aliquot (10 μg) of a DNA control sample was hydrolyzed, and aliquots of this control sample were run in duplicate with each batch of experimental samples; for this sample, the intra- and inter-assay CVs for %mC were 0.5 and 2.0%, respectively, and for %hmC, the intra- and inter-assay CVs were 7.0 and 14.4%, respectively. In the NIAT study, we selected a subset of 48 subjects for which different aliquots of their original DNA samples were hydrolyzed and analyzed in a different batch than the overall samples, using a different batch of [U-^{15}N]DNA internal standard; for these samples, the inter-assay CVs for %mC and %hmC were 3.0 and 11.8%, respectively. The run order of the experimental samples

was randomized in each study, and the LC-MS/MS operators were blinded to the identities of the samples.

Plasma folate and cobalamin

Plasma folate and cobalamin were analyzed by radioproteinbinding assay (NIAT: Quantaphase II, Bio-Rad Laboratories, Hercules, CA; FOX: SimulTRAC-S, MP Biomedicals, Orangeburg, NY). In NIAT, the intra- and inter-assay CVs for folate were 3% and 11%, respectively, and the intra- and inter-assay CVs for cobalamin were 4% and 8%, respectively. In FOX, the intra- and inter-assay CVs for folate were 6% and 14%, respectively, and the intra- and inter-assay CVs for cobalamin were 4% and 9%, respectively.

Plasma total homocysteine

Plasma total Hcys was assayed using the protocol of Pfieffer et al. (Pfeiffer et al. 1999), as previously described (Gamble et al. 2005) In NIAT, the intra- and inter-assay CVs for plasma total Hcys were x and x%, respectively; in FOX, the intra- and inter-assay CVs for plasma total Hcys were 4 and 9%, respectively.

Statistical methods

Descriptive statistics (means and standard deviations for continuous variables, proportions for dichotomous variables) were calculated for the FOX and NIAT samples. Spearman correlations were used to examine bivariate associations between continuous study characteristics and global %mC and %hmC, overall and stratified by gender. Since the global %mC and %hmC variables were normally distributed in the datasets, we used t-tests to compare mean global %mC and %hmC between levels of dichotomous variables (e.g., ever vs. never cigarette smoking).

Linear regression models were constructed with As exposure variables (wAs, uAs, bAs, and pAs) as predictors and global %mC and %hmC as outcomes, with and without adjusting for confounders. Since the directions of the bivariate associations between As variables and global %mC and %hmC differed by gender, we built linear regression models separately by gender. Confounders (age, BMI, cigarette smoking, and betelnut use) were selected based on biologic plausibility and their bivariate associations with As exposure variables and global %mC and %hmC in each dataset. Differences in parameter estimates by gender were examined using Wald tests.

Urinary As was adjusted for urinary Cr using the residual method. To estimate these adjusted values, linear regression models were constructed with log-transformed uCr as the predictor of log-transformed uAs. The residuals from this model were added back to the mean log-transformed uAs and exponentiated to get the final uCr-adjusted uAs values. The uCr-adjusted urinary As variable was used for all analyses involving uAs.

All statistical analyses were conducted using SAS (version 9.3; SAS Institute Inc., Cary, NC); statistical tests were two sided with a significance level of 0.05.

RESULTS

NIAT and FOX study characteristics

The demographic and clinical characteristics of the NIAT and FOX study populations are presented in Table 1. Both studies had equal numbers of males and females, and there were similar proportions of participants who reported ever smoking cigarettes or chewing betelnut. Since the minimum inclusion age differed between the FOX and NIAT studies (30 y vs. 18 y), the mean age was higher in FOX than in NIAT. Also due to differences in sampling designs between the studies, the mean wAs concentration was higher in FOX. Participants in NIAT were randomly selected from a subset of individuals who had previously been identified as having low folate (plasma folate $\leq$ 9 nmol/L) and sufficient cobalamin (plasma cobalamin > 185 pmol/L), whereas FOX participants were not selected based on folate or cobalamin status; as such, mean plasma cobalamin was higher in NIAT than in FOX, while mean plasma folate was lower.

Global %mC and %hmC in NIAT and FOX studies

We isolated DNA from two different subpopulations of peripheral blood cells: in NIAT, DNA was isolated from PBLs, while in FOX, DNA was isolated from PBMCs, a subset of PBLs comprised mainly of lymphocytes (Table 1). Mean global %mC was higher in NIAT (4.61%) than in FOX (4.57%) (Table 1). Mean global %hmC was two orders of magnitude lower than global %mC; mean global %hmC was slightly higher in NIAT (0.0325%) than FOX (0.0307%), but the range of global %hmC values in FOX (0.0147 – 0.0505%) was wider than in NIAT (0.0245 – 0.0443%) (Table 1). In NIAT, global %mC and %hmC were not correlated with one another (Spearman $r = 0.02$, $P = 0.82$), while in FOX, global %mC and %hmC were positively correlated (Spearman $r = 0.44$, $P < 0.0001$) (Figure 1).

Table 1. Demographic and clinical characteristics for FOX and NIAT samples

Variables	NIAT (N=190) Mean ± SD (range) or N(%)	FOX (N=376) Mean ± SD (range) or N(%)
Demographic		
Age (years)	38.4 ± 10.2 (19 - 66)	43.1 ± 8.3 (30 - 63)
Male	92 (48.4)	183 (48.7)
BMI (kg/m^2)	19.9 ± 3.1 (13.4- 32.5)	20.4 ± 3.5 (13.8 - 35.3)
Ever smoked cigarettes	76 (40.0)	137 (36.4)
Ever chewed betel nut	72 (37.9)	160 (42.6)
Education (years)		
0 years	78 (39.0)	150 (39.8)
1-5 years	75 (37.5)	134 (35.5)
> 5 years	47 (23.5)	92 (24.4)
Arsenic exposure		
Water As (µg/L)	105 ± 103 (0.1 - 435)	139 ± 124 (0.4 - 700)
Water As > 50 µg/L	118 (62.1)	226 (70.9)
Urinary As (µg/L)	136 ± 125 (7 - 741)	206 ± 236 (2 - 1800)
Urinary As adj. for uCr (µg/L)	121 ± 99 (12 - 543)	160 ± 120 (10 - 548)
Blood As (µg/L)	9.8 ± 5.1 (3.3 – 28.8)[c]	13.4 ± 9.8 (1.2 - 57.0)
Plasma As (µg/L)	6.9 ± 3.3 (2.2 – 19.4)	N/A
Nutritional status		
Plasma folate (nmol/L)	8.1 ± 4.0 (3.0 – 44.7)	12.9 ± 7.2 (2.4 - 60.6)[c]
Plasma Hcys (µmol/L)	10.9 ± 5.1 (0.3 – 40.0)	11.2 ± 13.0 (3.0 - 165.4)
Plasma cobalamin (pmol/L)[b]	285 ± 128 (118 - 920)	203 ± 113 (44 - 1183)[d]
DNA methylation		
Cell type for DNA extraction	Peripheral blood leukocytes	Peripheral blood mononuclear cells
Global %mC	4.61 ± 0.10 (4.36 – 4.99)	4.57 ± 0.12 (4.24 – 4.85)
Global %hmC	0.0325 ± 0.0038 (0.0245 – 0.0443)	0.0307 ± 0.0056 (0.0147 – 0.0505)[e]

[a.] N=375; [b.] N=369; [c.] N=375 [c] N=127

We examined the correlations between global %mC and %hmC and values from the [^{3}H]-methyl incorporation assay, which assesses global DNA methylation by measuring incorporation of tritiated methyl groups into unmethylated CpG sites (thus, values are negatively related to global DNA methylation). We found that global %mC was negatively correlated with [^{3}H]-methyl incorporation in both NIAT (Spearman r = -0.16, P = 0.03) and FOX (Spearman r = -0.24, P < 0.0001), demonstrating agreement between the two methods. Interestingly, global %hmC was also negatively correlated with [^{3}H]-methyl incorporation in NIAT (Spearman r = -0.21, P = 0.004) and FOX (Spearman r = -0.24, P < 0.0001).

Figure 1. Spearman correlations between global %mC and global %hmC in human DNA from two different subpopulations of WBCs. Global %mC (x-axis) and global %hmC (y-axis) are plotted for each subject in the NIAT (Figure 1A) and FOX (Figure 1B) samples.

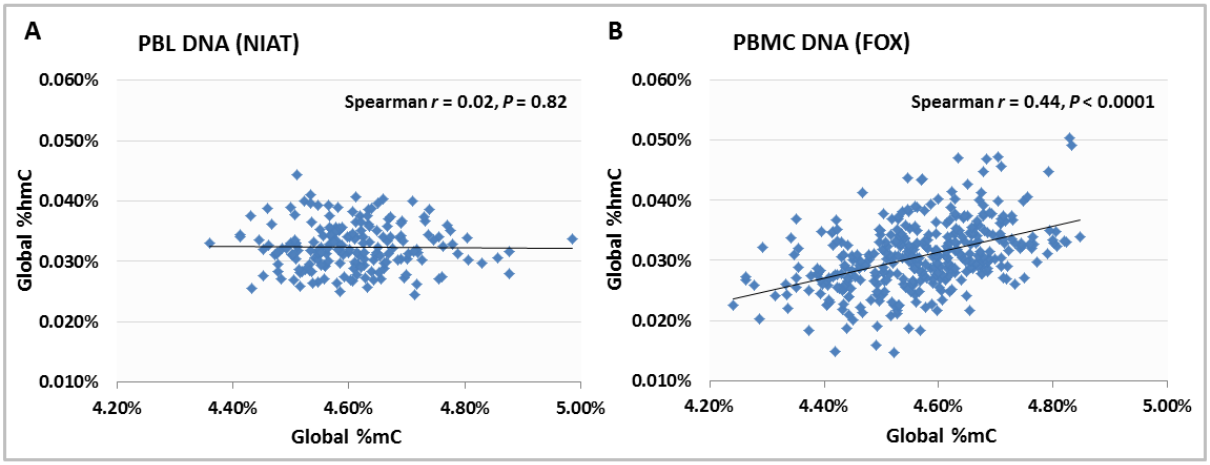

Global %mC is higher in males

Mean global %mC was 6% higher in males than females in both FOX (males vs. females, 4.60 vs. 4.54%, P < 0.0001) and NIAT (males vs. females, 4.64 vs. 4.58%, P < 0.0001). To examine whether the observed gender difference in mean global %mC was consistent across age

groups, we plotted mean global %mC in NIAT and FOX, stratified by gender and age group (Figures 2A and 2B). Males had higher mean global %mC than females across all age groups in both studies (Figures 2A and 2B). In NIAT, we did not observe a decline in global %mC with age in males, although in females, there was a borderline significant 0.05% decrease ($P = 0.06$) in mean global %mC in the 48-63 y age group compared to the 18-29 y group (Figure 2A). In FOX, mean global %mC decreased with increasing age in both genders, with a 0.05-0.06% decrease in in the 48-63 y age groups compared to the 30-35 y groups (Figure 2B).

To explore whether global %mC was associated with other demographic characteristics, we constructed regression models with demographic variables as predictors of global %mC and global %hmC, shown in Table 2. Based on results from bivariate analyses, we included gender, cigarette smoking, betelnut use, years of education, age, BMI, and wAs variables in the models simultaneously. The R^2 values for these models were 11.9 and 11.7% for NIAT and FOX, respectively (Table 2). The negative association between female gender and global %mC persisted after adjustment for covariates, with an estimated decrease in global %mC of 0.064% in NIAT (95% CI, -0.103, -0.024) and 0.042% in FOX (95% CI, -0.074, -0.011) compared to males (Table 2). Gender explained a large proportion of the variance in global %mC (Δ in R^2 = 4.9% in NIAT, 1.7% in FOX). Other predictors were not associated with global %mC consistently between the two study samples. In FOX, ever cigarette smoking was associated with a 0.034% increase (95% CI, 0.002, 0.067) and age (10-year unit increase) was associated with a 0.029% decrease (95% CI, -0.045, -0.045) in global %mC, but these associations were not observed in NIAT (Table 2).

Global %hmC declines with age

No gender differences were observed for mean global %hmC (NIAT, males vs. females, 0.032 vs. 0.033%, $P = 0.63$; FOX, males vs. females, 0.031 vs. 0.031%, $P = 0.71$). When mean global %hmC was assessed by gender and age range (Figures 2C and 2D), a steady decrease in mean global %hmC was observed with increasing age groups in both genders (Figures 2C and 2D). Parameter estimates for global %hmC from regression models adjusting for gender, cigarette smoking, betelnut use, years of education, age, BMI, and wAs are presented in Table 3. The R^2 values for the global %hmC models were 9.1 and 7.6% for NIAT and FOX, respectively (Table 2), indicating that these demographic variables explained a smaller proportion of the variance in global %hmC, compared to global %mC.

Consistent with the observations in Figure 1, a 10-year increase in age was associated with a 0.0011% decrease in global %hmC in NIAT (95% CI: -0.0017, -0.0004) and 0.0015% decrease in FOX (95% CI: -0.0023, -0.0007) (Table 3). Age explained the largest proportion of the variance in global %hmC by a wide margin (Δ in R^2 = 5.6% in NIAT, 3.3% in FOX). BMI (5-kg/m^2 unit increase) was associated with a decrease in global %hmC of 0.0006% in NIAT (95% CI: -0.0015, 0.0003) and 0.0009% in FOX (95% CI: -0.0018, -0.0001) and explained approximately 1% of the variance in global %hmC in both samples (Table 3). In FOX, females had an estimated 0.0017% increase in global %hmC compared to males (95% CI: 0.0001, 0.0033), but no difference in global %hmC by gender was found in NIAT (Table 3). Similarly, cigarette smoking and increased years of education were positively associated with global %hmC in FOX, but not in NIAT (Table 3).

Figure 2. Global %mC and %hmC, by gender and age range, in NIAT and FOX samples. Plots represent mean ± SD values for the specified gender and age range.

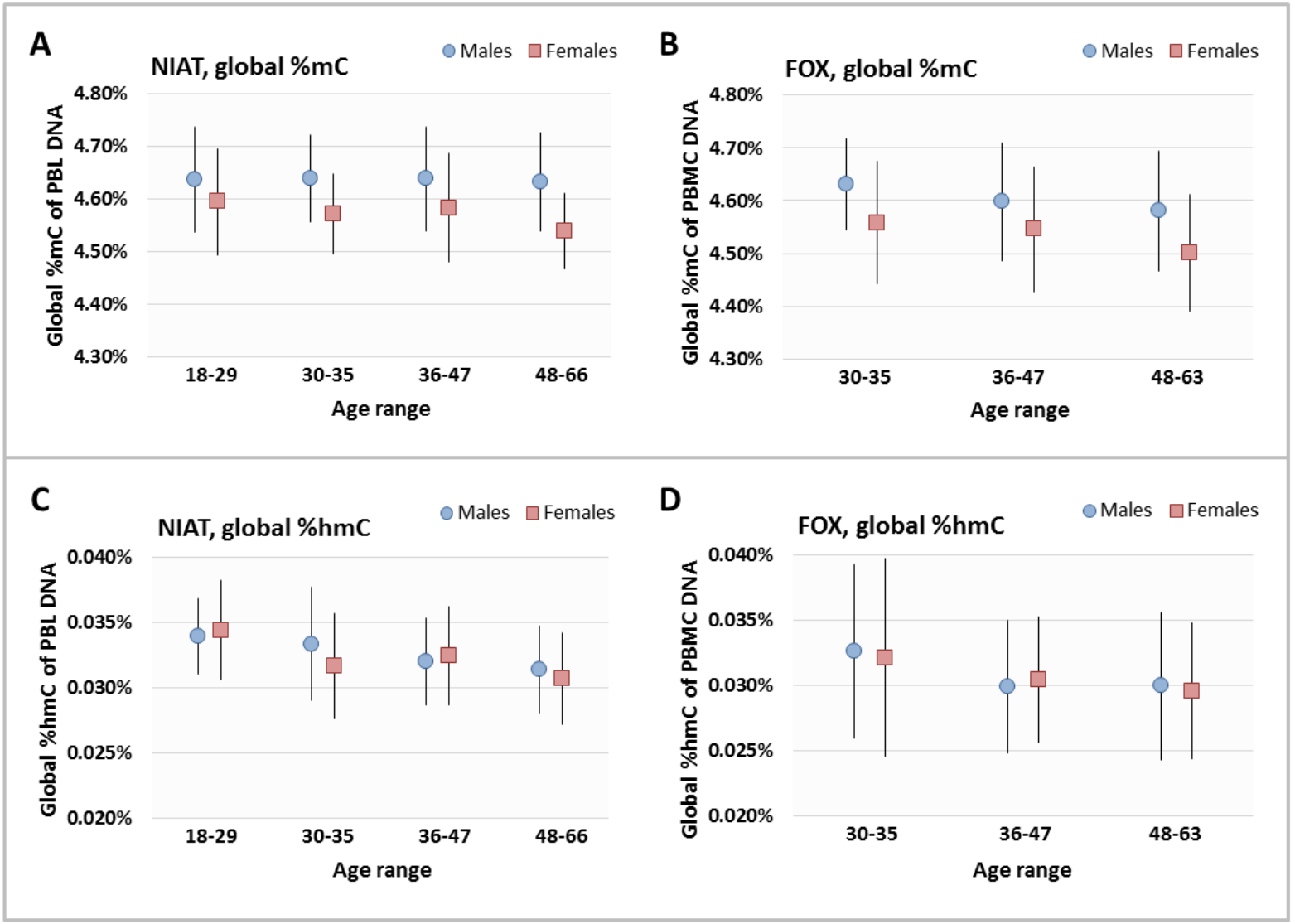

Table 2. Regression coefficients for associations between study characteristics and global %mC in NIAT and FOX samples.

Predictor	Level or unit	NIAT Global %mC, PBL DNA		FOX Global %mC, PBMC DNA	
		B (95% CI)	Δ in R^2 (%)	B (95% CI)	Δ in R^2 (%)
Gender			4.9		1.7
	Male	*ref.*		*ref.*	
	Female	-0.064** (-0.103, -0.024)		-0.043** (-0.074, -0.011)	
Age			0.4		3.3
	10-year	-0.007 (-0.023, 0.009)		-0.029** (-0.045, -0.014)	
Cigarette smoking			0.1		1.0
	Never	*ref.*		*ref.*	
	Ever	0.008 (-0.033, 0.050)		0.034* (0.002, 0.067)	
Betel chewing			0.3		0.0
	Never	*ref.*		*ref.*	
	Ever	-0.012 (-0.044, 0.020)		-0.003 (-0.029, 0.023)	
Education			0.2		0.7
	0 years	*ref.*		*ref.*	
	1-5 years	-0.007 (-0.038, 0.024)		0.022 (-0.005, 0.048)	
	5+ years	-0.010 (-0.047, 0.027)		0.014 (-0.017, 0.045)	
BMI			0.7		0.0
	5-kg/m^2	-0.005 (-0.028, 0.018)		-0.005 (-0.022, 0.013)	
wAs			0.0		0.0
	100-µg/L	0.000 (-0.013, 0.014)		-0.001 (-0.010, 0.085)	
R^2, model (%)			11.9		11.7

†p<0.10; *p<0.05; **p<0.01

Table 3. Regression coefficients for associations between study characteristics and global %hmC in NIAT and FOX samples.

		NIAT Global %hmC, PBL DNA		FOX Global %hmC, PBMC DNA	
Predictor	Level/unit	B (95% CI)	Δ in R^2 (%)	B (95% CI)	Δ in R^2 (%)
Gender			0.2		1.1
	Male	*ref.*		*ref.*	
	Female	-0.0004 (-0.0020, 0.0011)		0.0017* (0.0001, 0.0033)	
Age			5.6		3.3
	10-year	-0.0011** (-0.0017, -0.0004)		-0.0015** (-0.0023, -0.0007)	
Cigarette smoking			0.0		1.8
	Never	*ref.*		*ref.*	
	Ever	0.0001 (-0.0015, 0.0017)		0.0022** (0.006, 0.039)	
Betel chewing			0.6		0.0
	Never	*ref.*		*ref.*	
	Ever	0.0007 (-0.0005, 0.0020)		0.0000 (-0.0013, 0.0013)	
Education			1.0		2.0
	0 years	*ref.*		*ref.*	
	1-5 years	0.0002 (-0.0010, 0.0014)		0.0012† (-0.0002, 0.0025)	
	5+ years	-0.0009 (-0.0023, 0.0006)		0.0022** (0.0007, 0.0038)	
BMI			0.9		1.0
	5-kg/m^2	-0.0006 (-0.0015, 0.0003)		-0.0009* (-0.0018, -0.0001)	
wAs			0.0		0.2
	100-µg/L	0.0001 (-0.0005, 0.0006)		-0.0002 (-0.0007, 0.0002)	
R^2, model (%)			9.5		7.6

†p<0.10; *p<0.05; **p<0.01

Arsenic is associated with increased global %mC in males

We next examined the relationships between As exposure and global %mC. As shown in Table 2, water As was not associated with global %mC in the overall study samples in NIAT and FOX, and other As variables were not correlated with global %mC in bivariate analyses (Appendix, Table E1). Based on previous studies from our group (Pilsner et al. 2012) and others (Nohara et al. 2011) that reported associations between As exposure and DNA methylation that were modified by gender, we additionally examined the relationships between As exposure and global %mC separately in males and females. In bivariate analyses, As exposure was positively correlated with global %mC in males, but no consistent correlations between As exposure and global %mC was observed in females (Appendix, Table E1). We built regression models with As exposure variables predicting global %mC, adjusted for age, BMI, cigarette smoking, and years of education, stratified by gender (Figure 3). In males, As exposure was positively associated with global %mC at marginal statistical significance ($P < 0.10$ for wAs, uAs, and bAs in NIAT and FOX) (Figure 3). In females, no consistent associations between the As exposure variables and global %mC were observed (Figure 3).

Arsenic is associated with increased global %hmC in males, decreased global %hmC in females

We also examined the relationship between As exposure and global %hmC. In bivariate analyses, the As exposure variables were not correlated with global %hmC in the overall samples (Appendix, Table E1). Upon stratification by gender, As exposure was positively correlated with global %hmC in males and negatively correlated with global %hmC in females (Appendix, Table E1). Regression models for As exposure variables predicting global %hmC, stratified by gender and adjusted for age, BMI, cigarette smoking, and years of education, are presented in Figure 4.

Although the parameter estimates for the As variables predicting global %hmC were not all significant at $P < 0.05$, the estimates were consistently positive in males and negative in females, and the magnitudes of the estimates were similar between the two samples (Figure 4). The associations for the As exposure variables (wAs, uAs, bAs, and pAs) predicting global %hmC were significantly different by gender, as determined by Wald tests ($P < 0.05$ for all As exposure variables in NIAT and FOX).

Figure 3. Adjusted regression coefficients for As exposure variables predicting global %mC, stratified by gender, in NIAT and FOX samples. Plots represent B ± 95% CI for each As variable predicting global %mC from regression models adjusting for age, BMI, ever cigarette smoking, and years of education.

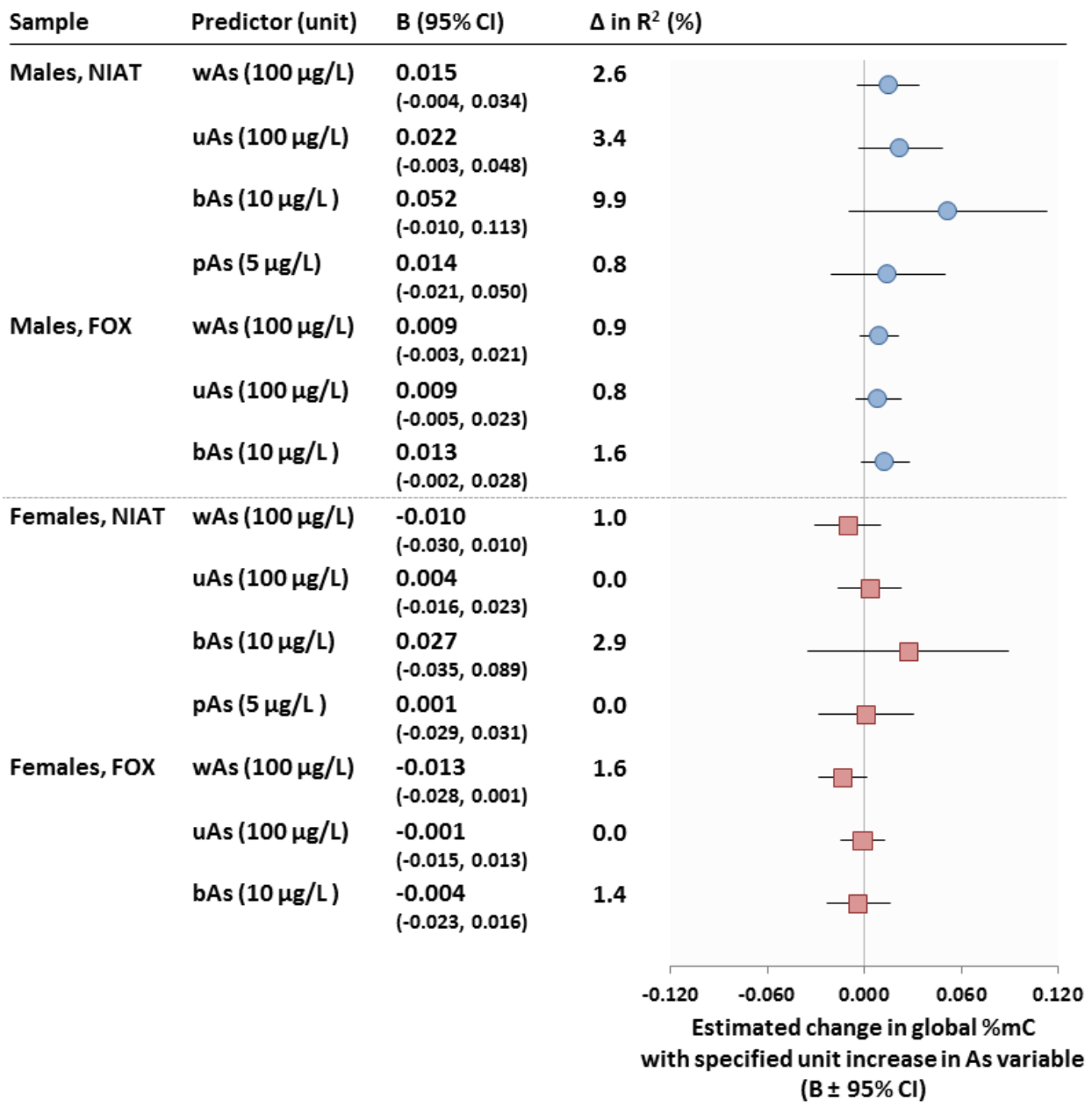

Figure 4. Adjusted regression coefficients for As exposure variables predicting global %hmC, stratified by gender, in NIAT and FOX samples. Plots represent B ± 95% CIs for each As variable predicting global %hmC from regression models adjusting for age, BMI, ever cigarette smoking, and years of education.

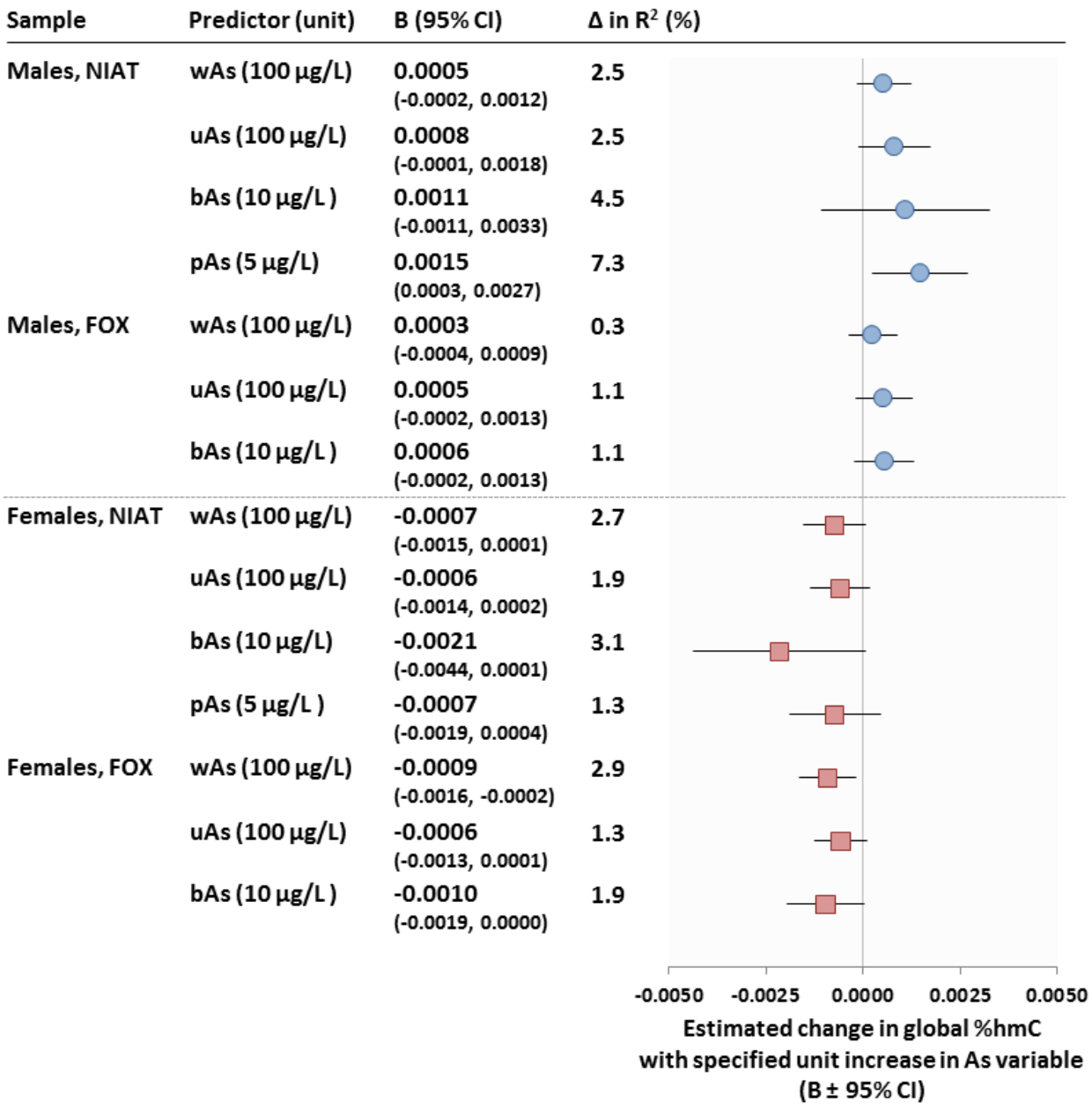

DISCUSSION

In this study, we examined the associations of gender, age, and As exposure with global %mC and %hmC in different subtypes of WBC DNA from two independent samples of Bangladeshi adults. We observed that global %mC was higher in males, and global %hmC decreased with age. Arsenic exposure was associated with global %hmC differentially by gender: In males, As exposure was positively associated with global %hmC, while in females, As exposure was negatively associated with global %hmC. The directions and magnitudes of the parameter estimates for age and As exposure variables were consistent between the two samples. Our results suggest that in DNA isolated from human PBLs and PBMCs, age is associated with a dose-dependent decrease in global %hmC, and chronic As exposure is associated with gender-specific changes in global %hmC.

Few studies have examined global 5hmC content in human blood cell DNA. While Nestor et al. (2012) found barely-detectable levels of 5hmC in human PBL DNA using an immuno dot-blot method (N=2 biological samples), Pronier et al. (2011) detected measurable 5hmC in PBLs using HPLC-MS-MS in myeloproliferative neoplasm patients and healthy controls. The range of global %hmC in PBL and PBMC DNA in our study (0.0147-0.0505% of total cytosine) was markedly lower than the global %hmC content in human brain (0.67% of total DNA, or 0.13% of total cytosines, assuming a cytosine proportion of 20% in human DNA) and liver (0.46% of total DNA, or 0.092% of total cytosines) and similar to global %hmC in lung (0.14% of total DNA, or 0.028% of total cytosines) and breast (0.05% of total DNA, or 0.010% of total cytosines), as reported by Li and Liu (2011). We found no correlation between global %mC and %hmC in DNA isolated from PBLs, consistent with a previous report that global 5mC and 5hmC levels were not correlated across human tissues (Nestor et al. 2012). However, global

%mC and %hmC were strongly correlated in DNA isolated from PBMCs, suggesting that global %mC and %hmC content might be correlated within a specific tissue or cell type.

Most of the current literature on the aging process and 5hmC dynamics has examined 5hmC in murine brain tissue. In mouse models, 5hmC content in the hippocampus increases from birth through 12 months (Song et al. 2011) and is preferentially acquired in developmentally-activated genes (K. E. Szulwach et al. 2011); through 24 months, 5hmC content has been shown to increase in hippocampal tissues (Chen et al. 2012; Chouliaras et al. 2012), as well as decrease in mitochrondrial DNA (mtDNA) in the frontal cortex (Dzitoyeva et al. 2012). Little has been reported on the relationship between age and 5hmC in other tissues. Age was positively correlated with global 5mC and 5hmC (measured by enzyme-linked immunosorbent assay) in a small study of human sperm DNA samples from 15 fertile donors (Jenkins et al. 2013), but to our knowledge, no other studies have examined the relationship between age and 5hmC in samples from non-diseased animals or humans.

We found that age was strongly associated with global %hmC depletion in blood cell DNA from healthy adults. Aging is associated with hematopoietic and immunological decline and increased risk of leukemias (Henry et al. 2011), which might result, in part, from a decline in hematopoietic stem cell integrity (Geiger et al. 2013). Busque et al. (2012) found a marked increase in the presence of *Tet2* somatic mutations in granulocyte DNA from elderly patients with age-associated skewing (AAS) of X-inactivation ratios in blood cells compared with age-matched healthy individuals, as well as a decrease in 5hmC levels in myeloid cells with age; the authors speculated that TET2-mediated 5hmC depletion may play an important role in the aging hematopoietic system (Busque et al. 2012). Our findings support the concept that global %5hmC in peripheral blood cell DNA might be an important biomarker of age-related hematopoietic

decline. We found that age was similarly associated with global %hmC decline in DNA isolated from both PBLs (primarily granulocytes) and PBMCs (primarily lymphocytes), suggesting that the age-related decrease in 5hmC occurs in both myeloid and lymphoid blood cells. Global loss of 5hmC is observed in numerous human cancers (Haffner et al. 2011); if aging is found to have a causal effect on 5hmC decline, it is possible that therapies to prevent 5hmC loss might reduce the risk of age-related leukemias and other malignancies.

Arsenic exposure was associated with gender-specific changes in global %hmC of PBL and PBMC DNA. The implications of this finding are unclear. As stated earlier, As_2O_3 in combination with ATRA is a successful treatment in APL, an AML subtype characterized by the fusion of the promyelocytic leukaemia (PML) gene to retinoic acid receptor alpha (RARα) (Goddard et al. 1991). One proposed mechanism of PML–RARα-induced leukaemogenesis is through its interaction with polycomb repressive complexes (PRC2) and subsequent transcriptional repression via tri-methylation of histone H3 lysine 27 (H3K27me3), which interferes with myeloid differentiation (Shih et al. 2012). Interestingly, in AML subtypes that are normally ATRA-resistant, lysine-specific demethylase 1 (LSD1) inhibitors "unlock" ATRA's pro-differentiation functionality: in both ATRA-responsive and insensitive cells, the co-treatment of LSD1 inhibitors with ATRA enhances the expression of genes associated with myeloid differentiation by increasing gene-specific dimethylation of histone H3 lysine 4 (H3K4me2) (Schenk et al. 2012), a mark associated with gene activation (Pekowska et al. 2010). This suggests that in APL, As_2O_3 induces epigenetic modifications that potentiate ATRA-driven myeloid differentiation. Since increased 5hmC content is associated with accessible chromatin structure (Mellén et al. 2012) and pluripotency (Ficz et al. 2011; Freudenberg et al. 2012), it is

plausible that the treatment effects of As_2O_3 occur through increases in global hmC levels, consistent with our observations in males.

Arsenic exposure might influence several key components involved in 5hmC dynamics. In cell culture, arsenite and its methylated metabolites have been shown to decrease BER activity (Ebert et al. 2011), which would interfere with active 5hmC demethylation. Arsenic is a known inhibitor of pyruvate dehydrogenase (PDH), an enzyme that transforms pyruvate into acetyl-CoA, a molecule involved in the Krebs cycle (Schiller et al. 1977). The TET cofactor α-ketoglutarate is a critical intermediate in the Krebs cycle, and deficiencies in the Krebs cycle enzyme succinate dehydrogenase (SDH) are associated with decreased 5hmC levels in mice (Letouzé et al. 2013) and humans (Mason and Hornick 2013), suggesting that aberrant Krebs cycle metabolism might contribute to epigenetic dyregulation during carcinogenesis (Garraway and Lander 2013). Arsenic exposure has also been linked with alterations of histone modifications in animal models (Cronican et al. 2013) and human studies (Cantone et al. 2011; Chervona et al. 2012), which could induce downstream effects on 5hmC. However, it is still not clear why we observed gender-specific associations of As exposure and global %hmC. Future research in experimental models should examine the potential mechanisms through which As exposure might induce changes in 5hmC content in blood cells and the biologic basis for a gender-specific effect.

Similar magnitudes of association for age and As exposure were observed in DNA isolated from different subtypes of WBCs in two independent samples of adults, which reduces the possibility that our findings were observed by chance and/or are explained by shifts in blood cell subtypes or counts. Nevertheless, given the observational nature of our study, we cannot dismiss the possibility that our findings might be explained by unmeasured confounding. We

also cannot determine the precise mechanisms through which the aging process and/or As exposure might induce global 5hmC changes, but our findings are useful for hypothesis generation for future experimental studies.

In conclusion, in two independent samples of Bangladeshi adults, we observed that age was associated with decreased global %hmC of PBL and PBMC DNA and that As exposure was associated with gender-specific changes in global %hmC. Future studies should examine the relevance of global 5hmC as a marker of age-related decline and disease risk, in addition to the potential causative role of aging on global 5hmC levels. Studies should also examine the mechanisms through which As exposure might induce changes in 5hmC content in human blood cells and the potential role of 5hmC in APL.

ACKNOWLEDGEMENTS

This work was supported by grants RO1 CA133595, RO1 ES017875, P42 ES10349, P30 ES09089, T32 CA009529-24, and RO1 ES011601 from the National Institutes of Health. The content is solely the responsibility of the authors and does not necessarily represent the official views of the National Institute of Environmental Health Sciences, the National Cancer Institute, or the National Institutes of Health.

REFERENCES

Ahsan H, Chen Y, Parvez F, Argos M, Hussain AI, Momotaj H, et al. 2006. Health effects of arsenic longitudinal study (heals): Description of a multidisciplinary epidemiologic investigation. J Expo Sci Environ Epidemiol 16:191-205.

Bergman Y, Cedar H. 2013. DNA methylation dynamics in health and disease. Nat Struct Mol Biol 20:274-281.

Bird A. 1992. The essentials of DNA methylation. Cell 70:5-8.

Busque L, Patel JP, Figueroa ME, Vasanthakumar A, Provost S, Hamilou Z, et al. 2012. Recurrent somatic tet2 mutations in normal elderly individuals with clonal hematopoiesis. Nat Genet 44:1179-1181.

Cantone L, Nordio F, Hou L, Apostoli P, Bonzini M, Tarantini L, et al. 2011. Inhalable metal-rich air particles and histone h3k4 dimethylation and h3k9 acetylation in a cross-sectional study of steel workers. Environ Health Perspect 119:964-969.

Chen H, Dzitoyeva S, Manev H. 2012. Effect of aging on 5-hydroxymethylcytosine in the mouse hippocampus. Restorative neurology and neuroscience 30:237-245.

Chervona Y, Hall MN, Arita A, Wu F, Sun H, Tseng HC, et al. 2012. Associations between arsenic exposure and global posttranslational histone modifications among adults in bangladesh. Cancer Epidemiol Biomarkers Prev 21:2252-2260.

Chouliaras L, van den Hove DL, Kenis G, Keitel S, Hof PR, van Os J, et al. 2012. Age-related increase in levels of 5-hydroxymethylcytosine in mouse hippocampus is prevented by caloric restriction. Current Alzheimer research 9:536-544.

Cronican AA, Fitz NF, Carter A, Saleem M, Shiva S, Barchowsky A, et al. 2013. Genome-wide alteration of histone h3k9 acetylation pattern in mouse offspring prenatally exposed to arsenic. PLoS ONE 8:e53478.

Dzitoyeva S, Chen H, Manev H. 2012. Effect of aging on 5-hydroxymethylcytosine in brain mitochondria. Neurobiol Aging 33:2881-2891.

Ebert F, Weiss A, Bultemeyer M, Hamann I, Hartwig A, Schwerdtle T. 2011. Arsenicals affect base excision repair by several mechanisms. Mutat Res 715:32-41.

Ficz G, Branco MR, Seisenberger S, Santos F, Krueger F, Hore TA, et al. 2011. Dynamic regulation of 5-hydroxymethylcytosine in mouse es cells and during differentiation. Nature 473:398-402.

Freudenberg JM, Ghosh S, Lackford BL, Yellaboina S, Zheng X, Li R, et al. 2012. Acute depletion of tet1-dependent 5-hydroxymethylcytosine levels impairs lif/stat3 signaling and results in loss of embryonic stem cell identity. Nucleic Acids Res 40:3364-3377.

Gamble MV, Ahsan H, Liu X, Factor-Litvak P, Ilievski V, Slavkovich V, et al. 2005. Folate and cobalamin deficiencies and hyperhomocysteinemia in bangladesh. Am J Clin Nutr 81:1372-1377.

Gamble MV, Liu X, Ahsan H, Pilsner JR, Ilievski V, Slavkovich V, et al. 2006. Folate and arsenic metabolism: A double-blind, placebo-controlled folic acid-supplementation trial in bangladesh. Am J Clin Nutr 84:1093-1101.

Garraway Levi A, Lander Eric S. 2013. Lessons from the cancer genome. Cell 153:17-37.

Geiger H, de Haan G, Florian MC. 2013. The ageing haematopoietic stem cell compartment. Nat Rev Immunol 13:376-389.

Goddard AD, Borrow J, Freemont PS, Solomon E. 1991. Characterization of a zinc finger gene disrupted by the t(15;17) in acute promyelocytic leukemia. Science 254:1371-1374.

Guo Junjie U, Su Y, Zhong C, Ming G-l, Song H. 2011. Hydroxylation of 5-methylcytosine by tet1 promotes active DNA demethylation in the adult brain. Cell 145:423-434.

Haffner MC, Chaux A, Meeker AK, Esopi DM, Gerber J, Pellakuru LG, et al. 2011. Global 5-hydroxymethylcytosine content is significantly reduced in tissue stem/progenitor cell compartments and in human cancers. Oncotarget 2:627-637.

Hall M, Chen Y, Ahsan H, Slavkovich V, van Geen A, Parvez F, et al. 2006. Blood arsenic as a biomarker of arsenic exposure: Results from a prospective study. Toxicology 225:225-233.

Hall MN, Niedzwiecki M, Liu X, Harper KN, Alam S, Slavkovich V, et al. 2013. Chronic arsenic exposure and blood glutathione and glutathione disulfide concentrations in bangladeshi adults. Environ Health Perspect 121:1068-74.

Henry CJ, Marusyk A, DeGregori J. 2011. Aging-associated changes in hematopoiesis and leukemogenesis: What's the connection? Aging 3:643-656.

Hughes MF, Beck BD, Chen Y, Lewis AS, Thomas DJ. 2011. Arsenic exposure and toxicology: A historical perspective. Toxicological Sciences 123:305-332.

Ito S, Dalessio AC, Taranova OV, Hong K, Sowers LC, Zhang Y. 2010. Role of tet proteins in 5mc to 5hmc conversion, es-cell self-renewal and inner cell mass specification. Nature 466:1129-1133.

Jenkins TG, Aston KI, Cairns BR, Carrell DT. 2013. Paternal aging and associated intraindividual alterations of global sperm 5-methylcytosine and 5-hydroxymethylcytosine levels. Fertil Steril 100:945-51.

Kass SU, Landsberger N, Wolffe AP. 1997. DNA methylation directs a time-dependent repression of transcription initiation. Current Biology 7:157-165.

Kile ML, Baccarelli A, Hoffman E, Tarantini L, Quamruzzaman Q, Rahman M, et al. 2012. Prenatal arsenic exposure and DNA methylation in maternal and umbilical cord blood leukocytes. Environ Health Perspect 120:1061-1066.

Kriaucionis S, Heintz N. 2009. The nuclear DNA base 5-hydroxymethylcytosine is present in purkinje neurons and the brain. Science 324:929-930.

Lambrou A, Baccarelli A, Wright RO, Weisskopf M, Bollati V, Amarasiriwardena C, et al. 2012. Arsenic exposure and DNA methylation among elderly men. Epidemiology 23:668-676.

Letouzé E, Martinelli C, Loriot C, Burnichon N, Abermil N, Ottolenghi C, et al. 2013. Sdh mutations establish a hypermethylator phenotype in paraganglioma. Cancer Cell 23:739-752.

Li W, Liu M. 2011. Distribution of 5-hydroxymethylcytosine in different human tissues. Journal of nucleic acids 2011:870726.

Lo-Coco F, Avvisati G, Vignetti M, Thiede C, Orlando SM, Iacobelli S, et al. 2013. Retinoic acid and arsenic trioxide for acute promyelocytic leukemia. N Engl J Med 369:111-121.

Loewenberg S. 2007. Scientists tackle water contamination in bangladesh. The Lancet 370:471-472.

Lorsbach RB, Moore J, Mathew S, Raimondi SC, Mukatira ST, Downing JR. 2003. Tet1, a member of a novel protein family, is fused to mll in acute myeloid leukemia containing the t(10;11)(q22;q23). Leukemia 17:637-641.

Majumdar S, Chanda S, Ganguli B, Mazumder DN, Lahiri S, Dasgupta UB. 2010. Arsenic exposure induces genomic hypermethylation. Environ Toxicol 25:315-318.

Mason EF, Hornick JL. 2013. Succinate dehydrogenase deficiency is associated with decreased 5-hydroxymethylcytosine production in gastrointestinal stromal tumors: Implications for mechanisms of tumorigenesis. Modern pathology : an official journal of the United States and Canadian Academy of Pathology, Inc.

Mellén M, Ayata P, Dewell S, Kriaucionis S, Heintz N. 2012. Mecp2 binds to 5hmc enriched within active genes and accessible chromatin in the nervous system. Cell 151:1417-1430.

Murati A, Brecqueville M, Devillier R, Mozziconacci MJ, Gelsi-Boyer V, Birnbaum D. 2012. Myeloid malignancies: Mutations, models and management. BMC cancer 12:304.

Nestor CE, Ottaviano R, Reddington J, Sproul D, Reinhardt D, Dunican D, et al. 2012. Tissue type is a major modifier of the 5-hydroxymethylcytosine content of human genes. Genome Res 22:467-477.

Nohara K, Baba T, Murai H, Kobayashi Y, Suzuki T, Tateishi Y, et al. 2011. Global DNA methylation in the mouse liver is affected by methyl deficiency and arsenic in a sex-dependent manner. Arch Toxicol 85:653-661.

Ono R, Taki T, Taketani T, Taniwaki M, Kobayashi H, Hayashi Y. 2002. Lcx, leukemia-associated protein with a cxxc domain, is fused to mll in acute myeloid leukemia with trilineage dysplasia having t(10;11)(q22;q23). Cancer Res 62:4075-4080.

Pekowska A, Benoukraf T, Ferrier P, Spicuglia S. 2010. A unique h3k4me2 profile marks tissue-specific gene regulation. Genome Res 20:1493-1502.

Pfeiffer CM, Huff DL, Gunter EW. 1999. Rapid and accurate hplc assay for plasma total homocysteine and cysteine in a clinical laboratory setting. Clin Chem 45:290-292.

Pilsner JR, Liu X, Ahsan H, Ilievski V, Slavkovich V, Levy D, et al. 2007. Genomic methylation of peripheral blood leukocyte DNA: Influences of arsenic and folate in bangladeshi adults. Am J Clin Nutr 86:1179-1186.

Pilsner JR, Liu X, Ahsan H, Ilievski V, Slavkovich V, Levy D, et al. 2009. Folate deficiency, hyperhomocysteinemia, low urinary creatinine, and hypomethylation of leukocyte DNA are risk factors for arsenic-induced skin lesions. Environ Health Perspect 117:254-260.

Pilsner JR, Hall MN, Liu X, Ilievski V, Slavkovich V, Levy D, et al. 2012. Influence of prenatal arsenic exposure and newborn sex on global methylation of cord blood DNA. PLoS One 7:e37147.

Pronier E, Almire C, Mokrani H, Vasanthakumar A, Simon A, da Costa Reis Monte Mor B, et al. 2011. Inhibition of tet2-mediated conversion of 5-methylcytosine to 5-hydroxymethylcytosine disturbs erythroid and granulomonocytic differentiation of human hematopoietic progenitors. Blood 118:2551-2555.

Quinlivan EP, Gregory JF. 2008. DNA methylation determination by liquid chromatography–tandem mass spectrometry using novel biosynthetic [u-15n]deoxycytidine and [u-15n]methyldeoxycytidine internal standards. Nucleic Acids Research 36:e119.

Reitman ZJ, Yan H. 2010. Isocitrate dehydrogenase 1 and 2 mutations in cancer: Alterations at a crossroads of cellular metabolism. Journal of the National Cancer Institute 102:932-941.

Ren X, McHale CM, Skibola CF, Smith AH, Smith MT, Zhang L. 2011. An emerging role for epigenetic dysregulation in arsenic toxicity and carcinogenesis. Environ Health Perspect 119:11-19.

Robertson KD. 2005. DNA methylation and human disease. Nat Rev Genet 6:597-610.

Schenk T, Chen WC, Gollner S, Howell L, Jin L, Hebestreit K, et al. 2012. Inhibition of the lsd1 (kdm1a) demethylase reactivates the all-trans-retinoic acid differentiation pathway in acute myeloid leukemia. Nature medicine 18:605-611.

Schiller CM, Fowler BA, Woods JS. 1977. Effects of arsenic on pyruvate dehydrogenase activation. Environ Health Perspect 19:205-207.

Shih AH, Abdel-Wahab O, Patel JP, Levine RL. 2012. The role of mutations in epigenetic regulators in myeloid malignancies. Nat Rev Cancer 12:599-612.

Siegfried Z, Eden S, Mendelsohn M, Feng X, Tsuberi BZ, Cedar H. 1999. DNA methylation represses transcription in vivo. Nat Genet 22:203-206.

Slot C. 1965. Plasma creatinine determination. A new and specific jaffe reaction method. Scand J Clin Lab Invest 17:381-387.

Smith ZD, Meissner A. 2013. DNA methylation: Roles in mammalian development. Nat Rev Genet 14:204-220.

Song C-X, Szulwach KE, Fu Y, Dai Q, Yi C, Li X, et al. 2011. Selective chemical labeling reveals the genome-wide distribution of 5-hydroxymethylcytosine. Nat Biotech 29:68-72.

Stroud H, Feng S, Morey Kinney S, Pradhan S, Jacobsen S. 2011. 5-hydroxymethylcytosine is associated with enhancers and gene bodies in human embryonic stem cells. Genome Biology 12:R54.

Szulwach KE, Li X, Li Y, Song C-X, Han JW, Kim S, et al. 2011. Integrating 5-hydroxymethylcytosine into the epigenomic landscape of human embryonic stem cells. PLoS Genet 7:e1002154.

Szulwach KE, Li X, Li Y, Song CX, Wu H, Dai Q, et al. 2011. 5-hmc-mediated epigenetic dynamics during postnatal neurodevelopment and aging. Nat Neurosci 14:1607-1616.

Tahiliani M, Koh KP, Shen Y, Pastor WA, Bandukwala H, Brudno Y, et al. 2009. Conversion of 5-methylcytosine to 5-hydroxymethylcytosine in mammalian DNA by mll partner tet1. Science 324:930-935.

Thurman RE, Rynes E, Humbert R, Vierstra J, Maurano MT, Haugen E, et al. 2012. The accessible chromatin landscape of the human genome. Nature 489:75-82.

Uribesalgo I, Di Croce L. 2011. Dynamics of epigenetic modifications in leukemia. Brief Funct Genomics 10:18-29.

Valinluck V, Sowers LC. 2007. Endogenous cytosine damage products alter the site selectivity of human DNA maintenance methyltransferase dnmt1. Cancer Res 67:946-950.

Vela NP, Heitkemper DT, Stewart KR. 2001. Arsenic extraction and speciation in carrots using accelerated solvent extraction, liquid chromatography and plasma mass spectrometry. The Analyst 126:1011-1017.

Wossidlo M, Nakamura T, Lepikhov K, Marques CJ, Zakhartchenko V, Boiani M, et al. 2011. 5-hydroxymethylcytosine in the mammalian zygote is linked with epigenetic reprogramming. Nat Commun 2:241.

Appendix, Table E1. Spearman correlations between As exposure variables and age with global %mC and %hmC, overall and stratified by gender, in NIAT and FOX samples.

a. Global %mC

Overall sample		Water As	Urinary As	Blood As	Plasma As	Age
	NIAT	-0.03	-0.07	0.20*	-0.01	0.03
	FOX	0.01	0.04	0.09	---	-0.12*
Males		Water As	Urinary As	Blood As	Plasma As	
	NIAT	0.09	-0.04	0.22	0.01	-0.01
	FOX	0.11	0.13†	0.15*	---	-0.18*
Females		Water As	Urinary As	Blood As	Plasma As	
	NIAT	-0.14	-0.03	0.10	-0.03	-0.13
	FOX	-0.12†	-0.04	-0.03	---	-0.16*

b. Global %hmC

Overall sample		Water As	Urinary As	Blood As	Plasma As	Age
	NIAT	0.05	0.15*	0.02	0.15*	-0.23**
	FOX	0.05	0.00	-0.02	---	-0.16**
Males		Water As	Urinary As	Blood As	Plasma As	
	NIAT	0.16	0.26*	0.05	0.31**	-0.19†
	FOX	0.11	0.14†	0.12†	---	-0.17*
Females		Water As	Urinary As	Blood As	Plasma As	
	NIAT	-0.05	0.05	-0.02	0.01	-0.29**
	FOX	-0.23**	-0.14*	-0.15*	---	-0.15*

†p<0.10; *p<0.05; **p<0.01

Chapter 5: Interactions of plasma glutathione redox and folate deficiency on arsenic methylation capacity

Megan M. Niedzwiecki[1], Megan N. Hall[2], Xinhua Liu[3], Vesna Slavkovich[1], Vesna Ilievski[1], Diane Levy[3], Shafiul Alam[4], Abu B. Siddique[4], Faruque Parvez[1], Joseph H. Graziano[1], and Mary V. Gamble[1]

Affiliations: [1]Department of Environmental Health Sciences, [2]Department of Epidemiology, [3]Department of Biostatistics, [1-3]Mailman School of Public Health, Columbia University, New York NY,10032, USA; [4]Columbia University Arsenic Project in Bangladesh, Dhaka, Bangladesh

Published: http://www.sciencedirect.com/science/article/pii/S0891584914001609

Niedzwiecki MM, Hall MN, Liu X, Slavkovich V, Ilievski V, Levy D, Alam S, Siddique AB, Parvez F, Graziano JH, Gamble MV. **Interaction of plasma glutathione redox and folate deficiency on arsenic methylation capacity in Bangladeshi adults.** Free Radic Biol Med. 2014 Apr 8. pii: S0891-5849(14)00160-9. doi: 10.1016/j.freeradbiomed.2014.03.042. [Epub ahead of print]

ABSTRACT

BACKGROUND: Inorganic arsenic (InAs) is metabolized through a series of methylation reactions catalyzed by arsenic(III)-methyltransferase (AS3MT), resulting in the generation of monomethylarsonic (MMAs) and dimethylarsinic acids (DMAs). AS3MT activity requires the presence of the methyl donor *S*-adenosylmethionine (SAM), a product of folate-dependent one-carbon metabolism, and a reductant. Redox-sensitive cysteine residues have been identified in the AS3MT active site, suggesting that AS3MT activity might be particularly sensitive to redox conditions. Although glutathione (GSH), the primary endogenous antioxidant, is not required for As methylation, GSH stimulates As methylation rates *in vitro*. However, the relationship between GSH redox and As methylation capacity in humans is unknown.

OBJECTIVE: To test the hypothesis that a more oxidized plasma GSH redox status is associated with decreased As methylation capacity, and examine whether these associations are modified by folate nutritional status.

METHODS: Concentrations of plasma GSH and GSSG, plasma folate, total blood As, total urinary As, and urinary As metabolites were assessed in 376 Bangladeshi adults who were chronically exposed to As in drinking water.

RESULTS: A decreased plasma GSH/GSSG ratio (reflecting a more oxidized redox state) was associated with increased urinary %MMA, decreased urinary %DMA, and increased total blood As among folate-deficient individuals (plasma folate $\leq$ 9.0 nmol/L). Concentrations of plasma GSH and GSSG were independently associated with increased and decreased As methylation capacity, respectively. No significant associations were observed in folate-sufficient individuals, and interactions by folate status were statistically significant.

CONCLUSIONS: An oxidized plasma GSH/GSSG redox state was associated with decreased As methylation capacity and increased bAs in folate-deficient Bangladeshi adults. GSH/GSSG

redox might contribute to the large interindividual variation in As methylation capacity observed in humans.

INTRODUCTION

Over 140 million people throughout Bangladesh, India, Vietnam, Nepal, and Cambodia are chronically exposed to arsenic (As) in drinking water at concentrations over 10 μg/L, the World Health Organization guideline (Ahmed et al. 2006). As a Class I human carcinogen (IARC 1987), As is associated with increased risk for cancers of the skin, lung, bladder, liver, and kidney (Navarro Silvera and Rohan 2007), although the carcinogenic mechanism of As is incompletely understood (Rossman 2003).

Inorganic arsenic (InAs) is metabolized, primarily in the liver, through a series of methylation reactions catalyzed by arsenic(III)-methyltransferase (AS3MT), resulting in the formation of monomethylarsonic acid (MMA) and dimethylarsinic acid (DMA) (Lin et al. 2002). The methyl group for the reaction is donated from *S*-adenosylmethionine (SAM) (Lin et al. 2002), a product of folate-dependent one-carbon metabolism (Chiang et al. 1996). Since methylation increases As excretion and reduces As body burden (Hughes et al. 2010), it is believed to be a detoxification process (Gebel 2002). However, *in vitro* and *in vivo* studies have identified MMA^{III} as the most toxic As form (Petrick et al. 2001; Styblo et al. 2000), suggesting that As methylation also involves bioactivation (Vahter and Concha 2001). Epidemiologic studies consistently find that a reduced capacity to fully methylate InAs, as indicated by higher $\%MMA^{(III+V)}$ and lower $\%DMA^{(III+V)}$ in urine, is associated with increased risk for As-induced skin lesions and cancers of the skin, lung, and bladder (Smith and Steinmaus 2009). As such, the identification of factors that facilitate complete methylation of InAs to DMA might provide insight into interventions to reduce risk for As-related diseases (Tseng 2007).

Although the proposed As methylation pathways presented in Figure 1 are distinct, they all require the presence of a reductant, such as glutathione (GSH) (Thomas 2009). As the

primary endogenous antioxidant, GSH readily donates an electron for reduction reactions, forming its oxidized form, glutathione disulfide (GSSG), in the process (Jones 2008). A lower ratio of GSH to GSSG reflects a more oxidized intracellular redox state (Jones 2008). While GSH is not required for As methylation to proceed, GSH can serve as the reducing agent necessary for AS3MT activity (Song et al. 2010; Thomas et al. 2007; Waters et al. 2004a; Waters et al. 2004b). The addition of GSH can stimulate AS3MT-catalyzed methylation rates in experimental systems already containing another reductant (Ding et al. 2012).

GSH might facilitate As methylation by donating electrons for the reduction of pentavalent arsenate (As^{V}) to trivalent arsenite (As^{III}), shown in the oxidative methylation pathway first proposed by Challenger (Challenger 1945, 1951), or by forming As-GSH complexes that are substrates for AS3MT, as proposed by Hayakawa et al. (Hayakawa et al. 2005). Recent work by Wang et al. found that a reductant (such as GSH) is needed to cleave a disulfide bond within AS3MT, which allows As^{III} to bind the enzyme (Wang et al. 2012). Additionally, active-site cysteine (Cys) residues that are potentially redox-sensitive have been identified in AS3MT (Fomenko et al. 2007). Redox-sensitive Cys residues are prone to oxidative modifications such as *S*-glutathionylation—the reversible formation of a mixed disulfide between a Cys residue and GSH or GSSG—which might also regulate AS3MT activity (Dalle-Donne et al. 2007).

We wished to test the hypothesis that a more reduced GSH redox state is associated with increased As methylation capacity, as indicated by a decrease in urinary %MMA, increase in urinary %DMA, and increase in the urinary secondary methylation index (SMI, defined as the ratio of DMA to MMA). We measured the GSH/GSSG ratio in plasma and in blood; the plasma ratio is believed to better reflect GSH/GSSG status in liver (Kombu et al. 2009), the primary site

of As methylation, and was therefore chosen for our focus in the present analyses. We also examined whether the associations were modified by plasma folate status. We used data from the Folate and Oxidative Stress (FOX) study (Hall et al. 2013), which was originally designed to assess the dose-response relationship between total As exposure and markers of oxidative stress.

SUBJECTS AND METHODS

Eligibility criteria and study design

The FOX study design is described in detail in Chapter 3.

Analytic techniques

Methods for sample collection and analysis of water As, urinary As, urinary Cr, blood As and plasma folate and cobalamin are described in detail in Chapter 3.

Blood and plasma glutathione and glutathione disulfide

Whole blood and plasma GSH and GSSG were assayed based on the protocol by Jones et al (Jones et al. 1998), as previously described (Hall et al. 2013). Briefly, blood was collected in the field laboratory in Bangladesh and immediately transferred into Eppendorf tubes containing 5% perchloric acid (PCA), 0.1 M boric acid, and γ-glutamyl glutamate (internal standard). Samples were derivatized in Bangladesh, and the derivatized samples were stored at -80°C until delivered to Columbia University on dry ice for HPLC analysis. Metabolites were detected using a Waters 474 scanning fluorescence detector, with 335 nm excitation and 515 nm emission (Waters Corp., Milford, MA). Intra-assay CVs were all between 5 and 10%, and inter-assay CVs were between 11 and 18%.

Calculation of the Reduction Potential

The reduction potential of the thiol/disulfide plasma GSH/GSSG redox pair (E_h) was calculated using the Nernst equation ($E_h = E_o + RT/nF \ln [\text{disulfide}]/[\text{thiol}]^2$ where E_o= standard potential for the redox couple, R= gas constant, T= absolute temperature, n=2 for the number of electrons transferred, and F= Faraday's constant) (Jones et al. 2002). A more positive E_h value reflects a more oxidized redox state.

Statistical methods

Descriptive statistics were calculated for the overall sample. Chi-square test and the Wilcoxon rank-sum test were used to detect group difference in categorical and continuous variables, respectively. Spearman correlations were used to examine bivariate associations between quantitative variables including covariates with urinary As metabolite percentages and plasma GSH and GSSG concentrations. Certain covariates (gender, age, ever cigarette smoking, and water As) were selected based on biologic plausibility and previous studies in the literature. Other biologically-plausible confounders (BMI, plasma cobalamin, ever betelnut use, television ownership, and uCr) were considered by examining their bivariate associations with plasma GSH variables and As exposure variables in this dataset; covariates were included in the regression models if they were associated with both exposure and outcome at significance level of 0.2. To reduce extraneous variation in plasma GSH and GSSG, we adjusted these variables for laboratory batch using the residual method using batch (day of run) as a categorical variable and used the batch-adjusted plasma GSH and GSSG variables in all analyses.

Linear regression models were constructed with plasma GSH variables as predictors and urinary As metabolite variables as the outcomes. Variables with skewed distributions were log-transformed to normalize the distributions of the variables and/or improve the linearity of the relationships between the predictors and outcomes; transformed variables included uAs, bAs, wAs, urinary SMI, plasma GSH, plasma GSSG, and plasma GSH/GSSG. Relationships were also examined by using plasma GSH/GSSG variables categorized at tertiles in the overall study sample, and linear models with categorized plasma GSH/GSSG variables to calculate gender and well water As adjusted mean urinary %MMA and %DMA within the categories, for the plasma folate strata. Differences in the associations between predictor (GSH, GSSG, GSH/GSSG ratio) and outcomes of methylation variables between plasma folate strata were also examined and

detected by Wald tests. Of the total N=378 participants in the study sample, two participants were excluded for missing data (N=1 participant with missing plasma folate, N=1 participant with missing plasma GSH), leaving N=376 participants in the analysis. All statistical analyses were conducted using SAS (version 9.3; SAS Institute Inc., Cary, NC).

RESULTS

Demographic and clinical characteristics of the study participants, overall and by plasma folate status, are shown in Table 1. In the overall sample, the average age was 43 y, and there were roughly equal numbers of males and females. Folate-deficient individuals (plasma folate concentrations < 9.0 nmol/L) comprised approximately 29% of the sample. The folate-deficient group had a higher proportion of males, ever cigarette smokers, and betel nut chewers; higher mean age; and lower mean BMI. The folate-deficient group also had higher %InAs and %MMA and lower %DMA in urine.

Males had significantly higher mean urinary %MMA (16.0% vs. 12.0%, $P < 0.0001$) and lower mean urinary %DMA (66.6% vs. 69.9%, $P < 0.0001$) and plasma GSH/GSSG ratio (1.25 vs. 1.34, $P = 0.04$). As shown in Table 2, the plasma GSH/GSSG ratio was negatively correlated with age in both folate groups. In support of previous findings from our group (Hall et al. 2009), plasma cobalamin was positively correlated with urinary %MMA. Total As exposures in well water, urine, and blood were positively correlated with %InAs and %MMA and negatively correlated with urinary %DMA, consistent with inhibition or saturation of AS3MT by InAs and MMA (Song et al. 2010).

Table 1. Descriptive characteristics for study sample by plasma folate status.

Baseline variables	Total sample N=376	Folate deficient (< 9.0 nmol/L) N=110	Folate sufficient (≥9.0 nmol/L) N=266	Group difference *P*
Age (yrs)	43.1 ± 8.03[a] (30 to 63)	44.4 ± 8.0 (30 to 62)	42.6 ± 8.3 (31 to 63)	0.02
Male	182 (48.4)[b]	70 (64.6)	112 (42.1)	<0.0001
BMI (kg/m^2)	20.4 ± 3.5 (13.8 to 35.3)	19.7 ± 3.0 (13.8 to 31.7)	20.7 ± 3.6 (14.5 to 35.3)	0.02
Ever cigarette smoking	136 (36.2)	59 (53.6)	77 (29.0)	<0.0001
Ever betel nut use	160 (42.6)	59 (53.6)	101 (38.0)	0.003
Television ownership	219 (58.2)	57 (51.8)	162 (60.9)	0.07
Plasma folate (nmol/L)	12.9 ± 7.2 (2.4 to 60.6)	7.1 ± 1.4 (2.4 to 8.9)	15.3 ± 7.2 (9.1 to 60.6)	<0.0001
Plasma cobalamin (µM)	204 ± 113 (44 to 1183)	191 ± 93 (59 to 557)	209 ± 119 (44 to 1183)	0.20
Plasma GSH (µmol/L)	2.6 ± 0.7 (1.0 – 5.8)	2.5 ± 0.7 (1.2 – 4.8)	2.7 ± 0.8 (1.0 to 5.8)	0.25
Plasma GSSG (µmol/L)	2.1 ± 0.6 (0.8 – 4.8)	2.0 ± 0.7 (0.9 – 4.8)	2.2 ± 0.6 (0.8 to 4.0)	0.02
Plasma GSH/GSSG	1.3 ± 0.4 (0.4 to 2.9)	1.3 ± 0.4 (0.6 to 2.6)	1.3 ± 0.5 (0.4 to 2.9)	0.38
Plasma GSH E_h (mV)	-98.7 ± 7.3 (-118.0 to -73.4)	-98.6 ± 6.8 (-112.6 to -83.6)	-98.7 ± 7.5 (-118.0 to -73.4)	0.92
Water As (µg/L)	138 ± 124 (0.4 to 700)	164 ± 143 (0.4 to 700)	128 ± 114 (0.4 to 447)	0.04
Blood As, total (µg/L)	13.4 ± 9.8 (1.2 to 57.0)	15.4 ± 10.9 (1.3 to 51.3)	12.5 ± 9.1 (1.2 to 57.0)	0.03
Urinary As, total (µg/L)	202 ± 226 (3 to 1990)	209 ± 207 (7 to 992)	119 ± 223 (3 to 1990)	0.43
Urinary Cr (mg/dL)	53 ± 44 (4 to 224)	53 ± 42 (4 to 212)	55 ± 44 (6 to 224)	0.83
Urinary As/Cr (µg/g Cr)	417 ± 329 (16 to 1832)	464 ± 361 (16 to 1743)	397 ± 312 (18 to 1832)	0.14
Urinary %InAs	17.7 ± 5.5 (6.7 to 51.8)	18.6 ± 5.9 (8.3 to 42.9)	17.4 ± 5.3 (6.7 to 51.8)	0.05
Urinary %MMA	13.9 ± 5.0 (3.6 to 30.0)	15.3 ± 5.5 (3.6 to 30.0)	13.4 ± 4.7 (4.2 to 28.5)	0.002
Urinary %DMA	68.3 ± 7.9 (38.3 to 88.0)	66.1 ± 8.5 (39.5 to 88.0)	69.3 ± 7.4 (38.3 to 85.7)	0.004

[a.] Mean ± SD (all such values); [b.] N(%) (all such values)

Table 2. Spearman correlations of continuous sample characteristics with plasma glutathione variables and urinary As metabolite percentages.

Total sample N=376	Plasma GSH/GSSG	Urinary %InAs	Urinary %MMA	Urinary %DMA
Age	-0.23***	-0.17**	0.15**	0.01
BMI	-0.12*	-0.05	-0.18**	0.14**
Plasma cobalamin	-0.15**	-0.08	0.13*	-0.04
Water As	0.05	0.21***	0.21***	-0.26***
Urinary As/Cr	0.04	0.19**	0.22***	-0.25***
Blood As	0.01	0.25***	0.30***	-0.35***
Folate deficient N=110	Plasma GSH/GSSG	Urinary %InAs	Urinary %MMA	Urinary %DMA
Age	-0.29***	-0.24**	0.23**	-0.01
BMI	-0.19*	-0.08	-0.22**	0.20**
Plasma cobalamin	-0.18	0.05	0.13	-0.10
Water As	0.16	0.21*	0.29**	-0.27**
Urinary As/Cr	0.11	0.25**	0.22*	-0.28**
Blood As	0.03	0.29**	0.36**	-0.38***
Folate sufficient N=266	Plasma GSH/GSSG	Urinary %InAs	Urinary %MMA	Urinary %DMA
Age	-0.22***	-0.17**	0.09	0.05
BMI	-0.08	-0.03	-0.14*	0.10
Plasma cobalamin[a]	-0.14*	-0.13*	0.14*	-0.02
Water As	0.00	0.20**	0.14**	-0.22**
Urinary As/Cr	0.01	0.16**	0.19**	-0.22**
Blood As	-0.01	0.22**	0.25***	-0.31***

a. N=260; *p<0.05; **p<0.01; ***p<0.0001

In multiple linear regression models stratified by plasma folate status (Table 3), the plasma GSH/GSSG ratio was negatively associated with urinary %MMA (B ± SE, -4.7 ± 1.6, *P* = 0.004) and positively associated with urinary %DMA (B ± SE, 5.7 ± 2.7, *P* = 0.04) in the folate-deficient stratum, indicating that a more reduced plasma GSH/GSSG ratio is associated with increased As methylation capacity. No significant associations were observed in the folate-sufficient stratum, and the interactions by folate status were significant for %MMA (*P* = 0.01) and %DMA (*P* = 0.04). The plasma GSH/GSSG ratio was not associated with urinary %InAs in adjusted models in either folate stratum (folate-deficient, *P* = 0.62; folate-sufficient, *P* = 0.47). Additionally, the plasma GSH/GSSG ratio was positively associated with urinary SMI in the folate-deficient group (folate-deficient, B ± SE, 0.44 ± 0.14, *P* = 0.002; folate-sufficient, B ± SE, 0.00 ± 0.08, *P* = 0.98; *P* interaction = 0.01). The change in R^2 values for urinary SMI models were 6.1% in the folate-deficient group and 0.0% in the folate-sufficient group; the change in R^2 represents the percentage of the variance in urinary SMI explained by the plasma GSH/GSSG ratio after adjustment for covariates. Additionally, in the folate-deficient group, the plasma GSH/GSSG ratio was negatively associated with total bAs concentrations (B ± SE, -0.43 ± 0.17, *P* = 0.02). Similar patterns of association were observed when plasma GSH E_h, as calculated by the Nernst equation, was used as the predictor: in adjusted models, a more oxidized plasma GSH E_h was associated with decreased urinary SMI (*P* = 0.03), increased urinary %MMA (*P* = 0.03), decreased urinary %DMA (*P* = 0.17), and increased blood As concentrations (*P* = 0.08) in the folate-deficient stratum.

Table 3. Regression coefficients for associations between log-transformed plasma GSH/GSSG ratio and arsenic methylation capacity indicators, stratified by plasma folate status.

Outcome	Model	Total sample N=376	Folate-deficient N=110			Folate-sufficent N=266			*P* interaction[b]
		B ± SE	B ± SE	R^2 (%)	Δ in R^2 (%)	B ± SE	R^2 (%)	Δ in R^2 (%)	
Urinary %MMA	Adj. for gender, age, and wAs[c]	-1.03 ± 0.70	-4.60 ± 1.51**	29.6	6.4	-0.18 ± 0.77	19.2	0.0	0.001
	Extended model[a]	-0.81 ± 0.71	-5.21 ± 1.58**	36.3	7.1	0.17 ± 0.78	24.8	0.0	0.002
Urinary %DMA	Adj. for gender, age, and wAs[c]	0.09 ± 1.16	4.93 ± 2.56†	15.2	2.9	-0.92 ± 1.28	12.0	0.2	0.04
	Extended model[a]	0.28 ± 1.20	6.53 ± 2.66*	23.4	4.5	-0.89 ± 1.33	13.7	0.1	0.01
Urinary SMI[c]	Adj. for gender, age, and wAs[c]	0.07 ± 0.07	0.41 ± 0.14**	30.0	6.4	-0.01 ± 0.07	16.9	0.0	0.007
	Extended model[a]	0.06 ± 0.07	0.49 ± 0.14**	37.1	7.7	-0.04 ± 0.07	23.0	0.0	0.001
Blood As[c]	Adj. for gender, age, and wAs[c]	-0.04 ± 0.08	-0.26 ± 0.17	61.6	0.8	0.02 ± 0.09	62.4	0.0	0.15
	Extended model[a]	-0.10 ± 0.08	-0.39 ± 0.18*	63.5	1.7	-0.01 ± 0.09	64.0	0.0	0.06

[a] Adjusted for gender, log-transformed water As, age, cigarette smoking (ever/never), betelnut chewing (ever/never), television ownership, plasma cobalamin, and BMI; N=110 in folate deficient, N=259 in folate sufficient

[b] p-value was from Wald test for group difference in the regression coefficient

[c] Log-transformed

†p<0.10; *p<0.05; **p<0.01

To examine whether concentrations of plasma GSH or GSSG were independently associated with As methylation capacity, we built regression models with GSH and GSSG concentrations as predictors of urinary As metabolites, shown in Table 4. Since plasma GSH and GSSG were positively correlated with one another (Spearman $r = 0.29$, $P < 0.0001$), we included both variables in the models simultaneously. After adjustment, in the folate-deficient stratum, plasma GSH was positively associated with urinary SMI (B ± SE, 0.37 ± 0.18, $P = 0.04$), while plasma GSSG was negatively associated with urinary SMI (B ± SE, -0.49 ± 0.15, $P = 0.002$). Again, no significant associations were observed in the folate-sufficient stratum.

Least squares mean urinary %MMA and %DMA by plasma GSH/GSSG tertiles, stratified by plasma folate status, are presented in Figure 1. In the folate-deficient stratum, the most oxidized plasma GSH/GSSG category (Category 1, ratios of 0.39-1.06) had a 4.4% higher adjusted mean urinary %MMA compared to the least oxidized plasma GSH/GSSG category (Category 3, ratios of 1.42-2.92) ($P = 0.0001$) (Figure 1A). Category 2 (ratios of 1.07-1.41) had a 2.7% increase in mean urinary %MMA compared to Category 3 ($P = 0.01$) (Figure 1A). Adjusted mean urinary %MMA did not differ by plasma GSH/GSSG category in the folate-sufficient stratum (Figure 1B). Similarly, Category 1 had a 3.5% lower mean urinary %DMA compared to Category 3 in the folate-deficient ($P = 0.07$) (Figure 1C), but no differences by category were observed in the folate-sufficient group (Figure 1D).

Table 4. Regression coefficients for associations between log-transformed plasma GSH and plasma GSSG concentrations and arsenic methylation capacity indicators, stratified by plasma folate status.

Outcome	Predictor	Total sample N=376 B ± SE	Folate-deficient N=110 B ± SE	Folate-sufficent N=266 B ± SE	*P* interaction[b]
Urinary %MMA	Plasma GSH[a]	-0.02 ± 0.88	-4.75 ± 2.00*	1.16 ± 0.98	0.008
	Plasma GSSG[a]	1.59 ± 0.87[†]	5.46 ± 1.72**	0.93 ± 1.02	0.0003
Urinary %DMA	Plasma GSH[a]	-0.60 ± 1.50	4.93 ± 3.37	-1.24 ± 1.68	0.10
	Plasma GSSG[a]	-1.13 ± 1.48	-7.40 ± 2.90*	0.50 ± 1.76	0.02
Urinary SMI [c]	Plasma GSH[a]	-0.04 ± 0.08	0.41 ± 0.18*	-0.14 ± 0.09	0.006
	Plasma GSSG[a]	-0.15 ± 0.08[†]	-0.53 ± 0.15**	-0.07 ± 0.10	0.01
Blood As[c]	Plasma GSH[a]	-0.10 ± 0.10	-0.34 ± 0.22	-0.05 ± 0.12	0.25
	Plasma GSSG[a]	0.09 ± 0.10	0.41 ± 0.19*	-0.03 ± 0.12	0.05

[a] Adjusted for gender, log-transformed water As, age, cigarette smoking (ever/never), betelnut chewing (ever/never), television ownership, plasma cobalamin, BMI, , and other plasma variable (GSH or GSSG); N=110 in folate deficient, N=259 in folate sufficient

[b] p-value was from Wald test for group difference in the regression coefficient

[c] Log-transformed

[†]p<0.10; *p<0.05; **p<0.01

Figure 1. Adjusted mean urinary %MMA and %DMA by plasma GSH/GSSG category, stratified by plasma folate status.

Bars represent mean ± SE urinary %MMA and %DMA for each plasma GSH/GSSG tertile, adjusted for gender and well water As.

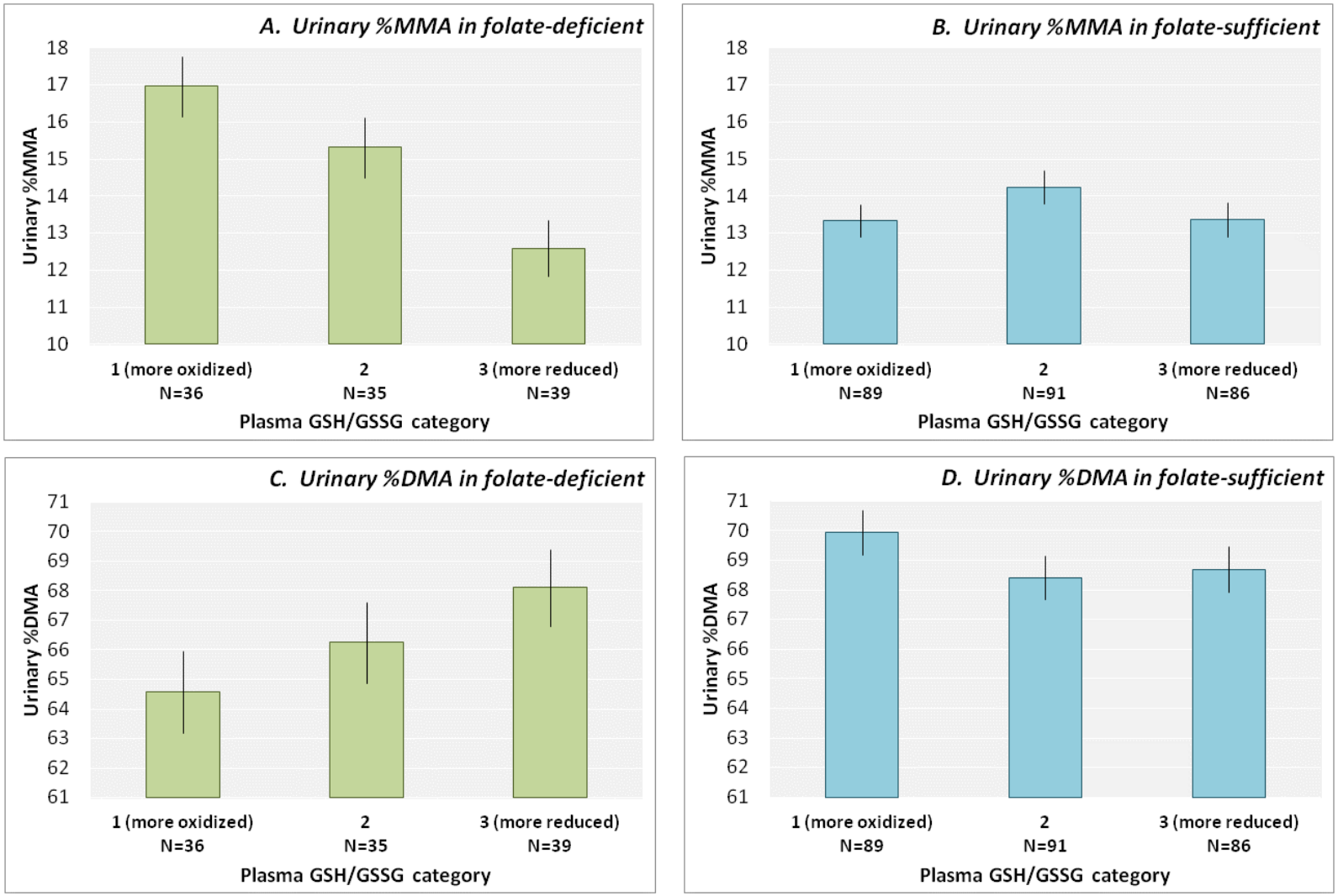

DISCUSSION

The primary objective of this study was to examine the associations of the plasma GSH/GSSG ratio with indicators of As methylation capacity (urinary %MMA, %DMA, and SMI) and to further examine whether these associations were modified by plasma folate status. In the folate-deficient stratum, we observed that the plasma GSH/GSSG ratio was negatively associated with urinary %MMA and positively associated with urinary %DMA and urinary SMI. No significant associations were observed in the folate-sufficient stratum, and the interaction by folate status was statistically significant. Additionally, the plasma GSH/GSSG ratio was negatively associated with total bAs concentrations in the folate-deficient stratum. Our findings suggest that a more reduced plasma GSH redox state is associated with increased As methylation capacity and decreased bAs concentrations, and plasma folate status is a modifier of these associations.

We found that an oxidized plasma GSH redox state was negatively associated with As methylation capacity, with concentrations of plasma GSH and GSSG having independent—and opposite—associations with urinary As metabolite percentages. We speculate that these observations might be explained by *S*-glutathionylation, i.e., direct binding of GSH and GSSG to AS3MT (Dalle-Donne et al. 2007). Unpublished *in vitro* results from David Thomas's group using biotinylated GSH and GSSG found that both molecules bind to the AS3MT protein, with GSH and GSSG leading to an increase and decrease in catalytic activity, respectively (David Thomas, personal communication). Furthermore, GSH and GSSG are antagonists: binding of GSH is reduced by the addition of GSSG (David Thomas, personal communication). These *in vitro* findings, along with the results of our study, suggest that the GSH/GSSG ratio influences

AS3MT activity and might be one of several mechanisms that determines As methylation capacity.

Since the association between plasma GSH/GSSG and As methylation capacity was only observed in the folate-deficient group, it is possible that *S*-glutathionylation of AS3MT, if present, might have a regulatory purpose. For example, GSSG inhibits the Na,K-ATPase enzyme through *S*-glutathionylation of Cys residues in its ATP binding site, but this inhibition does not occur when ATP concentrations are above a certain threshold (Petrushanko et al. 2012). The authors spectulated that *S*-glutathionylation of Na,K-ATPase is a regulatory mechanism to prevent irreversible loss of ATP under ATP-deficient conditions (Petrushanko et al. 2012). It is possible that an analogous mechanism occurs with AS3MT, where exposure to GSSG under folate-deficient conditions increases *S*-glutathionylation of redox-sensitive Cys residues near the SAM binding site, thereby conserving SAM. Interestingly, the AS3MT Cys residues that were previously identified as redox-sensitive, Cys^{156} and Cys^{206}, are located in the SAM binding pocket (Li et al. 2013a; Li et al. 2013b) . While we cannot definitively establish that this mechanism explains our observations, it would be of interest to explore this potential regulatory mechanism in experimental models.

It is also possible that our observed associations might be explained by differential biliary transport of As metabolite species. For example, efflux of As^{III} and MMA^{III} from hepatocytes to the bile via multidrug resistance protein 2 (Mrp2) requires the formation of As-GSH conjugates (Leslie 2012). If plasma GSH redox state indeed influences biliary As excretion, we would expect that plasma GSH redox would be associated with urinary As concentrations. However, we found no significant associations between plasma GSH, GSSG, or GSH/GSSG ratio with total urinary As or urinary As metabolite concentrations (InAs, MMA, or DMA) (data not

shown). This suggests that the plasma GSH redox state is only associated with the *distribution* of urinary As metabolites for a given As exposure. The absence of associations between plasma GSH redox and urinary As concentrations also suggests that our observations are less likely to be explained by reverse causality, e.g., inhibition of glutathione reductase (GR) by As metabolites seen at very high As concentrations *in vitro* (Chouchane and Snow 2001; Styblo and Thomas 1995; Styblo et al. 1997) and *in vivo* (Rodríguez et al. 2005).

We are aware of only one other study that examined the associations between GSH and urinary As metabolites in humans (Xu et al. 2008). Xu et al. found that total non-protein sulfhydryls (primarily GSH + GSSG) measured in whole blood was strongly associated with increased urinary %MMA and decreased urinary %DMA in children and adults in Inner Mongolia, China (Xu et al. 2008). In our study, we did not observe any significant associations between whole blood GSH or the sum of whole blood GSH and GSSG and urinary As metabolite percentages, either in the overall sample or within the folate strata (data not shown). The reason for this discrepancy is unclear, but it might be related to differing laboratory methodologies used to measure GSH or differences in the study populations. Conversely, numerous studies have examined the associations of genetic variants in the glutathione *S*-transferase (GST) family of enzymes with urinary As metabolite profiles, although no consistent associations have been observed (Agusa et al. 2012; Ahsan et al. 2007; Caceres et al. 2010; Chiou et al. 1997; Chung et al. 2010; Hwang et al. 2010; Lindberg et al. 2007; Marnell et al. 2003; Paiva et al. 2010; Schlawicke Engstrom et al. 2007; Steinmaus et al. 2007). It is possible that the inconsistent findings might be due to differences in folate nutritional status among the populations included in these studies.

Our study has several limitations. First, we used plasma measurements of GSH, GSSG, and folate as proxies for liver measurements of GSH, GSSG, and SAM. Since the liver is the primary site of As methylation in the body, we would ideally measure GSH, GSSG, and SAM concentrations in hepatic tissue. However, mathematical models of hepatic folate and GSH metabolism indicate that plasma biomarkers might be informative: Based on model predictions, plasma folate is strongly related to liver SAM (Duncan et al. 2013), and plasma GSH/GSSG tracks liver GSH/GSSG over a range of steady-state oxidative stress (H_2O_2) concentrations (Reed et al. 2008). Second, evidence from Currier et al. suggests that our method for measuring urinary As metabolites, HPLC-ICP-MS, might underestimate the concentrations of the trivalent methylated As metabolites, i.e., MMA^{III} and DMA^{III} (Currier et al. 2013). Finally, due to the cross-sectional nature of our study, we are unable to establish the directionality of the relationship between plasma GSH redox status and As methylation capacity.

In conclusion, we found that an oxidized plasma GSH/GSSG redox state was associated with decreased As methylation capacity (increased urinary %MMA, decreased urinary %DMA, and decreased urinary SMI) and increased total bAs among folate-deficient Bangladeshi adults. GSH/GSSG redox might be one of several mechanisms controlling intracellular AS3MT activity and might contribute to the large interindividual variation in As methylation capacity observed in humans.

ACKNOWLEDGEMENTS

This work was supported by grants RO1 CA133595, RO1 ES017875, P42 ES10349, P30 ES009089, and T32 CA009529-24 from the National Institutes of Health. The content is solely the responsibility of the authors and does not necessarily represent the official views of the National Institute of Environmental Health Sciences, the National Cancer Institute, or the National Institutes of Health.

REFERENCES

Agusa T, Kunito T, Tue NM, Lan VT, Fujihara J, Takeshita H, et al. 2012. Individual variations in arsenic metabolism in vietnamese: The association with arsenic exposure and gstp1 genetic polymorphism. Metallomics 4:91-100.

Ahmed MF, Ahuja S, Alauddin M, Hug SJ, Lloyd JR, Pfaff A, et al. 2006. Epidemiology. Ensuring safe drinking water in bangladesh. Science 314:1687-1688.

Ahsan H, Chen Y, Kibriya MG, Slavkovich V, Parvez F, Jasmine F, et al. 2007. Arsenic metabolism, genetic susceptibility, and risk of premalignant skin lesions in bangladesh. Cancer Epidemiology Biomarkers & Prevention 16:1270-1278.

Caceres DD, Werlinger F, Orellana M, Jara M, Rocha R, Alvarado SA, et al. 2010. Polymorphism of glutathione s-transferase (gst) variants and its effect on distribution of urinary arsenic species in people exposed to low inorganic arsenic in tap water: An exploratory study. Arch Environ Occup Health 65:140-147.

Challenger F. 1945. Biological methylation. Chemical Reviews 36:315–361.

Challenger F. 1951. Biological methylation. Advances in enzymology and related subjects of biochemistry 12:429-491.

Chiang PK, Gordon RK, Tal J, Zeng GC, Doctor BP, Pardhasaradhi K, et al. 1996. S-adenosylmethionine and methylation. FASEB J 10:471-480.

Chiou HY, Hsueh YM, Hsieh LL, Hsu LI, Hsu YH, Hsieh FI, et al. 1997. Arsenic methylation capacity, body retention, and null genotypes of glutathione s-transferase m1 and t1 among current arsenic-exposed residents in taiwan. Mutat Res 386:197-207.

Chouchane S, Snow ET. 2001. In vitro effect of arsenical compounds on glutathione-related enzymes. Chem Res Toxicol 14:517-522.

Chung CJ, Pu YS, Su CT, Chen HW, Huang YK, Shiue HS, et al. 2010. Polymorphisms in one-carbon metabolism pathway genes, urinary arsenic profile, and urothelial carcinoma. Cancer Causes Control 21:1605-1613.

Currier J, Saunders RJ, Ding L, Bodnar W, Cable P, Matousek T, et al. 2013. Comparative oxidation state specific analysis of arsenic species by high-performance liquid chromatography-inductively coupled plasma-mass spectrometry and hydride generation-cryotrapping-atomic absorption spectrometry. J Anal At Spectrom 28:843-852.

Dalle-Donne I, Rossi R, Giustarini D, Colombo R, Milzani A. 2007. S-glutathionylation in protein redox regulation. Free Radic Biol Med 43:883-898.

Ding L, Saunders RJ, Drobna Z, Walton FS, Xun P, Thomas DJ, et al. 2012. Methylation of arsenic by recombinant human wild-type arsenic (+3 oxidation state) methyltransferase and its

methionine 287 threonine (m287t) polymorph: Role of glutathione. Toxicol Appl Pharmacol 264:121-130.

Duncan TM, Reed MC, Nijhout HF. 2013. The relationship between intracellular and plasma levels of folate and metabolites in the methionine cycle: A model. Mol Nutr Food Res 57:628-636.

Fomenko DE, Xing W, Adair BM, Thomas DJ, Gladyshev VN. 2007. High-throughput identification of catalytic redox-active cysteine residues. Science 315:387-389.

Gebel TW. 2002. Arsenic methylation is a process of detoxification through accelerated excretion. International Journal of Hygiene and Environmental Health 205:505-508.

Hall MN, Liu X, Slavkovich V, Ilievski V, Mi Z, Alam S, et al. 2009. Influence of cobalamin on arsenic metabolism in bangladesh. Environ Health Perspect 117:1724-1729.

Hall MN, Niedzwiecki M, Liu X, Harper KN, Alam S, Slavkovich V, et al. 2013. Chronic arsenic exposure and blood glutathione and glutathione disulfide concentrations in bangladeshi adults. Environ Health Perspect 121:1068-74.

Hayakawa T, Kobayashi Y, Cui X, Hirano S. 2005. A new metabolic pathway of arsenite: Arsenic-glutathione complexes are substrates for human arsenic methyltransferase cyt19. Arch Toxicol 79:183-191.

Hughes MF, Edwards BC, Herbin-Davis KM, Saunders J, Styblo M, Thomas DJ. 2010. Arsenic (+3 oxidation state) methyltransferase genotype affects steady-state distribution and clearance of arsenic in arsenate-treated mice. Toxicol Appl Pharmacol 249:217-223.

Hwang YH, Chen YH, Su YN, Hsu CC, Yuan TH. 2010. Genetic polymorphism of as3mt and delayed urinary dma excretion after organic arsenic intake from oyster ingestion. J Environ Monit 12:1247-1254.

IARC. 1987. Overall evaluations of carcinogenicity: An updating of iarc monographs volumes 1 to 42. IARC monographs on the evaluation of carcinogenic risks to humans Supplement / World Health Organization, International Agency for Research on Cancer 7:1-440.

Jones DP, Carlson JL, Samiec PS, Sternberg P, Jr., Mody VC, Jr., Reed RL, et al. 1998. Glutathione measurement in human plasma. Evaluation of sample collection, storage and derivatization conditions for analysis of dansyl derivatives by hplc. Clin Chim Acta 275:175-184.

Jones DP, Mody VC, Jr., Carlson JL, Lynn MJ, Sternberg P, Jr. 2002. Redox analysis of human plasma allows separation of pro-oxidant events of aging from decline in antioxidant defenses. Free Radic Biol Med 33:1290-1300.

Jones DP. 2008. Radical-free biology of oxidative stress. American Journal of Physiology - Cell Physiology 295:C849-C868.

Kombu RS, Zhang G-F, Abbas R, Mieyal JJ, Anderson VE, Kelleher JK, et al. 2009. Dynamics of glutathione and ophthalmate traced with 2h-enriched body water in rats and humans. American Journal of Physiology - Endocrinology And Metabolism 297:E260-E269.

Leslie EM. 2012. Arsenic–glutathione conjugate transport by the human multidrug resistance proteins (mrps/abccs). Journal of Inorganic Biochemistry 108:141-149.

Li X, Cao J, Wang S, Geng Z, Song X, Hu X, et al. 2013a. Residues in human arsenic (+3 oxidation state) methyltransferase forming potential hydrogen bond network around s-adenosylmethionine. PLoS ONE 8:e76709.

Li X, Geng Z, Wang S, Song X, Hu X, Wang Z. 2013b. Functional evaluation of asp76, 84, 102 and 150 in human arsenic(iii) methyltransferase (has3mt) interacting with s-adenosylmethionine. FEBS Letters 587:2232-2240.

Lin S, Shi Q, Nix FB, Styblo M, Beck MA, Herbin-Davis KM, et al. 2002. A novel s-adenosyl-l-methionine:Arsenic(iii) methyltransferase from rat liver cytosol. J Biol Chem 277:10795-10803.

Lindberg AL, Kumar R, Goessler W, Thirumaran R, Gurzau E, Koppova K, et al. 2007. Metabolism of low-dose inorganic arsenic in a central european population: Influence of sex and genetic polymorphisms. Environ Health Perspect 115:1081-1086.

Marnell LL, Garcia-Vargas GG, Chowdhury UK, Zakharyan RA, Walsh B, Avram MD, et al. 2003. Polymorphisms in the human monomethylarsonic acid (mma v) reductase/hgsto1 gene and changes in urinary arsenic profiles. Chem Res Toxicol 16:1507-1513.

Navarro Silvera SA, Rohan TE. 2007. Trace elements and cancer risk: A review of the epidemiologic evidence. Cancer Causes Control 18:7-27.

Paiva L, Hernandez A, Martinez V, Creus A, Quinteros D, Marcos R. 2010. Association between gsto2 polymorphism and the urinary arsenic profile in copper industry workers. Environ Res 110:463-468.

Petrick JS, Jagadish B, Mash EA, Aposhian HV. 2001. Monomethylarsonous acid (mma(iii)) and arsenite: Ld(50) in hamsters and in vitro inhibition of pyruvate dehydrogenase. Chem Res Toxicol 14:651-656.

Petrushanko IY, Yakushev S, Mitkevich VA, Kamanina YV, Ziganshin RH, Meng X, et al. 2012. S-glutathionylation of the na,k-atpase catalytic alpha subunit is a determinant of the enzyme redox sensitivity. J Biol Chem 287:32195-32205.

Reed MC, Thomas RL, Pavisic J, James SJ, Ulrich CM, Nijhout HF. 2008. A mathematical model of glutathione metabolism. Theor Biol Med Model 5:8.

Rodríguez VM, Del Razo LM, Limón-Pacheco JH, Giordano M, Sánchez-Peña LC, Uribe-Querol E, et al. 2005. Glutathione reductase inhibition and methylated arsenic distribution in cd1 mice brain and liver. Toxicological Sciences 84:157-166.

Rossman TG. 2003. Mechanism of arsenic carcinogenesis: An integrated approach. Mutat Res 533:37-65.

Schlawicke Engstrom K, Broberg K, Concha G, Nermell B, Warholm M, Vahter M. 2007. Genetic polymorphisms influencing arsenic metabolism: Evidence from argentina. Environ Health Perspect 115:599-605.

Smith AH, Steinmaus CM. 2009. Health effects of arsenic and chromium in drinking water: Recent human findings. Annu Rev Public Health 30:107-122.

Song X, Geng Z, Li X, Hu X, Bian N, Zhang X, et al. 2010. New insights into the mechanism of arsenite methylation with the recombinant human arsenic (+3) methyltransferase (has3mt). Biochimie 92:1397-1406.

Steinmaus C, Moore LE, Shipp M, Kalman D, Rey OA, Biggs ML, et al. 2007. Genetic polymorphisms in mthfr 677 and 1298, gstm1 and t1, and metabolism of arsenic. J Toxicol Environ Health A 70:159-170.

Styblo M, Thomas DJ. 1995. In vitro inhibition of glutathione reductase by arsenotriglutathione. Biochemical pharmacology 49:971-977.

Styblo M, Serves SV, Cullen WR, Thomas DJ. 1997. Comparative inhibition of yeast glutathione reductase by arsenicals and arsenothiols. Chem Res Toxicol 10:27-33.

Styblo M, Del Razo LM, Vega L, Germolec DR, LeCluyse EL, Hamilton GA, et al. 2000. Comparative toxicity of trivalent and pentavalent inorganic and methylated arsenicals in rat and human cells. Arch Toxicol 74:289-299.

Thomas DJ, Li J, Waters SB, Xing W, Adair BM, Drobna Z, et al. 2007. Arsenic (+3 oxidation state) methyltransferase and the methylation of arsenicals. Experimental biology and medicine (Maywood, NJ) 232:3-13.

Thomas DJ. 2009. Unraveling arsenic--glutathione connections. Toxicol Sci 107:309-311.

Tseng CH. 2007. Arsenic methylation, urinary arsenic metabolites and human diseases: Current perspective. J Environ Sci Health C Environ Carcinog Ecotoxicol Rev 25:1-22.

Vahter M, Concha G. 2001. Role of metabolism in arsenic toxicity. Pharmacol Toxicol 89:1-5.

Wang S, Li X, Song X, Geng Z, Hu X, Wang Z. 2012. Rapid equilibrium kinetic analysis of arsenite methylation catalyzed by recombinant human arsenic (+3 oxidation state) methyltransferase (has3mt). J Biol Chem 287:38790-38799.

Waters SB, Devesa V, Del Razo LM, Styblo M, Thomas DJ. 2004a. Endogenous reductants support the catalytic function of recombinant rat cyt19, an arsenic methyltransferase. Chem Res Toxicol 17:404-409.

Waters SB, Devesa V, Fricke MW, Creed JT, Styblo M, Thomas DJ. 2004b. Glutathione modulates recombinant rat arsenic (+3 oxidation state) methyltransferase-catalyzed formation of trimethylarsine oxide and trimethylarsine. Chem Res Toxicol 17:1621-1629.

Xu Y, Wang Y, Zheng Q, Li X, Li B, Jin Y, et al. 2008. Association of oxidative stress with arsenic methylation in chronic arsenic-exposed children and adults. Toxicol Appl Pharmacol 232:142-149.

Chapter 6: Blood glutathione redox status and global methylation of peripheral blood mononuclear cell DNA

Megan M. Niedzwiecki[1], Megan N. Hall[2], Xinhua Liu[3], Julie Oka[1], Kristin N. Harper[1],Vesna Slavkovich[1], Vesna Ilievski[1], Diane Levy[3], Alexander van Geen[4], Jacob L. Mey[4], Shafiul Alam[5], Abu B. Siddique[5], Faruque Parvez[1], Joseph H. Graziano[1], and Mary V. Gamble[1]

Affiliations: [1]Department of Environmental Health Sciences, [2]Department of Epidemiology, [3]Department of Biostatistics, [1-3]Mailman School of Public Health, Columbia University, New York NY,10032, USA; [4]Lamont-Doherty Earth Observatory of Columbia University, Palisades, NY, USA; [5]Columbia University Arsenic Project in Bangladesh, Dhaka, Bangladesh

Published: https://www.landesbioscience.com/journals/epigenetics/article/25012/

Niedzwiecki MM, Hall MN, Liu X, Oka J, Harper KN, Slavkovich V, Ilievski V, Levy D, van Geen A, Mey JL, Alam S, Siddique AB, Parvez F, Graziano JH, Gamble MV. **Blood glutathione redox status and global methylation of peripheral blood mononuclear cell DNA in Bangladeshi adults**. Epigenetics. 2013 Jul;8(7):730-8. PMID: 23803688

ABSTRACT

BACKGROUND: Oxidative stress and DNA methylation are metabolically linked through the relationship between one-carbon metabolism and the transsulfuration pathway, but possible modulating effects of oxidative stress on DNA methylation have not been extensively studied in humans. Enzymes involved in DNA methylation, including DNA methyltransferases and histone deacetylases, may show altered activity under oxidized cellular conditions. Additionally, *in vitro* studies suggest that glutathione (GSH) depletion leads to global DNA hypomethylation, possibly through the depletion of *S*-adenosylmethionine (SAM).

OBJECTIVE: We tested the hypothesis that a more oxidized blood GSH redox status is associated with decreased global peripheral blood mononuclear cell (PBMC) DNA methylation in a sample of Bangladeshi adults.

METHODS: Global PBMC DNA methylation and whole blood GSH, glutathione disulfide (GSSG), and SAM concentrations were measured in 320 adults. DNA methylation was measured by using the [^{3}H]-methyl incorporation assay; values are inversely related to global DNA methylation. Whole blood GSH redox status (E_h) was calculated using the Nernst equation.

RESULTS: We found that a more oxidized blood GSH E_h was associated with decreased global DNA methylation (B ± SE, 271 ± 103, $P = 0.009$). Blood SAM and blood GSH were associated with global DNA methylation, but these relationships did not achieve statistical significance.

CONCLUSIONS: Our findings support the hypothesis that a more oxidized blood GSH redox status is associated with decreased global methylation of PBMC DNA. Furthermore, blood SAM does not appear to mediate this association. Future research should explore mechanisms through which cellular redox might influence global DNA methylation.

INTRODUCTION

Methylation of cytosines in CpG dinucleotides is an epigenetic mechanism involved in the regulation of gene expression and cellular differentiation (Jones and Taylor 1980; Razin and Riggs 1980). The methyl donor for this reaction is *S*-adenosylmethionine (SAM), whose synthesis is regulated by folate-dependent one-carbon metabolism. Decreased levels of global DNA methylation are associated with increased chromatin accessibility and gene transcriptional activity (Thurman et al. 2012), as well as genomic instability (Lengauer et al. 1997). Consequently, global DNA hypomethylation, along with site-specific DNA hypermethylation of tumor suppressor genes, is commonly found in tumor tissue and transformed cells (Das and Singal 2004) and is believed to play a role in carcinogenesis (Robertson and Jones 2000).

Oxidative stress is a risk factor also commonly implicated in carcinogenesis (Klaunig and Kamendulis 2004). The body's primary antioxidant is glutathione (GSH), a thiol-containing tri-peptide (γ-glutamyl-cysteinyl-glycine) that readily donates an electron to reactive oxygen species (ROS) via glutathione peroxidase (GPx) and quickly reacts with another free radical GSH molecule to form glutathione disulfide (GSSG) (Forman et al. 2009). Reduced levels of GSH, increased levels of GSSG, and a decrease of the ratio of GSH to GSSG are indicative of a more oxidized intracellular environment (Jones 2008). Since the GSH-GSSG couple is the most abundant intracellular redox pair, their absolute concentrations can be used in the Nernst equation to estimate the intracellular redox state, E_h (in mV) (Schafer and Buettner 2001). Approximately 50% of the cysteine (Cys) used in the production of GSH is derived from the conversion of homocysteine (Hcys) to cystathionine in the first step of the transsulfuration pathway (Beatty and Reed 1980).

Increased oxidative stress and aberrant DNA methylation often co-occur in carcinogenesis (Franco et al. 2008). Although DNA methylation and oxidative stress are metabolically linked through the relationship between one-carbon metabolism and the transsulfuration pathway, possible modulating effects of oxidative stress on DNA methylation have not been extensively studied in humans. Two mechanisms have been proposed in the literature.

First, a more oxidized cellular redox state may lead to a decrease in genomic DNA methylation through redox regulation of related enzymes. A BLAST analysis of gene sequences containing possible redox-sensitive cysteine residues identified the SAM-dependent methyltransferases as potentially redox-sensitive (Fomenko et al. 2007). Additionally, the activity of methionine adenosyltransferase (MAT), which catalyzes the enzymatic addition of methionine to adenosine for the synthesis of SAM, is decreased in environments with a more oxidized GSH:GSSG ratio (Pajares et al. 1992).

Second, it has been hypothesized by others that GSH depletion under conditions of chronic oxidative stress may lead to decreased global DNA methylation through the depletion of SAM (Hitchler and Domann 2007). Under oxidizing conditions, cystathionine-β-synthase (CBS) activity increases to direct Hcys flux through the transsulfuration pathway for the generation of GSH (Mosharov et al. 2000). Consequently, less Hcys is directed toward the regeneration of methionine, which may result in decreased SAM levels. In support of this hypothesis, treatment with the GSH-depleting hepatotoxin bromobenzene led to extensive depletion of liver methionine pools and hypomethylation of genomic liver DNA in Syrian hamsters (Lertratanangkoon et al. 1996; Lertratanangkoon et al. 1997).

We tested the hypothesis that increased oxidative stress is associated with decreased global DNA methylation in a cohort of Bangladeshi adults by examining the associations of blood GSH concentrations and blood GSH redox state (E_h) with global methylation of peripheral blood mononuclear cell (PBMC) DNA. To evaluate whether the association of blood GSH redox state with global PBMC DNA methylation might be due to depletion of SAM, we also examined the associations of blood SAM with the blood GSH redox variables and DNA methylation to test for possible mediation.

SUBJECTS AND METHODS

Eligibility criteria and study design

The details of the FOX study design are described in Chapter 3.

Analytic techniques

Methods for sample collection and analysis of water As, PBMC DNA isolation, genomic DNA methylation, plasma folate, plasma homocysteine, and urinary Cr are described in detail in Chapter 3. Analytic methods for whole blood GSH and GSSG, blood SAM and SAH, urinary 8-oxodG, and the calculation of the whole blood GSH reduction potential (E_h) are outlined here.

Whole blood and plasma glutathione and glutathione disulfide

Whole blood and plasma GSH and GSSG were assayed by the method of Jones et al. (1998), as previously described (Hall et al. 2013). Briefly, blood samples were collected in the field laboratory with a butterfly syringe, immediately processed for derivatization, and stored at -80°C until delivered to Columbia University for analysis. 20 µl of each sample was injected onto the HPLC, and metabolites were detected using a Waters 474 scanning fluorescence detector with 335 nm excitation and 515 nm emission (Waters Corp., Milford, MA). Intra-assay CVs were between 5 and 10%, and inter-assay CVs were between 11 and 18%.

Blood *S*-adenosylmethionine and *S*-adenosylhomocysteine

SAM and SAH were measured in whole blood, as previously described (Poirier et al. 2001). Briefly, blood was thawed, vortexed, and 400 µl were added to an equal volume of 0.1 M sodium acetate, pH 6.0, plus 40% TCA. SAM and SAH were detected at 254 nm using a 996 Photodiode Array ultraviolet absorbance detector (Waters Inc, Milford, MA) and quantified relative to standard curves generated using purified compounds (Sigma, St. Louis, MO). The inter-assay coefficient of variation was 9.6% for SAM and 16.1% for SAH.

Urinary 8-oxodG

Urinary 8-oxodG was measured using the 'New 8-OHdG Check' ELISA kit at the Genox Corporation's laboratory (Baltimore, MD). Samples were measured in triplicate. The detection level for this assay was 0.64 ng/mL urine. A significant proportion of the study sample (N=56 individuals, or 18%) had urinary 8-oxodG levels below the detection limit; levels for these individuals were set to one-half of the detection limit, or 0.32 ng/mL. The intra- and inter-assay coefficients of variation were 7.5% and 7.7%, respectively. Urinary Cr was analyzed with a colorimetric assay based on the Jaffe reaction (Slot 1965) to adjust for urine concentration.

Calculation of the reduction potential (E_h)

The reduction potentials of the blood GSH/GSSG redox pair was calculated using the Nernst equation, $E_h = Eo + (RT/nF)\ln([acceptor]/[donor])$, where Eo is the standard potential for the redox couple at the defined pH, R is the gas constant, T is the absolute temperature, F is Faraday's constant, and n is the number of electrons transferred (Jones 2002). For GSH and GSSG, the equation simplifies to $E_h\,(mV) = -264 - 30\log([GSH]^2/[GSSG])$, where [GSH] and [GSSG] are molar concentrations and the Eo value assumes a physiologic pH of 7.4 (Jones 2002). A more positive E_h value reflects a more oxidized state.

Statistical methods

Descriptive statistics (means and standard deviations) were calculated for the characteristics of the sample. Spearman correlations were used to examine bivariate associations between blood GSH variables, [^{3}H]-methyl incorporation, and other continuous covariates. Wilcoxon rank-sum test was used to detect differences in continuous measures between categories of binary variables.

Linear regression analyses were constructed with blood GSH redox variables and blood SAM as predictors and [^{3}H]-methyl incorporation as the outcome, with and without controlling for confounding factors. Proper transformations were applied to the continuous independent variables with skewed distribution to reduce the impact of extreme values. Certain confounders (gender, age, cigarette smoking, and water As) were selected *a priori* based on biologic plausibility and previous studies in the literature (Pilsner et al. 2007). Other potential confounders (plasma folate, plasma Hcys, plasma vitamin B_{12}, betel nut chewing, BMI, television ownership, education) were considered by examining their bivariate associations with blood GSH redox variables, blood SAM, and [^{3}H]-methyl incorporation. The control variables in the final models were those that were related to the outcome and main predictors and resulted in an appreciable (>5%) change in the regression coefficient for the association between a predictor and the outcome. Since cigarette smoking did not predict [^{3}H]-methyl incorporation independently of gender, it was excluded from the final model. The final regression models contained gender, age, and water As as covariates.

Blood SAM was considered to be a partial mediator of the association between blood GSH and [^{3}H]-methyl incorporation if it met the following criteria: (I) Blood GSH (predictor) was significantly associated with blood SAM (mediator); (II) Blood GSH was significantly associated with [^{3}H]-methyl incorporation (outcome); (III) Blood SAM was significantly associated with [^{3}H]-methyl incorporation; (IV) inclusion of blood SAM in a model of blood GSH predicting [^{3}H]-methyl incorporation resulted in attenuation of the regression coefficient.

Values for [^{3}H]-methyl incorporation were excluded from the analysis if duplicates had coefficients of variation > 15% (N=48), DNA assay inputs below 10 µg/ml (N=8), or values that were extreme outliers, defined as values that exceeded the boxplot of the DPM values by more

than three interquartile ranges (N=2). Additionally, we were unable to isolate DNA from N=1 lysate, resulting in a final sample size of 320. All statistical analyses were conducted using SAS (version 9.3; SAS Institute Inc., Cary, NC).

RESULTS

Demographic and clinical characteristics of the study participants are shown in Table 1. The average age was 43 years, and there were roughly equal numbers of males and females. Approximately 35% of the population was classified as underweight (BMI < 18.5 kg/m^2), and 31.3% of the participants were folate deficient (plasma folate < 9 nmol/L). Due to the Folate and Oxidative Stress (FOX) study sampling design, nearly 71% of the participants used wells with water arsenic (As) > 50 ug/L (the Bangladeshi standard) as their primary drinking source. Mean blood GSH and GSSG concentrations were 491.0 and 37.3 µmol/L, respectively, and the mean blood GSH E_h was –198 mV.

In our evaluation of potential covariates for inclusion in the regression models, we observed that water As was negatively correlated with blood GSH (Spearman r = -0.15, P = 0.008), as reported in an earlier study from our group.(Hall et al. 2013) Males had higher blood GSH concentrations, less oxidized blood GSH E_h values, and higher blood SAM levels than females ($P < 0.0001$). Ever-smokers also had higher GSH concentrations, less oxidized blood GSH E_h values, and higher SAM levels than never-smokers. Since most ever-smokers were male (113/123, 91.9%), we stratified the ever-smoking analyses by gender: no significant associations were found between GSH and smoking status after stratification, indicating that the observed differences in GSH, GSH E_h, and SAM by smoking status were due to the preponderance of males in the ever-smoking group (data not shown).

Table 1. Descriptive characteristics for study sample (N=320).

Baseline variables	**Mean ± SD (range) or N(%)**
Age (yrs)	43.2 ± 8.3 (30 – 63)
Male	159 (49.7)
BMI (kg/m^2)	20.3 ± 3.5 (13.8 – 35.3)
Underweight (BMI < 18.5 kg/m^2)	112 (35.1)
Ever cigarette smoking	123 (38.4)
Ever betel nut use	142 (44.4)
Television ownership	185 (57.8)
Water As (µg/L)	144.9 ± 122.5 (0.4 – 699.9)
Water As > 50 µg/L	226 (70.9)
Plasma folate (nmol/L)[a]	12.6 ± 7.0 (2.4 – 60.6)
Folate deficiency (folate < 9.0 nmol/L) [a]	100 (31.3)
Plasma Hcys (µmol/L)	11.2 ± 12 (3.0 – 165.4)
Hyperhomocystinemia (Hcys > 13 µmol/L)	56 (17.5)
DPM per µg DNA	149,123 ± 23,932 (61,398 – 215,666)
Blood GSH (µmol/L)	491.0 ± 170.6 (104.6 – 1072.1)
Plasma GSH (µmol/L)	2.6 ± 0.7 (1.0 – 5.8)
Blood GSSG (µmol/L)	37.3 ± 18.8 (9.6 - 121.8)
Plasma GSSG (µmol/L)	2.1 ± 0.6 (0.8 – 4.8)
Blood GSH E_h (mV)	-198.0 ± 13.0 (-227.9 to -144.4)
Plasma GSH E_h (mV)	-98.5 ± 7.2 (-118.0 to -73.4)
Blood SAM[b] (µM)	1.29 ± 0.50 (0.44 – 3.38)
Blood SAH[b] (µM)	0.31 ± 0.17 (0.10 – 1.37)

[a] N=319; [b] N=312

To support the validity of whole blood GSH E_h as a marker of intracellular redox in blood cells, we examined relationships of blood GSH redox variables with plasma Hcys and blood *S*-adenosylhomocysteine (SAH), shown in Table 2. Cellular oxidative stress has been shown experimentally to decrease plasma Hcys *in vitro* (Hultberg and Hultberg 2007) and *in vivo* (Rogers et al. 2007). As expected, a more oxidized blood GSH E_h was negatively correlated with both plasma Hcys (Spearman r = -0.27, P < 0.0001) and blood SAH (Spearman r = -0.42, P < 0.0001). We did not find that plasma GSH E_h was correlated with plasma Hcys (Spearman r = 0.07, P = 0.22) or blood SAH (Spearman r = 0.02, P = 0.74).

Table 2. Spearman correlation coefficients of blood and plasma glutathione redox variables with plasma Hcys and blood SAH (N=320).

		Blood GSH	Blood GSSG	Blood E_h GSH	Plasma E_h GSH
Plasma Hcys	*r*	0.22	-0.09	-0.27	0.07
	P	(<0.0001)	(0.10)	(<0.0001)	(0.22)
Blood SAH[a]	*r*	0.22	-0.38	-0.42	0.02
	P	(<0.0001)	(<0.0001)	(<0.0001)	(0.74)

[a] N=312

A more oxidized blood GSH E_h was significantly correlated with increased [^{3}H]-methyl incorporation in bivariate analyses (Spearman r = 0.17, P = 0.002). Since [^{3}H]-methyl incorporation is inversely related to genomic DNA methylation, this indicated that a more oxidized blood GSH E_h is associated with reduced global DNA methylation. In covariate-adjusted linear regression models shown in Table 3, a 1 mV increase in blood GSH E_h was associated with an increase in [^{3}H]-methyl incorporation of 271 disintegrations per minute (DPM) per µg DNA (P = 0.009). Similarly, a 1 µM decrease in blood GSH was associated with

an increase in [^{3}H]-methyl incorporation of 12.7 DPM per µg DNA, but this association was not statistically significant (P = 0.11).

For statistical evidence to support blood SAM as a mediator of the association between blood GSH redox and global DNA methylation, we examined associations of blood SAM with blood GSH, blood GSH E_h, and [^{3}H]-methyl incorporation. Blood SAM was negatively associated with [^{3}H]-methyl incorporation at borderline significance (B ± SE = -4803 ± 2747, P = 0.08, Table 3). Blood GSH concentration was a significant predictor of log-transformed blood SAM in a covariate-adjusted model (B ± SE = 0.026 ± 0.012 for a 100 µM increase in blood GSH, P = 0.04), but blood GSH E_h was not associated with blood SAM (P = 0.23). Since the association of blood GSH and [^{3}H]-methyl incorporation did not reach statistical significance, and since blood GSH E_h and blood SAM were not associated, the result did not support the role of blood SAM as a mediator.

In exploratory analyses, we also examined associations of other variables with [^{3}H]-methyl incorporation. Neither blood SAH nor the blood SAM/SAH ratio were significantly associated with [^{3}H]-methyl incorporation in adjusted models (P = 0.65 and P = 0.79, respectively). An oxidized blood GSH E_h correlated positively with urinary 8-oxodG levels per g urinary creatinine (Cr) (Spearman r = 0.17, P = 0.004); since oxidative damage of guanines in CpG dinucleotides has been hypothesized to decrease global DNA methylation (Valinluck et al. 2004; Weitzman et al. 1994), we also examined the association between urinary 8-oxodG/Cr levels and [^{3}H]-methyl incorporation. However, the covariate-adjusted association was not significant (B ± SE = 293 ± 207, P = 0.16).

Table 3. Unadjusted and adjusted regression coefficients for associations between predictors and [^{3}H]-methyl incorporation of PBMC DNA (N=320).

Predictor	Model	[^{3}H]-methyl incorporation			
		B ± SE	*P*	R^2 %	Δ in R^2 %
Blood GSH E_h	Unadjusted	303 ± 102	0.003	2.7	
	Adjusted[a]	271 ± 103	0.009	5.5	2.0
Blood GSH	Unadjusted	-13.0 ± 7.8	0.10	0.9	
	Adjusted[a]	-12.7 ± 8.0	0.11	4.2	0.7
Blood SAM[b]	Unadjusted	-4799 ± 2698	0.08	1.0	
	Adjusted[a]	-4803 ± 2747	0.08	5.2	1.7

[a] Adjusted for gender, age, and well water As, N=319; [b] N=312

DISCUSSION

The objective of this study was to examine whether oxidative stress is associated with decreased global methylation of PBMC DNA in a cross-sectional study of Bangladeshi adults. We tested this hypothesis by examining the associations of blood GSH and blood GSH E_h with PBMC DNA methylation, and we also examined whether these associations were mediated by blood SAM levels. We observed that a more oxidized blood GSH E_h was associated with decreased DNA methylation. Decreased blood GSH was not significantly associated with decreased DNA methylation, indicating that the association of blood GSH E_h with global DNA methylation depended on the concentrations and balance of blood GSH and GSSG and was not simply explained by the concentration of blood GSH. Finally, although blood SAM was positively associated with PBMC DNA methylation at marginal significance, blood GSH E_h was not associated with blood SAM. Taken together, our observations are consistent with the hypothesis that an oxidized intracellular redox state, as measured by blood GSH E_h, is associated with decreased global DNA methylation, but blood SAM does not appear to mediate this association.

Only a few other epidemiologic studies have examined the association between oxidative stress and DNA methylation. A study of 45 infertile men found that seminal ROS production was negatively correlated with sperm global DNA methylation, and three-month supplementation with antioxidants produced a significant decrease in seminal ROS and significant increase in sperm global DNA methylation (Tunc and Tremellen 2009). Additionally, in a study of 61 bladder cancer patients and 45 healthy controls, total antioxidant status in urine was positively correlated with methylation of long interspersed nuclear element-1 (LINE-1) in peripheral blood leukocyte (PBL) DNA from all subjects (Patchsung et al. 2012). To our

knowledge, this is the first study to find an association between blood glutathione redox status and global DNA methylation in a generally healthy population.

While methylation of DNA is known to be a dynamic process, a mechanism for demethylation has not been clearly established. Recent work has shown that the ten-eleven translocation (Tet) family of proteins can convert 5-methylcytosine (5mC) into 5-hydroxymethylcytosine (5hmC) (Ito et al. 2010; Tahiliani et al. 2009), which is believed to be an intermediary in passive and/or active DNA demethylation (Guo et al. 2011; Wu and Zhang 2010). Interestingly, Chen et al. found that the *de novo* methyltransferases DNMT3a and DNMT3b act as both DNA methyltransferases and DNA dehydroxymethylases, depending upon the redox environment: treatment with dithiothreitol (DTT) or hydrogen peroxide (H_2O_2) inhibited and enhanced the dehydroxymethylation activities of the enzymes, respectively (Chen et al. 2012). Chen et al. speculated that the dual methylation and dehydroxymethylation activities of the DNMT3 enzymes might explain the paradoxical observation that DMNT3 expression is up-regulated and gene-specific DNA methylation is increased in cancer cells, yet global DNA methylation is decreased (Chen et al. 2012).

Histone deacetylase (HDAC) inhibition has been shown experimentally to induce DNA hypomethylation (Selker 1998), and it has been hypothesized that HDAC activities might also be influenced directly by cellular redox (Cyr and Domann 2011). In human neuroblastoma cells, exposure to H_2O_2 induces global DNA hypomethylation, along with downregulation of HDAC3, DNMT1, and DNMT3a expression (Gu et al. 2013). One potential mechanism of redox inhibition of HDACs might occur through alteration of cysteine residues: reactive carbonyl species inactivate HDAC1 through covalent modification of conserved cysteine residues (Doyle

and Fitzpatrick 2010), and exposure to ROS-producing compounds induces intramolecular disulfide bond formation in conserved cysteine residues in HDAC4 (Ago et al. 2008).

We did not find that blood SAM was significantly associated with global DNA methylation or blood GSH E_h. Mathematical modeling of one-carbon metabolism predicts that the DNMT methylation rate is remarkably stable over wide fluctuations of SAM concentrations, primarily due to the low K_m for the DNMT reaction and long-range allosteric regulation of CBS and methylenetetrahydrofolate reductase (MTHFR) by SAM (Nijhout et al. 2006). Furthermore, the hypothesis that increased demand for GSH production depletes SAM levels is complicated by the discovery that CBS is allosterically activated by SAM but destabilized under SAM-deficient conditions (Prudova et al. 2006). These findings, along with the observations in this study, do not lend strong support to the hypothesis that oxidative stress leads to DNA hypomethylation through SAM depletion.

It is not clear whether whole blood concentrations of SAM and GSH reflect intracellular concentrations in other tissues. Although *in vitro* evidence suggests that SAM is not easily transported across cell membranes (McMillan et al. 2005; Van Phi and Soling 1982), in a cohort of healthy adults, the plasma SAM/SAH ratio was strongly correlated with the intracellular lymphocyte SAM/SAH ratio (r = 0.73) (Melnyk et al. 2000). A study in rats showed that an increase in reduced oxygen species in liver initiated changes in the erythrocytic GSH:GSSG ratio; the authors concluded that the erythrocytic GSH:GSSG ratio reflects oxidative stress in liver and other tissues (Siems et al. 1987). Additionally, an intact transsulfuration pathway has been identified in blood cells, including macrophages (Garg et al. 2006) and T cells (Garg et al. 2011), and transsulfuration pathway flux is upregulated in naïve and activated T cells after exposure to peroxide (Garg et al. 2011). Even if SAM and GSH measurements in blood do not

directly reflect the absolute concentrations in other tissues, the presence of intact one-carbon metabolism and transsulfuration pathways in blood cells suggests that blood biomarkers might be appropriate to study perturbations of these pathways by oxidative stress.

We observed that an oxidized blood GSH E_h was correlated with decreased blood SAH and plasma Hcys, which is consistent with an increase in Hcys flux through the transsulfuration pathway under oxidized intracellular conditions (Mosharov et al. 2000). Although some studies have used plasma GSH E_h as a marker of intracellular redox (Ashfaq et al. 2006; Mannery et al. 2010), we did not observe significant correlations of Hcys or SAH with plasma GSH E_h, which suggests that whole blood GSH E_h might be a better indicator of the intracellular redox environment, at least within blood cells. However, an oxidized plasma GSH E_h is thought to reflect oxidative stress in other tissues (Jones 2002) or systemic oxidative stress (Calabrese et al. 2012) and is observed in aging (Samiec et al. 1998), obesity (Joao Cabrera et al. 2010), and disease states such as asthma (Fitzpatrick et al. 2011) and heart disease (Huang et al. 2006). Indeed, we found that plasma GSH E_h, but not blood GSH E_h, was positively correlated with age (Spearman $r = 0.14$, $P = 0.01$) and BMI (Spearman $r = 0.11$, $P = 0.05$). As such, the measurements of GSH redox pairs in both plasma and whole blood might be informative to fully understand the influence of "oxidative stress" in an organism.

Redox regulation is known to influence white blood cell cycle progression and proliferation (Iwata et al. 1994), and thus, it is possible that our observations are explained by redox-induced shifts in PBMC cell type distributions or counts. However, the overall level of global DNA methylation across cell types would have to vary dramatically for cell distribution shifts to explain our observations. While site-specific CpG methylation levels at certain loci have been found to be associated with blood cell type (Talens et al. 2010), global DNA

methylation levels were not significantly different among DNA samples from granulocytes, mononuclear cells, and white blood cells in adult women (Wu et al. 2011). Furthermore, since PBMCs are a subset of total WBCs, the influence of cell type variability is reduced to some extent in our study.

Our study has several limitations. First, the cross-sectional design precludes us from establishing the directionality of the relationship between blood GSH redox state and global DNA methylation. Epigenetic alterations might induce changes in the cellular redox status: for example, mice exposed to d-β-hydroxybutyrate, an inhibitor of class I HDACs, exhibit an increase in global H3 acetylation, increase in expression of oxidative stress resistance genes, and a reduction in oxidative damage from ROS (Shimazu et al. 2013). We also cannot establish whether the observed association with global DNA methylation is explained by an upstream factor (e.g., H_2O_2), the GSH redox state itself, or another redox-associated event, e.g., alterations of the citric acid cycle and/or the NAD^+/NADH ratio (Cyr and Domann 2011). Finally, we were unable to adjust for PBMC cell type counts or distributions in our regression models.

In conclusion, we observed that a more oxidized intracellular redox state, as measured by blood GSH E_h, was associated with a decrease in global methylation of PBMC DNA. Furthermore, blood SAM was marginally associated with an increase in global DNA methylation, but it did not mediate the association between blood GSH E_h and global DNA methylation. Future research should examine whether alteration of intracellular redox is a mechanism through which environmental exposures and other factors influence DNA methylation. It might also be of interest to examine whether redox therapies might help to prevent progressive loss of global DNA methylation in cancer and other diseases.

ACKNOWLEDGEMENTS

This work was supported by grants RO1 CA133595, RO1 ES017875, P42 ES10349, P30 ES009089, and T32 CA009529-24 from the National Institutes of Health. The content is solely the responsibility of the authors and does not necessarily represent the official views of the National Institute of Environmental Health Sciences, the National Cancer Institute, or the National Institutes of Health. We wish to thank Dr. Frederick Domann for his help with the preparation of this manuscript.

REFERENCES

Ago T, Liu T, Zhai P, Chen W, Li H, Molkentin JD, et al. 2008. A redox-dependent pathway for regulating class ii hdacs and cardiac hypertrophy. Cell 133:978-993.

Ashfaq S, Abramson JL, Jones DP, Rhodes SD, Weintraub WS, Hooper WC, et al. 2006. The relationship between plasma levels of oxidized and reduced thiols and early atherosclerosis in healthy adults. J Am Coll Cardiol 47:1005-1011.

Beatty PW, Reed DJ. 1980. Involvement of the cystathionine pathway in the biosynthesis of glutathione by isolated rat hepatocytes. Archives of Biochemistry and Biophysics 204:80-87.

Calabrese V, Cornelius C, Leso V, Trovato-Salinaro A, Ventimiglia B, Cavallaro M, et al. 2012. Oxidative stress, glutathione status, sirtuin and cellular stress response in type 2 diabetes. Biochim Biophys Acta 1822:729-736.

Chen CC, Wang KY, Shen CK. 2012. The mammalian de novo DNA methyltransferases dnmt3a and dnmt3b are also DNA 5-hydroxymethylcytosine dehydroxymethylases. J Biol Chem 287:33116-33121.

Cyr AR, Domann FE. 2011. The redox basis of epigenetic modifications: From mechanisms to functional consequences. Antioxid Redox Signal 15:551-589.

Das PM, Singal R. 2004. DNA methylation and cancer. Journal of Clinical Oncology 22:4632-4642.

Doyle K, Fitzpatrick FA. 2010. Redox signaling, alkylation (carbonylation) of conserved cysteines inactivates class i histone deacetylases 1, 2, and 3 and antagonizes their transcriptional repressor function. J Biol Chem 285:17417-17424.

Fitzpatrick AM, Stephenson ST, Hadley GR, Burwell L, Penugonda M, Simon DM, et al. 2011. Thiol redox disturbances in children with severe asthma are associated with posttranslational modification of the transcription factor nuclear factor (erythroid-derived 2)-like 2. J Allergy Clin Immunol 127:1604-1611.

Fomenko DE, Xing W, Adair BM, Thomas DJ, Gladyshev VN. 2007. High-throughput identification of catalytic redox-active cysteine residues. Science 315:387-389.

Forman HJ, Zhang H, Rinna A. 2009. Glutathione: Overview of its protective roles, measurement, and biosynthesis. Mol Aspects Med 30:1-12.

Franco R, Schoneveld O, Georgakilas AG, Panayiotidis MI. 2008. Oxidative stress, DNA methylation and carcinogenesis. Cancer Lett 266:6-11.

Garg S, Vitvitsky V, Gendelman HE, Banerjee R. 2006. Monocyte differentiation, activation, and mycobacterial killing are linked to transsulfuration-dependent redox metabolism. J Biol Chem 281:38712-38720.

Garg SK, Yan Z, Vitvitsky V, Banerjee R. 2011. Differential dependence on cysteine from transsulfuration versus transport during t cell activation. Antioxid Redox Signal 15:39-47.

Gu X, Sun J, Li S, Wu X, Li L. 2013. Oxidative stress induces DNA demethylation and histone acetylation in sh-sy5y cells: Potential epigenetic mechanisms in gene transcription in abeta production. Neurobiol Aging 34:1069-1079.

Guo Junjie U, Su Y, Zhong C, Ming G-l, Song H. 2011. Hydroxylation of 5-methylcytosine by tet1 promotes active DNA demethylation in the adult brain. Cell 145:423-434.

Hall MN, Niedzwiecki M, Liu X, Harper KN, Alam S, Slavkovich V, et al. 2013. Chronic arsenic exposure and blood glutathione and glutathione disulfide concentrations in bangladeshi adults. Environ Health Perspect 121:1068-74.

Hitchler MJ, Domann FE. 2007. An epigenetic perspective on the free radical theory of development. Free Radical Biology and Medicine 43:1023-1036.

Huang YS, Zhi YF, Kong SY, Wang QL, Xu BS, Wang SR. 2006. [plasma glutathione of patients with coronary heart disease measured by fluorospectrophotometer]. Guang Pu Xue Yu Guang Pu Fen Xi 26:936-940.

Hultberg M, Hultberg B. 2007. Oxidative stress decreases extracellular homocysteine concentration in human hepatoma (hepg2) cell cultures. Chem Biol Interact 165:54-58.

Ito S, Dalessio AC, Taranova OV, Hong K, Sowers LC, Zhang Y. 2010. Role of tet proteins in 5mc to 5hmc conversion, es-cell self-renewal and inner cell mass specification. Nature 466:1129-1133.

Iwata S, Hori T, Sato N, Ueda-Taniguchi Y, Yamabe T, Nakamura H, et al. 1994. Thiol-mediated redox regulation of lymphocyte proliferation. Possible involvement of adult t cell leukemia-derived factor and glutathione in transferrin receptor expression. J Immunol 152:5633-5642.

Joao Cabrera E, Valezi AC, Delfino VD, Lavado EL, Barbosa DS. 2010. Reduction in plasma levels of inflammatory and oxidative stress indicators after roux-en-y gastric bypass. Obes Surg 20:42-49.

Jones DP, Carlson JL, Samiec PS, Sternberg P, Jr., Mody VC, Jr., Reed RL, et al. 1998. Glutathione measurement in human plasma. Evaluation of sample collection, storage and derivatization conditions for analysis of dansyl derivatives by hplc. Clin Chim Acta 275:175-184.

Jones DP. 2002. Redox potential of gsh/gssg couple: Assay and biological significance. Methods Enzymol 348:93-112.

Jones DP. 2008. Radical-free biology of oxidative stress. American Journal of Physiology - Cell Physiology 295:C849-C868.

Jones PA, Taylor SM. 1980. Cellular differentiation, cytidine analogs and DNA methylation. Cell 20:85-93.

Klaunig JE, Kamendulis LM. 2004. The role of oxidative stress in carcinogenesis. Annu Rev Pharmacol Toxicol 44:239-267.

Lengauer C, Kinzler KW, Vogelstein B. 1997. DNA methylation and genetic instability in colorectal cancer cells. Proceedings of the National Academy of Sciences 94:2545-2550.

Lertratanangkoon K, Orkiszewski RS, Scimeca JM. 1996. Methyl-donor deficiency due to chemically induced glutathione depletion. Cancer Res 56:995-1005.

Lertratanangkoon K, Wu CJ, Savaraj N, Thomas ML. 1997. Alterations of DNA methylation by glutathione depletion. Cancer Lett 120:149-156.

Mannery YO, Ziegler TR, Park Y, Jones DP. 2010. Oxidation of plasma cysteine/cystine and gsh/gssg redox potentials by acetaminophen and sulfur amino acid insufficiency in humans. J Pharmacol Exp Ther 333:939-947.

McMillan JM, Walle UK, Walle T. 2005. S-adenosyl-l-methionine: Transcellular transport and uptake by caco-2 cells and hepatocytes. J Pharm Pharmacol 57:599-605.

Melnyk S, Pogribna M, Pogribny IP, Yi P, James SJ. 2000. Measurement of plasma and intracellular s-adenosylmethionine and s-adenosylhomocysteine utilizing coulometric electrochemical detection: Alterations with plasma homocysteine and pyridoxal 5′-phosphate concentrations. Clinical Chemistry 46:265-272.

Mosharov E, Cranford MR, Banerjee R. 2000. The quantitatively important relationship between homocysteine metabolism and glutathione synthesis by the transsulfuration pathway and its regulation by redox changes. Biochemistry 39:13005-13011.

Nijhout HF, Reed MC, Anderson DF, Mattingly JC, James SJ, Ulrich CM. 2006. Long-range allosteric interactions between the folate and methionine cycles stabilize DNA methylation reaction rate. Epigenetics 1:81-87.

Pajares MA, Duran C, Corrales F, Pliego MM, Mato JM. 1992. Modulation of rat liver s-adenosylmethionine synthetase activity by glutathione. J Biol Chem 267:17598-17605.

Patchsung M, Boonla C, Amnattrakul P, Dissayabutra T, Mutirangura A, Tosukhowong P. 2012. Long interspersed nuclear element-1 hypomethylation and oxidative stress: Correlation and bladder cancer diagnostic potential. PLoS One 7:e37009.

Pilsner JR, Liu X, Ahsan H, Ilievski V, Slavkovich V, Levy D, et al. 2007. Genomic methylation of peripheral blood leukocyte DNA: Influences of arsenic and folate in bangladeshi adults. Am J Clin Nutr 86:1179-1186.

Poirier LA, Wise CK, Delongchamp RR, Sinha R. 2001. Blood determinations of s-adenosylmethionine, s-adenosylhomocysteine, and homocysteine: Correlations with diet. Cancer Epidemiol Biomarkers Prev 10:649-655.

Prudova A, Bauman Z, Braun A, Vitvitsky V, Lu SC, Banerjee R. 2006. S-adenosylmethionine stabilizes cystathionine beta-synthase and modulates redox capacity. Proc Natl Acad Sci U S A 103:6489-6494.

Razin A, Riggs AD. 1980. DNA methylation and gene function. Science 210:604-610.

Robertson KD, Jones P. 2000. DNA methylation: Past, present and future directions. Carcinogenesis 21:461-467.

Rogers EJ, Chen S, Chan A. 2007. Folate deficiency and plasma homocysteine during increased oxidative stress. New England Journal of Medicine 357:421-422.

Samiec PS, Drews-Botsch C, Flagg EW, Kurtz JC, Sternberg P, Jr., Reed RL, et al. 1998. Glutathione in human plasma: Decline in association with aging, age-related macular degeneration, and diabetes. Free Radic Biol Med 24:699-704.

Schafer FQ, Buettner GR. 2001. Redox environment of the cell as viewed through the redox state of the glutathione disulfide/glutathione couple. Free Radic Biol Med 30:1191-1212.

Selker EU. 1998. Trichostatin a causes selective loss of DNA methylation in neurospora. Proceedings of the National Academy of Sciences 95:9430-9435.

Shimazu T, Hirschey MD, Newman J, He W, Shirakawa K, Le Moan N, et al. 2013. Suppression of oxidative stress by β-hydroxybutyrate, an endogenous histone deacetylase inhibitor. Science 339:211-214.

Siems W, Mueller M, Garbe S, Gerber G. 1987. Damage of erythrocytes by activated oxygen generated in hypoxic rat liver. Free Radic Res Commun 4:31-39.

Slot C. 1965. Plasma creatinine determination. A new and specific jaffe reaction method. Scand J Clin Lab Invest 17:381-387.

Tahiliani M, Koh KP, Shen Y, Pastor WA, Bandukwala H, Brudno Y, et al. 2009. Conversion of 5-methylcytosine to 5-hydroxymethylcytosine in mammalian DNA by mll partner tet1. Science 324:930-935.

Talens RP, Boomsma DI, Tobi EW, Kremer D, Jukema JW, Willemsen G, et al. 2010. Variation, patterns, and temporal stability of DNA methylation: Considerations for epigenetic epidemiology. FASEB J 24:3135-3144.

Thurman RE, Rynes E, Humbert R, Vierstra J, Maurano MT, Haugen E, et al. 2012. The accessible chromatin landscape of the human genome. Nature 489:75-82.

Tunc O, Tremellen K. 2009. Oxidative DNA damage impairs global sperm DNA methylation in infertile men. J Assist Reprod Genet 26:537-544.

Valinluck V, Tsai HH, Rogstad DK, Burdzy A, Bird A, Sowers LC. 2004. Oxidative damage to methyl-cpg sequences inhibits the binding of the methyl-cpg binding domain (mbd) of methyl-cpg binding protein 2 (mecp2). Nucleic Acids Res 32:4100-4108.

Van Phi L, Soling HD. 1982. Methyl group transfer from exogenous s-adenosylmethionine on to plasma-membrane phospholipids without cellular uptake in isolated hepatocytes. Biochem J 206:481-487.

Weitzman SA, Turk PW, Milkowski DH, Kozlowski K. 1994. Free radical adducts induce alterations in DNA cytosine methylation. Proc Natl Acad Sci U S A 91:1261-1264.

Wu HC, Delgado-Cruzata L, Flom JD, Kappil M, Ferris JS, Liao Y, et al. 2011. Global methylation profiles in DNA from different blood cell types. Epigenetics 6:76-85.

Wu SC, Zhang Y. 2010. Active DNA demethylation: Many roads lead to rome. Nature Reviews Molecular Cell Biology 11:607-620.

Chapter 7: Genetic variants associated with serum homocysteine concentrations and arsenic-induced skin lesions: a candidate-gene and genome-wide association study

Megan M. Niedzwiecki[1], Megan N. Hall[2], Xinhua Liu[3], Vesna Slavkovich[1], Vesna Ilievski[1], Diane Levy[3], Abu B. Siddique,[5] Faruque Parvez,[1] Joseph H. Graziano,[1] and Mary V. Gamble[1]

Affiliations: [1]Department of Environmental Health Sciences, [2]Department of Epidemiology, [3]Department of Biostatistics, [1-3]Mailman School of Public Health, Columbia University, New York NY,10032, USA; [4]Lamont-Doherty Earth Observatory of Columbia University, Palisades, NY, USA; [5]Columbia University Arsenic Project in Bangladesh, Dhaka, Bangladesh

ABSTRACT

BACKGROUND: Elevated homocysteine (Hcys), a condition known as hyperhomocysteinemia (HHcys), is highly prevalent in Bangladesh. HHcys is a risk factor for arsenic (As)-induced skin lesions in Bangladeshis, but the role of HHcys in skin lesion pathogenesis is unknown. Single nucleotide polymorphisms (SNPs) in one-carbon metabolism genes, particularly *MTHFR* 677 C→T (rs1801133), are associated with Hcys in other populations, but the influences of gene variants on serum Hcys and skin lesion development in Bangladesh has not been examined previously.

OBJECTIVE: To identify gene variants associated with serum Hcys in Bangladesh and examine whether Hcys-associated gene variants are associated with risk for As-induced skin lesions.

METHODS: We conducted a nested case-control study in which 876 incident skin lesion cases were matched to controls on gender, age, and follow-up time. Homocysteine was measured in 701 cases and 703 controls with serum from baseline, and 64 SNPs in one-carbon metabolism genes were measured with OpenArray. A genome-wide association study (GWAS) of serum Hcys was conducted in a subset of 358 cases and 149 controls.

RESULTS: Compared to subjects with serum Hcys < 10 μM, the odds ratios (ORs) and 95% confidence intervals (CIs) for skin lesion incidence for subjects with serum Hcys 10-15 μM, 15-25 μM, and > 25 μM were 1.29 (0.94 to 1.79), 1.60 (1.12 to 2.27), and 1.83 (1.12 to 3.01), respectively. MTHFR 677 C→T was strongly associated with serum Hcys; in the overall sample, geometric mean (± standard deviation [SD]) serum Hcys in 677 CC, CT, and TT genotypes were 13.1 ± 1.5 μM, 16.7 ± 1.6 μM, and 34.4 ± 2.0 μM, respectively. Diplotypes constructed from MTHFR SNPs (rs1801133, rs1801131, and rs1476413) explained 19.6% of the variance in serum Hcys among controls and 9.1% among cases. However, MTHFR variants

were not associated with skin lesion incidence ($P > 0.05$). GWAS results identified one SNP in NR1I2 (rs6438549) associated with serum Hcys at genome-wide significance ($P = 4.69 \times 10^{-8}$). Top hits were in genes involved in epithelial cell polarity, cell adhesion, and squamous cell carcinoma.

CONCLUSIONS: Serum Hcys was associated with a dose-dependent increase in odds for incident skin lesions, and MTHFR variants were associated with serum Hcys. However, MTHFR variants were not significantly associated with skin lesion risk. The GWAS for serum Hcys identified genes relevant to skin cancer, suggesting that HHcys might not be causally-related to skin lesion development but might instead reflect increased susceptibility to As-induced epithelial cell dysregulation.

INTRODUCTION

Elevated homocysteine (Hcys) concentrations (often defined as plasma Hcys > 15 μM), a condition known as hyperhomocystenemia (HHcys), is a well-established risk factor for numerous diseases, including cardiovascular disease (CVD) (Refsum et al. 1998), neurologic conditions (Diaz-Arrastia 2000), and cancer (Wu and Wu 2002). Homocysteine is endogenously synthesized via one-carbon metabolism (Figure 1): the donation of a methyl group from the methyl donor *S*-adenosylmethionine (SAM) yields the byproduct *S*-adenosylhomocysteine (SAH), which is then hydrolyzed to form Hcys (Scott and Weir 1998). Although Hcys induces oxidative stress and inflammation in experimental models (Dayal et al. 2004; Eberhardt et al. 2000), whether HHcys is a causative factor in human disease, or merely a biomarker of disease risk, is under debate (Brattström and Wilcken 2000). For example, numerous studies have found that HHcys is a risk factor for CVD, yet folic acid supplementation for Hcys lowering has failed to reduce the risk of secondary CVD events (Group 2010; Lonn et al. 2006). Since Hcys is often examined as a disease biomarker, it is essential to understand precisely what the measurement of Hcys reflects about the disease of interest.

Chronic exposure to inorganic arsenic (InAs), a Class I human carcinogen (IARC 1987), has been linked to elevated risk for cancers of the skin, lung, bladder, liver, and kidney (Navarro Silvera and Rohan 2007). Inorganic arsenic is metabolized through a series of methylation reactions to monomethyl (MMA) and dimethyl (DMA) arsenical species, with methyl groups donated by SAM via one-carbon metabolism (Lin et al. 2002). Previously, our group identified that several factors associated with aberrant one-carbon metabolism—namely, global hypomethylation of blood cell DNA, folate deficiency, and HHcys— were risk factors for As-induced precancerous skin lesions (melanosis, leukomelanosis, and keratosis) in a Bangladeshi

population (Pilsner et al. 2009). Interestingly, the association of HHcys with skin lesion risk was observed even after adjustment for folate deficiency, global DNA methylation, and As exposure (Pilsner et al. 2009).

Figure 1. Determinants of serum Hcys concentrations: one-carbon metabolism, transsulfuration pathway, and Hcys cellular efflux. Genes with SNPs examined in the current study are displayed in orange.

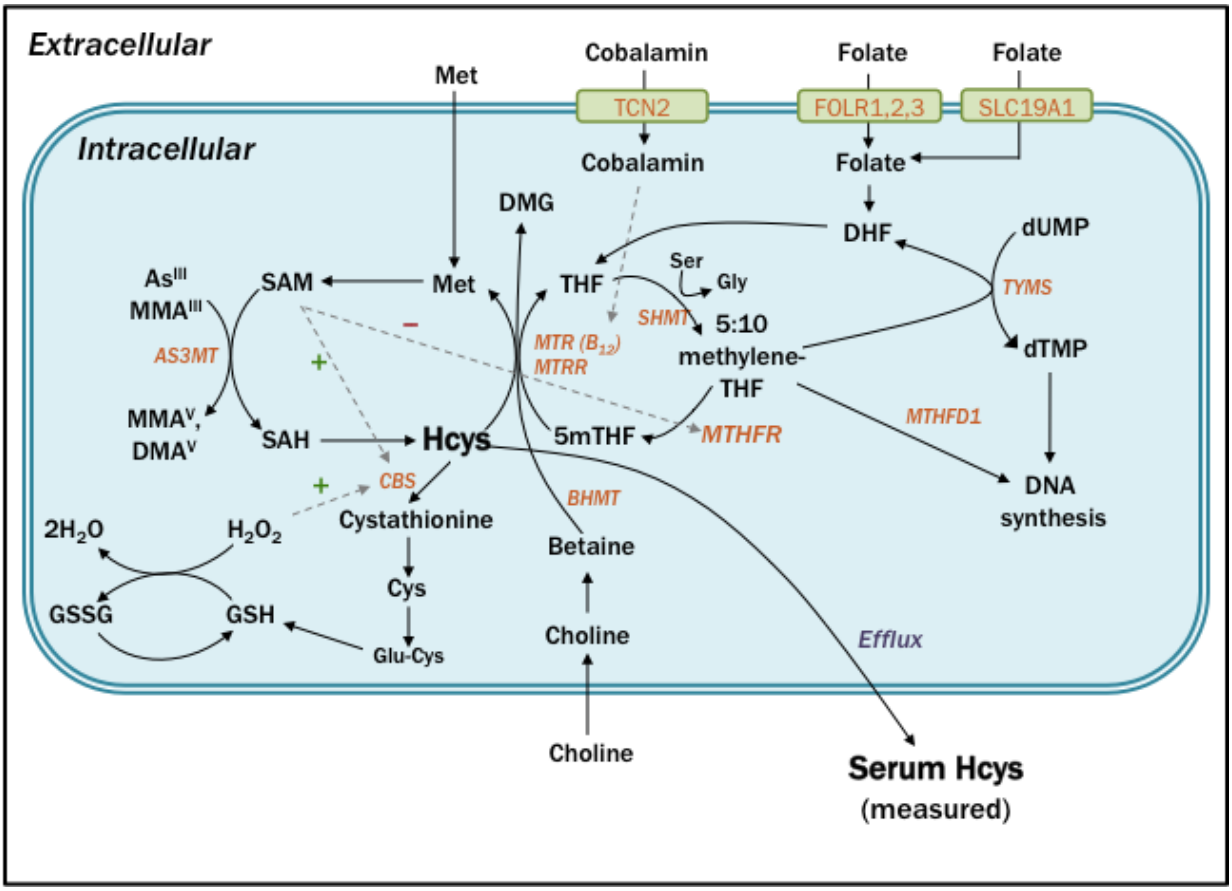

Plasma Hcys concentrations are influenced by single nucleotide polymorphisms (SNPs) in genes involved in one-carbon metabolism. The most widely studied Hcys-associated gene variant is the nonsynonymous 677 C→T polymorphism (rs1801133) in the methylenetetrahydrofolate reductase (MTHFR) gene. MTHFR synthesizes 5-

methyltetrahydrofolate (5mTHF), a substrate for the remethylation of Hcys to methionine (Met), and the C677T variant is associated with reduced enzyme activity and elevated Hcys concentrations, particularly in populations with low folate intakes (Jacques et al. 1996). Another common nonsynonymous MTHFR variant, 1298 A→C (rs1801131), is also associated with reduced enzyme activity (Chango et al. 2000) and elevated Hcys concentrations (Castro et al. 2003). Importantly, genetic association studies can provide evidence about the causality of biomarker-disease relationships: gene variants are randomly distributed during gamete formation, and associations should not be subject to confounding or explained by reverse causation (Bochud et al. 2008). Since the 677 C→T variant is strongly associated with HHcys, it is commonly used as a genetic "proxy" for HHcys to examine the causal nature of HHcys-disease associations (Clarke et al. 2012; Wald et al. 2002).

The prevalence of HHcys is particularly high among individuals of South Asian descent compared to other populations, which is believed to reflect folate and cobalamin deficiencies and/or genetic factors (Chandalia et al. 2003; Senaratne et al. 2001). A cross-sectional survey of 1,650 Bangladeshi adults found a high prevalence of HHcys, and plasma folate and cobalamin explained just 15% and 5% of the variance in plasma Hcys, respectively (Gamble et al. 2005). It is unknown whether MTHFR 677 C→T and 1298 A→C are associated with Hcys concentrations in Bangladesh: these SNPs have variable effects on Hcys concentrations across populations (Wald et al. 2012), and the associations of these variants with Hcys concentrations has not been examined previously in a Bangladeshi population.

The objectives of the current study were to (1) identify gene variants that are associated with Hcys concentrations in Bangladesh; (2) confirm our group's previous findings that HHcys is a risk factor for As-induced skin lesions in a larger sample of incident skin lesion cases; and

(3) examine whether gene variants associated with HHcys are also associated with As-induced skin lesion incidence. To address these objectives, we conducted a nested case-control study of As-induced skin lesions in the Health Effects of Arsenic Longitudinal Study (HEALS) cohort. We used two approaches to identify genetic variants associated with serum Hcys. First, we examined a panel of SNPs in candidate genes involved one-carbon metabolism, with a particular focus on the two aforementioned nonsynonymous MTHFR SNPs, 677 C→T and 1298 A→C. Second, in a subset of 507 subjects with available GWAS data, we conducted an exploratory GWAS of serum Hcys to identify genetic loci using an "unbiased" approach.

SUBJECTS AND METHODS

Eligibility criteria and study design

The Gene-Environment-Nutrition Interactions (GENI) study is a case-control study of incident As-induced skin lesions nested within a parent cohort, the Health Effects of Arsenic Longitudinal Study (HEALS) cohort, an ongoing prospective cohort study of As-exposed adults in Araihazar, Bangladesh (Ahsan et al. 2006). GENI cases and controls were identified from the original cohort of 11,746 married men and women between 18 and 65 years, of which 9,727 participants completed the baseline physical examination, provided urine and blood samples, and were free of skin lesions. Initial HEALS recruitment was completed from October 2000 to May 2002, and active follow-up of the cohort was done every 2 years: the first follow-up was completed from September 2002 to May 2004; second follow-up from June 2004 to August 2006; and third follow-up from January 2007 to February 2009. At baseline and at every follow-up visit, trained physicians conducted comprehensive examinations to identify arsenicosis skin lesions (melanosis, leukomelanosis, and keratosis) across the entire body; the details of the structured examination protocol have been reported previously (Ahsan et al. 2006). Melanosis is characterized by skin hyperpigmentation over a wide surface area; leukomelanosis is characterized by both skin hyperpigmentation and skin hypopigmentation over a wide surface area; and keratosis is characterized by bilateral skin thickening of the palms and soles (Ahsan et al. 2006b).

The GENI study includes 876 incident skin lesion cases identified through the end of the third follow-up period in HEALS (February 2009). The 876 skin lesion cases were individually matched to controls on gender, age (± 3 years), and follow-up time in the study (± 500 days). Since it was known *a priori* that some of the HEALS subjects did not have remaining serum

and/or DNA samples from the baseline recruitment visit for analysis, we devised a matching scheme to maximize the number of controls with biological samples. Up to 3 possible controls were identified for each case, without prior knowledge of whether these controls had biological samples available. Sample availability (serum and/or DNA) was then determined for each possible control, and the control with the greatest number of biological samples in the freezers (serum and/or DNA) was preferentially selected for each case.

We had 703 cases and 705 controls with serum samples, and 701 matched pairs where both the case and control had a serum sample available. There were 732 successfully matched pairs in which a control was identified with a DNA and/or serum sample, and 608 matched pairs in which both the case and control have both DNA and serum samples. There were 144 skin lesion cases for which none of the three possible controls had either a serum or DNA sample in the freezers; for these cases, a control match was randomly selected from the three identified controls.

Oral informed consent was obtained by our Bangladeshi field staff physicians, who read an approved consent form to the study participants. This study was approved by the Institutional Review Boards of Columbia University Medical Center and the Bangladesh Medical Research Council.

Analytic techniques

Methods for analysis of water As, urinary As, and urinary Cr are described in detail in Chapter 3. Analytic methods for serum Hcys, DNA extraction, and genotyping are outlined here.

Serum Hcys

Serum Hcys was measured using HPLC, as described in Chapter 3. Serum samples in case-control pairs were assayed in the same laboratory batch, and all samples were run in

duplicate; samples were repeated if the coefficient of variation (CV) within the duplicates was >10%. Samples were randomized in a two-step process such that the run order of the case-control pairs was randomized, as well as the run order of the case and control samples within each matched pair. The intra- and inter-day CVs were 3 and 8%, respectively.

DNA extraction

DNA was extracted from blood clots using the Flexigene DNA kit (Qiagen), and the DNA concentration and quality (260/280 and 260/230 ratios) was determined using Nanodrop 1000. DNA samples were shipped to Columbia University on dry ice and stored at −80°C.

TaqMan OpenArray SNP genotyping

125 ng of DNA was processed with the TaqMan OpenArray Genotyping System (Life Technologies, Carlsbad, California, USA) according to the manufacturer's protocol using custom-designed chips with 64 SNPs in candidate genes involved in one-carbon metabolism and folate transport (full list of SNPs in Appendix Table E1). DNA samples in case-control pairs were processed on the same array chip, and the run order was determined using the same two-step randomization process as for serum Hcys, but with different sample randomization orders. Genotype calls were generated using the OpenArray SNP Genotyping analysis software 1.0.3.

Of the original 64 SNPs on the array, 11 SNP assays had call rates < 90% and were excluded, and of the remaining 53 SNPs, 21 SNPs had minor allele frequencies (MAF) < 1% in our sample and were additionally excluded. The final dataset contained 32 SNPs with a mean call rate of 97.1%.

Illumina Infinium HD SNP array

A subset of GENI subjects had GWAS data available from the Illumina Infinium HD SNP array (Illumina). For these subjects, 250 ng of DNA was processed on HumanCytoSNP-12

v2.1 chips according to manufacturer's protocol and read on the BeadArray Reader, and genotype calls were generated using BeadStudio software. The 299,140 measured genotypes were used to impute for 1,211,988 SNPs using HapMap 2 data with the Gujarati Indians in Houston, Texas (GIH) reference panel.

Statistical methods

Descriptive statistics (mean ± standard deviation [SD] for continuous variables, N [%] for categorical variables) were calculated separately for the cases and control groups. Differences between case and control groups were examined using Wilcoxon test (continuous variables) and chi-square test (categorical variables), and differences in matched case-control pairs were examined using Wilcoxon signed-rank test (continuous variables), McNemar's test (dichotomous variables), and Bowker's test (categorical variables).

We examined whether genotype distributions were in accordance with Hardy-Weinberg equilibrium by comparing the expected vs. observed genotype frequencies in controls using Chi-square tests. Differences in genotype distributions between case and control groups were also examined using Chi-square tests. Linkage disequilibrium parameters (pairwise D' and R^2) among MTHFR SNPs were calculated using Haploview version 4.2 (Barrett et al. 2005), and haplotype pairs (diplotypes) for each subject were constructed using PHASE version 2.1.1 (Stephens et al. 2001; Stephens and Scheet 2005) for all subjects with complete data for rs1801133, rs1801131, and rs1476413. Associations between SNP genotypes/haplotypes and serum Hcys were examined in the overall sample and separately in the cases and controls using general linear models. Associations between serum Hcys and SNPs with risk of skin lesions were examined using conditional logistic regression with matched case-control pairs, with and without adjustment for covariates. Genome-wide associations with serum Hcys were examined

using a linear mixed model adjusted for age, sex, genotype batch, and cryptic relatedness using Genome-wide Efficient Mixed Model Association (GEMMA) software (Zhou and Stephens 2012, 2013).

Unless specified, statistical tests were conducted using SAS software, version 9.3 (SAS Institute Inc., Cary, NC); statistical tests were two sided with a significance level of 0.05.

RESULTS

Characteristics of GENI study participants

Demographic and clinical characteristics of the GENI skin lesion cases and controls are presented in Table 1. Controls were matched to skin lesion cases on gender, age (± 3 years), and study follow-up time (± 60 days). At baseline, skin lesion cases were more likely to report use of betelnut ($P = 0.07$), were less likely to own a television ($P = 0.009$), and had higher As concentrations in well water ($P < 0.0001$) and urine ($P < 0.0001$). Serum Hcys concentrations were higher in skin lesion cases ($P = 0.003$), as well as the proportion of individuals who were classified as having HHcys, defined here as serum Hcys > 15 uM ($P = 0.02$). The demographic and clinical data did not differ between GENI subjects with and without serum and/or DNA samples (data not shown). The breakdown of the skin lesion types (melanosis, keratosis, and/or leukomelanosis) among the total 876 incident skin lesions cases is in Appendix Table E2.

Genotype frequencies of the three MTHFR SNPs on the OpenArray panel are shown in Table 2. In addition to 677 C→T (rs1801133) and 1298 A→C (rs1801131), we measured rs1476413, a G→A variant in intron 10 that is 2,176 bp away from 1298 A→C. The MAF for 677 C→T was 0.12 in both cases and controls, and approximately 20% and 1.6% of the total sample were CT heterozygous and TT homozygous, respectively. The MAFs for 1298 A→C and Intron 10 G→A were higher than the MAF for 677 C→T (overall sample, 0.38 and 0.43, respectively). Genotype frequencies were in accordance with Hardy-Weinberg equilibrium for all three MTHFR SNPs ($P > 0.05$), and genotype distributions did not differ between cases and controls for any of the SNPs ($P > 0.05$).

Table 1. Baseline descriptive and clinical characteristics for GENI participants with serum.

Variable	Controls N=705	Cases N=703	Diff. among N=701 matched pairs (*P*)
Demographic			
Gender (male)	497 (70.5)[a]	495 (70.4)	1.0
Age (years)	44.3 ± 9.5 (20 to 65)[b]	44.3 ± 9.5 (20 to 65)	0.03
BMI (kg/m^2)	19.8 ± 3.3 (13.0 to 32.3)	19.5 ± 2.8 (14.0 to 31.4)	0.05
Cigarette smoking (ever)	400 (56.7)	420 (59.7)	0.15
Betelnut use (ever)	351 (49.8)	381 (54.2)	0.07
Education			0.004
0 years	297 (42.1)	341 (48.5)	
1-5 years	101 (14.3)	115 (16.4)	
> 5 years	307 (43.6)	247 (35.1)	
Television ownership (yes)	270 (38.3)	222 (31.6)	0.009
Arsenic exposure			
Well water As (µg/L)	85 ± 97 (0.1 to 571)	138 ± 134 (0.1 to 790)	<0.0001
Well water As category			<0.0001
< 10 µg/L	178 (25.3)	106 (15.1)	
10-50 µg/L	166 (23.6)	116 (16.5)	
50-100 µg/L	128 (18.2)	121 (17.2)	
100-200 µg/L	147 (20.9)	172 (24.5)	
>200 µg/L	86 (12.2)	188 (26.7)	
Urinary As (µg/L)[c]	124 ± 125 (4 to 1228)	167 ± 177 (1 to 1278)	<0.0001
Urinary Cr (mg/dL)[c]	63 ± 46 (4 to 290)	61 ± 47 (3 to 376)	0.29
Homocysteine			
Serum Hcys (µM)	15.3 ± 9.6 (3.1 to 108.2)	16.2 ± 9.1 (3.5 to 119.0)	0.003
HHcys (Hcys > 15 µM)	272 (38.6)	309 (44.0)	0.02
Serum Hcys category			0.10
< 10 µM	169 (19.3)	133 (15.2)	
10-15 µM	264 (30.1)	261 (29.8)	
15-25 µM	217 (24.8)	235 (26.8)	
> 25 µM	55 (6.3)	74 (8.5)	

a. N (%) (all such values); b. mean ± SD (range) (all such values); c. N=677 pairs

Table 2. Genotype frequencies for MTHFR SNPs, overall and by skin lesion case status.

SNP		Controls	Cases	Overall	Overall with serum
677 C→T rs1801133					
	CC	501 (77.2)[a]	563 (77.9)	1064 (77.6)	1008 (78.1)
	CT	136 (21.0)	147 (20.3)	283 (20.6)	262 (20.3)
	TT	12 (1.8)	13 (1.8)	25 (1.8)	21 (1.6)
	MAF	0.12	0.12	0.12	0.12
1298 A→C rs1801131					
	AA	255 (40.0)	278 (39.3)	533 (39.6)	505 (39.8)
	AC	287 (45.0)	315 (44.5)	602 (44.7)	566 (44.6)
	CC	96 (15.0)	115 (16.2)	211 (15.7)	198 (15.6)
	MAF	0.38	0.38	0.38	0.38
Intron 10 G→A rs1476413					
	GG	226 (34.8)	239 (33.0)	465 (33.8)	436 (33.7)
	GA	301 (46.4)	338 (46.6)	639 (46.5)	604 (46.6)
	AA	122 (18.8)	148 (20.4)	270 (19.7)	255 (19.7)
	MAF	0.42	0.44	0.43	0.43

a. N (%) (all such values), b. mean ± SD (all such values)

Elevated serum Hcys is a risk factor for arsenic-induced skin lesions

To confirm our group's previous finding that HHcys was a risk factor for As-induced skin lesions (Pilsner et al 2009), we used conditional logistic regression to examine the unadjusted and adjusted odds ratios (ORs) for serum Hcys and other study covariates, shown in Table 3. Consistent with Pilsner et al. 2009, serum Hcys at baseline was associated with a dose-dependent increase in odds for incident skin lesions.

Table 3. Unadjusted and adjusted ORs (95% CIs) for serum homocysteine and demographic characteristics as predictors of skin lesions (N=701 matched pairs).

Predictor	Level/unit	Unadjusted OR (95% CI)	Adjusted OR[a] (95% CI)
Serum Hcys			
	< 10 µM	*ref.*	*ref.*
	10-15 µM	1.34 (0.99 to 1.80)	1.29 (0.94 to 1.79)
	15-25 µM	1.53 (1.10 to 2.13)	1.60 (1.12 to 2.27)
	> 25 µM	1.98 (1.25 to 3.14)	1.83 (1.12 to 3.01)
Age			
	1-year	1.38 (1.04 to 1.83)	1.37 (1.01 to 1.79)
Betelnut use			
	Never	*ref.*	*ref.*
	Ever	1.21 (0.97 to 1.52)	1.17 (0.91 to 1.49)
Television ownership			
	No	*ref.*	*ref.*
	Yes	0.74 (0.59 to 0.92)	0.86 (0.67 to 1.11)
Education			
	0 years	*ref.*	*ref.*
	1-5 years	0.84 (0.65 to 1.09)	0.83 (0.63 to 1.09)
	> 5 years	0.67 (0.51 to 0.87)	0.70 (0.52 to 0.94)
Well water As			
	< 10 µg/L	*ref.*	*ref.*
	10-50 µg/L	1.32 (0.91 to 1.91)	1.38 (0.95 to 2.01)
	50-100 µg/L	1.81 (1.22 to 2.66)	1.90 (1.28 to 2.84)
	100-200 µg/L	2.16 (1.51 to 3.10)	2.15 (1.49 to 3.11)
	>200 µg/L	4.12 (2.78 to 6.11)	4.16 (2.78 to 6.21)

a. Adjusted for other predictors listed in table

MTHFR 677 C→T is associated with elevated serum Hcys

We next examined associations of MTHFR SNPs with serum Hcys concentrations. The 677 C→T variant was strongly associated with serum Hcys concentrations in both cases and controls (P < 0.0001, Appendix Table E3). Boxplots displaying serum Hcys concentrations by 677 C→T genotype for the overall sample are shown in Figure 2. In the overall sample, compared to CC wildtype, geometric mean serum Hcys concentrations were approximately 3 µM higher in CT heterozygotes (P < 0.0001) and approximately 19 µM higher in TT homozygotes (P < 0.0001). The 677 C→T genotype explained 15.8% of the variance in log-transformed serum Hcys in controls and 7.4% in cases (Appendix Table E3). The 1298 A→C and Intron 10 G→A variants were not associated with serum Hcys in cases or controls after conditioning on 677 C→T (Appendix Table E3).

Figure 2. Boxplots of serum Hcys by MTHFR 677 C→T genotype for all subjects.
Whiskers, red X's, and asterisks represent 1st and 99th percentiles, geometric mean, and outliers, respectively, for serum Hcys in the overall sample. Numerical values reflect median serum Hcys values.

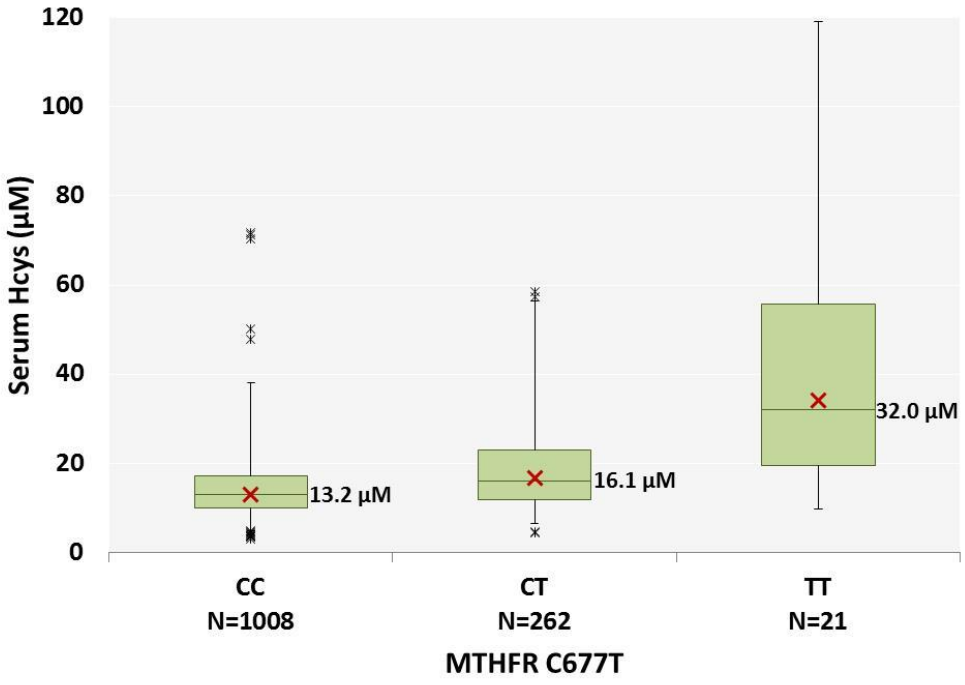

MTHFR Intron 10 G→A is marginally associated with increased odds for skin lesions

Next, we examined associations of MTHFR SNPs with incident skin lesions in matched case-control pairs (Table 4). Although 677 C→T was strongly associated with serum Hcys in our sample, there was no association of the 677 C→T variant with skin lesion risk (Table 4). Conversely, although Intron 10 G→A was not associated with serum Hcys, those who were homozygous for the risk allele of Intron 10 G→A had an OR for skin lesions of 1.29 (95% CI, 0.96 to 1.75) in adjusted models, although this did not reach statistical significance (Table 4).

MTHFR SNPs are in linkage disequilibrium

The three MTHFR SNPs are in linkage disequilibrium (LD): In the HapMap GIH population, the pairwise D' values for 677 C→T with 1298 A→C and Intron 10 G→ A are 1.0 and 0.93, respectively, and the pairwise D' between 1298 A→C and Intron 10 G→ A is 0.90. Using Haploview, we examined LD parameters in our sample and observed similar pairwise D' values (Figure 3), indicating that the three SNPs were nearly in complete LD. The R^2 values were smaller than the D' values (Figure 1) since the MAF for 677 C→T was considerably lower than the MAFs for 1298 A→C and Intron 10 G→ A.

We constructed MTHFR haplotypes for all subjects with complete data for the three SNPs (Table 5). The most common haplotype was wildtype CAG (677 C-1298 A-Intron 10 G). The C allele of 1298 A→C was most commonly in phase with the A allele of Intron 10 G→A, and the T allele of 677 C→T was almost always in phase with 1298 A and Intron 10 G. Haplotypes containing both 677 T and 1298 C variant alleles were rare and occurred mainly in the case group. Diplotype (haplotype pair) frequencies are listed in Appendix Table E4. Approximately 20% of the overall sample had wildtype diplotypes (GAC/GAC haplotype pairs).

Table 4. Unadjusted and adjusted ORs (95% CIs) for MTHFR SNPs as independent predictors of arsenic-induced skin lesions in conditional logistic regression models.

SNP	Model		Unadjusted OR (95% CI)	Adjusted OR[a] (95% CI)
677 C→T				
N=606 pairs	General	CC	*ref.*	*ref.*
		CT	0.95 (0.71 to 1.27)	0.87 (0.64 to 1.19)
		TT	0.91 (0.41 to 2.07)	0.84 (0.36 to 1.97)
	Dominant	CC	*ref.*	*ref.*
		CT+TT	0.95 (0.72 to 1.24)	0.87 (0.65 to 1.16)
	Recessive	CC+CT	*ref.*	*ref.*
		TT	0.92 (0.40 to 2.08)	0.84 (0.36 to 1.98)
1298 A→C				
N=585 pairs	General	AA	*ref.*	*ref.*
		AC	0.98 (0.77 to 1.25)	0.97 (0.75 to 1.26)
		CC	1.11 (0.79 to 1.57)	1.21 (0.84 to 1.74)
	Dominant	AA	*ref.*	*ref.*
		AC+CC	1.01 (0.81 to 1.27)	1.03 (0.81 to 1.31)
	Recessive	AA+AC	*ref.*	*ref.*
		CC	1.13 (0.82 to 1.55)	1.22 (0.87 to 1.73)
Intron 10 G→A				
N=608 pairs	General	GG	*ref.*	*ref.*
		GA	1.05 (0.82 to 1.35)	1.04 (0.80 to 1.36)
		AA	1.16 (0.85 to 1.58)	1.32 (0.95 to 1.84)
	Dominant	GG	*ref.*	*ref.*
		GA+AA	1.09 (0.86 to 1.37)	1.12 (0.88 to 1.43)
	Recessive	GG+GA	*ref.*	*ref.*
		AA	1.13 (0.85 to 1.49)	1.29 (0.96 to 1.75)

a. Adjusted for water As, age, and years of education (categorical)

Figure 3. Linkage disequilibrium parameters for MTHFR SNPs. Pairwise D' and R^2 values calculated using Haploview are shown for controls (A), cases (B), and the overall sample (C).

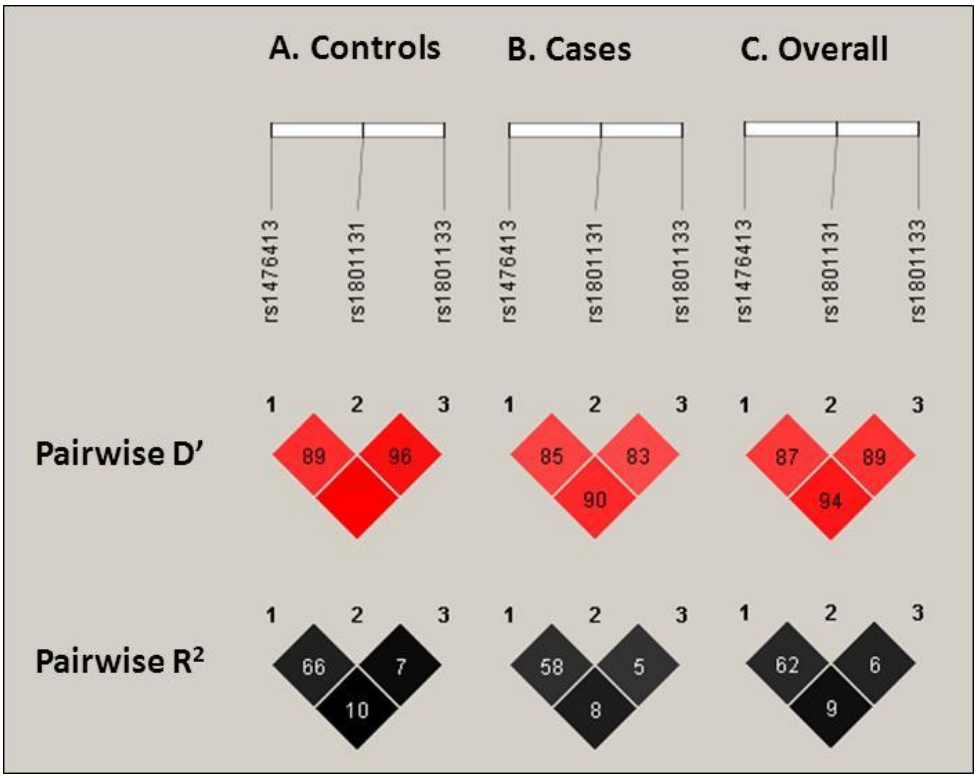

Table 5. Inferred haplotype counts and frequencies.

Haplotype			Controls	Cases	Overall
677 C→T	1298 A→C	Int. 10 G→A			
C	A	G	552 (43.7)	588 (41.9)	1140 (42.8)
C	A	A	84 (6.6)	114 (8.1)	198 (7.4)
	Total 677 C-1298 A		636 (50.3)	702 (50.1)	1338 (50.2)
C	C	G	25 (2.0)	39 (2.8)	64 (2.4)
C	C	A	448 (35.4)	496 (35.4)	944 (35.4)
	Total 677 C-1298 C		473 (37.4)	535 (38.2)	1008 (37.8)
T	A	G	154 (12.2)	158 (11.3)	312 (11.7)
T	A	A	0 (0.0)	1 (0.1)	1 (0.0)
	Total 677 T-1298 A		154 (12.2)	159 (11.3)	313 (11.7)
T	C	G	1 (0.1)	3 (0.2)	4 (0.2)
T	C	A	0 (0.0)	3 (0.2)	3 (0.1)
	Total 677 T-1298 C		1 (0.1)	6 (0.4)	7 (0.3)

MTHFR haplotypes are not significantly associated with increased odds for skin lesions

To attempt to tease apart the independent effects of each MTHFR SNP on skin lesion risk, we examined associations of MTHFR diplotypes with incident skin lesions (Table 6). Those with diplotypes containing a CAA haplotype (wildtype for 677 C→T and 1298 A→C, risk allele for Intron 10 G→A) had an OR for skin lesions of 1.42 (95% CI, 0.92 to 2.19) compared to those with the wildtype diplotype (CAG/CAG). Similarly, those with diplotypes containing the CCG haplotype (wildtype for 677 C→T and Intron 10 G→A, risk allele for 1298 A→C) had an OR for skin lesions of 1.48 (95% CI, 0.76 to 2.90) compared to wildtype (Table 6). However, diplotypes containing the haplotype with risk alleles for both Intron 10 G→A and 1298 A→C (haplotype CCA) did *not* have an elevated risk for skin lesions compared to wildtype (OR 1.11, 95% CI 0.80 to 1.53). Diplotypes containing a TAG haplotype were also not significantly associated with skin lesion incidence (OR 0.82, 95% CI 0.61 to 1.12).

MTHFR haplotypes and diplotypes are associated with serum Hcys

We also examined associations of MTHFR diplotypes with serum Hcys concentrations. Plots of geometric mean (± SD) serum Hcys concentrations by MTHFR diplotype in cases and controls are displayed in Figure 4. The diplotype variable explained 19.6% of the variance in log-transformed serum Hcys in controls (Figure 4A), which is approximately 4% higher than the variance explained by 677 C→T alone. In cases, the MTHFR diplotype explained only 9.1% of the variance in serum Hcys (Figure 4B). Compared to wildtype diplotype carriers, diplotypes containing the CAA haplotype had higher geometric mean serum Hcys concentrations ($P < 0.05$), indicating that the Intron 10 G→A risk allele is associated with increased serum Hcys. The CCG diplotype was not associated with serum Hcys, suggesting that 1298 A→C is not

independently associated with Hcys in this population. In agreement with the findings for 677 C→T, the TAG haplotype was strongly associated with serum Hcys ($P < 0.0001$).

Table 6. Unadjusted and adjusted ORs (95% CIs) for MTHFR diplotypes as predictors of skin lesions from conditional logistic regression models.

Predictor	Referent group	Unadjusted OR (95% CI)	Adjusted OR[a] (95% CI)
Diplotypes containing CAA			
	Wildtype	1.29 (0.86 to 1.95)	1.42 (0.92 to 2.19)
	Wildtype + other	1.21 (0.86 to 1.70)	1.33 (0.93 to 1.91)
Diplotypes containing CCG		.	.
	Wildtype	1.36 (0.72 to 2.54)	1.48 (0.76 to 2.90)
	Wildtype + other	1.25 (0.69 to 2.25)	1.36 (0.73 to 2.55)
Diplotypes containing CCA			
	Wildtype	1.09 (0.80 to 1.47)	1.11 (0.80 to 1.53)
	Wildtype + other	0.97 (0.77 to 1.22)	0.98 (0.77 to 1.26)
Diplotypes containing TAG			
	Wildtype	0.99 (0.68 to 1.44)	0.95 (0.64 to 1.42)
	Wildtype + other	0.88 (0.66 to 1.17)	0.82 (0.61 to 1.12)

Figure 4. Geometric mean Hcys concentrations by MTHFR diplotype. Bars represent geometric mean (± SD) serum Hcys in controls (Figure 4A) and cases (Figure 4B).

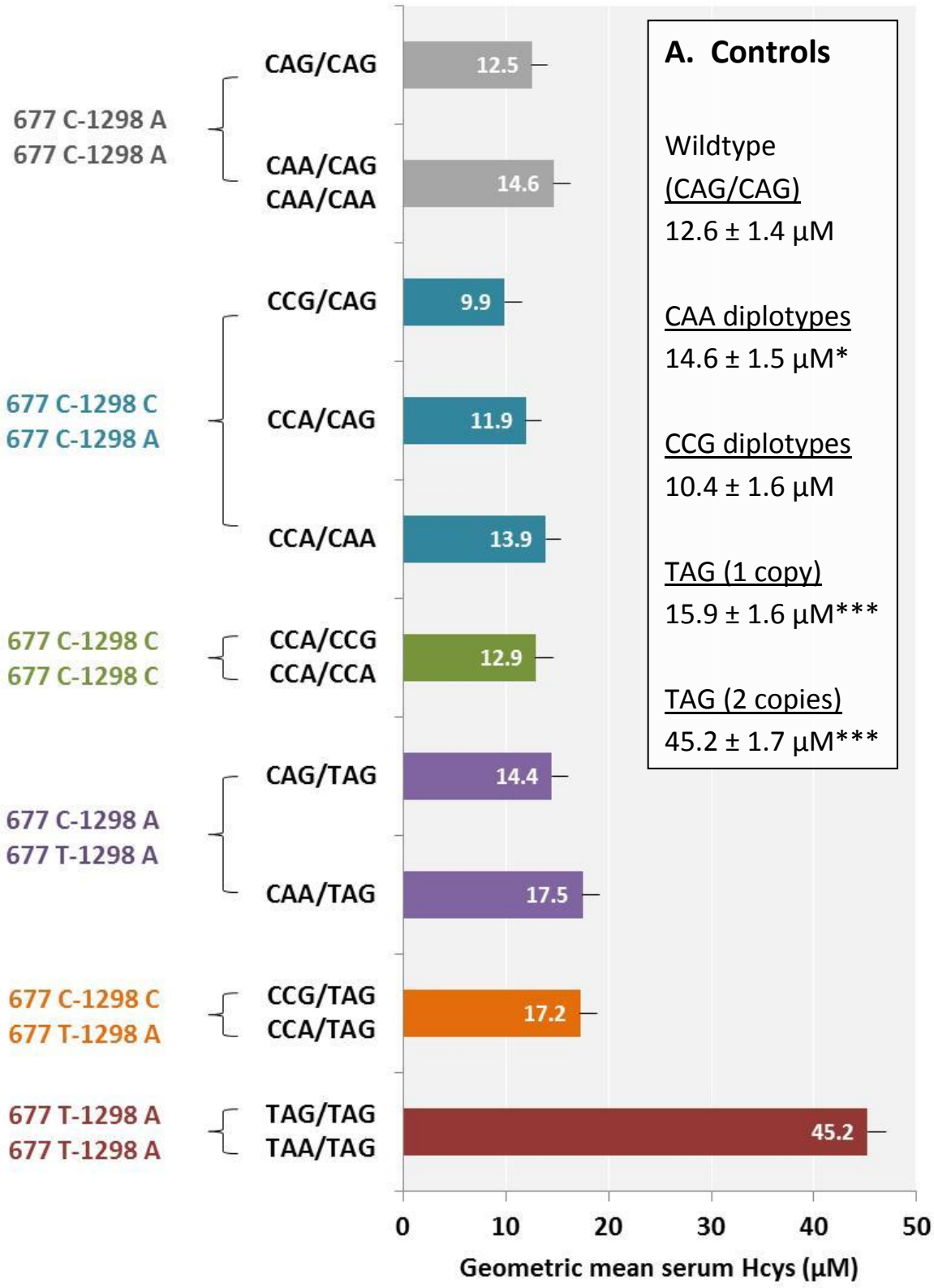

Figure 4. Geometric mean Hcys concentrations by MTHFR diplotype. Bars represent geometric mean (± SD) serum Hcys in controls (Figure 4A) and cases (Figure 4B).

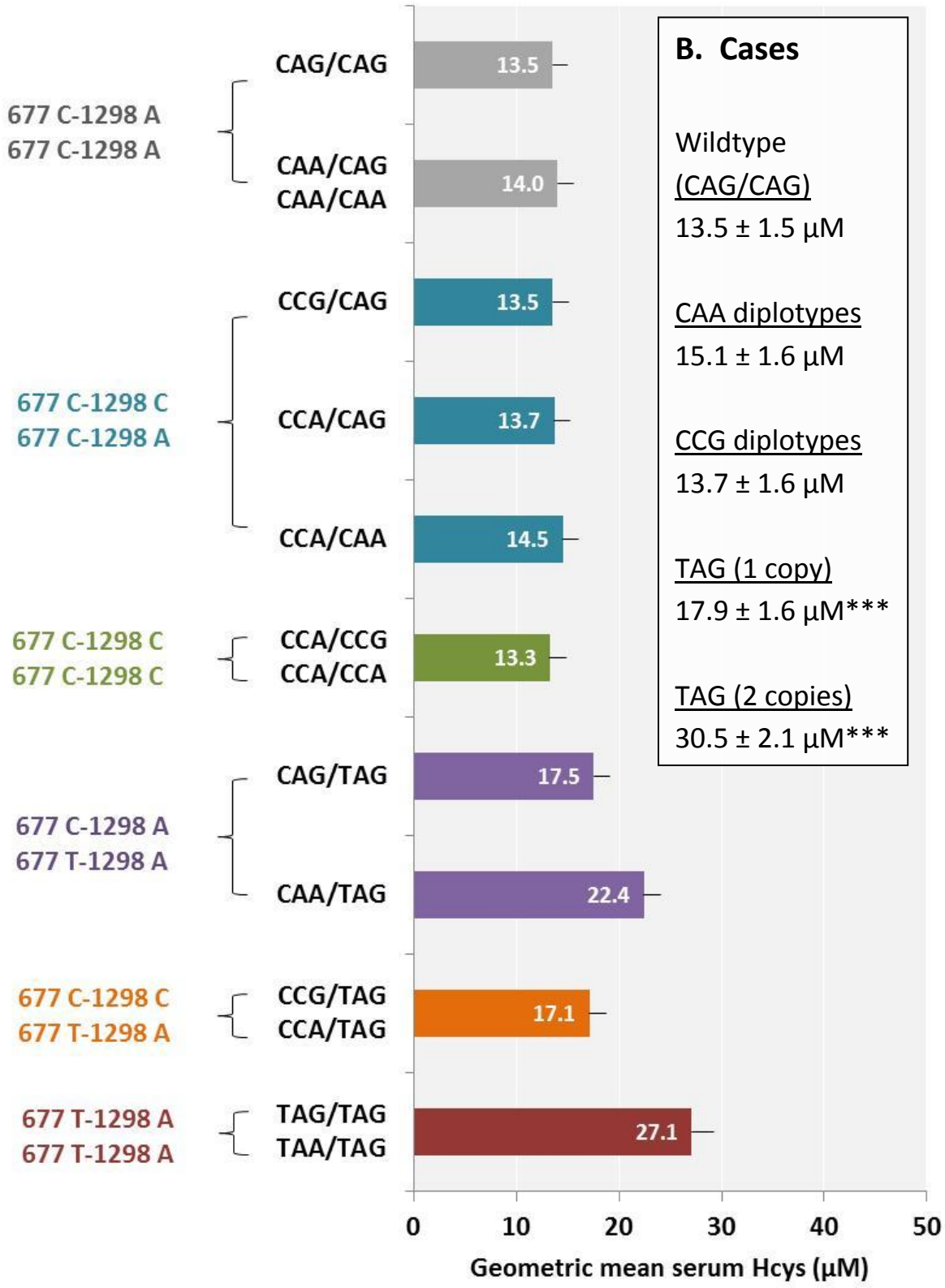

MTHFR 677 C→T is associated with urinary As metabolite percentages

Since MTHFR 677 C→T genotypes had the strongest associations with serum Hcys, we also assessed the associations of 677 C→T genotypes with urinary As metabolite percentages. The majority of skin lesion cases with genotype data also had urinary As metabolite data (657/723), but only a small proportion of controls had urinary As metabolite data (203/651). As shown in Appendix Table E5, in cases, adjusted mean urinary %MMA was higher in 677 T allele carriers (adjusted mean ± SE, 13.9 ± 0.2% in CC wildtype, 14.9 ± 0.4% in T allele carriers, P = 0.05), and urinary %DMA was lower (adjusted mean ± SE, 71.4 ± 0.4% in CC wildtype, 69.7 ± 0.7% in T allele carriers, P = 0.04). In controls, 677 T allele carriers also had higher urinary %MMA and lower urinary %DMA (Appendix Table E5). No significant associations between urinary As metabolites and 1298 A→C or Intron 10 G→A were observed (data not shown).

Other one-carbon metabolism variants are not associated with serum Hcys or skin lesions

In addition to MTHFR gene variants, we examined the associations of the other OpenArray SNPs with both serum Hcys concentrations and skin lesion risk. However, in preliminary analyses, we did not observe any significant associations ($P < 0.05$) between these SNPs with serum Hcys or skin lesion incidence (data not shown).

GWAS of serum Hcys reveals novel genetic loci

The MTHFR diplotypes explained a smaller proportion of the variance in serum Hcys among skin lesion cases (9.1%) compared to controls (19.6%), indicating that there might be other important genetic determinants of serum Hcys concentrations in the skin lesion group. To examine whether we could identify novel genetic loci associated with serum Hcys among skin lesion cases, we conducted an exploratory GWAS of serum Hcys in a subset of 507 subjects in which cases were overrepresented (358 skin lesion cases and 149 controls). The results are

presented in Figure 5, and the quantile-quantile (Q-Q) plot is shown in Figure 6. We identified one SNP that was associated with serum Hcys at genome-wide significance ($P < 5.0 \times 10^{-8}$) (Figure 4). This SNP (rs6438549, A→G) is located in an intronic region of the NR1I2 gene on chromosome 3. Another SNP in NR1I2 (rs2461818), in LD with rs6438549, was the 8th most significant SNP genome-wide according to *P*-value ($P = 9.81 \times 10^{-7}$).

The top gene-associated SNPs are listed in Table 7; when multiple SNPs were identified in an LD block at a gene locus, only the lead SNP was included in the table. Since the GWAS was conducted in a convenience sample, we examined top hits that did not meet the genome-wide $P < 5.0 \times 10^{-8}$ significance cutoff and explored the biologic significance of the identified genes (Appendix Table E6). Among the top ranked SNPs in our analysis, there were hits in genes that had been identified in previous GWAS analyses. Among our top 20 hits, there were two SNPs in PRICKLE2, which was a gene identified in a GWAS of serum folate concentrations in an Italian cohort (Tanaka et al. 2009). Additionally, we identified an LD block of 8 SNPs in *PTPRT*; another member of the protein tyrosine phosphatase (PTP) family, PTPRD, was associated with plasma Hcys in a Spanish GWAS study (Malarstig et al. 2009).

Although 677 C→T (rs1801133) was strongly associated with serum Hcys in our overall sample, in the GWAS of serum Hcys in the subset of 507 subjects, we did not identify 677 C→T among the top 1,000 hits genome-wide (SNPs with $P < 6.23 \times 10^{-4}$). However, 677 C→T was in LD with the 43rd most significant SNP (rs2639453, $P = 1.17 \times 10^{-5}$). No candidate-gene SNPs included on the OpenArray platform, and no SNPs in any of the one-carbon metabolism genes included on the platform, were among the top 1,000 GWAS hits.

Figure 5. Manhattan plot from GWAS of serum Hcys. Genomic coordinates for all GWAS SNPs are plotted on the x-axis, and the negative logarithm of the *P*-value for the association of each SNP with serum Hcys is plotted on the y-axis. Datapoints above the red line represent SNPs with genome-wide significant *P*-values ($P < 5.0 \times 10^{-8}$) for associations with serum Hcys. Chromosomes are color-coded by the alternating black/gray color scheme (SNPs within Chromosome 1=black, Chromosome 2=gray, Chromosome 3=black, etc.).

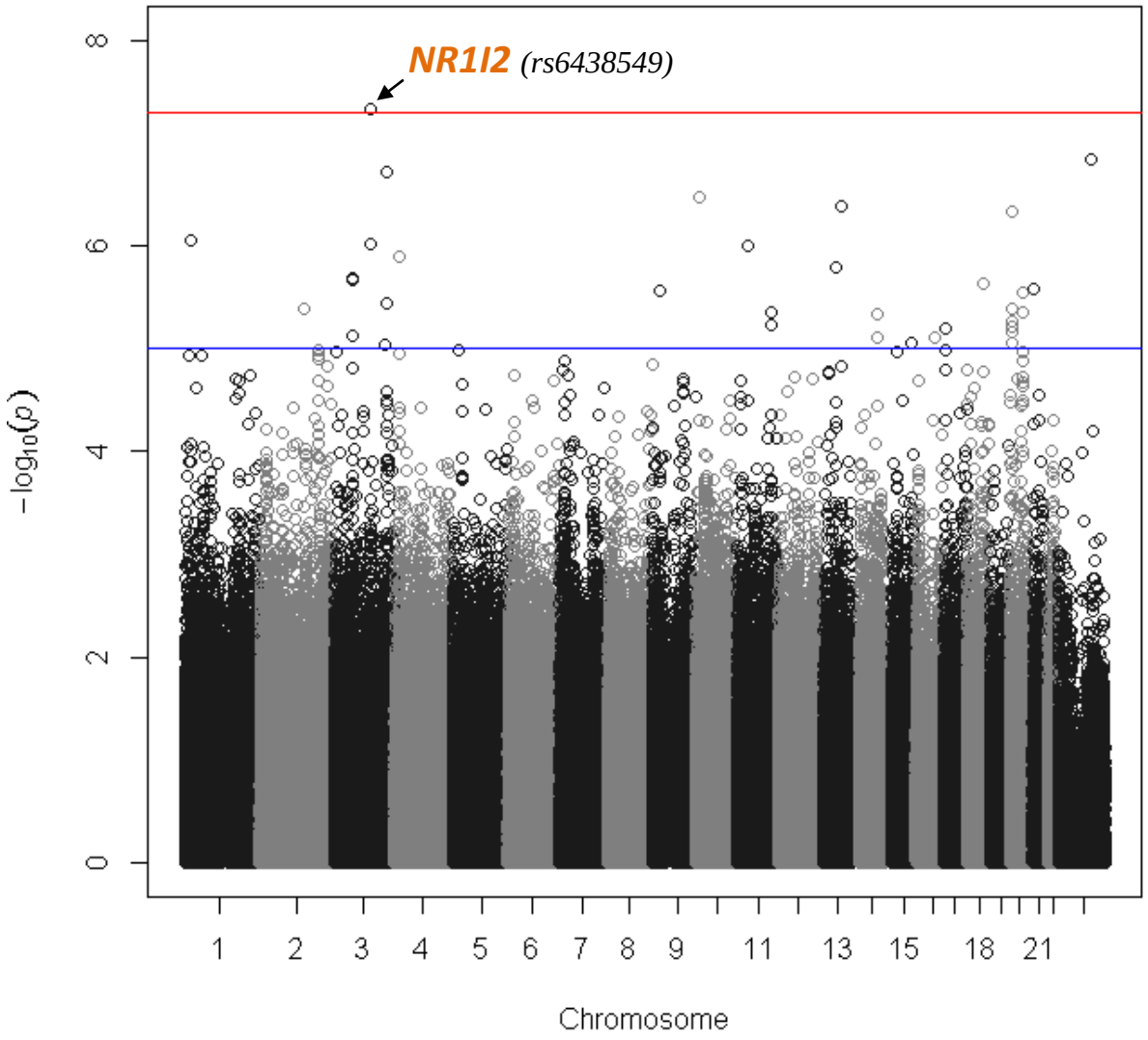

Figure 6. Quantile-quantile (Q-Q) plot from GWAS of serum Hcys. The figure displays the expected distribution of negative log-transformed *P*-values (x-axis) plotted against the observed distribution of negative log-transformed *P*-values (y-axis).

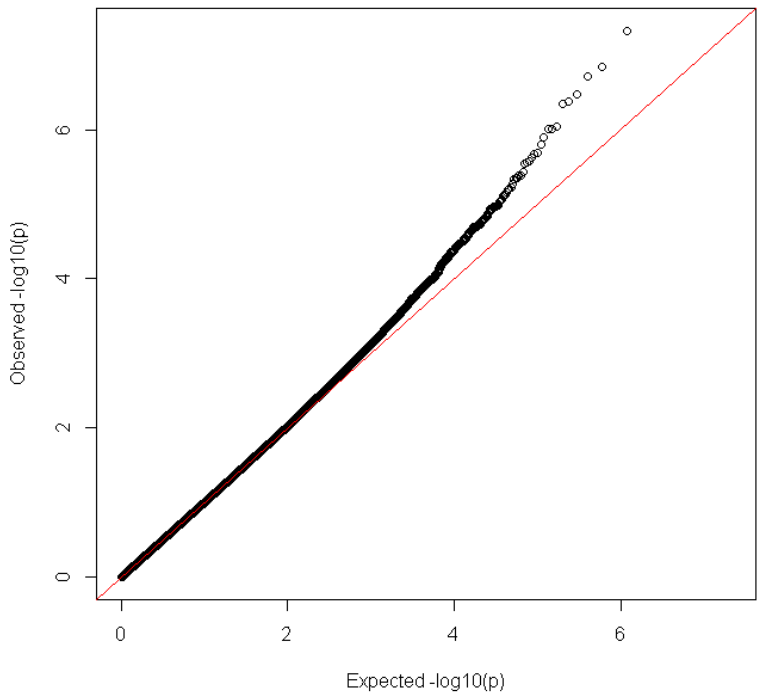

Table 7. List of top gene-associated SNPs from GWAS of serum Hcys.

RS#	Gene	Chr.	Ref. allele	B	SE	*P*
rs6438549	NR1I2	3	A	-7.53	1.36	4.69×10^{-8}
rs7611474	NLGN1	3	A	-6.47	1.23	1.94×10^{-7}
rs17155012	FRMD4A	10	C	-4.95	0.96	3.40×10^{-7}
rs6077536	PLCB4	20	T	-4.13	0.81	4.60×10^{-7}
rs10916959	ECE1	1	A	-2.86	0.57	8.98×10^{-7}
rs16927009	CD44	11	T	-7.97	1.61	9.94×10^{-7}
rs6791571	PRICKLE2	3	G	-3.03	0.63	2.04×10^{-6}
rs2425556	PTPRT	20	G	-3.69	0.78	2.89×10^{-6}
rs9880289	TNIK	3	C	-4.20	0.90	3.67×10^{-6}

DISCUSSION

In this nested case-control study of incident As-induced skin lesions in a cohort of Bangladeshi adults, we measured Hcys in baseline serum samples and SNPs in various one-carbon metabolism genes to address three primary objectives: first, to confirm that HHcys was a risk factor for As-induced skin lesions; second, to identify genetic determinants of serum Hcys concentrations in this population; and third, to explore the causal nature of the association between HHcys and As-induced skin lesion incidence. We focused on the nonsynonymous MTHFR variants 677 C→T and 1298 A→C, which are known to influence Hcys concentrations in other populations. First, we confirmed our group's previous finding (Pilsner et al. 2009) that serum HHcys was a risk factor for incident As-induced skin lesions. Next, we found that MTHFR 677 C→T was strongly associated with serum Hcys among both skin lesion cases and matched controls, and analysis of MTHFR diplotypes constructed from 677 C→T, 1298 A→C, and Intron 10 A→G found that the Intron 10 G→A variant had a modest association with Hcys concentrations independent of 677 C→T. MTHFR diplotypes explained approximately 20% of the variance in serum Hcys among controls, but only explained 9% of the variance in serum Hcys among skin lesion cases. Despite the strong associations between MTHFR variants and serum Hcys, these gene variants were not significantly associated with skin lesion risk. An exploratory GWAS of serum Hcys in a sample comprised predominately of skin lesion cases identified novel genetic loci associated with serum Hcys, which may provide information about the source of HHcys among individuals with As-induced skin lesions.

Homocysteine—measured in serum samples from the baseline cohort, which were drawn prior to disease onset—was associated with a dose-dependent increase in risk for As-induced skin lesions. Based on this observation, we could surmise that (1) extracellular Hcys is causally

related to skin lesion incidence and/or (2) extracellular Hcys is correlated with endogenous or exogenous causal risk factor(s). However, we did not find that the MTHFR SNPs and haplotypes that were associated with serum Hcys were associated with skin lesion incidence. Since MTHFR is causally related to Hcys, and MTHFR diplotypes explained a substantial proportion of the variance in serum Hcys in our population, we would expect to observe an association between MTHFR gene variants and skin lesion incidence if the serum Hcys association with skin lesions were indeed causal. However, it is important to distinguish what the MTHFR finding does—and does not—imply about the causal nature of the HHcys-skin lesions association.

First, many of the proposed mechanisms of HHcys-induced carcinogenesis involve intracellular Hcys, and serum Hcys might not perfectly reflect intracellular Hcys, particularly in relation to folate. A small randomized controlled trial (RCT) of 50 subjects randomized to 500 µg daily folic acid vs. placebo found only a moderate correlation between plasma Hcys and intracellular Hcys (measured in peripheral blood mononuclear cells [PBMCs]) at baseline (r = 0.35, P = 0.01), and folic acid supplementation significantly reduced plasma Hcys but had no effect on intracellular Hcys concentrations (Smith et al. 2013). The authors speculated that folate increases intracellular Hcys remethylation, resulting in reduced Hcys transport to the plasma, but homeostatic mechanisms keep intracellular Hcys concentrations within a tight range over a wide range of folate concentrations (Smith et al. 2013). If *intracellular* Hcys is casually related to skin lesions, serum Hcys and skin lesion incidence would be associated, but since the folate-related component of serum Hcys would not be associated with intracellular Hcys, we would not see an association between MTHFR variants and skin lesions. Thus, the findings from the

current study can only provide evidence that increased extracellular Hcys directly related to MTHFR variants is not associated with skin lesion risk.

Second, although MTHFR SNPs are often used as proxies for HHcys in Mendelian randomization studies, MTHFR is involved in numerous biologic processes that could also influence As-induced skin lesion development. For example, 5:10-methylenetetrahydrofolate (5:10 methylene-THF), the substrate used by MTHFR for 5mTHF synthesis, is involved in the *de novo* production of thymidines, and it has been hypothesized that 677 C→T variants, while having negative impacts on methylation capacity, might also have protective health effects by increasing DNA repair capacity and minimizing uracil-induced DNA double strand breaks (DSBs) (Blount et al. 1997; Kennedy et al. 2012). Given that a recent study found that As^{III} was a direct inducer of DSBs in *Saccharomyces cerevisiae* (Litwin et al. 2013), it is plausible that the different 677 C→T genotypes might each have protective and deleterious effects on As-induced skin lesion risk. At the very least, MTHFR SNPs are not likely to be appropriate proxies for HHcys in the study of As-induced skin lesion pathogenesis.

Although we did not find that MTHFR variants were associated with risk of skin lesions, we observed significant associations of MTHFR variants with increased serum Hcys and decreased As methylation (increased urinary %MMA and decreased urinary %DMA), indicating that MTHFR variants, particularly 677 C→T, explain a substantial proportion of the inter-individual variation in these As toxicity markers. A previous RCT of folic acid supplementation in folate-deficient Bangladeshis found that 400 μg folic acid significantly enhanced As methylation, decreased blood As, and decreased plasma Hcys compared to placebo, although the treatment response varied widely among individuals in the folic acid group (Gamble et al. 2006; Gamble et al. 2007). The results from the current study suggest that the subset of Bangladeshis

with 677 CT or TT genotypes might not be as responsive to folic acid treatment as CC genotypes; for these individuals, additional supplementation with 5mTHF might enhance As methylation capacity and reduce serum Hcys.

Since the subset of GENI participants with GWAS data was predominantly comprised of skin lesion cases, the results of the GWAS of serum Hcys might provide insight into the source of HHcys among individuals who are predisposed to As toxicity. The exploratory GWAS of serum Hcys identified a SNP in the NR1I2 gene, rs6438549, which was associated with serum Hcys at genome-wide significance. In humans, the NR1I2 gene encodes the pregnane X receptor (PXR), a nuclear receptor (as a heterodimer with retinoid X receptor [RXR]) involved in CYP3A4-mediated xenobiotic detoxification (Luo et al. 2002). PXR regulates the expression of Phase II enzymes (including glutathione *S*-transferases) and drug transporters (including multidrug resistance proteins [MRPs]) (Kakizaki et al. 2008), which are both involved in As detoxification and transport (Leslie et al. 2004; Liu et al. 2001). Upregulation of PXR expression is found in a variety of human cancers (Qiao et al. 2013), and As^{III} exposure induces PXR expression in mouse models (Medina-Diaz et al. 2009). Although there are not obvious biologic mechanisms linking PXR and serum Hcys, *N*-3 polyunsatured fatty acids (PUFAs) upregulate the expression of Hcys-metabolizing enzymes, including MTHFR, in a mechanism that might involve the binding of PXR to fatty acid-responsive elements in the promoters of MTHFR and other genes (Huang et al. 2012).

Among the top 1,000 GWAS hits, we did not identify any SNPs in genes involved in Hcys-related metabolic pathways. Instead, the top hits were in genes involved in a range of biological processes, including epithelial cell polarity establishment (FRMD4A, PRICKLE2), cell adhesion (NLGN1, CD44, PTPRT), and the Wnt signaling pathway (CD44, TNIK). We

identified multiple genes that are associated with human squamous cell carcinomas: CD44 is a marker of tumor initiation in head and neck squamous cell carcinomas (HNSCCs) (Prince et al. 2007), and FRMD4A expression is upregulated in primary HNSCCs (Goldie et al. 2012). Interestingly, a recent study of cultured human keratinocytes found that chronic exposure to environmentally-relevant concentrations of sodium arsenite (0.05 ppm) induced malignant transformation through NF-κB-mediated CD44 upregulation, suggesting that CD44 might be a molecular marker of As-induced neoplastic transformation in skin lesions (Huang et al. 2013). Possibly, the elevated serum Hcys that we observed among individuals who went on to develop skin lesions did not play a causal role in skin lesion pathogenesis, but instead reflected increased susceptibility to As-induced dysregulation of epithelial cell adhesion and polarity.

This study had several limitations. First, we did not have As metabolite measures (InAs, MMA, and DMA) for all of our participants, and we were thus unable to fully examine the relationships among the As metabolites, Hcys, and one-carbon metabolism gene variants. We plan to incorporate this data into the analysis once the As metabolite measures becomes available for our entire study sample. Second, we did not have biologic samples (serum and/or DNA) for a small proportion of the cases and controls, which could bias our results. Third, we did not have serum and/or plasma samples that had not undergone a freeze-thaw cycle, and thus, we were unable to measure plasma folate to assess folate nutritional status. Fourth, we did not replicate the results of the GWAS of serum Hcys to verify our findings. However, we plan to measure the top SNP hits in the entire GENI study sample to verify the associations of these SNPs with serum Hcys concentrations and additionally, to examine whether these SNPs are associated with skin lesion incidence.

In conclusion, we observed that serum Hcys was a risk factor for As-induced skin lesions, in accordance with previous findings from our group (Pilsner et al. 2009), and that gene variants in MTHFR were associated with elevated serum Hcys concentrations in skin lesion cases and controls. However, these MTHFR variants were not associated with skin lesion risk. A GWAS of serum Hcys in a subset of GENI subjects identified mulitple genes involved in xenobiotic detoxification and epithelial cell polarity and adhesion, providing new information regarding the role of HHcys as a biomarker of As-induced skin lesions.

ACKNOWLEDGEMENTS

This work was supported by grants RO1 CA133595, RO1 ES017875, P42 ES10349, P30 ES009089, and T32 CA009529-24 from the National Institutes of Health. The content is solely the responsibility of the authors and does not necessarily represent the official views of the National Institute of Environmental Health Sciences, the National Cancer Institute, or the National Institutes of Health.

REFERENCES

Ahsan H, Chen Y, Parvez F, Argos M, Hussain AI, Momotaj H, et al. 2006. Health effects of arsenic longitudinal study (heals): Description of a multidisciplinary epidemiologic investigation. J Expo Sci Environ Epidemiol 16:191-205.

Banno M, Hanada H, Kamide K, Kokubo Y, Kada A, Yang J, et al. 2007. Association of genetic polymorphisms of endothelin-converting enzyme-1 gene with hypertension in a japanese population and rare missense mutation in preproendothelin-1 in japanese hypertensives. Hypertension research : official journal of the Japanese Society of Hypertension 30:513-520.

Barrett JC, Fry B, Maller J, Daly MJ. 2005. Haploview: Analysis and visualization of ld and haplotype maps. Bioinformatics (Oxford, England) 21:263-265.

Blount BC, Mack MM, Wehr CM, MacGregor JT, Hiatt RA, Wang G, et al. 1997. Folate deficiency causes uracil misincorporation into human DNA and chromosome breakage: Implications for cancer and neuronal damage. Proc Natl Acad Sci U S A 94:3290-3295.

Bochud M, Chiolero A, Elston RC, Paccaud F. 2008. A cautionary note on the use of mendelian randomization to infer causation in observational epidemiology. Int J Epidemiol 37:414-416; author reply 416-417.

Brattström L, Wilcken DE. 2000. Homocysteine and cardiovascular disease: Cause or effect? The American Journal of Clinical Nutrition 72:315-323.

Castro R, Rivera I, Ravasco P, Jakobs C, Blom HJ, Camilo ME, et al. 2003. 5,10-methylenetetrahydrofolate reductase 677c-->t and 1298a-->c mutations are genetic determinants of elevated homocysteine. QJM : monthly journal of the Association of Physicians 96:297-303.

Chandalia M, Abate N, Cabo-Chan AV, Devaraj S, Jialal I, Grundy SM. 2003. Hyperhomocysteinemia in asian indians living in the united states. Journal of Clinical Endocrinology & Metabolism 88:1089-1095.

Chango A, Boisson F, Barbe F, Quilliot D, Droesch S, Pfister M, et al. 2000. The effect of 677c-->t and 1298a-->c mutations on plasma homocysteine and 5,10-methylenetetrahydrofolate reductase activity in healthy subjects. The British journal of nutrition 83:593-596.

Chattopadhyay I, Singh A, Phukan R, Purkayastha J, Kataki A, Mahanta J, et al. 2010. Genome-wide analysis of chromosomal alterations in patients with esophageal squamous cell carcinoma exposed to tobacco and betel quid from high-risk area in india. Mutat Res 696:130-138.

Clarke R, Bennett DA, Parish S, Verhoef P, Dötsch-Klerk M, Lathrop M, et al. 2012. Homocysteine and coronary heart disease: Meta-analysis of *mthfr* case-control studies, avoiding publication bias. PLoS Med 9:e1001177.

Dayal S, Arning E, Bottiglieri T, Boger RH, Sigmund CD, Faraci FM, et al. 2004. Cerebral vascular dysfunction mediated by superoxide in hyperhomocysteinemic mice. Stroke; a journal of cerebral circulation 35:1957-1962.

Diaz-Arrastia R. 2000. Homocysteine and neurologic disease. Archives of neurology 57:1422-1427.

Eberhardt RT, Forgione MA, Cap A, Leopold JA, Rudd MA, Trolliet M, et al. 2000. Endothelial dysfunction in a murine model of mild hyperhomocyst(e)inemia. J Clin Invest 106:483-491.

Funalot B, Ouimet T, Claperon A, Fallet C, Delacourte A, Epelbaum J, et al. 2004. Endothelin-converting enzyme-1 is expressed in human cerebral cortex and protects against alzheimer's disease. Molecular psychiatry 9:1122-1128, 1059.

Gamble MV, Ahsan H, Liu X, Factor-Litvak P, Ilievski V, Slavkovich V, et al. 2005. Folate and cobalamin deficiencies and hyperhomocysteinemia in bangladesh. Am J Clin Nutr 81:1372-1377.

Gamble MV, Liu X, Ahsan H, Pilsner JR, Ilievski V, Slavkovich V, et al. 2006. Folate and arsenic metabolism: A double-blind, placebo-controlled folic acid-supplementation trial in bangladesh. Am J Clin Nutr 84:1093-1101.

Gamble MV, Liu X, Slavkovich V, Pilsner JR, Ilievski V, Factor-Litvak P, et al. 2007. Folic acid supplementation lowers blood arsenic. Am J Clin Nutr 86:1202-1209.

Glessner JT, Wang K, Cai G, Korvatska O, Kim CE, Wood S, et al. 2009. Autism genome-wide copy number variation reveals ubiquitin and neuronal genes. Nature 459:569-573.

Goldie SJ, Mulder KW, Tan DW, Lyons SK, Sims AH, Watt FM. 2012. Frmd4a upregulation in human squamous cell carcinoma promotes tumor growth and metastasis and is associated with poor prognosis. Cancer Res 72:3424-3436.

Group SC. 2010. Effects of homocysteine-lowering with folic acid plus vitamin b12 vs placebo on mortality and major morbidity in myocardial infarction survivors: A randomized trial. JAMA 303:2486-2494.

Huang S, Guo S, Guo F, Yang Q, Xiao X, Murata M, et al. 2013. Cd44v6 expression in human skin keratinocytes as a possible mechanism for carcinogenesis associated with chronic arsenic exposure. Eur J Histochem 57:e1.

Huang T, Wahlqvist ML, Li D. 2012. Effect of n-3 polyunsaturated fatty acid on gene expression of the critical enzymes involved in homocysteine metabolism. Nutrition journal 11:6.

Jacques PF, Bostom AG, Williams RR, Ellison RC, Eckfeldt JH, Rosenberg IH, et al. 1996. Relation between folate status, a common mutation in methylenetetrahydrofolate reductase, and plasma homocysteine concentrations. Circulation 93:7-9.

Kakizaki S, Yamazaki Y, Takizawa D, Negishi M. 2008. New insights on the xenobiotic-sensing nuclear receptors in liver diseases--car and pxr. Current drug metabolism 9:614-621.

Kennedy DA, Stern SJ, Matok I, Moretti ME, Sarkar M, Adams-Webber T, et al. 2012. Folate intake, mthfr polymorphisms, and the risk of colorectal cancer: A systematic review and meta-analysis. Journal of cancer epidemiology 2012:952508.

Lambert JC, Grenier-Boley B, Harold D, Zelenika D, Chouraki V, Kamatani Y, et al. 2013. Genome-wide haplotype association study identifies the frmd4a gene as a risk locus for alzheimer's disease. Molecular psychiatry 18:461-470.

Leslie EM, Haimeur A, Waalkes MP. 2004. Arsenic transport by the human multidrug resistance protein 1 (mrp1/abcc1): Evidence that a tri-glutathione conjugate is required. Journal of Biological Chemistry 279:32700-32708.

Lewis CM, Ng MY, Butler AW, Cohen-Woods S, Uher R, Pirlo K, et al. 2010. Genome-wide association study of major recurrent depression in the u.K. Population. The American journal of psychiatry 167:949-957.

Lin S, Shi Q, Nix FB, Styblo M, Beck MA, Herbin-Davis KM, et al. 2002. A novel s-adenosyl-l-methionine:Arsenic(iii) methyltransferase from rat liver cytosol. J Biol Chem 277:10795-10803.

Litwin I, Bocer T, Dziadkowiec D, Wysocki R. 2013. Oxidative stress and replication-independent DNA breakage induced by arsenic in <italic>saccharomyces cerevisiae</italic>. PLoS Genet 9:e1003640.

Liu J, Chen H, Miller DS, Saavedra JE, Keefer LK, Johnson DR, et al. 2001. Overexpression of glutathione s-transferase ii and multidrug resistance transport proteins is associated with acquired tolerance to inorganic arsenic. Molecular pharmacology 60:302-309.

Lonn E, Yusuf S, Arnold MJ, Sheridan P, Pogue J, Micks M, et al. 2006. Homocysteine lowering with folic acid and b vitamins in vascular disease. N Engl J Med 354:1567-1577.

Luo G, Cunningham M, Kim S, Burn T, Lin J, Sinz M, et al. 2002. Cyp3a4 induction by drugs: Correlation between a pregnane x receptor reporter gene assay and cyp3a4 expression in human hepatocytes. Drug metabolism and disposition: the biological fate of chemicals 30:795-804.

Malarstig A, Buil A, Souto JC, Clarke R, Blanco-Vaca F, Fontcuberta J, et al. 2009. Identification of znf366 and ptprd as novel determinants of plasma homocysteine in a family-based genome-wide association study. Blood 114:1417-1422.

Medina-Diaz IM, Estrada-Muniz E, Reyes-Hernandez OD, Ramirez P, Vega L, Elizondo G. 2009. Arsenite and its metabolites, mma(iii) and dma(iii), modify cyp3a4, pxr and rxr alpha expression in the small intestine of cyp3a4 transgenic mice. Toxicol Appl Pharmacol 239:162-168.

Okada Y, Kamatani Y, Takahashi A, Matsuda K, Hosono N, Ohmiya H, et al. 2010. Common variations in psmd3-csf3 and plcb4 are associated with neutrophil count. Human molecular genetics 19:2079-2085.

Pilsner JR, Liu X, Ahsan H, Ilievski V, Slavkovich V, Levy D, et al. 2009. Folate deficiency, hyperhomocysteinemia, low urinary creatinine, and hypomethylation of leukocyte DNA are risk factors for arsenic-induced skin lesions. Environ Health Perspect 117:254-260.

Prince ME, Sivanandan R, Kaczorowski A, Wolf GT, Kaplan MJ, Dalerba P, et al. 2007. Identification of a subpopulation of cells with cancer stem cell properties in head and neck squamous cell carcinoma. Proc Natl Acad Sci U S A 104:973-978.

Qiao E, Ji M, Wu J, Ma R, Zhang X, He Y, et al. 2013. Expression of the pxr gene in various types of cancer and drug resistance. Oncology letters 5:1093-1100.

Ramsahoye BH, Biniszkiewicz D, Lyko F, Clark V, Bird AP, Jaenisch R. 2000. Non-cpg methylation is prevalent in embryonic stem cells and may be mediated by DNA methyltransferase 3a. Proceedings of the National Academy of Sciences 97:5237-5242.

Refsum H, Ueland PM, Nygard O, Vollset SE. 1998. Homocysteine and cardiovascular disease. Annual review of medicine 49:31-62.

Scott JM, Weir DG. 1998. Folic acid, homocysteine and one-carbon metabolism: A review of the essential biochemistry. Journal of cardiovascular risk 5:223-227.

Senaratne MP, MacDonald K, De Silva D. 2001. Possible ethnic differences in plasma homocysteine levels associated with coronary artery disease between south asian and east asian immigrants. Clinical cardiology 24:730-734.

Smith DE, Hornstra JM, Kok RM, Blom HJ, Smulders YM. 2013. Folic acid supplementation does not reduce intracellular homocysteine, and may disturb intracellular one-carbon metabolism. Clinical chemistry and laboratory medicine : CCLM / FESCC 51:1643-1650.

Stephens M, Smith NJ, Donnelly P. 2001. A new statistical method for haplotype reconstruction from population data. American journal of human genetics 68:978-989.

Stephens M, Scheet P. 2005. Accounting for decay of linkage disequilibrium in haplotype inference and missing-data imputation. American journal of human genetics 76:449-462.

Tanaka T, Scheet P, Giusti B, Bandinelli S, Piras MG, Usala G, et al. 2009. Genome-wide association study of vitamin b6, vitamin b12, folate, and homocysteine blood concentrations. American journal of human genetics 84:477-482.

Wald DS, Law M, Morris JK. 2002. Homocysteine and cardiovascular disease: Evidence on causality from a meta-analysis. BMJ 325:1202.

Wald DS, Bestwick JP, Wald NJ. 2012. Homocysteine as a cause of ischemic heart disease: The door remains open. Clinical Chemistry 58:1488-1490.

Wang Y, Liu Y, Peng W, Wang M, Sun J, Zhang Z, et al. 2012. Ece1 polymorphisms may contribute to the susceptibility of sporadic congenital heart disease in a chinese population. DNA and cell biology 31:1425-1430.

Wu LL, Wu JT. 2002. Hyperhomocysteinemia is a risk factor for cancer and a new potential tumor marker. Clin Chim Acta 322:21-28.

Yoon D, Kim YJ, Cui WY, Van der Vaart A, Cho YS, Lee JY, et al. 2012. Large-scale genome-wide association study of asian population reveals genetic factors in frmd4a and other loci influencing smoking initiation and nicotine dependence. Human genetics 131:1009-1021.

Zhou X, Stephens M. 2012. Genome-wide efficient mixed-model analysis for association studies. Nat Genet 44:821-824.

Zhou X, Stephens M. 2013. Efficient algorithms for multivariate linear mixed models in genome-wide association studies. Arxiv:1305.4366.

Appendix

Table E1. List of SNPs on OpenArray platform.

SNP assays with call rates < 90% (N=11)		
Symbol(s)	**Gene Name(s)**	**RS#**
AS3MT	arsenic (+3 oxidation state) methyltransferase	rs3740400
AS3MT	arsenic (+3 oxidation state) methyltransferase	rs11191439
AS3MT	arsenic (+3 oxidation state) methyltransferase	rs11191453
FOLR1	folate receptor 1 (adult)	rs1801932
FOLR1	folate receptor 1 (adult)	rs9282688
FOLR3	folate receptor 3 (gamma)	rs2229185
SLC19A1	solute carrier family 19 (folate transporter), member 1	rs12659
SLC19A1	solute carrier family 19 (folate transporter), member 1	rs1051266
SLC19A1	solute carrier family 19 (folate transporter), member 1	rs56822323
SLC19A1	solute carrier family 19 (folate transporter), member 1	rs79091853
SLC19A1	solute carrier family 19 (folate transporter), member 1	rs113642554
SNP assays with MAF < 0.01 (N=21)		
Symbol(s)	**Gene Name(s)**	**RS#**
AS3MT	arsenic (+3 oxidation state) methyltransferase	rs34556438
AS3MT	arsenic (+3 oxidation state) methyltransferase	rs35232887
CBS	cystathionine-β-synthase	rs34040148
FOLR1	folate receptor 1 (adult)	rs112062510
FOLR1	folate receptor 1 (adult)	rs121918405
FOLR1	folate receptor 1 (adult)	rs121918406
FOLR1	folate receptor 1 (adult)	rs35179028
FOLR1	folate receptor 1 (adult)	rs61735636
FOLR1	folate receptor 1 (adult)	rs76191655
FOLR1	folate receptor 1 (adult)	rs77405781

FOLR1	folate receptor 1 (adult)	rs77771906
FOLR1	folate receptor 1 (adult)	rs7928649
FOLR2	folate receptor 2 (fetal)	rs13908
FOLR3	folate receptor 3 (gamma)	rs34970007
FOLR3	folate receptor 3 (gamma)	rs61746271
FOLR3	folate receptor 3 (gamma)	rs7925545
FOLR3	folate receptor 3 (gamma)	rs7926875
FOLR3	folate receptor 3 (gamma)	rs7926987
MTHFD1	methylenetetrahydrofolate dehydrogenase (NADP+ dependent) 1	rs1803951
SLC19A1	solute carrier family 19 (folate transporter), member 1	rs35786590
--	--	rs117782026
SNP assays included in current study (N=32)		
Symbol(s)	**Gene Name(s)**	**RS#**
AS3MT	arsenic (+3 oxidation state) methyltransferase	rs10748835
AS3MT	arsenic (+3 oxidation state) methyltransferase	rs12416687
AS3MT	arsenic (+3 oxidation state) methyltransferase	rs3740393
AS3MT	arsenic (+3 oxidation state) methyltransferase	rs7085104
BHMT	betaine-homocysteine S-methyltransferase	rs3733890
FOLR1	folate receptor 1 (adult)	rs1540087
FOLR1	folate receptor 1 (adult)	rs2071010
FOLR1	folate receptor 1 (adult)	rs7109250
FOLR2	folate receptor 2 (fetal)	rs2298444
FOLR2	folate receptor 2 (fetal)	rs514933
FOLR2	folate receptor 2 (fetal)	rs651646
FOLR2	folate receptor 1 (adult)	rs651933
FOLR3	folate receptor 3 (gamma)	rs1802608
FOLR3	folate receptor 3 (gamma)	rs61734430
MTHFD1	methylenetetrahydrofolate dehydrogenase (NADP+ dependent) 1 CHR14	rs11627387

MTHFD1	methylenetetrahydrofolate dehydrogenase (NADP+ dependent) 1	rs1950902
MTHFD1	methylenetetrahydrofolate dehydrogenase (NADP+ dependent) 1	rs2236224
MTHFD1	methylenetetrahydrofolate dehydrogenase (NADP+ dependent) 1	rs2236225
MTHFR	methylenetetrahydrofolate reductase (NAD(P)H)	rs1476413
MTHFR	methylenetetrahydrofolate reductase (NAD(P)H)	rs1801131
MTHFR	methylenetetrahydrofolate reductase (NAD(P)H)	rs1801133
MTR	5-methyltetrahydrofolate-homocysteine methyltransferase	rs1805087
MTRR	5-methyltetrahydrofolate-homocysteine methyltransferase reductase	rs1801394
SHMT1	serine hydroxymethyltransferase 1 (soluble)	rs1979277
SLC19A1	solute carrier family 19 (folate transporter), member 1	rs1888530
SLC19A1	solute carrier family 19 (folate transporter), member 1	rs3788200
SLC46A1	solute carrier family 46 (folate transporter), member 1	rs1128162
TCN2	transcobalamin II	rs1801198
TYMS	thymidylate synthetase	rs1001761
TYMS	thymidylate synthetase	rs2847149
TYMS	thymidylate synthetase	rs502396
TYMS	thymidylate synthetase	rs596909

Table E2. Skin lesion types among N=876 incident skin lesion cases.

Skin lesion type	N	% of total cases	% of subgroup
Lesion types among all cases			
Melanosis	655	74.8	--
Leukomelanosis	358	40.9	--
Keratosis	199	22.7	
Cases with 1 lesion type			
Melanosis only	392	44.7	67.0
Leukomelanosis only	193	22.0	33.0
Keratosis only	0	0.0	0.0
Total cases with 1 lesion type	585	66.9	100.0
Cases with 2 lesion types			
Melanosis + keratosis	126	14.4	51.2
Melanosis + leukomelanosis	92	10.5	37.4
Leukomelanosis + keratosis	28	3.2	11.4
Total cases with 2 lesion types	246	28.1	100.0
Cases with 3 lesion types			
Total cases with 3 lesion types	45	5.1	--

Table E3. Regression coefficients for MTHFR genotypes predicting log-transformed serum Hcys.

SNP	Model		Controls B (95% CI)	Cases B (95% CI)
677 C→T	Unadjusted	CC	*Ref.*	*Ref.*
		CT	0.23 (0.14 to 0.31)***	0.26 (0.18 to 0.35)***
		TT	1.28 (1.02 to 1.54)***	0.61 (0.33 to 0.88)***
		P	<0.0001	<0.0001
		R^2 (%)	15.8	7.4
1298 A→C	Unadjusted	AA	*Ref.*	*Ref.*
		AC	-0.09 (-0.17 to -0.01)*	-0.06 (-0.14 to 0.02)
		CC	-0.10 (-0.22 to 0.01)	-0.14 (-0.24 to -0.03)*
		P	0.06	0.04
		R^2 (%)	0.9	1.0
	Conditioned on 677 C→T	AA	*Ref.*	*Ref.*
		AC	-0.02 (-0.10 to 0.05)	-0.01 (-0.08 to 0.07)
		CC	0.01 (-0.10 to 0.12)	-0.05 (-0.16 to 0.05)
		P	0.77	0.59
		R^2 (%)	16.0	7.7
Intron 10 C→T	Unadjusted	CC	*Ref.*	*Ref.*
		CT	-0.03 (-0.11 to 0.06)	-0.04 (-0.12 to 0.04)
		TT	-0.03 (-0.14 to 0.07)	-0.09 (-0.19 to 0.01)
		P	0.76	0.21
		R^2 (%)	0.0	0.0
	Conditioned on 677 C→T	CC	*Ref.*	*Ref.*
		CT	0.05 (-0.03 to 0.13)	0.02 (-0.06 to 0.09)
		TT	0.10 (0.00 to 0.20)	0.02 (-0.08 to 0.12)
		P	0.15	0.91
		R^2 (%)	16.2	7.4

*$P < 0.05$; ** $P < 0.01$; *** $P < 0.0001$

Table E4. MTHFR diplotype counts and frequencies.

677 CT/ 1298 AC/ Int. 10 GA Diplotype			N overall/ N with serum	N (%) cases	N (%) controls
677-1298 CA/CA					
	CAG	CAG	259/249	126 (18.0)	133 (21.0)
	CAG	CAA	86/82	49 (7.0)	37 (5.9)
	CAA	CAA	7/7	5 (0.7)	2 (0.3)
		Total	352/338	180 (25.7)	172 (27.2)
677-1298 CA/CC					
	CAG	CCG	33/30	21 (3.0)	12 (1.9)
	CAG	CCA	374/354	196 (28.0)	178 (28.2)
	CAA	CCA	75/72	41 (5.8)	34 (5.4)
		Total	482/456	258 (36.8)	224 (35.4)
677-1298 CC/CC					
	CCA	CCG	23/22	13 (1.9)	10 (1.6)
	CCA	CCA	180/168	97 (13.8)	83 (13.1)
		Total	203/190	110 (15.7)	93 (14.7)
677-1298 CA/TA					
	CAG	TAG	129/120	70 (10.0)	59 (9.3)
	CAA	TAG	23/22	14 (2.0)	9 (1.4)
		Total	152/142	84 (12.0)	68 (10.8)
677-1298 CC/TA					
	CCG	TAG	7/5	5 (0.7)	2 (0.3)
	CCA	TAG	108/101	48 (6.8)	60 (9.5)
		Total	115/106	53 (7.6)	62 (9.8)
677-1298 TA/TA					
	TAG	TAG	22/18	10 (1.4)	12 (1.9)
	TAA	TAG	1/1	1 (0.1)	0 (0.0)
		Total	23/19	11 (1.6)	12 (1.9)
677-1298 CC/TC or TC/TC					
	CCG	TCG	1/1	0 (0.0)	1 (0.2)
	CCA	TCG	3/3	3 (0.4)	0 (0.0)
	CCA	TCA	1/1	1 (0.1)	0 (0.0)
	TCA	TCA	1/1	1 (0.1)	0 (0.0)
		Total	6/6	5 (0.7)	1 (0.2)

Table E5. Least squares mean (± SE) urinary %InAs, %MMA, and %DMA by MTHFR 677 C→T genotype in cases, adjusted for age, total urinary arsenic, and urinary creatinine.

		Cases[a]		Controls[b]	
		Urinary %MMA	**Urinary %DMA**	**Urinary %MMA**	**Urinary %DMA**
677 C→T	CC	13.9 ± 0.2	71.4 ± 0.4	14.2 ± 0.4	72.2 ± 0.6
	CT	14.8 ± 0.5	69.9 ± 0.7†	15.4 ± 0.7	69.3 ± 1.0*
	TT	16.5 ± 1.6	67.5 ± 2.5	17.3 ± 2.2	61.0 ± 3.3*
	P	0.09	0.07	0.16	0.0006
	CC	13.9 ± 0.2	71.4 ± 0.4	14.2 ± 0.4	72.2 ± 0.6
	CT+TT	14.9 ± 0.4*	69.7 ± 0.7*	15.6 ± 0.7	68.6 ± 1.0*
	P	0.05	0.04	0.08	0.002

a. Cases: CC, N=514; CT, N=132; TT, N=11; b. Controls: CC, N=148; CT, N=50; TT, N=5; † $P < 0.10$; * $P < 0.05$ compared to wildtype

Table E6. Description of genes identified in GWAS of serum Hcys.

Symbol	Gene Name	Process	Function	Known associations of genes with Hcys or related conditions
NR1I2	nuclear receptor subfamily 1, group I, member 2	drug, metal, protein, zinc ion, sequence-specific DNA binding; steroid hormone receptor activity; transcription coactivator activity	encodes Pregnane X Receptor (PXR); exogenous drug catabolic process; steroid metabolic process; xenobiotic metabolic process and transport	
NLGN1	Neuroligin 1	calcium-dependent cell-cell adhesion; positive regulation of intracellular protein kinase cascade	cell adhesion molecule binding; receptor activity	Identified in GWAS of autism (Glessner et al. 2009), recurrent depression (Lewis et al. 2010)
FRMD4A	FERM domain containing 4A	establishment of epithelial cell polarity	protein binding, bridging	Identified in GWAS of Alzheimer's (Lambert et al. 2013), nicotine dependence (Yoon et al. 2012) Upregulation of FRMD4A in squamous cell carcinoma (Goldie et al. 2012)
PLCB4	phospholipase C, beta 4	intracellular signal transduction; negative regulation of potassium ion transport; lipid catabolic process	signal transducer activity; mitogen-activated protein kinase binding; calcium ion binding; phospholipase C activity; phosphoinositide phospholipase C activity	Identified in GWAS of neutrophil count (Okada et al. 2010)
ECE1	endothelin converting	apoptotic process; hormone catabolic process; peptide	endopeptidase activity; metalloendopeptidase	Gene variants associated with CHD (Wang et al. 2012), hypertension (Banno et al.

	enzyme 1	hormone processing; regulation of systemic arterial blood pressure by endothelin	activity; protein homodimerization activity; metal ion, peptide hormone binding	2007), Alzheimer's (Funalot et al. 2004)
CD44	CD44 molecule (Indian blood group)	Wnt receptor signaling pathway; cell-cell, cell-matrix adhesion; monocyte aggregation	collagen, hyaluronic acid, protein binding; transmembrane signaling receptor activity	Associated with esophageal squamous cell carcinoma in Indians exposed to tobacco and betel (Chattopadhyay et al. 2010) Biomarker of arsenic-induced neoplastic transformation in human keratinocytes (Huang et al. 2013)
PRICKLE2	prickle homolog 2	establishment or maintenance of epithelial cell apical/basal polarity; neuron projection development	metal and zinc ion binding: zinc-finger transcription factor	Identified in GWAS of folate (Tanaka et al. 2009)
PTPRT	Receptor-type tyrosine-protein phosphatase T	cell adhesion; protein dephosphorylation; transmembrane receptor protein tyrosine kinase signaling pathway	actinin, catenin, cadherin, protein binding; protein tyrosine phosphatase activity	PTPRD (PTP family) identified in GWAS of plasma Hcys (Malarstig et al. 2009) Interacts with cadherin 2 (CDH2): SNP in CDH2, rs1108325, was 78^{th} top hit, $P = 2.4 \times 10^{-5}$; SNP in another cadherin gene, CDH1, (rs347694), was 36^{th} top hit, $P = 1.0 \times 10^{-5}$
TNIK	TRAF2 and NCK interacting kinase	Wnt receptor signaling pathway; activation of JNKK activity; cytoskeleton organization; intracellular protein kinase cascade; protein phosphorylation; response to stress	ATP, protein binding; protein serine/threonine kinase activity; small GTPase regulator activity	

Chapter 8: Conclusions and future directions

Summary of major findings

The five epidemiologic studies contained in this dissertation were designed to address the overarching hypothesis that one-carbon metabolism and the transsulfuration pathway interact to influence susceptibility to As toxicity in humans. We addressed this overall hypothesis by testing three working hypotheses, as outlined below:

Hypothesis 1:

We hypothesize that chronic As exposure is associated with alterations of global DNA methylation and hydroxymethylation.

Principle findings from Specific Aim 1:

In **Chapter 3,** we observed that chronic As exposure was associated with increased global methylation of peripheral blood mononuclear cell (PBMC) DNA, as measured by [^{3}H]-methyl incorporation, in support of previous epidemiologic findings (Lambrou et al. 2012; Majumdar et al. 2010; Pilsner et al. 2007, 2009). Additionally, our findings suggest that this positive association is linear over a wide range of environmentally-relevant As doses. In **Chapter 4**, we found that the association between As exposure and global percent 5-hydroxymethylcytosine (%hmC) of blood cell DNA was modified by gender, with a positive association in males and negative association in females. The mechanism underlying this gender-specific observation is unclear. We also found that age was negatively associated with global %hmC. To our knowledge, this is the first study to examine global DNA hydroxymethylation in an epidemiologic study in a non-diseased population, and the first to report an association between As exposure and 5hmC in any study. There are multiple

mechanisms through which As exposure might influence 5hmC—aberrant Krebs cycle regulation via inhibition of pyruvate dehydrogenase (PDH), disruption of base excision repair (BER) pathways, and so forth—which should be explored experimentally.

Hypothesis 2:

We hypothesize that an oxidized intracellular GSH redox state is associated with a reduced capacity to methylate DNA and As.

Principle findings from Specific Aim 2:

In **Chapter 5**, consistent with our hypothesis, we observed that an oxidized plasma GSH redox state was associated with decreased As methylation capacity and increased blood As concentrations, but only among folate-deficient individuals. We speculated that this association might be explained by *S*-glutathionylation of critical redox-sensitive cysteine (Cys) residues within the arsenic(III)-methyltransferase (AS3MT) active site (Fomenko et al. 2007) and that *S*-glutathionylation might be a regulatory mechanism to prevent consumption of methyl groups during conditions of folate deficiency, when methyl groups are limiting. Alternatively, our observations might simply indicate that under folate-sufficient conditions, AS3MT kinetics are not measurably influenced by the reducing environment. Given this uncertainty, to avoid any "unintended consequences," we would not advise a redox-based intervention to improve As methylation capacity among the folate deficient.

Also consistent with our hypothesis, in **Chapter 6**, we found that an oxidized blood GSH redox state was associated with decreased global methylation of PBMC DNA. Since it had been postulated by others that oxidative stress might lead to DNA hypomethylation by increasing transsulfuration flux, thereby leading to *S*-adenosylmethione (SAM) depletion (Hitchler and

Domann 2007), we examined whether there was evidence that blood SAM mediated this association in our study. We observed that an oxidized blood GSH redox state was correlated with decreased plasma homocysteine (Hcys) and blood *S*-adenosylhomocysteine (SAH), providing evidence that intracellular oxidative stress increases Hcys flux through the transsulfuration pathway (Hultberg and Hultberg 2007; Rogers et al. 2007). However, we did not find evidence that blood SAM was a mediator of the association between blood GSH redox state and global DNA methylation, suggesting that this relationship is explained by another mechanism. We propose that this association might be explained by direct redox regulation of DNA methyltransferases (DNMTs) or histone deacetylases (HDACs), which should be explored in experimental models.

Moreover, these two studies highlight the importance of selecting biologically-relevant biomarkers to address mechanistic hypotheses and fully understanding the biochemistry underlying each mechanism. In both studies, we were interested in examining "intracellular" GSH redox status and SAM concentrations. However, we used plasma biomarkers of GSH redox and folate in **Chapter 5**—which are predicted by mathematical models to reflect hepatic GSH redox and hepatic SAM, respectively (Duncan et al. 2013; Reed et al. 2008)—and used whole blood biomarkers of GSH redox and SAM in **Chapter 6**, which should better reflect intracellular concentrations within PBMCs. These two analyses were dependent upon separate measurements of GSH and glutathione disulfide (GSSG), which requires careful planning and sample preparation since GSH rapidly oxidizes to GSSG upon sample collection (Winters et al. 1995). In **Chapter 5**, if we had used total plasma GSH (plasma GSH+GSSG), as is common in many epidemiological studies, we would not have observed significant associations. In addition, had we not considered in **Chapter 5** that the influence of GSH on AS3MT activity might depend

upon the availability of its methyl group substrate and thus, had not stratified by folate nutritional status, we would have concluded that plasma GSH redox was not associated with As methylation—even though the plasma GSH/GSSG ratio explained a substantial proportion of the variance in the urinary As metabolite percentages in the folate-deficient group.

Hypothesis 3:

We predict that aberrant regulation of one-carbon metabolism contributes to increased susceptibility to As-induced skin lesions. Specifically, we predict that nonsynonymous variants in one-carbon metabolism genes, specifically variants that are known to influence enzymatic activities, and elevated serum Hcys are risk factors for As-induced skin lesion incidence.

Principle findings from Specific Aim 3:

In **Chapter 7**, we confirmed our group's previous findings (Pilsner et al. 2009) that hyperhomocystenemia (HHcys) at baseline was a risk factor for As-induced skin lesion development. We found that MTHFR haplotypes explained a large proportion of the variance in serum Hcys concentrations among both cases and controls. Of the single nucleotide polymorphisms (SNPs) that we examined, the MTHFR 677 C→T variant had the strongest association with serum Hcys concentrations: mean serum Hcys concentrations in CT heterozygotes and TT homozygotes were 3.6 and 21.3 μM higher than wildtype, respectively. Across human populations, the MTHFR 677 CT genotype is not consistently associated with elevated Hcys concentrations (Wald et al. 2012), but our findings indicate that in Bangladesh, MTHFR 677 CT heterozygotes, in addition to TT homozygotes, have elevated Hcys and impaired MTHFR enzymatic activity. Over one-fifth of our study population were CT heterozygotes, and thus, the MTHFR 677 C→T variant had measurable effects on one-carbon

metabolism regulation on the population level. We predict that in the Bangladeshi population, supplementation with 5mTHF, as opposed to folic acid, might be more effective to reduce Hcys and improve methylation capacity.

However, we did not find that one-carbon metabolism gene variants were risk factors for As-induced skin lesions. Specifically, even though HHcys was a risk factor for skin lesions and MTHFR 677 C→T was strongly associated with serum Hcys, we found no association between MTHFR 677 C→T variants and skin lesion risk. Although it would be easy to conclude that HHcys does not have a causal role in As-induced skin lesion development, MTHFR could influence skin lesion risk through pathways that are independent of HHcys. Many Mendelian randomization studies use MTHFR to infer causal effects of HHcys; this approach operates under the assumption that the effects of MTFHR on disease would only occur through a HHcys intermediate, which is a gross oversimplification of the underlying biology.

To examine genetic determinants of serum Hcys concentrations in our population using an "unbiased" approach, we conducted an exploratory GWAS of serum Hcys in a subset of participants, which was predominately comprised of skin lesion cases. Interestingly, we did not identify any one-carbon metabolism genes, or other genes known to directly influence Hcys, among our top-ranked SNPs. We identified one genome-wide significant SNP in the gene encoding the pregnane X receptor (PXR), along with other SNPs in genes involved in redox signaling (PTPRT) and the establishment of epithelial cell polarity (PRICKLE2) that have been identified in other GWAS analyses (Malarstig et al. 2009; Tanaka et al. 2009).

Using GWAS to identify genetic determinants of circulating disease biomarkers might provide novel insights into mechanisms of disease pathophysiology. This approach has been used to identify candidate gene susceptibility loci in chronic obstructive pulmonary disorder

(COPD): Several genes identified in GWAS analyses of Clara cell secretory protein and surfactant protein D, two important biomarkers of COPD, were found to be associated with COPD risk (Kim et al. 2012). This approach might be particularly useful to study the biological source of HHcys as a disease biomarker. The determinants of blood Hcys concentrations are multifactorial: For example, in **Chapter 6**, we observed that an oxidized blood GSH redox state was significantly associated with decreased Hcys concentrations. We plan to measure our top GWAS hits in the full GENI study sample to examine whether these gene variants are also associated with susceptibility for As-induced skin lesions.

Future directions

Systems biology and mathematical modeling

Given the astounding level of complexity in redox regulation, it is nearly impossible to predict the effects of an "antioxidant intervention," such as *N*-acetyl-*L*-cysteine (NAC) or *L*-ascorbic acid (vitamin C) supplementation, without implementing a systems-based approach (de Graaf et al. 2009). In our studies, information from mathematical models of human one-carbon metabolism and transsulfuration pathways (Duncan et al. 2013; Reed et al. 2008) aided our selection of biologically-relevant biomarkers, and members of our group have collaborated with mathematicians at Duke University to create models of As metabolism to predict the effects of folate supplementation on As methylation and detoxification (Lawley et al. 2011). There are numerous instances in the literature in which randomized controlled trials of antioxidant supplementation for disease prevention have yielded unintended adverse effects (ATBC 1994; Michailidis et al. 2013; Omenn et al. 1996); mathematical models of cellular redox signaling pathways would allow *in silico* experimentation of the potential effects of antioxidant

supplemention, as well as the discovery of novel biomarkers of redox dysregulation (Vicini et al. 2002).

Substantial evidence from experimental studies indicates that As exposure induces oxidative stress and redox disturbances: Arsenic generates ROS through upregulation of NAPDH oxidase (NOX) enzymes (Chou et al. 2004; Zhang et al. 2011), inhibits redox-sensitive protein tyrosine phosphatases (PTPs) (Rehman et al. 2012), and perturbs the Nrf2, AP-1, and NF-κB redox signaling pathways (Barchowsky et al. 1996; Hu et al. 2002; Lau et al. 2013a; Lau et al. 2013b; Simeonova et al. 2001). However, evidence from human population studies is lacking, and the limited number of epidemiologic studies of As exposure and oxidative stress have overwhelmingly examined markers of oxidative damage (reviewed in De Vizcaya-Ruiz et al. 2009). Just this year, our group was the first to report that As exposure was associated with decreased blood GSH and altered blood GSH/GSSG and plasma Cys/CySS redox states in a population-based study (Hall et al. 2013), providing evidence that in humans, As exposure might perturb redox homeostasis. Metabolomic profiling has been used to study perturbations of redox pathways (Suh et al. 2012), and metabolomic profiles can be combined with genetic and epigenetic data to examine pathways and interactions in complex diseases (Liu et al. 2012); this approach might be useful to study the influences of As exposure on oxidative stress and redox regulation in humans.

Conclusions

Taken together, our findings suggest that the complex metabolic interplay between one-carbon metabolism and the transsulfuration pathway influences susceptibility to As toxicity in humans. For the first time, we report a gender-specific association between As exposure and

global DNA hydroxymethylation. We observed evidence that the GSH redox state contributes to the interindividual variation in As methylation capacity in humans, in addition to evidence that the GSH redox state influences global DNA methylation. We confirmed that HHcys is an important risk factor for As-induced skin lesion incidence, and the strong associations between MTHFR gene variants and serum Hcys suggest that in the Bangladeshi population, supplementation with 5mTHF might be more effective for Hcys lowering than folic acid. In addition, we used GWAS to identify novel genetic determinants of serum Hcys concentrations, which must be confirmed in future studies. Perhaps most importantly, we have emphasized the importance of understanding the complexities of biologic systems in molecular epidemiology.

REFERENCES

The Alpha-Tocopherol Beta Carotene Cancer Prevention Study Group. 1994. The effect of vitamin e and beta carotene on the incidence of lung cancer and other cancers in male smokers. New England Journal of Medicine 330:1029-1035.

Barchowsky A, Dudek EJ, Treadwell MD, Wetterhahn KE. 1996. Arsenic induces oxidant stress and nf-kappa b activation in cultured aortic endothelial cells. Free Radic Biol Med 21:783-790.

Chou WC, Jie C, Kenedy AA, Jones RJ, Trush MA, Dang CV. 2004. Role of nadph oxidase in arsenic-induced reactive oxygen species formation and cytotoxicity in myeloid leukemia cells. Proc Natl Acad Sci U S A 101:4578-4583.

de Graaf AA, Freidig AP, De Roos B, Jamshidi N, Heinemann M, Rullmann JAC, et al. 2009. Nutritional systems biology modeling: From molecular mechanisms to physiology. PLoS Comput Biol 5:e1000554.

De Vizcaya-Ruiz A, Barbier O, Ruiz-Ramos R, Cebrian ME. 2009. Biomarkers of oxidative stress and damage in human populations exposed to arsenic. Mutation Research/Genetic Toxicology and Environmental Mutagenesis 674:85-92.

Duncan TM, Reed MC, Nijhout HF. 2013. The relationship between intracellular and plasma levels of folate and metabolites in the methionine cycle: A model. Mol Nutr Food Res 57:628-636.

Fomenko DE, Xing W, Adair BM, Thomas DJ, Gladyshev VN. 2007. High-throughput identification of catalytic redox-active cysteine residues. Science 315:387-389.

Hall MN, Niedzwiecki M, Liu X, Harper KN, Alam S, Slavkovich V, et al. 2013. Chronic arsenic exposure and blood glutathione and glutathione disulfide concentrations in bangladeshi adults. Environ Health Perspect 121:1068-74.

Hitchler MJ, Domann FE. 2007. An epigenetic perspective on the free radical theory of development. Free Radical Biology and Medicine 43:1023-1036.

Hu Y, Jin X, Snow ET. 2002. Effect of arsenic on transcription factor ap-1 and nf-kappab DNA binding activity and related gene expression. Toxicol Lett 133:33-45.

Hultberg M, Hultberg B. 2007. Oxidative stress decreases extracellular homocysteine concentration in human hepatoma (hepg2) cell cultures. Chem Biol Interact 165:54-58.

Kim DK, Cho MH, Hersh CP, Lomas DA, Miller BE, Kong X, et al. 2012. Genome-wide association analysis of blood biomarkers in chronic obstructive pulmonary disease. American journal of respiratory and critical care medicine 186:1238-1247.

Lambrou A, Baccarelli A, Wright RO, Weisskopf M, Bollati V, Amarasiriwardena C, et al. 2012. Arsenic exposure and DNA methylation among elderly men. Epidemiology 23:668-676.

Lau A, Whitman SA, Jaramillo MC, Zhang DD. 2013a. Arsenic-mediated activation of the nrf2-keap1 antioxidant pathway. Journal of biochemical and molecular toxicology 27:99-105.

Lau A, Zheng Y, Tao S, Wang H, Whitman SA, White E, et al. 2013b. Arsenic inhibits autophagic flux, activating the nrf2-keap1 pathway in a p62-dependent manner. Mol Cell Biol 33:2436-2446.

Lawley S, Cinderella M, Hall M, Gamble M, Nijhout HF, Reed M. 2011. Mathematical model insights into arsenic detoxification. Theoretical Biology and Medical Modelling 8:31.

Liu Y, Koyuturk M, Barnholtz-Sloan J, Chance M. 2012. Gene interaction enrichment and network analysis to identify dysregulated pathways and their interactions in complex diseases. BMC Systems Biology 6:65.

Majumdar S, Chanda S, Ganguli B, Mazumder DN, Lahiri S, Dasgupta UB. 2010. Arsenic exposure induces genomic hypermethylation. Environ Toxicol 25:315-318.

Malarstig A, Buil A, Souto JC, Clarke R, Blanco-Vaca F, Fontcuberta J, et al. 2009. Identification of znf366 and ptprd as novel determinants of plasma homocysteine in a family-based genome-wide association study. Blood 114:1417-1422.

Michailidis Y, Karagounis LG, Terzis G, Jamurtas AZ, Spengos K, Tsoukas D, et al. 2013. Thiol-based antioxidant supplementation alters human skeletal muscle signaling and attenuates its inflammatory response and recovery after intense eccentric exercise. The American Journal of Clinical Nutrition 98:233-245.

Omenn GS, Goodman GE, Thornquist MD, Balmes J, Cullen MR, Glass A, et al. 1996. Risk factors for lung cancer and for intervention effects in caret, the beta-carotene and retinol efficacy trial. Journal of the National Cancer Institute 88:1550-1559.

Pilsner JR, Liu X, Ahsan H, Ilievski V, Slavkovich V, Levy D, et al. 2007. Genomic methylation of peripheral blood leukocyte DNA: Influences of arsenic and folate in bangladeshi adults. Am J Clin Nutr 86:1179-1186.

Pilsner JR, Liu X, Ahsan H, Ilievski V, Slavkovich V, Levy D, et al. 2009. Folate deficiency, hyperhomocysteinemia, low urinary creatinine, and hypomethylation of leukocyte DNA are risk factors for arsenic-induced skin lesions. Environ Health Perspect 117:254-260.

Reed MC, Thomas RL, Pavisic J, James SJ, Ulrich CM, Nijhout HF. 2008. A mathematical model of glutathione metabolism. Theor Biol Med Model 5:8.

Rehman K, Chen Z, Wang WW, Wang YW, Sakamoto A, Zhang YF, et al. 2012. Mechanisms underlying the inhibitory effects of arsenic compounds on protein tyrosine phosphatase (ptp). Toxicol Appl Pharmacol 263:273-280.

Rogers EJ, Chen S, Chan A. 2007. Folate deficiency and plasma homocysteine during increased oxidative stress. New England Journal of Medicine 357:421-422.

Simeonova PP, Wang S, Kashon ML, Kommineni C, Crecelius E, Luster MI. 2001. Quantitative relationship between arsenic exposure and ap-1 activity in mouse urinary bladder epithelium. Toxicol Sci 60:279-284.

Suh J, Kim R, Lee D. 2012. A new metabolomic assay to examine inflammation and redox pathways following lps challenge. Journal of Inflammation 9:37.

Tanaka T, Scheet P, Giusti B, Bandinelli S, Piras MG, Usala G, et al. 2009. Genome-wide association study of vitamin b6, vitamin b12, folate, and homocysteine blood concentrations. American journal of human genetics 84:477-482.

Vicini P, Gastonguay MR, Foster DM. 2002. Model-based approaches to biomarker discovery and evaluation: A multidisciplinary integrated review. Critical reviews in biomedical engineering 30:379-418.

Wald DS, Bestwick JP, Wald NJ. 2012. Homocysteine as a cause of ischemic heart disease: The door remains open. Clinical Chemistry 58:1488-1490.

Winters RA, Zukowski J, Ercal N, Matthews RH, Spitz DR. 1995. Analysis of glutathione, glutathione disulfide, cysteine, homocysteine, and other biological thiols by high-performance liquid chromatography following derivatization by n-(1-pyrenyl)maleimide. Analytical biochemistry 227:14-21.

Zhang Z, Wang X, Cheng S, Sun L, Son YO, Yao H, et al. 2011. Reactive oxygen species mediate arsenic induced cell transformation and tumorigenesis through wnt/beta-catenin pathway in human colorectal adenocarcinoma dld1 cells. Toxicol Appl Pharmacol 256:114-121.